Carderock Division
Naval Surface Warfare Center
9500 MacArthur Blvd.
West Bethesda, MD 20817-5700

NSWCCD-70-TR-2000/037 March 2000
Signatures Directorate
Research and Development Report

Normalized Outputs to Turbulent Boundary Layer (TBL) of Pressure and Velocity Transducers and Their Sensitivities

by

G. Maidanik
K. J. Becker

NSWCCD-70-TR-2000/037 Normalized Outputs to Turbulent Boundary Layer (TBL) of Pressure and Velocity Transducers and Their Sensitivities

SECURITY CLASSIFICATION OF THIS PAGE

REPORT DOCUMENTATION PAGE

Form Approved OMB No. 0704-0188

1a. REPORT SECURITY CLASSIFICATION Unclassified	1b. RESTRICTIVE MARKINGS None
2a. SECURITY CLASSIFICATION AUTHORITY	3. DISTRIBUTION / AVAILABILITY OF REPORT Approved for public release. Distribution is unlimited.
2b. DECLASSIFICATION/DOWNGRADING SCHEDULE	
4. PERFORMING ORGANIZATION REPORT NUMBER(S) NSWCCD-70-TR—2000/037	5. MONITORING ORGANIZATION REPORT NUMBER(S)
6a. NAME OF PERFORMING ORGANIZATION Carderock Division, NSWC 6b. OFFICE SYMBOL *(if applicable)* Code 7030	7a. NAME OF MONITORING ORGANIZATION
6c. ADDRESS *(City, State, and ZIP Code)* 9500 MacArthur Blvd. West Bethesda, MD 20817-5700	7b. ADDRESS *(City, State, and ZIP Code)*
8a. NAME OF FUNDING/SPONSORING ORGANIZATION 8b. OFFICE SYMBOL *(if applicable)*	9. PROCUREMENT INSTRUMENT IDENTIFICATION NUMBER
8c. ADDRESS *(City, State, and ZIP Code)*	10. SOURCE OF FUNDING NUMBERS PROGRAM ELEMENT NO. / PROJECT NO. / TASK NO. / WORK UNIT ACCESSION NO.

11. TITLE *(Include Security Classification)*

Induced Damping by a Nearly Continuous Distribution of Nearly Undamped Oscillators: Linear Analysis

12. PERSONAL AUTHOR(S)

G. Maidanik

13a. TYPE OF REPORT	13b. TIME COVERED	14. DATE OF REPORT *(Year, Month, Day)*	15. PAGE COUNT
Research & Development	FROM 01/01/00 TO 03/01/00	2000 March 31	163

16. SUPPLEMENTARY NOTATION

17. COSATI CODES			18. SUBJECT TERMS *(Continue on reverse if necessary and identify by block number)*
FIELD	GROUP	SUB-GROUP	Damping Pressure Transducers Turbulent Boundary Layer Velocity Transducer

18. ABSTRACT *(Continue on reverse if necessary and identify by block number)*

This report rudimentarily assesses and compares the performances of three types of arrays: The first comprises flush-mounted pressure transducers placed on a conditioning plate, and the second and third comprise flush-mounted pressure transducers and velocity transducers, respectively, placed on the compliant layer; the conditioning plate is absent in these second and third arrays. The performance of an array is specified by the *normalized output* $S(\Omega)$ and the *sensitivity* $C(\Omega)$ of the array, where (Ω) is the normalized frequency variable. The quantity $S(\Omega)$ of an array is related to the noise that the array insitu registered; the form of $S(\Omega)$ is rendered commensurate with a sea-state rating for the array. The quantity $C(\Omega)$ of an array is related to the capability of the array insitu to register a normally incident signal from a distant source. The maximum value of quantity $C(\Omega)$ is equal to four (4), indicating a signal doubling (compared with the free-field) at the boundary on which the transducers are flush-mounted. For an array to perform adequately, the normalized output quantity $S(\Omega)$ must be *viable* and the sensitivity $C(\Omega)$ needs to be *acceptable*. The array is viable if $S(\Omega)$ lies below a specified criterion; e.g., $S(\Omega)<10^{8}$ re$[(\mu Pa)^2/Hz.] \cong$ Sea-State (0-2). The array is acceptable if $C(\Omega)$ lies above a specified criterion; e.g., $C(\Omega)>(10^{-1})$, say. The more these criteria are satisfied, the superior is the performance of the array. An analysis is developed and examples are cited in this report to enable these assessments and comparisons to be made.

20. DISTRIBUTION / AVAILABILITY OF ABSTRACT	21. ABSTRACT SECURITY CLASSIFICATION	
☐ UNCLASSIFIED/UNLIMITED ☐ SAME AS RPT. ☐ DTIC USERS	Unclassified	
22a. NAME OF RESPONSIBLE INDIVIDUAL Maidanik, G.	22b. TELEPHONE (Including Area Code) (301) 227-1292	22c. OFFICE SYMBOL NSWCCD 7030

DD Form 1473, JUN 86 *Previous editions are obsolete*

SECURITY CLASSIFICATION OF THIS PAGE

Contents

Abstract

This report rudimentarily assesses and compares the performances of three types of arrays: The first comprises flush-mounted pressure transducers placed on a conditioning plate, and the second and third comprise flush-mounted pressure transducers and velocity transducers, respectively, placed on the compliant layer; the conditioning plate is absent in these second and third arrays. The performance of an array is specified by the *normalized output* $S(\Omega)$ and the *sensitivity* $C(\Omega)$ of the array, where (Ω) is the normalized frequency variable. The quantity $S(\Omega)$ of an array is related to the noise that the array insitu registered; the form of $S(\Omega)$ is rendered commensurate with a sea-state rating for the array. The quantity $C(\Omega)$ of an array is related to the capability of the array insitu to register a normally incident signal from a distant source. The maximum value of $C(\Omega)$ is equal to four (4), indicating a signal doubling (compared with the free-field) at the boundary on which the transducers are flush-mounted. For an array to perform adequately, the normalized output $S(\Omega)$ must be *viable* and the sensitivity $C(\Omega)$ needs to be *acceptable*. The array is viable if $S(\Omega)$ lies below a specified criterion; e.g., $S(\Omega) < 10^8 \,\mathrm{re}[(\mu Pa)^2 / \mathrm{Hz.}] \cong \mathrm{Sea-State}\ (0-2)$. The array is acceptable if $C(\Omega)$ lies above a specified criterion; e.g., $C(\Omega) > (10^{-1})$, say. The more these criteria are satisfied, the superior is the performance of the array. An analysis is developed and examples are cited in this report to enable these assessments and comparisons to be made.

Introduction

Two recent reports addressed the wavevector-frequency spectral density of a turbulent boundary layer (TBL) and the manner by which the filtering efficiencies of the boundaries, blankets, transducers and arrays challenge this spectral density. Whereas the goal of a design is to maintain largely intact the output to a signal (a supersonic incident pressure field), the output to a (TBL) must be largely subdued; i.e., a component in the (TBL) must be largely rejected from inducing an output in the transducer. The rejection of (TBL) that can be mustered by a flush-mounted pressure transducer and by a flush-mounted velocity transducer are compared in these reports. In the present report the comparison is extended to transducer configurations that are not merely designated flush-mounted. Also, the comparison is made not just on the raw basis of the wavevector-frequency filtering efficiencies and the wavevector-frequency spectral density of (TBL), but, in addition, by evaluating the frequency spectral densities registered by the two sets of transducers. The frequency spectral densities are quantities that are more commensurate with the outputs of actual transducers and arrays. However, the evaluation of the frequency spectral densities provide for more specific assessments than those afforded by consideration of the wavevector-frequency spectral densities. In this sense, this report sacrifices generality in an attempt to render the material discussed in the two referenced reports more akin in format to the kind of information that is usually requested by designers of naval sonar systems. Moreover, whereas, in the two reports the spatial size of the flush-mounted transducers in the planar array are associated with the steering filtering efficiency of the array, in this report transducers are of equal sizes and the filtering efficiency due to the spatial extent of the transducers are incorporated in the passive filtering efficiency of the array. Then only the true steering filtering efficiency of a matrix of point transducers is the active element in the combined filtering efficiency of the array. Moreover, only the passive filtering efficiency, including that of the spatial size of the transducer, is considered herein; the steering filtering efficiencies in the pressure and velocity arrays are assumed to be equal.

In order to conform more closely with other similarly attempted estimates, the wavevector-frequency spectral density of a (TBL) is modified slightly from that stated in the referenced reports. The non-convective wavevector-frequency spectral density is given a nearly quadratic dependence on the mach number of the convective speed with respect to the speed of sound in the fluid. This modification encourages a frequency spectral density that is proportional to the sixth power in the convective speed when the overall passive filtering efficiency of the array is strong enough. It is understood that this dependence is apparently in agreement with observations. On the other hand, except for accommodating a nonflush-mounted transducer, the passive filtering efficiencies of the boundaries and the blankets remain intact in the present report. Nonetheless, computational consideration in this report is limited to essentially flush-mounted transducers; consideration of transducers that are not flush-mounted is deferred.

A major question addressed in this report is the normalization of the filtering efficiencies of the pressure transducer and the velocity transducer by a "unit" spectral density of a normally incident pressure field. This normalizing quantity is termed the sensitivity of the transducer insitu; it qualifies the transducer as a signal responder. In turn, the normalized filtering efficiency may be conveniently calibrated with known noise sources such as sea-state noise. In this way the normalized output to (TBL) of a transducer or an array may be given sea-state rating.

The performance of the transducers, and the arrays in which the transducers are elements, are assessed here largely on the basis of the direct response induced by (TBL); other noise sources are not considered. However, the direct response that (TBL) generates is subdued efficiently by a blanket and the spatial sizes of the transducers; usually the blanket is by far the more effective mitigator to (TBL). Other noise sources than (TBL) may not be so efficiently mitigated by a blanket, if at all. How do these noise sources compete with the response that is generated directly by (TBL) especially when the latter is significantly reduced. In this connection one recalls the eternal dilemma: A design modification to achieve an advantage in one noise control and endeavor may adversely affect other noise control requirements. Coupled with this consideration are questions relating to the influence of modifications in the design of a boundary,

not only on the shielding of the transducers and arrays from the motions of the hull, but also on the auxiliary functions of the cladding; e.g., anti-radiation properties and specular reflection efficiencies. These influences are formulated under the same mantle and are demonstrated in this report. However, no attempt is made to assign quantitative estimates of these attributes; a flag waving is all that is done here. Nonetheless, even this flag waving cannot be dismissed as trivial; in the final design, these raised questions cannot be ignored.

Finally, the influence, of modifications to the designed boundary on the filtering efficiencies that relate to the anti-radiation properties, to the specular reflection efficiencies and to the shielding of the transducers and arrays from mechanical drives on the hull, are also formulated and demonstrated in this report. Thus, questions relating to anti-radiation, questions relating to stealth and questions relating to signal-to-noise of the transducers and arrays in consequence of hull excitation, are cast under the same mantle. In this form, a design modification to achieve an advantage in one noise control endeavor can be appropriately judged as to its affects on the other endeavors of noise control.

I. Elemental Analysis

In this essay it is intended to decipher the response of a pressure transducer or of a velocity transducer that is placed just on or just above a boundary. The placement is considered to be nonintrusive in the sense that the transducer introduces no impedance discontinuity either locally or globally. The fluid above the boundary and the boundary itself are considered to possess uniform impedances. The fluid characteristic impedance is designated (ρc) where (ρ) is the density and (c) is the speed of sound. On the other hand, the mechanical surface impedance of the boundary is designated, in spectral space, by $Z_b(\underset{\sim}{k},\omega)$, where $(\underset{\sim}{k})$ is the wavevector variable in the plane of the boundary and (ω) is the frequency variable. A sketch of the physical situation to be investigated with respect to a pressure transducer is presented in Fig. 1. Considering that the boundary is subjected to an external "incident" pressure field designated by $P(\underset{\sim}{k},\omega)$ and the pressure reflection coefficient at the boundary is designated $R_p(\underset{\sim}{k},\omega)$, the response $O_p(\underset{\sim}{k},\omega)$ of a point pressure sensing device is given by

$$O_p(\underset{\sim}{k},\omega) = \exp(-ihk_3)[1+R_p(\underset{\sim}{k},\omega)\ \exp(-2id_0k_3)]P(\underset{\sim}{k},\omega)\ , \tag{1}$$

where

$$R_p(\underset{\sim}{k},\omega) = [Z_b(\underset{\sim}{k},\omega) - Z_w(\underset{\sim}{k},\omega)]\ [Z_b(\underset{\sim}{k},\omega) + Z_w(\underset{\sim}{k},\omega)]\ , \tag{2}$$

$$d_0 = dU(b-d) + bU(d-b)\ ;\quad \underset{\sim}{k} = \{k_x,k_y\}\ ;\quad |\underset{\sim}{k}| = k\ ;\quad \bar{k}_3 = (k_3c/\omega)\ ;$$

$$\bar{k}_3 = [1-(kc/\omega)^2]^{1/2}\ U[1-(kc/\omega)^2]-i[(kc/\omega)^2-1]^{1/2}\ U[(kc/\omega)^2-1]\ ;$$

$$U(b-d)=\begin{cases}1, & b>d\\ 0 & b<d\end{cases}\ . \tag{3}$$

In Eqs. (2) and (3), $Z_w(\underset{\sim}{k},\omega)$ is the surface impedance of the fluid in the plane of the boundary; namely

$$Z_w(\underset{\sim}{k},\omega) = (\rho c)(\bar{k}_3)^{-1} \; ; \; \bar{Z}_w(\underset{\sim}{k},\omega) = (\bar{k}_3) \; ; \; \bar{Z}_w(\underset{\sim}{k},\omega) = (\rho c)^{-1} Z_w(\underset{\sim}{k},\omega) \; , \quad (4a)$$

and, similarly, the normalization of the surface impedance of the boundary is carried out in the form

$$\bar{Z}_b(\underset{\sim}{k},\omega) = (\rho c)^{-1} \; Z_b(\underset{\sim}{k},\omega) \; , \quad (4b)$$

and, finally, (h), (b) and (d) are the separation distances between parallel planes as defined in Fig. 1. From Eqs. (1) – (4) one obtains

$$\Phi_p(\underset{\sim}{k},\omega) = C_p(\underset{\sim}{k},\omega) \; \Phi^p(\underset{\sim}{k},\omega) \; , \quad (5)$$

where

$$C_p(\underset{\sim}{k},\omega) \; |\exp(-i\bar{h}\bar{k}_3) \; \{1 + R_p(\underset{\sim}{k},\omega) \; \exp(-2i\bar{d}_0\bar{k}_3)\}|^2 \; ;$$

$$\bar{d}_0 = \bar{d}U(b-d) + \bar{b}U(d-b) \; ; \quad \bar{h} = (\omega h/c) \; ; \quad \bar{d}_0 = (\omega d_0/c) \; , \quad (6)$$

$$\langle O_p(\underset{\sim}{k},\omega) \; O_p^*(\underset{\sim}{k}',\omega')\rangle = \Phi_p(\underset{\sim}{k},\omega) \; \delta(\underset{\sim}{k}-\underset{\sim}{k}') \; \delta(\omega-\omega') \; , \quad (7a)$$

$$\langle P(\underset{\sim}{k},\omega) \; P^*(\underset{\sim}{k}',\omega')\rangle = \Phi^p(\underset{\sim}{k},\omega) \; \delta(\underset{\sim}{k}-\underset{\sim}{k}') \; \delta(\omega-\omega') \; , \quad (7b)$$

DEPARTMENT OF THE NAVY
NAVAL SURFACE WARFARE CENTER
CARDEROCK DIVISION

CARDEROCK DIVISION HEADQUARTERS
DAVID TAYLOR MODEL BASIN
9500 MACARTHUR BOULEVARD
WEST BETHESDA, MD 20817-5700

IN REPLY REFER TO:

9073
Ser 72505/020
19 May 00

From: Commander, Carderock Division, Naval Surface Warfare Center
To: Commander, Naval Sea Systems Command

Subj: TRANSMITTAL OF REPORT

Encl: (1) NSWCCD-70-TR-2000-037, "Normalized Outputs to Turbulent Boundary Layer (TBL) of Pressure and Velocity Transducers and Their Sensitivities", Mar 00

1. Enclosure (1) is forwarded for your information. This document was prepared by the Naval Surface Warfare Center, Carderock Division (NSWCCD).

2. Please contact Dr. Gideon Maidanik, 301-227-1292, or Mr. Ken Becker, 301-227-3137 for further inquiries.

G.A. Smith

G.A. SMITH
By direction

Distribution:
NAVSEA 05T2 (Taddeo, Biancardi)
ONR/ONT 334 (Tucker, Radlinski, Vogelsong, Main, Library)
NRL 5130 (Bucaro, Williams, Photiadis, Library)
NUWC/NPT (Sandman, Harari, 3332 Lee, Library)
DTIC
John Hopkins Univ. (Green, Dickey)
ARL/Penn State Univ. (Burroughs, Hwang)
R.H. Lyons
Cambridge Collaborative (Manning)
Cambridge Acoustical Associates (Garrelick)
J.G. Engineering Research (Greenspan)
MIT (Dyer)
Catholic Univ. of America Engineering Dept. (McCoy)
Boston Univ. (Pierce, Barbone)
Penn State Univ. (Koopman)
Virginia Tech (Knight, Fuller)

Subj: TRANSMITTAL OF NSWC REPORT

Distribution: (continued)
NSWCCD
0100 (Corrado)
0112 (Douglas, Halsall)
20
2040 (Everstine)
70 (Covich)
701 (Sevik)
7015 (Fisher)
7020 (Strasberg)
7030 (Maidanik)
7205 (Dlubac)
7200 (Shang)
7207 (Becker)
725 (Bowers, Maga)
722 (Niemiec, Carroll, Vasudevan)
842 (Graesser)

Writer: G. Maidanik, 7030, x1292
Typist: J. Patino, 19 MAY 00

and (U), in Eq. (6), is the conventional unit step function, as defined in Eq. (3), and $\delta(\underset{\sim}{k}-\underset{\sim}{k}') = \delta(k_x - k_x')\ \delta(k_y - k_y')$. If $\Phi_p(\underset{\sim}{k},\omega)$ is to be normalized by a standard, normally incident pressure wave, the normalization is executed by dividing Eq. (5) by

$$\Phi_{pI}(0,\omega) = (2)^2 \,|[\bar{Z}_b(0,\omega)\ \cos(\bar{d}) + i\sin(\bar{d})]\ [Z_b(0,\omega) + 1]^{-1}\,|^2 \ , \qquad (8a)$$

where $\Phi_{pI}(o,\omega)$ is the quadratic insitu output of the pressure transducer to a wavevector-frequency spectral density $\Phi_I^p(0,\omega)$ that is set equal to unity; namely

$$C_p(0,\omega) = (2)^2 \,|[\bar{Z}_b(0,\omega)\ \cos(\bar{d}) + i\sin(\bar{d})\ [Z_b(0,\omega) + 1]^{-1}\,|^2 \ ;$$

$$\Phi_{pI}(0,\omega) = C_p(0,\omega) \ . \qquad (8b)$$

The normalized wavevector-frequency spectral density $\Phi_p(\underset{\sim}{k},\omega)$ as registered by a point pressure transducer is, from Eqs. (1) – (8), given by

$$\Phi_p(0,\omega) = \bar{C}_p(\underset{\sim}{k},\omega)\ \Phi^p(\underset{\sim}{k},\omega) \ ; \quad \bar{C}_p(\underset{\sim}{k},\omega) = [C_p(\underset{\sim}{k},\omega) / C_p(0,\omega)] \ , \ (9)$$

where the normalized boundary-filtering efficiency $\bar{C}_p(\underset{\sim}{k},\omega)$ may be expressed in the form

$$\bar{C}_p(\underset{\sim}{k},\omega) = |\exp(-i\bar{h}\bar{k}_3)\ [\bar{k}_3\bar{Z}_b(\underset{\sim}{k},\omega)\ \{1+\exp(-2i\bar{d}_0\bar{k}_3)\} + \{1-\exp(-2i\bar{d}_0\bar{k}_3)\}]$$

$$[\bar{Z}_b(0,\omega)+1]\ [\bar{k}_3\bar{Z}_b(\underset{\sim}{k},\omega)+1]^{-1}\ [\bar{Z}_b(0,\omega)\cos(\bar{d})+i\sin(\bar{d})]^{-1}\,|^2 \ . \quad (10)$$

Were one to compare the viability of one mechanical boundary versus another, and/or one transducer configuration versus another, one may need to evaluate the frequency spectral density in the form

$$S_p^{(n)}(\omega) = \int d\underset{\sim}{k}\ \Phi_p^{(n)}(\underset{\sim}{k},\omega)\ , \tag{11}$$

where (n) designates a particular boundary and/or a pressure transducer configuration. However, the comparison afforded by Eq. (11) is only partial; to complete the comparison one is required to evaluate, in addition, the quadratic outputs in response to a unit normal incidence. Thus, from Eqs. (8) and (11), to complete the comparison one needs to evaluate also

$$C_p^{(n)}(\omega) = (2)^2\, |[\overline{Z}_b^{(n)}(0,\omega)\cos(\overline{d}^{(n)}) + i\sin(\overline{d}^{(n)})]\ [\overline{Z}_b^{(n)}(0,\omega) + 1]^{-1}\,|^2 \tag{12}$$

Equation (12) determines whether the sensitivity of the pressure transducer, in the (n)th designation of the boundary and configuration is acceptable. It is assumed in Eqs. (11) and (12) that the "incident" wavevector-frequency spectral density $\Phi^p(\underset{\sim}{k},\omega)$ remains unchanged on the boundary, whatever the normalized mechanical surface impedance is as a function of $\{\underset{\sim}{k},\omega\}$, even in extreme cases; i.e., $\Phi^p(\underset{\sim}{k},\omega)$ is the normalized wavevector-frequency spectral density of an "external drive." Moreover, the pressure transducer is nonintrusive; i.e., its placement on or above the boundary does not change the impedances involved, neither locally nor globally.

Situations may arise in which the placement of a velocity transducer on or just above a boundary is contemplated. A sketch of the physical situation for investigating a velocity transducer is presented in Fig. 2. [cf. Fig 1.] The output $O_v(\underset{\sim}{k},\omega)$ of a point velocity sensing device is given by

$$O_v(\underset{\sim}{k},\omega) = \exp(-ihk_3)\ [1 + R_v(\underset{\sim}{k},\omega)\ \exp(-2id_0k_3)]\ V(\underset{\sim}{k},\omega)\ , \tag{13}$$

where

$$R_v(\underset{\sim}{k},\omega) \;=\; -R_p(\underset{\sim}{k},\omega)\;, \tag{14}$$

and the other quantities and parameters are as defined in Eqs. (3) and (4). [cf. Figs. 1 and 2.] From Eq. (13) one obtains

$$\Phi_v(\underset{\sim}{k},\omega) \;=\; C_v(\underset{\sim}{k},\omega)\;\Phi^v(\underset{\sim}{k},\omega) \;=\; C_v(\underset{\sim}{k},\omega)\,|\,\bar{k}_3\,/\,(\rho c)\,|^2\;\Phi^p(\underset{\sim}{k},\omega)\;, \tag{15}$$

where

$$C_v(\underset{\sim}{k},\omega) \;=\; \left|\exp(-i\bar{h}\bar{k}_3)\;\{1-R_p(\underset{\sim}{k},\omega)\;\exp(-2i\bar{d}_0\bar{k}_3)\}\right|^2\;, \tag{16}$$

$$\langle O_v(\underset{\sim}{k},\omega)\;\;O_v^*(\underset{\sim}{k},\omega)\rangle \;=\; \Phi_v(\underset{\sim}{k}',\omega')\;\;\delta(\underset{\sim}{k}-\underset{\sim}{k}')\;\;\delta(\omega-\omega')\;, \tag{17a}$$

$$\langle V(\underset{\sim}{k},\omega)\;\;V^*(\underset{\sim}{k}',\omega')\rangle \;=\; \Phi^v(\underset{\sim}{k}',\omega')\;\;\delta(\underset{\sim}{k}-\underset{\sim}{k}')\;\;\delta(\omega-\omega')\;, \tag{17b}$$

and it is tacitly assumed that

$$V(\underset{\sim}{k},\omega) \;=\; [\bar{k}_3\,/\,(\rho c)]\;\;P(\underset{\sim}{k},\omega)\quad. \tag{17c}$$

[cf. Eqs. (5) – (7).] If $\Phi_v(\underset{\sim}{k},\omega)$ is to be normalized by a standard, normally incident pressure wave, the normalization is executed by dividing Eq. (15) by

$$\Phi_{vI}(0,\omega) \;=\; (2)^2\,\left|[i\bar{Z}_b(0,\omega)\sin(\bar{d}) \;+\; \cos(\bar{d})]\;[\bar{Z}_b(0,\omega)+1]^{-1}\right|^2\quad. \tag{18a}$$

where $\Phi_{vI}(0,\omega)$ is the quadratic insitu output in the spectral domain, of the velocity transducer to a unit normally incident pressure wave registered by a point velocity transducer on the boundary, namely

$$C_v(\omega) \;=\; (2)^2 \,|\, \bar{Z}_b^{(m)}(0,\omega)\sin(\bar{d}) + \cos\bar{d}\,]\;[\bar{Z}_b^{(n)}(0,\omega) \;+\; 1]^{-1}\,|^2 \;\;;$$

$$\Phi_{vI}(0,\omega) \;=\; C_v(\omega)(\rho c)^{-2} \;\;. \tag{18b}$$

The normalized wavevector-frequency spectral density $\Phi_v(\underset{\sim}{k},\omega)$ registered by a point velocity transducer is, from Eqs. (15) – (18), given by

$$\Phi_v(\underset{\sim}{k},\omega) \;=\; \bar{C}_v(\underset{\sim}{k},\omega)\;\; \Phi^v(\underset{\sim}{k},\omega) \;=\; \bar{C}_v(\underset{\sim}{k},\omega)\;\; |\,\bar{k}_3\,|^2 \;\; \Phi^p(\underset{\sim}{k},\omega)\;\;;$$

$$\bar{C}_v(\underset{\sim}{k},\omega) \;=\; [C_v(\underset{\sim}{k},\omega)/\,C_v(\omega)]\;\;, \tag{19}$$

where the normalized boundary filtering efficiency $\bar{C}_v(\underset{\sim}{k},\omega)$ may be derived from Eqs. (13), (18a) and (19) to be

$$\bar{C}_v(\underset{\sim}{k},\omega) \;=\; (1/2)^2\,|\exp(-i\bar{h}\bar{k}_3)\;[\bar{k}_3\bar{Z}_b(\underset{\sim}{k},\omega)\;\{1-\exp(-2i\bar{d}_0\bar{k}_3)\} \;+\; \{1+\exp(-2i\bar{d}_0\bar{k}_3)\}]$$

$$[1+\bar{Z}_b(0,\omega)]\;[\bar{k}_3\bar{Z}_b(\underset{\sim}{k},\omega)+1]^{-1}\;\;[i\bar{Z}_b(0,\omega)\sin(\bar{d})+\cos(\bar{d})]^{-1}\,|^2 \;\;. \tag{20}$$

Were one to compare the viability of one mechanical boundary versus another, one may need to evaluate the frequency spectral density in the form

$$S_v^{(n)}(\omega) \;=\; \int d\,\underset{\sim}{k}\;\Phi_v^{(n)}(\underset{\sim}{k},\omega)\;\;, \tag{21}$$

where, again, (n) designates a particular boundary and/or a velocity transducer configuration. However, again, the comparison afforded by Eq. (21) is only partial; to complete the comparison one is required to evaluate, in addition, the quadratic output in response to a unit normal incidence. Thus, from Eqs. (18) – (21), to complete the comparison one needs to evaluate also

$$C_v^{(n)}(\omega) = (2)^2 \left| [iZ_b^{(n)}(0,\omega)\sin(\bar{d})^{(n)} + \cos(\bar{d})^{(n)}] \, [\bar{Z}_b^{(n)}(0,\omega) + 1]^{-1} \right|^2 \qquad (22)$$

Again, Eq. (22) determines whether the sensitivity of the velocity transducer, in the $(n)th$ configuration is absolutely acceptable. Again, it is assumed in Eqs. (21) and (22) that the "incident" wavevector-frequency spectral density $\Phi^v(\underset{\sim}{k},\omega)$ remains unchanged on the boundary, whatever the normalized mechanical surface impedance is as a function of $\{\underset{\sim}{k},\omega\}$, even in extreme cases; i.e., $\Phi^v(\underset{\sim}{k},\omega)$ is the normalized wavevector-frequency spectral density of an "external drive." Moreover, the velocity transducer is nonintrusive; i.e., its placement on or above the boundary does not change the impedances involved, neither locally nor globally.

Clearly, there exist distinctions, as well as commonalties, between a *pressure* transducer and a *velocity* transducer. In part, the distinctions and the commonalties between these two types of transducers are analyzed and contrasted in two recent reports [1,2]. In the reports the transducers are flush-mounted on the boundary; namely $(\bar{d})$ is set essentially equal to zero. Both types of transducers merely sense the *pressure* and the *velocity* on the boundary. The ideal boundary for the pressure transducer is designated to be *rigid* and for the velocity transducer is designated to be *pressure release*. Deviations of the boundary from these defined ideals are also considered in these reports [1,2]. In particular, it is argued in these reports that if the pressure release boundary is stiffened, the resonance between the surface stiffness and the surface mass of the fluid tends to render the filtering efficiency of a velocity transducer more like that of a pressure transducer on a rigid boundary. That is, the resonance, with the exception of the wavenumber in the narrow region of resonance, subdues the favor held by the velocity transducer for accepting the higher subsonic components. Indeed, so much so that in certain regions about

the convective range, a velocity transducer may possess a filtering efficiency that is superior to that of a pressure transducer on a rigid boundary [1,2]. Thus, it is suggested that stiffening the compliant layer on which the velocity transducer may be placed, might bring into contention an array incorporating velocity transducers that are placed on this stiffened boundary. Thus, if (m) designates a largely rigid boundary and (n) designates a specifically stiffened pressure release boundary, then from Eqs. (11) and (21), one may expect that in certain frequency ranges the ratio

$$S^{v(n)}_{p(m)}(\omega) \;=\; [S^{(n)}_{v}(\omega) \,/\, S^{m}_{p}(\omega)] \;, \tag{23}$$

where

$$S^{(n)}_{v}(\omega) \;=\; \int d\underset{\sim}{k}\; \Phi^{(n)}_{v}(\underset{\sim}{k},\omega) \;; \qquad S^{(m)}_{p}(\omega) \;=\; \int d\underset{\sim}{k}\; \Phi^{(m)}_{p}(\underset{\sim}{k},\omega) \;, \tag{24}$$

will exceed unity. In these frequency ranges, because of the resonance between the surface stiffness and the surface mass of the fluid, the velocity transducer may exhibit a frequency spectral density $S^{(n)}_{v}(\omega)$ that is less than $S^{(m)}_{p}(\omega)$ of a pressure transducer, even if the external wavevector-frequency spectral density is rich in higher subsonic components; e.g., as is the external drive of a turbulent boundary layer (TBL). Notwithstanding that for such an external drive, were the boundary for the velocity transducer to be largely pressure release, this ratio will exceed unity, by several orders of magnitude throughout the relevant frequency range [1-3]. [The relevant frequency range extends from about 200 Hz to 10 KHz. The *lower* limit is determined largely by the ring frequency of the hull and the *upper* limit largely by the failure of a two-dimensional analysis.]

Although the comparisons, stated in Eqs. (11), (21) and (23), are advocated on the basis of the frequency spectral densities, nonetheless, the raw wavevector-frequency domain may serve to design and assess the functional viability of one boundary versus another, of one configuration versus another and of one type of transducer versus another. In these kinds of assessments one

relies on the nature of the signal and noise fields to be encountered and on the filtering efficiencies of the boundary. These filtering efficiencies are functionals of the configuration and of the type of transducers [1, 2].

Last, but not least, the model of the boundaries employed herein can be readily used to assess the other functions that they may need to serve. These functions may include tasks relating to anti-radiation, stealth, and force and velocity controlled motions of the hull. The advantage is that all these functions, that are assigned to the boundary, come under a single cover. Then clashes between requirements and design criteria of these boundaries may be judged within the same context. Thus, for the assessment of the anti-radiation function it is necessary to evaluate the normalized velocity $\overline{V}_b^{(n)}(\underset{\sim}{k},\omega)$ on the boundary for a particular arrangement (n) and for a mechanical external drive $P_e(\underset{\sim}{k},\omega)$ on the hull. [cf. Figs. 3 and 4 [3].] Before the cladding on the boundary is implemented, the normalized velocity $V_h(\underset{\sim}{k},\omega)$ is ascertained. The anti-radiation efficiency $A_h^{(n)}(\underset{\sim}{k},\omega)$ of that modification is evaluated in the form

$$A_h^{(n)}(\underset{\sim}{k},\omega) \;=\; |\overline{V}_b^{(n)}(\underset{\sim}{k},\omega)|^2 \;,\quad V_b^{(n)}(\underset{\sim}{k},\omega) \;=\; V_b^{(n)}(\underset{\sim}{k},\omega)/V_h(\underset{\sim}{k},\omega)] \;, \qquad (25)$$

where, again, $V_b^{(n)}(\underset{\sim}{k},\omega)$ is the insitu velocity on the boundary for a particular arrangement (n) and $V_h(\underset{\sim}{k},\omega)$ is typically the response of the hull to a corresponding external drive in the absence of any cladding. It is readily derived, with the help of Fig. 4, that

$$\overline{V}_b(\underset{\sim}{k},\omega) \;=\; \overline{Z}_c(\underset{\sim}{k},\omega)\;[1+\overline{k}_3(\underset{\sim}{k},\omega)\overline{Z}_h(\underset{\sim}{k},\omega)][\overline{Z}_c(\underset{\sim}{k},\omega)+\overline{Z}_h(\underset{\sim}{k},\omega)]^{-1}$$

$$\{[1+\overline{k}_3(\underset{\sim}{k},\omega)\{\overline{Z}_t(\underset{\sim}{k},\omega)+\overline{Z}_{ch}(\underset{\sim}{k},\omega)\}]\}^{-1} \quad , \qquad (26a)$$

$$\overline{Z}_{ch}(\underset{\sim}{k},\omega) \;=\; \overline{Z}_h(\underset{\sim}{k},\omega)\overline{Z}_c(\underset{\sim}{k},\omega)[\overline{Z}_c(\underset{\sim}{k},\omega)+\overline{Z}_h(\underset{\sim}{k},\omega)]^{-1} \quad . \qquad (26b)$$

[cf. Eqs. (11), (12), (21) and (22).] One is reminded that substantially only the supersonic components, for which $(kc/\omega)^2 < 1$, need to be evaluated in $\overline{V}_b(\underset{\sim}{k},\omega)$ or $A_h^{(n)}(\underset{\sim}{k},\omega)$.

On the other hand, the stealth function is evaluated via determining the modification that is rendered unto the specular reflection coefficient $R_p^{(n)}(\underset{\sim}{k},\omega)$. Again, substantially, only supersonic components need to be evaluated. Two categories may be distinguished and compared. One is with the conditioning plate in place, and the other in its absence; namely

$$R_{Np}(\underset{\sim}{k},\omega) = [1-\overline{k}_3(\underset{\sim}{k},\omega)\ \overline{Z}_N(\underset{\sim}{k},\omega)]\ [1+\overline{k}_3(\underset{\sim}{k},\omega)\overline{Z}_N(\underset{\sim}{k},\omega)]^{-1} \quad ;$$

$$N=1 \text{ or } 2 \quad , \tag{27}$$

$$\overline{Z}_1(\underset{\sim}{k},\omega) = \overline{Z}_t(\underset{\sim}{k},\omega)+\overline{Z}_2(\underset{\sim}{k},\omega) \quad , \tag{28a}$$

$$\overline{Z}_2(\underset{\sim}{k},\omega) = \overline{Z}_{ch}(\underset{\sim}{k},\omega) \quad , \tag{28b}$$

where $\overline{Z}_{ch}(\underset{\sim}{k},\omega)$ is stated in Eq. (26b) [5]. The stealth function is assessed in terms of specular reflection efficiency that is simply equal to the absolute square value of the reflection coefficient.

Finally, the transfer of the motions of the hull to velocity and pressure wavenumber-frequency spectral densities on the boundary are determined. These densities; $\Phi_v^e(\underset{\sim}{k},\omega)$ and $\Phi_p^e(\underset{\sim}{k},\omega)$, due to a force spectral density $\Phi_{Ip}^e(\underset{\sim}{k},\omega)$ acting on the hull, and $\Phi_v^o(\underset{\sim}{k},\omega)$ and $\Phi_p^o(\underset{\sim}{k},\omega)$ due to a velocity spectral density $\Phi_{Iv}^e(\underset{\sim}{k},\omega)$ that is specified on the hull, may be expressed in the forms

$$[\Phi_p^e(\underset{\sim}{k},\omega)/\Phi_{Ip}^e(\underset{\sim}{k},\omega)] = T_{Ip}^p(\underset{\sim}{k},\omega) \quad , \tag{29a}$$

$$[\Phi_v^e(\underset{\sim}{k},\omega)/\Phi_{Iv}^e(\underset{\sim}{k},\omega)] \;=\; |Z_w(\underset{\sim}{k},\omega)|^{-2}\, T_{Ip}^p(\underset{\sim}{k},\omega) \quad , \tag{29b}$$

and

$$[\Phi_v^o(\underset{\sim}{k},\omega)/\Phi_{Iv}^o(\underset{\sim}{k},\omega)] \;=\; T_{Iv}^v(\underset{\sim}{k},\omega) \quad , \tag{30a}$$

$$[\Phi_p^o(\underset{\sim}{k},\omega)/\Phi_{Iv}^o(\underset{\sim}{k},\omega)] \;=\; |Z_w(\underset{\sim}{k},\omega)|^{-2}\, T_{Iv}^v(\underset{\sim}{k},\omega) \quad , \tag{30b}$$

$$T_{Ip}^p(\underset{\sim}{k},\omega) \;=\; |\overline{Z}_c(\underset{\sim}{k},\omega)[\overline{Z}_c(\underset{\sim}{k},\omega)+\overline{Z}_h(\underset{\sim}{k},\omega)]^{-1}$$

$$[1+\bar{k}_3(\underset{\sim}{k},\omega)\{\overline{Z}_t(\underset{\sim}{k},\omega)+\overline{Z}_{ch}(\underset{\sim}{k},\omega)\}]^{-1}|^2 \quad , \tag{31a}$$

$$T_{Iv}^v(\underset{\sim}{k},\omega) \;=\; |\bar{k}_3(\underset{\sim}{k},\omega)\overline{Z}_c(\underset{\sim}{k},\omega)[1+\bar{k}_3(\underset{\sim}{k},\omega)\{\overline{Z}_t(\underset{\sim}{k},\omega)+\overline{Z}_c(\underset{\sim}{k},\omega)\}]^{-1}|^2 \quad , \tag{31b}$$

and, again $\overline{Z}_{ch}(\underset{\sim}{k},\omega)$ is stated in Eq. (26b).

II. The Tale of Two Boundaries and the Surface Impedances Involved

Two boundary forms are sketched in Figs. 3a and 3b. It is recognized that the difference between the two boundaries is that in the first, as depicted in Fig. 3a, a *conditioning plate* is incorporated as compared with the second, as depicted in Fig. 3b; the second boundary is derived from the first by the removal of that plate [6, 7]. From a weight consideration this removal is welcomed. The question to be asked is whether this removal introduces a significant decrease in the signal-to-noise ratio as perceived by arrays that are to be placed on one boundary or the other. The equivalent circuit diagrams depicting the two forms of boundaries are shown in Figs. 4a and 4b, respectively. Designating the respective normalized mechanical surface impedances of the boundaries in the first and in the second forms by $\overline{Z}_b^{(1)}(\underset{\sim}{k},\omega)$ and $\overline{Z}_b^{(2)}(\underset{\sim}{k},\omega)$, respectively, the expressions for these normalized quantities are:

$$\overline{Z}_b^{(1)}(\underset{\sim}{k},\omega) = [Z_b^{(1)}(\underset{\sim}{k},\omega)/(\rho c)] = i\omega\overline{m}_h\ [(m_t/m_h)\{1-g_t(\underset{\sim}{k},\omega)\}+g_c(\underset{\sim}{k},\omega)]\ , \quad (32a)$$

$$\overline{Z}_b^{(2)}(\underset{\sim}{k},\omega) = [Z_b^{(2)}(\underset{\sim}{k},\omega)/(\rho c)] = i\omega\overline{m}_h\ g_c(\underset{\sim}{k},\omega)\ ; \qquad \overline{m}_h = [m_h/\rho c]\ , \quad (32b)$$

where

$$g_c(\underset{\sim}{k},\omega) = \{1-g_h(\underset{\sim}{k},\omega)\}\ (1+i\eta_c)\ [(1+i\eta_c)-(\omega/\omega_o)\ \{1-g_h(\underset{\sim}{k},\omega)\}]^{-1}\ , \quad (33)$$

$$g_t(\underset{\sim}{k},\omega) = (k/k_t)^4\ (1+i\eta_t)\ ; \qquad k_t^2 = [(\omega/\omega_t/c^2]\ , \quad (34a)$$

$$g_h(\underset{\sim}{k},\omega) = (k/k_h)^4\ (1+i\eta_h)\ ; \qquad k_b^2 = [(\omega/\omega_h/c^2]\ , \quad (34b)$$

$$(\omega_t/\omega_h) = (h_h/h_t)\ ; \quad \omega_0^2 = (K/m_h)\ ; \quad Z_c(\underset{\sim}{k},\omega) = (K/i\omega)(1+i\eta_c)\ , \quad (35)$$

and the three parameters (η_t), (η_h) and (η_c) are the loss factors associated with the top-plate, the bottom-plate (the hull) and the compliant layer, respectively, (m_t), (h_t) and (ω_t), and (m_h), (h_h) and (ω_h) are the surface mass, thickness and critical frequency, respectively, associated with the top-plate and the bottom-plate (the hull), respectively, and (ω_o) is the resonance frequency associated with the surface stiffness of the compliant layer and the surface mass of the bottom-plate. Clearly, $\overline{Z}_b^{(2)}(\underset{\sim}{k},\omega)$ is derived from $\overline{Z}_b^{(1)}(\underset{\sim}{k},\omega)$ by merely setting the surface mass ratio (m_t / m_h) equal to zero; i.e., when (m_t / m_h) is equal to zero, the conditioning top-plate is essentially removed. In particular, from Eqs. (31) – (34), one obtains

$$\overline{Z}_b^{(1)}(0,\omega) = (i\omega\overline{m}_h)\,[(m_t / m_h)+(1+i\eta_c)\{1+i\eta_c)-(\omega/\omega_o)^2\}^{-1}]\,, \qquad (36a)$$

$$\overline{Z}_b^{(2)}(0,\omega) = i\omega\overline{m}_h\,(1+i\eta_c)\,\{(1+i\eta_c)-(\omega/\omega_o)^2\}^{-1}\,. \qquad (36b)$$

It is noted at this stage that although the model of the boundaries depicted herein are relatively simple, more elaborate and compounded boundaries may be readily introduced. In part, such an introduction may be used to render the model more realistic and in part to examine whether specific elaborations and complexities in the composition of the boundaries may be advantaged [3, 6, 7]. In this report, however, a limited scope is pursued. This scope is first to establish the lines of the analysis of the model and second to tackle questions that seem to have escaped direct and clear answers. Indeed, in many cases there appears to be a desire to conduct experiments to acquire some fundamental answers. However, if the experiments are to provide answers, one must acquire clear definition and understanding of the questions. In this report, definition and understanding of the questions are sought through rudimentary analysis and computations.

III. A Model for the Wavevector-Frequency Spectral Density of a Turbulent Boundary Layer (TBL)

One of the major contributors to the noise perceived by a transducer, that is placed near a boundary in the presence of flow, is due to the formation of a turbulent boundary layer (TBL). A (TBL) describes the instabilities that are generated in a fluid that flows (beyond a certain speed) over a boundary. These instabilities are usually confined to a narrow layer (thickness) adjacent to the boundary. The description of a (TBL) is usually given in terms of the pressure $P_{TBL}(\underset{\sim}{k},\omega)$ that is generated on the boundary on which it forms. One may approximately cast the description of this pressure in terms of its wavevector-frequency spectral density $\Phi_{TBL}(\underset{\sim}{k},\omega)$ so that

$$\langle P_{TBL}(\underset{\sim}{k},\omega)P_{TBL}(\underset{\sim}{k}',\omega')\rangle \;=\; \Phi_{TBL}(\underset{\sim}{k},\omega)\delta(\underset{\sim}{k}-\underset{\sim}{k}')\delta(\omega-\omega') \quad , \tag{37}$$

where the angular bracket indicates an appropriate averaging and $\delta(\underset{\sim}{k}-\underset{\sim}{k}')$ stands equal to $\delta(k_x-k_x')\delta(k_y-k_y')$. The functional form for the wavevector-frequency spectral density $\Phi_{TBL}(\underset{\sim}{k},\omega)$ for a (TBL) is here defined by

$$\Phi_{TBL}(\underset{\sim}{k},\omega) \;=\; A[U,(\delta/U)]\;\; a_1\;\; [(c/\omega)M]^2\;\; \Phi_{xy}(x,y,M)\;, \tag{38}$$

where (M) is the convective mach number $M=(U/C)$ and (U) is the convective speed, which is related to the free-stream speed (U_∞) in the form

$$U \;=\; f\,U_\infty\;; \qquad f\;<\;1\;; \qquad f\;\simeq\;0.6\;, \tag{39}$$

the thickness of the (TBL) is designated (δ), (a_1) is a constant and the function (A) is then explicitly expressed in the form

$$A[U,(\delta/U)] \;=\; [(1/2)\rho U^2]^2\;\;(\delta/U)\;, \tag{40}$$

and finally the variables (x) and (y) are, respectively and conveniently, defined

$$x = (k_x c/\omega)M \ , \qquad y = (k_y c/\omega)M \ . \tag{41a}$$

From Eqs. (39) and (40) one obtains

$$A[U,(\delta/U)] = (f)^3 \ A[U_\infty,(\delta/U_\infty)] \ . \tag{42}$$

It follows from Eqs. (38) and (42) that

$$\int d\underset{\sim}{k} \ \Phi_{TBL}(\underset{\sim}{k},\omega) = S_{TBL}(\omega) = A[U_\infty,(\delta/U_\infty)] \ (f)^3 a_1 S_{xy}(\omega,M) \ , \tag{43}$$

where

$$S_{xy}(\omega,M) = \int dx \int dy \ \Phi_{xy}(x,y,M) \ , \tag{44}$$

and it is imposed that

$$\Phi_{xy}(x,y,M) = [\Phi_{nx}(x,M)+\Phi_{cx}(x)] \ \Phi_{ny}(y) \ , \tag{45}$$

$$\Phi_{nx}(x,M) = M^2 \ [M^2+\alpha^4(1+|x|)^2]^{-1} \ , \tag{46a}$$

$$\Phi_{cx}(x) = [\{\alpha^2+(1-x)^2\}^{-1} - \{\alpha^2+(1+|x|)^2\}^{-1}] \ , \tag{46b}$$

$$\Phi_{ny}(x) = \beta^2[\beta^2+(x)^2]^{-1} \ . \tag{46c}$$

The nature of $\Phi_{xy}(x, y, M)$ as a function of (x) is depicted in Fig. 5 for three typical values of (M); $M = (5/3)x10^{-3}$, $M = (15/3)x10^{-3}$ and $M = (25/3)x10^{-3}$, with $x > 0$ and $y \rightarrow 0$. [$M = M_o = (15/3)x10^{-3}$ is considered to be the standard mach number. The standard mach number (M_o) is equivalently a 15 knots speed. When the mach number is not stated, it is assumed that the standard mach number (M_o) prevails.] The prominence of $\Phi_{xy}(x, y, M)$ in the range where $x \approx 1$ and its dependence on (M) when it levels in the range where (x) is small compared unity; $x \lesssim 10^{-3}$, is clearly exhibited in Fig. 5. The sonic point, in Fig. 5, is defined by $x = M$.

Experimental data suggest that [3, 6]

$$S_{TBL}(\omega) \{A[U_\infty, (\delta / U_\infty)]\}^{-1} = 2x10^{-5} . \tag{47a}$$

Calculations suggest that

$$S_{xy}(\omega, M) = 30 , \tag{47b}$$

as can be verified from Eq. (44), and Fig. 6. From Eqs. (39), (43) and (47), one deduces that

$$\Phi_{TBL}(\underset{\sim}{k}, \omega) = 3x10^{-6} \; A[U, (\delta / U)] \; [(c/\omega)M]^2 \; \Phi_{xy}(x, y, M) . \tag{48}$$

The wavevector-frequency spectral density $\Phi_{TBL}(\underset{\sim}{k}, \omega)$, as stated in Eq. (48), is taken as basic to the calculations that follow. Thus, the elemental equivalence becomes

$$\Phi_{TBL}(\underset{\sim}{k}, \omega) \; d\underset{\sim}{k} \equiv S_o(M/M_o) \; \Phi_{xy}(x, y, M) \; dx\, dy ;$$

$$S_o(M/M_o) = 2x10^{12}(M/M_o)^4 . \tag{49}$$

The quantity $\Phi_{TBL}(\underset{\sim}{k},\omega)d\underset{\sim}{k}$ is measured in units of $(\mu Pa)^2 / Hz$, where $M_o = 5\text{x}10^{-3}$, which corresponds to a 15 knots speed and then $(\delta / U) = 6.7\text{x}10^{-3}$ sec.

[Note: $10 \log_{10} 2x10^{12} \simeq 123$.]

Just as the normalization of the wavenumber (k_x) and (k_y) are cast in terms of (x) and (y), respectively, in Eq. (41a), it is convenient to cast the frequency variable (ω) in terms of the normalized frequency (Ω) such that

$$\Omega = (\omega \, \delta / U) \quad . \tag{41b}$$

The normalizing frequency (U / δ) is assumed to be a constant independent of the mach number (M).

IV. The Size Filtering Efficiency of a Transducer

The filtering efficiency $H(\underset{\sim}{k},\omega)$ of the transducer's size may be expressed in the form

$$H(\underset{\sim}{k},\omega) = \begin{cases} |2J_1(kr)/(kr)|^2 & , \quad (50a) \\ |[\sin(k_x L_x/2)\sin(k_y/2)][(k_x L_x/2)(k_y L_y/2)]^{-1}|^2 & , \quad (50b) \end{cases}$$

where Eq. (50a) pertains to a uniformly sensitive circular transducer of radius (r) and Eq. (50b) pertains to a uniformly sensitive rectangular transducer of $(L_x \cdot L_y)$ on the sides. Normalization of the variables alá Eq. (41) yields for Eq. (50) the form

$$H(x,y,\Omega) = \begin{cases} |2J_1[(x^2+y^2)^{1/2}(\gamma_r\Omega)]/[(x^2+y^2)^{1/2}(\gamma_r\Omega)]|^2 & , \quad (51a) \\ |[\sin(x\gamma_x\Omega)\sin(y\gamma_y\Omega)]/[(x\gamma_x\Omega)(y\gamma_y\Omega)]^{-1}|^2 & , \quad (51b) \end{cases}$$

where, again, (δ) is the (TBL) thickness and

$$\gamma_r = (r/\delta) \;\; ; \;\; \gamma_x = (L_x/2\delta) \text{ and } \gamma_y = (L_y/2\delta) \quad . \qquad (52)$$

In particular, for point transducers

$$H(x,y,\Omega) = 1 \quad . \qquad (53)$$

Also, since in this report (U/δ) is assumed to be a constant, it follows from Eq. (52) that

$$\gamma_\alpha(M) = \gamma_\alpha(M_o)(M_o/M) \quad , \qquad (54)$$

where (γ_α) is a typical normalized distance (length). This normalization renders (γ_α) a function of the mach number (M). A typical filtering efficiency of the transducer size is depicted in Fig. 7a. In this figure $H(x,y,\Omega)$, stated in Eq. (51b), is plotted as a function of (x), with

$y \to 0$, $\gamma_x = (1/2)$, and $M_o = M = 5x10^{-3}$, for three normalized frequencies (Ω); $\Omega = 1$, 10 and 100. [The *displayed* normalized frequency range in this report is $1 \leq \Omega \leq 10^3$, whereas the validity of the analysis can be hardly justified on either side of a normalized frequency range of $8 \leq \Omega \leq 400$. This latter range is designated the *relevant* normalized frequency range.] Also, note that $\gamma_x = (1/2)$ with $\delta = 2$ inches relates to a transducer of size $L_x = 2$ inches. A standard transducer's size is defined by $\gamma = \gamma_x = \gamma_y = (1/2)\ (M_o / M)$. Thus, a standard transducer is a square transducer. When the size of the transducer is not explicitly stated, it is assumed that the standard size just defined prevails.] Clearly, from Fig. 7a the filtering efficiency diminishes more pronouncedly at the higher frequencies. In the normalized wavenumber range depicted, at the lower frequency range, where $\Omega \lesssim 1$, the filtering efficiency due to size is largely equal to unity. One also observes that the diminishing in the filtering efficiency at the higher frequency range, where $\Omega \geq 10$, is accompanied by fluctuations in this quantity; the origin of these fluctuations is commonly recognized [6]. Anticipating that such fluctuations in the integrad will drive to grief the integrations to be performed, a way to mitigate these fluctuations, without interfering with the diminished filtering efficiency, must be devised. Thus, in subsequent calculations, Eq. (51b) is replaced by

$$H(x,y,\Omega) = \left| [(1-\exp(-|x\gamma_x\Omega|)(1-\exp(-|y\gamma_y\Omega|)] \right.$$

$$\left. [(x\gamma_x\Omega)(y\gamma_y\Omega)]^{-1} \right|^{-2} \qquad (51c)$$

The nature of $H(x,y,\Omega)$, as stated in Eq. (51c), is depicted in Fig. 7b; Fig. 7b is to be compared with Fig. 7a. Except for the fluctuations, that are purposely suppressed in Fig. 7b, the diminishing in the filtering efficiency with increase in the normalized frequency in the two figures are commensurate. As already mentioned, to ease the complications that the fluctuations in the integrad bring to the evaluation of the integrals, in subsequent calculations Eq. (51c) is used rather than Eq. (51b). In particular, the frequency spectral density $S_{TBL}(\Omega)$ for a largely point

transducer and $S^{H}_{TBL}(\Omega)$ for a square transducer of a standard size, given by $\gamma_x = \gamma_y = (1/2)\ (M_o / M)$, are computed and displayed in Fig. 8. In this figure $S_{TBL}(\Omega)$ and $S^{H}_{TBL}(\Omega)$ are explicitly defined by

$$S_{TBL}(\Omega) \ = \ 2x10^{12}(M/M_o)^4 \int \ \Phi_{xy}(x,y,M)\,dxdy \quad , \tag{55a}$$

$$S^{H}_{TBL}(\Omega) \ = \ 2x10^{12}(M/M_o)^4 \int \ H(x,y,\Omega)\Phi_{xy}(x,y,\Omega)dxdy \quad . \tag{55b}$$

[cf. Eqs. (44) and (49).] These normalized frequency spectral densities are evaluated for the standard mach number (M_o); $M_o = 5x10^{-3}$ and are plotted as functions of the normalized frequency (Ω). The size of the transducer is manifested, in Fig. 8, in that the frequency spectral density is diminishing at the higher normalized frequency (Ω). [Since the point transducer is small, but only approximating a point, at the higher normalized frequency (Ω) even in Fig. 8, a tinge of diminution exist in $S_{TBL}(\Omega)$. This diminution is due to a corresponding diminution caused by the *size* of the *point* transducer in the filtering efficiency in this higher range of the normalized frequency.] In Fig. 8 the normalized frequency range extends $1 \leq \Omega \leq 10^3$; this normalized frequency range is the *displayed* range.

V. Computations of the Passive Filtering Efficiencies of Ideal Boundaries for Pressure and Velocity Transducers

In this section typical passive filtering efficiencies are depicted. For the pressure transducer the filtering efficiency $\overline{C}_p(\underset{\sim}{k},\omega)$ is stated in Eq. (10) and for the velocity transducer the filtering efficiency $\overline{C}_v(\underset{\sim}{k},\omega)$ is stated in Eq. (20). Accompanying the filtering efficiencies are the respective sensitivities of the transducers to a unit normally incident pressure wave; the sensitivity $C_p(\omega)$ of the pressure transducer is stated in Eqs. (8b) and (12) and the sensitivity $C_v(\omega)$ of the velocity transducer is stated in Eqs. (18b) and (22). It is instructive to begin the computations and their interpretation using largely ideal boundaries [1-3]. An ideal boundary for the pressure transducer is a *rigid* boundary and for the velocity transducer is a *pressure release* boundary. To achieve these ideal conditions the surface impedance of the standard conditioning plate is artificially increased by a factor of 10^3. [The standard conditioning plate is a factor of $(1.61)^{-1}$ of the thickness of the plating of the hull.] This factor of 10^3, thus, largely renders the conditioning plate rigid. On the other hand, the compliant layer is endowed with a normalized resonance frequency (Ω_o) that is equal to 10^{-2}, which describes a boundary, such that in the absence of the conditioning plate, is largely pressure released. One remembers that (Ω_o) is the normalized resonance frequency between the surface stiffness of the compliant layer with the surface mass of the hull. [cf. Eq. (35) and it is noted that $\Omega_o = (\omega_o \delta / U)$.] The surface impedance of the hull remains intact in this artificial rendering of the ideal boundaries. Thus, the ideal boundaries are defined such that in the presence of a conditioning plate the surface impedance of the boundary is largely *rigid* and in the absence of a conditioning plate the surface impedance of the boundary is largely *pressure release*. [cf. Figs. 4a and 4b, respectively.] To render $\overline{C}_p(\underset{\sim}{k},\omega)$ and $\overline{C}_v(\underset{\sim}{k},\omega)$ compatible with the format assigned to the (TBL) in Eq. (49), via Eq. (41), the passive filtering efficiency of the transducers may be cast in the forms

$$\overline{C}_p(\underset{\sim}{k},\omega)\,H(\underset{\sim}{k},\omega) \rightarrow \begin{cases} \overline{C}_{1p}(x,y,\Omega) \quad , & \text{(56a)} \\ \overline{C}_{2p}(x,y,\Omega) \quad , & \text{(56b)} \end{cases}$$

$$\overline{C}_v(\underset{\sim}{k},\omega)\,H(\underset{\sim}{k},\omega)\rightarrow\begin{cases}\overline{C}_{1v}(x,y,\Omega) & , \quad (57a)\\ \overline{C}_{2v}(x,y,\Omega) & , \quad (57b)\end{cases}$$

where the subscript (1) pertains to a boundary in which a conditioning plate is present and the subscript (2) pertains to a corresponding boundary in the absence of a conditioning plate. The filtering efficiency of the transducer's size is included in these passive filtering efficiencies. [cf. Eq (51).] In this format, distances (lengths) are cast in the form

$$\overline{h}=(\gamma_h)(M\,\Omega)\quad;\quad \overline{d}=(\gamma_d)(M\,\Omega)\quad;\quad \overline{b}=(\gamma_b)(M\,\Omega)\quad, \qquad (58)$$

where $\gamma_h=(h/\delta)$; $\gamma_d=(d/\delta)$ and $\gamma_b=(b/\delta)$ and $(\overline{h})$, $(\overline{d})$ and $(\overline{d})$ are defined in Eq. (6) and a typical (γ_α) is defined in Eq. (54). Similarly, the sensitivities, to a unit of normally incident pressure wave, may be cast in the forms

$$C_p(\omega)\rightarrow\begin{cases}C_{1p}(\Omega) & , \quad (59a)\\ \quad ;\quad H(0,0,\Omega)=1 & \\ C_{2p}(\Omega) & , \quad (59b)\end{cases}$$

$$C_v(\omega)\rightarrow\begin{cases}C_{1v}(\Omega) & , \quad (60a)\\ \quad ;\quad H(0,0,\Omega)=1 & \\ C_{2v}(\Omega) & , \quad (60b)\end{cases}$$

respectively. In Fig. 9 the filtering efficiency of a standard blanket for which $\gamma_b=(1.5)\ (M_o/M)$ is depicted as a function of (x) with $y\rightarrow 0$ and for three values of the normalized frequency (Ω); $\Omega=1$, 10 and 100. Comparing Figs. 7 and 9 clearly shows that in

the higher normalized wavenumber range and the higher normalized frequency, a standard size transducer does less to reduce the passive filtering efficiency of the transducer than does the standard blanket. The blanket is the most effective reducer for the passive filtering efficiency of a transducer. For the ideal boundaries, Figs. 10-13 depict $\overline{C}_{1p}(x,y,\Omega)$, $\overline{C}_{2p}(x,y,\Omega)$, $\overline{C}_{1v}(x,y,\Omega)$ and $\overline{C}_{2v}(x,y,\Omega)$, respectively, as functions of the normalized wavenumber (x) for $y \rightarrow 0$ and for three values of the normalized frequency (Ω); $\Omega = 1$, 10 and 100. The range of (x) extends from (10^{-4}) to (10) with the sonic point at $(x = M)$. The corresponding sensitivities are depicted in pairs $\{C_{1p}(\Omega), C_{2p}(\Omega)\}$, $\{C_{1v}(\Omega), C_{2v}(\Omega)\}$ and $\{C_{2p}(\Omega), C_{2v}(\Omega)\}$ in Figs. 14-16, respectively. The sensitivities are cast in these figures as functions of (Ω) extending over the normalized frequency range $1 \leq \Omega \leq 10^3$. In particular, the following conditions are imposed in Figs. 10a-13a

$$M = M_o = 5x10^{-3} \ , \gamma_x = \gamma_y = \gamma = 10^{-3} \ , \ \gamma_d = 10^{-5} \ \text{and} \ \gamma_b = 10^{-5} \ , \quad (61a)$$

in Figs. 10b-13b

$$M = M_o = 5x10^{-3} \ ; \ \gamma_x = \gamma_y = \gamma = 10^{-3} \ ; \ \gamma_d = 10^{-5} \ \text{and} \ \gamma_b = 1.5 \ , \quad (61b)$$

in Figs. 10c-13c

$$M = M_o = 5x10^{-3} \ ; \ \gamma_x = \gamma_y = \gamma = (1/2) \ ; \ \gamma_d = 10^{-5} \ \text{and} \ \gamma_b = 10^{-5} \ , \quad (61c)$$

and in Figs. 10d-13d

$$M = M_o = 5x10^{-3} \ ; \ \gamma_x = \gamma_y = \gamma = (1/2) \ ; \ \gamma_d = 10^{-5} \ \text{and} \ \gamma_b = 1.5 \ . \quad (61d)$$

What are these figures saying? By and large, the (normalized) filtering efficiencies depicted in Figs. 10-13 are readily interpretable. For example, the (normalized) filtering efficiencies $\overline{C}_{2p}(x, y, \Omega)$ and $\overline{C}_{2v}(x, y, \Omega)$ are identical in Figs. 11 and 13. Thus a pressure release boundary turns a pressure transducer that lies close to the boundary into an *acting* velocity transducer. [Note: Remember that the filtering efficiency depicted in Figs. 10-13 are normalized quantities.] An adjunct information to the (normalized) filtering efficiencies is the information provided by the sensitivities. The corresponding sensitivities, as functions of the normalized frequency, are depicted in Figs. 14-16. First, it is realized that Figs. 14-16 cover all the cases depicted in Figs. 10-13. Also note that Figs. 14a and 14b are identical except for the ordinate scale. Clearly, then, although Figs. 11 and 13 are identical, the sensitivity relating to Fig. 11 is several orders of magnitude deficient compared with the sensitivity relating to Fig. 13. Thus, whereas a pressure transducer flush-mounted on an essentially pressure release boundary may exhibit an identical (normalized) filtering efficiency to that of a velocity transducer essentially flush-mounted on a corresponding pressure release boundary, the former transducer is disqualified on the basis of its sensitivity. This exemplifies the significance that the sensitivity information carries.

VI. Computations of the Frequency Spectral Densities Due to (TBL) on Ideal Boundaries

The filtering efficiencies $\overline{C}(x, y, \Omega)$ and the spectral density of (TBL) $\Phi_{xy}(x, y, M)$, on ideal boundaries that are defined in the preceding sections, are now used to evaluate the corresponding frequency spectral densities -- normalized outputs to (TBL). The frequency spectral densities -- the normalized outputs -- due to (TBL) on the ideal boundaries, as defined in the preceding section, are now evaluated. The corresponding frequency spectral densities due to (TBL) are derived from Eqs. (49), (56) and (57) in the forms

$$\left.\begin{matrix} S_{1p}(\Omega) \\ S_{2p}(\Omega) \\ S_{1v}(\Omega) \\ S_{2v}(\Omega) \end{matrix}\right\} = S_o(M/M_o)\int \Phi_{xy}(x, y, M)dxdy \begin{cases} \overline{C}_{1p}(x, y, \Omega) & , \quad (62a) \\ \overline{C}_{2p}(x, y, \Omega) & , \quad (62b) \\ \overline{C}_{1v}(x, y, \Omega) & , \quad (62c) \\ \overline{C}_{2v}(x, y, \Omega) & , \quad (62d) \end{cases}$$

where, again, the subscript (1) pertains to a boundary in which a conditioning plate is present, the subscript (2) pertains to a corresponding boundary in the absence of a conditioning plate and $S_o(M/M_o)$ is stated in Eq. (49). In Fig. 17, the pair $\{S_{1p}(\Omega), \quad S_{2v}(\Omega)\}$ is depicted as a function of the normalized frequency (Ω) extending over the normalized frequency range $1 \leq \Omega \leq 10^3$. Figures 17a-17d correspond to the conditions stated in Eqs. (61a)-(61d), respectively. Figures 11 and 13 suggest that on an essentially pressure release boundary, the filtering efficiency $\overline{C}_{2p}(x, y, \Omega)$ of a pressure transducer is largely the same as the filtering efficiency $\overline{C}_{2v}(x, y, \Omega)$ of a velocity transducer on a corresponding boundary and that this sameness is independent of any variations stated in Eqs. (61a)-(61d). Then, from Eqs. (62b) and (62d), it follows that on an ideal boundary $S_{2p}(\Omega)$ is correspondingly identical to $S_{2v}(\Omega)$. Therefore, the pair depicted in Fig. 17 may be cast in the form $\{S_{1p}(\Omega), \; S_{2p}(\Omega) \equiv S_{2v}(\Omega)\}$. The identity, in this essentially two-vector, is explicitly stated in this figure. To confirm this statement of identify, Fig. 18a is offered as an indirect proof and Fig. 18b as a direct proof. In Fig. 18a the pair $\{S_{1p}(\Omega), \; S_{2v}(\Omega)\}$ is depicted, as a function of the normalized frequency (Ω),

for the condition stated in Eq. (61a). This figure, when compared with Fig. 17a, establishes the identity of $S_{2p}(\Omega)$ and $S_{2v}(\Omega)$ for an ideal boundary. In Fig. 18b the pair $\{S_{2p}(\Omega),\ S_{2v}(\Omega)\}$ is depicted, as a function of the normalized frequency (Ω), for the condition stated in Eq. (61d). This figure exhibits clearly the sameness of the outputs to (TBL) of a pressure transducer and of a corresponding velocity transducer, both placed on essentially a pressure release boundary. This identity brings in a remarkable inquiry: When contemplating removal of the conditioning plate, why introduce a velocity transducer in the first place? Would not a pressure transducer do just as well? Again, the reason lies in the sensitivity; the sensitivity of the pressure transducer on a pressure release boundary is very poor. The corresponding sensitivities in the pair $\{C_{2p}(\Omega),\ C_{2v}(\Omega)\}$ are indicated in Fig.18c. [cf. Fig. 14a and b.] The sensitivities, as is again emphasized in this special example, play a major role in the design criteria of whether to employ pressure transducers or velocity transducers as the appropriate elements in an array.

Variations on the theme as depicted in Fig. 17, are now briefly considered. Figure 17d is repeated in Figs. 19 and 20, except that the (convective) mach number (M) is changed from the standard value of $5x10^{-3}$ to $(5/3)x10^{-3}$ and to $(25/3)x10^{-3}$, respectively. The major difference between Fig. 17d and Figs. 19 and 20 is manifested by the lower value of the normalized output to (TBL) in the first; i.e., as exhibited in Fig. 19, and the higher value of the normalized output to (TBL), in the second; i.e., as exhibited in Fig. 20. These results are to be expected; the proportionality is approximately $(M/M_o)^6$ at the higher normalized frequency, where the effect of the blanket is most pronounced in rejecting subsonic components. It is also noted that the normalized frequency in all the three figures, Figs. 17b, 19 and 20, is identical. This is in consequence of maintaining the invariability of the frequency normalizing factor (U/δ). [cf. Eq. (41b).]

It is emerging that if the options are: A pressure transducer on a rigid boundary or a velocity transducer on a pressure release boundary, the pressure transducer wins every time, see Figs. 16 and 18a. Although the sensitivity of both transducers, on their respective ideal boundaries, is the same, as shown in Fig. 16, the normalized output to (TBL) is worse in the

velocity transducer by some 50 dB, see Fig. 17a and 18a. As shown in Figs. 17b-d blankets and transducer's sizes may help bring the normalized outputs to (TBL) closer, but that help is mostly at the very high normalized frequency; see Figs. 17b, 19 and 20. Ideal boundaries, in each case, tend to reject the employment of velocity transducers as well as the employment of pressure transducers on an essentially pressure release boundary. [cf. Figs. 17a and 18a.]. As discussed in the two previous reports, the situation, indicating the overwhelming superiority of the pressure transducer on a conditioning plate over that of a velocity transducer without a conditioning plate, is not, however, desperate [1,2]. A relief may come if the boundary, in the absence of the conditioning plate, is stiff enough to accommodate a resonance condition between the surface stiffness of the compliant layer and the now adjacent surface mass of the fluid. In this connection, it is noted that the fluid possesses a surface mass for subsonic components only. One recalls that the influence of this resonance is to significantly subdue the filtering efficiency of the velocity transducer for subsonic components that lie above that resonance [1,2]. With the exception of a peak at that resonance, the filtering efficiency of a velocity transducer, above the resonance, may become more like that of a pressure transducer on an ideal conditioning plate [1,2]. That is fortunate, for the velocity transducer has a high normalized filtering efficiency for subsonic components and it becomes higher at the higher subsonic range. With respect to (TBL) this is not an unhappy circumstance. If the resonance can, on balance, curb the appetite of a velocity transducer to higher and higher subsonic components, the velocity transducer may stand a chance [1,2]. In this context and simultaneously, if the compliant layer is endowed with a finite surface stiffness, it may also render the pressure transducer more viable when the conditioning plate is removed. In this case, the normalized output to (TBL) $S_{2p}(\Omega)$ and the sensitivity $C_{2p}(\Omega)$ of the pressure transducer, on a compliant layer of finite surface stiffness, may no longer be as poor as indicated in Figs. 14, 17 and18. All these conjectures are briefly considered in subsequent sections. In particular, means to evaluate and interpret the various design proposals are to emerge. Also, an adjunct computer program for these purposes is being prepared under separate cover.

Before bestowing the compliant layer with a measure of surface stiffness, it may be in order to quantify some of the qualitative arguments just presented.

VII. Purpose and Criteria of Viability and Acceptability

A major consideration in this report relates to the desire to dispense with the conditioning plate. The conditioning plate is required, so goes the argument, to render the normalized outputs to (TBL) and the sensitivities of the flush-mounted transducers, that populate an array, *viable* and *acceptable*. Can the viability and the acceptability of a transducer mounted on a boundary be so quantified? Consulting Figs. 17, 19 and 20, one finds that in the displayed normalized frequency range a viable normalized noise output to (TBL) that is less than sea-state 0 to 2; i.e., the normalized frequency spectral density $S(\Omega)$ of the normalized output to (TBL) of a transducer must lie below a nominated criterion to qualify as viable. This kind of qualification is possible because of the normalization of the output to a unit normally incident pressure wave. Sea-state rating is similarly normalized. This nomination of viability is quantified as follows:

$$S(\Omega) \leq 10^{8} \quad , \tag{63}$$

where $S(\Omega)$ is as stated in Eq. (62). In stating these criteria of viability, a 20 dB gain between a transducer and an array is assumed in Eq. (63). Thus, from Fig. 17a neither the pressure transducer in the presence of an ideal conditioning plate nor the velocity transducer on an ideal pressure release boundary qualify as viable at any of the quoted mach numbers and in any portion of the normalized frequency defined in the range $1 \leq \Omega \leq 10^{3}$. Notwithstanding, as already discussed, the pressure transducer is superior to a velocity transducer in this case. [Again, one is reminded in this connection that the normalized output to (TBL) of a pressure transducer on an essentially pressure release boundary matches that of a velocity transducer on the same boundary as indicated in Figs. 17a, and 18a.] When the transducers are of a standard size, for which $\gamma = (1/2)\ (M_o / M)$, and are cladded by a standard blanket, for which $\gamma_b = (1.5)\ (M_o / M)$, the situation improves. This situation is depicted in Figs. 17d, 18b, 19, and 20. In the presence of a effective blanket; e.g., a standard blanket, and a standard transducer's size, $S(\Omega)$, as a function of the normalized frequency (Ω), for the standard mach

number (M_o); e.g., Fig. 17a, may account for the normalized output to (TBL) for the mach number (M) if its magnitude is multiplied by $(M/M_o)^6$ and the normalized frequency axis by (M/M_o); e.g., Figs. 19 and 20. In certain normalized frequency ranges the outputs to (TBL) are viable as follows: For a speed of 5 knots, for which the mach number (M) is equal to $(5/3)x10^{-3}$ one finds

$$\left.\begin{array}{r} S_{1p}(\Omega) \\ S_{2p}(\Omega)=S_{2v}(\Omega) \end{array}\right\} \lesssim 10^8 \quad \begin{array}{l} \text{in the range } 2\lesssim\Omega \ ; \\ \text{in the range } 7\lesssim\Omega \ , \end{array} \tag{64a}$$

for the standard speed of 15 knots, for which the mach number (M); $M=M_o$, is equal to $(15/3)x10^{-3}$ one finds

$$\left.\begin{array}{r} S_{1p}(\Omega) \\ S_{2p}(\Omega)=S_{2v}(\Omega) \end{array}\right\} \lesssim 10^8 \quad \begin{array}{l} \text{in the range } 13\lesssim\Omega \ ; \\ \text{in the range } 27\lesssim\Omega \ , \end{array} \tag{64b}$$

and for a speed of 25 knots, for which the mach number (M) is equal to $(25/3)x10^{-3}$, one finds

$$\left.\begin{array}{r} S_{1p}(\Omega) \\ S_{2p}(\Omega)=S_{2v}(\Omega) \end{array}\right\} \lesssim 10^8 \quad \begin{array}{l} \text{in the range } 35\lesssim\Omega \ ; \\ \text{in the range } 50\lesssim\Omega \ . \end{array} \tag{64c}$$

The normalized frequency (Ω) at which the viability of an array commences may be designated (Ω_+). This normalized frequency parameter is a function of the type of the array, the definition of the cladding, the size of the transducers and, of course, the mach number (M). Thus, for example, for array $(1p)$ and for $M=(5/3)x10^3$, $\Omega_+(1p)\simeq 2$, as stated in Eq. (64a) and for array $(2p)$ and array $(2v)$ and for $M=(15/3)x10^3$, $\Omega_+(2p)=\Omega_+(2v)\cong 13$, as stated in Eq. (64b), etc. However, when (Ω_+) is stated without a reference to an array, it invariably pertains to the initial normalized frequency of viability of array $(1p)$. Also, unless explicitly

stated the cladding, the size of the transducers and the convective mach number all are at their standard values. [Only minimal explicit use of (Ω_+) is made in this report.] Similarly, a sensitivity that is less than (10^{-1}) is to be considered unacceptable; i.e., the acceptability criterion for the sensitivity is nominated as follows:

$$C(\Omega) \gtrsim 10^{-1} \quad , \tag{65}$$

where the sensitivity $C(\Omega)$ is as stated in Eqs. (59) and (60). As Fig. 14 shows, the pressure transducer on an ideal conditioning plate is acceptable, whereas the pressure transducer on an ideal pressure release boundary is definitely not acceptable. In both cases this applies throughout the displayed normalized frequency range. As Fig. 15 shows, the velocity transducer on an ideal conditioning plate is far from being acceptable whereas the velocity transducer on an ideal pressure release boundary is acceptable. Again, in both cases this applies throughout the displayed normalized frequency range. The acceptability of the pressure transducer on an ideal conditioning plate and the velocity transducer on an ideal pressure release boundary is depicted in Fig. 16. Both cases are highly acceptable; the sensitivities of both are at the maximum value of four (4), signifying a pressure and a velocity doubling at the respective boundaries. On the other hand, as Figs. 15 and 18c show, a pressure transducer on an essentially pressure release boundary is not acceptable throughout the displayed normalized frequency range.

Again, before embarking on consideration of boundaries that are non-ideal, it may be useful to assess the anti-radiation, the specular reflection efficiency and the transference from the hull to the transducers via the compliant layer and the conditioning plate, when the latter is present. The assessment on the ideal boundaries, in these matters, is conducted briefly in the coming section.

VIII. Evaluations of the Filtering Efficiencies on the Ideal Boundaries Relating to Anti-Radiation, Reflections and Transferences from the Hull

These quantities are derived and stated in Eqs. (25), (27) and (31), respectively. Again, these quantities need to be expressed in terms of (x) for (k_x), (y) for (k_y) and (Ω) for (ω). These expressions are readily derived. The anti-radiation measures are shown in Figs. 21a and b. In Fig. 21a the ideal conditioning plate is present and $A_h^{(1)}(x, y, \Omega)$ is plotted as a function of the normalized wavenumber (x) with $y \to 0$ for three values of the normalized frequency (Ω), $\Omega = 1$, 10 and 100. In Fig. 21b the conditioning plate is absent exposing an ideal pressure release boundary and $A_h^{(2)}(x, y, \Omega)$ is plotted as a function of (x) with $y \to 0$ for three values of the normalized frequency (Ω); $\Omega = 1$, 10 and 100. The specular reflection efficiencies are shown in Figs. 22a and b. In Fig. 22a the ideal conditioning plate is present and $|R_{1p}(x, y, \Omega)|^2$ is plotted as a function of the normalized wavenumber (x) with $y \to 0$ for three values of the normalized frequency (Ω); $\Omega = 1$, 10 and 100. In Fig. 22b the conditioning plate is absent exposing an ideal pressure release boundary and $|R_{2p}(x, y, \Omega)|^2$ is plotted as a function of (x) with $y \to 0$ for three values of the normalized frequency (Ω); $\Omega = 1$, 10 and 100. Finally, the transferences from the hull onto the boundary are presented in Figs. 23a, b, c and d. In Figs. 23a and b the pair $\{T_{I1p}^p(x, y, \Omega),\ T_{I2p}^p(x, y, \Omega)\}$ is depicted as a function of (x) with $y \to 0$ for the three values of the normalized frequency (Ω); $\Omega = 1$, 10 and 100. The first element $T_{I1p}^p(x, y, \Omega)$ pertains to the transference of a force drive on the hull to a pressure on a boundary that accommodates an ideal conditioning plate, the second element $T_{I2p}^p(x, y, \Omega)$ is the same as the first except that the conditioning plate is removed, thereby, exposing an ideal pressure release boundary. In Figs. 23c and d the pair $\{T_{I1v}^v(x, y, \Omega),\ T_{I2v}^v(x, y, \Omega)\}$ is depicted as a function of the normalized wavenumber (x) with $y \to 0$ for three values of the normalized frequency (Ω); $\Omega = 1$, 10 and 100. The first element $T_{I1v}^v(x, y, \Omega)$ pertains to the transference of a velocity drive on the hull to a velocity on a boundary that accommodates an ideal conditioning plate. The second element $T_{I2v}^v(x, y, \Omega)$ is the same as the first except that the conditioning plate is removed, thereby, again, exposing an ideal pressure release boundary.

A brief interpretation of the result may be useful:

a. The anti-radiation quantity of $A_h^{(1)}(x, y, \Omega)$, as depicted in Fig. 21a, shows that the high compliance (low stiffness) of the compliant layer is beneficial, giving the boundary excellent anti-radiation property as may be expected. Similarly, $A_h^{(2)}(x, y, \Omega)$, as depicted in Fig. 21b, shows also an excellent anti-radiation property, again, on account of the high compliance (low stiffness) of the compliant layer. The relevance of the anti-radiation is confined to the supersonic range only, notwithstanding that a portion of the subsonic range is also displayed in Fig. 21.

b. The specular reflection efficiencies, depicted in Fig. 22, as may be expected, remain, in the supersonic range, largely equal to unity. Again, although the relevant range is the supersonic range, a portion of the subsonic range is also displayed in Fig. 22.

c. The transfer from the drive (force-like and velocity-like) on the hull to the ideal boundaries on which the transducers are placed are depicted in terms of the two-vectors $\{T_{I1p}^{p}(x, y, \Omega),\ T_{I1p}^{p}(x, y, \Omega),\}$ and $\{T_{I1v}^{v}(x, y, \Omega),\ T_{I2v}^{v}(x, y, \Omega)\}$, where the subscript (1) designates quantities in reference to a *rigid* conditioning plate and the subscript (2) designates quantities in reference to the removal of the conditioning plate, thereby, exposing essentially a *pressure release* boundary. These quantities are evaluated and displayed, as function of (x) with $y \rightarrow 0$ for three values of the normalized frequency (Ω); $\Omega = 1$, 10 and 100, in Fig. 23. In this figure, the relevant range is the entire normalized wavevector range; i.e., the supersonic as well as the subsonic range. [In this connection and in a passing, one is to remember that the subsonic noise induced by this transference is not controlled by a blanket placed above the boundary.] Due to the low stiffness (high compliance) of the compliant layer that separates the hull from the top surface of the boundary, in either case, with and without the conditioning plate, the transference is low and may be considered, by and large, to be insignificant.

IX. Computations of the Passive Filtering Efficiencies of Boundaries for Pressure and Velocity Transducers and Their Corresponding Normalized Outputs in Response to Turbulent Boundary Layer – Normalized Outputs to (TBL)

In order to simplify the analyses and discussions it may be conducive to treat here only three cases; the pressure transducer with and without the conditioning plate and the velocity transducer without the conditioning plate. The fourth case, of the velocity transducer with the conditioning plate, is not discarded, but is suppressed in subsequent consideration. In this manner, the question of removal of the conditioning plate remains paramount. Consideration of the velocity transducer in the presence of a conditioning plate is, hereby, deferred.

Although the ideal boundaries; either *rigid* or *pressure release* are instructive, one needs approach boundaries that are more commensurate with those that may be employed in practical situations. In this connection, the conditioning plate is apriori specified. The conditioning plate is of thickness which is a fraction $(1.61)^{-1}$ of the hull plating [6,7]. This conditioning plate is designated standard. [The standard thickness of the hull is set to be (1.61) inches [6,7].] This standard conditioning plate is used exclusively in subsequent consideration and computations in which a conditioning plate is employed. The variable in the composition of the boundary is then embodied in the surface stiffness of the compliant layer. [cf. Figs. 3 and 4.]

Can one find a compliant layer that is not commensurate with the pressure release condition that will render the output to (TBL) of a velocity transducer more like that of a pressure transducer? In the ideal boundaries' case the velocity transducer fares badly, on this account, compared with the pressure transducer; see Figs. 17, 18a, 19 and 20. It is noted, however, that in the ideal boundaries' case and in the range of the normalized frequency of interest, the sensitivities of the two distinct transducers are well nigh the same and are highly acceptable; see Fig. 16. The corresponding passive filtering efficiencies for these boundaries are depicted in Figs. 10-13. Examination of these figures together with Fig. 5, amply explains the character of the results shown in Fig. 17, 18a, 19 and 20.

The compliant layer is now given measures of surface stiffness. For the purposes of this report the surface stiffness is defined in terms of a normalized frequency dependent resonance frequency, in the manner

$$\Omega_o^o(\Omega,\Omega_s,\Omega^o) = (\Omega^o)[\Omega(\Omega+\Omega_s)^{-1}] \quad , \tag{66}$$

where (Ω_s) and (Ω^o) are parameters to be specified. Thus, a compliant layer that is defined by (Ω_s) that is essentially equal to zero may be referred to as having ten (10), thirty (30) and one hundred (100) measures of surface stiffness defined by a constant normalized frequency (Ω^o) that is equal to these measures. The surface stiffness measure (Ω_o^o) so defined, is independent of the normalized frequency. These are expressed in the respective forms

$$\Omega_o^o = \begin{cases} 10 \\ 30 \\ 100 \end{cases} \; ; \; \Omega^o = \begin{cases} 10 \\ 30 \\ 100 \end{cases} \; ; \; \Omega_s = 10^{-10} \; ; \; \begin{aligned} \Omega_o &= 10 \quad , \quad (67a) \\ \Omega_o &= 30 \quad , \quad (67b) \\ \Omega_o &= 100 \quad . \quad (67c) \end{aligned}$$

In addition, three more measures of surface stiffness are defined in this report for analytical and computational purposes. These definitions of surface stiffness measures (Ω_o^o) are dependent on the normalized frequency. These are expressed in the respective forms

$$\Omega_o^o = \begin{cases} \Omega_o^o\ (\Omega,\ 25,\ 30) \; ; \; \Omega_o = 5 \quad , \quad (67d) \\ \Omega_o^o\ (\Omega,\ 25,\ 70) \; ; \; \Omega_o = 50 \quad , \quad (67e) \\ \Omega_o^o\ (\Omega,\ 5,\ 70) \; ; \; \Omega_o = 65 \quad . \quad (67f) \end{cases}$$

The measure of surface stiffness (Ω_o^o), as a function of the normalized frequency (Ω), for the cases stated in Eqs. (67b) and (67 d-f) are depicted in Fig. 24. In this figure, in addition, a measure of a surface stiffness such that $\Omega_s = 0$ and $\Omega^o = \Omega$, is represented by the dashed curve. Then, each intersection of the solid curves, in Fig. 24, with the dashed curve, define, for a

condition specified in Eq. (67), a normalized resonance frequency (Ω_o). [cf. Appendix.] The resonance is between the surface impedance of the compliant layer and the surface impedance of the plating of the hull for a negligible normalized wavenumber; namely, $(x^2 + y^2)^{1/2} << (M)$. This wavenumber is commensurate with that defining a normally incident pressure wave. Since these surface impedances enter in parallel to yield the boundary surface impedance, in the normalized frequency range defined by $\Omega < \Omega_o$, the resulting surface impedance is surface mass control, in the region $\Omega \approx \Omega_o$, it is surface resistance control and in the range $\Omega > \Omega_o$, it is surface stiffness control. [It is adopted in the report that a normalized frequency range, defined by $\Omega < \Omega_o$, refers to a *range* that lies an octave or two below (Ω_o). It is further adopted that a normalized frequency range, defined by $\Omega > \Omega_o$, refers to *range* that that lies an octave or two *above* (Ω_o). Finally it is adopted that a normalized frequency region, defined by $\Omega \approx \Omega_o$, refers to a *region* that spans the range from an octave or two *below* (Ω_o) to an octave or two *above* (Ω_o).] When the conditioning plate is present, the surface impedance of the boundary entertains, in addition, the surface impedance of the conditioning plate. [cf. Eq. (28) and Figs. 3 and 4.] With this scheme in mind, much of the values for the sensitivities, as functions of the normalized frequency, for the three transducer types here considered, may be deciphered and explained.

Consideration in this section focuses on a compliant layer that is given ten (10) measures of surface stiffness. This case is defined in Eq. (67a). Again, one is reminded that now a standard conditioning plate is in place when a conditioning plate is employed. Since the passive filtering efficiencies of a pressure transducer and a velocity transducer are affected equally by the size of the transducer and the blanket, it may be of interest, initially, to compare the raw filtering efficiencies of these two types of transducers. For this purpose the filtering efficiencies $\overline{C}_{1p}(x, y, \Omega)$, $\overline{C}_{2p}(x, y, \Omega)$, and $\overline{C}_{2v}(x, y, \Omega)$ stated in Eqs. (56a), (56b) and (57b) are depicted in Figs. 25 a–c as functions of (x) with $y \rightarrow 0$ for three values of the normalized frequency (Ω); $\Omega = 1$, 10 and 100. In these figures Eq. (61a) is imposed; namely, the transducers are flush-mounted and are largely of point size and the blanket is absent. [cf. Figs. 10 a-d.] The

corresponding sensitivities of the transducers, as functions of the normalized frequency (Ω), are depicted in Figs. 26a and b. [cf. Figs. 14-16.] A few observations are emerging:

1. In the normalized frequency ranged defined by $\Omega < \Omega_o = 10$, the filtering efficiencies in Figs. 25a and b are about the same. Then, in this range, where the surface stiffness is higher than linear, the normalized outputs to (TBL) $S_{1p}(\Omega)$ and $S_{2p}(\Omega)$ of a pressure transducer with and without a standard conditioning plate, respectively, must be largely the same. This observation is substantiated in Fig. 27a. [In this figure the normalized outputs, $S_{1p}(\Omega)$ and $S_{2p}(\Omega)$ of a pressure transducer, with and without a conditioning plate, and $S_{2v}(\Omega)$ of a velocity transducer, without the conditioning plate, are depicted as functions of the normalized frequency (Ω)]. Also, in this lower normalized frequency range, Fig. 26a shows that the sensitivities $C_{1p}(\Omega)$ and $C_{2p}(\Omega)$ are largely the same, and, naturally, with $C_{1p}(\Omega) > C_{2p}(\Omega)$. However, both $C_{1p}(\Omega)$ and $C_{2p}(\Omega)$ are unacceptable in the normalized frequency range an octave or two below the normalized resonance frequency. On the other hand, in this lower normalized frequency range, the filtering efficiency in Fig. 25c is lower, especially in the subsonic range, than the corresponding filtering efficiencies in Figs. 25a and b. Again, this observation is substantiated in Fig. 27a. Moreover, and significantly, in this lower normalized frequency range, the sensitivity $C_{2v}(\Omega)$ is largely at its maximum value of four (4); see Fig.26b.

2. In the normalized frequency region, where $\Omega \approx \Omega_o = 10$, the surface stiffness, as given by (Ω_o^o), is about linear in (Ω). Figures 25 a-c shows that whereas the filtering efficiency $\overline{C}_{1p}(x,0,10)$ and $\overline{C}_{2p}(x,0,10)$ are nearly the same in the subsonic range, $\overline{C}_{2v}(x,0,10)$ is higher in this subsonic range. This is confirmed, after performing the integrations, in Fig. 27a; i.e., in this region $S_{1p}(\Omega) \approx S_{2p}(\Omega)$ but $S_{2v}(\Omega)$ is slightly higher. In particular, it is observed that localized peaks in the outputs to (TBL) occur in this region of the normalized frequency. These peaks occur where valleys occur in the corresponding sensitivities. Indeed, the normalized output $S_{2p}(\Omega)$ of the pressure transducer in the absence of a conditioning plate, does not exhibit a localized peak at any of the normalized frequency in Fig. 27a. The corresponding sensitivity

$C_{2p}(\Omega)$ is valleyless as exhibited in Fig. 26a or 28a. Figure 28a is a composite of Fig. 26a and b; Fig. 28a is more compatible with Fig. 27a.

3. At the higher normalized frequency range, where $\Omega > \Omega_o = 10$, a comparison between Figs. 25a and 25b reveals that the pressure transducer on a standard conditioning plate registers less normalized output to (TBL) then it does in the absence of that plate. This revelation is again confirmed in Fig. 27a. Worse yet, at this higher normalized frequency range, Fig. 26a indicates that the sensitivity $C_{2p}(\Omega)$ of the pressure transducer in the absence of the conditioning plate is significantly less than the sensitivity $C_{1p}(\Omega)$ in the presence of the standard conditioning plate; the latter reaching its maximum value of four (4) and the former becoming unacceptable at a normalized frequency that exceeds the normalized resonance frequency by an octave or two. Thus, at this higher normalized frequency range; $\Omega > \Omega_o = 10$ for a pressure transducer, the conditioning plate plays a major role; in this range, a conditioning plate is essential for a pressure transducer. At this higher normalized frequency range a comparison between Figs. 25b and 25c reveals that the pressure transducer and the velocity transducer without the conditioning plate register largely identical outputs to (TBL). This is confirmed in Fig. 27a. Indeed, an octave or two past the normalized resonance frequency, the outputs to (TBL) and the sensitivities of all three transducer types gradually commence a reversion to values they sustained on the ideal boundaries as displayed in Figs. 14-16, 17a and 18a, respectively. For example, the identity between the normalized outputs to (TBL) $S_{2p}(\Omega)$ and $S_{2v}(\Omega)$ in Fig. 27a, commences and is sustained as soon as (Ω) is an octave or two past (Ω_o). Also, the sensitivities $C_{1p}(\Omega)$ and $C_{2v}(\Omega)$ in Fig. 28a are both acceptable and are improving with increase in the normalized frequency (Ω), but $C_{2p}(\Omega)$ in Fig. 28a deteriorates, becoming unacceptable an octave or two past (Ω_o). [Figs. 14-16, 17a and 18a.]

Restating, in the lower normalized frequency range defined by $\Omega < \Omega_o = 10$, the resonance between the surface stiffness of the compliant layer and the surface mass of the fluid is an effective device that significantly subdues the normalized output to (TBL) of a velocity transducer, so much so that, in this range, this transducer becomes superior (including the

sensitivity) to a pressure transducer with and without a standard conditioning plate [1,2]. Moreover, in this lower range of the normalized frequency, apparently the ten (10) measures of surface stiffness renders identical the pressure transducers with and without the standard conditioning plate. In the higher normalized frequency range, where $\Omega > \Omega_o = 10$, the pressure transducer on a standard conditioning plate gradually recovers the superiority it had when the boundaries were ideal; see Figs. 14-16, 17a and 18a. Nonetheless, although the sensitivities in some of the normalized frequency ranges may qualify as acceptable, in Fig. 27a none of the normalized outputs qualify as viable. In this case then introduction of a blanket becomes essential.

Can a blanket help? One is reminded first that the blanket does not influence the sensitivity of any type of transducers i.e., Figs. 26 and 28a remain intact when a blanket is introduced. Second, the influence of a standard blanket on the output to (TBL) exceeds, by far, that of a standard size transducer. The influence of a standard blanket; $\gamma_b = (1.5)(M / M_o)$, on the raw filtering efficiencies is depicted in Figs. 29 a-c, these figures are to be compared, respectively, with Figs. 25 a-c, in which the blanket is absent. The *equalizing* influence of the blanket on the filtering efficiencies is clearly deciphered in this comparison of the two sets of figures; the blanket reduces the filtering efficiency at the higher normalized wavenumber range where the differences among the pressure transducer, with and without the conditioning plate, and the velocity transducer, without the conditioning plate, are the more pronounced. The equalizing influence of the blanket is confirmed in Fig. 30a. Thus, for example, in the lower normalized frequency range defined by $\Omega < \Omega_o = 10$, the superiority of the normalized output to (TBL) $S_{2v}(\Omega)$ of the velocity transducers (without the conditioning plate) in Fig. 27a is reduced, but is not eliminated in Fig. 30a. In the higher normalized frequency range; $\Omega > \Omega_o = 10$, the superiority of the output to (TBL) $S_{1p}(\Omega)$ over $S_{2p}(\Omega)$ and $S_{2v}(\Omega)$ in Fig. 27a is reduced, but, again, is not eliminated in Fig. 30a. Also, in this higher range, the identity of $S_{2p}(\Omega)$ and $S_{2v}(\Omega)$ in Fig. 27a is not eliminated in Fig. 30a. In the region defined by $\Omega \approx \Omega_o = 10$, the

mixture and localized peaks in the values of the normalized outputs in Fig. 27a, remain largely intact in Fig. 30a.

The viabilities and acceptabilities of the pressure transducer, with and without a conditioning plate and the velocity transducer, without a conditioning plate, are sketched in Figs. 31 a-c, respectively. In these figures the standard conditions prevail and the compliant layer is defined by ten (10) measures of surface stiffness. The design criteria emerges in Figs. 31 a-c with the following interpretations:

1. Provided a standard blanket is incorporated, there exist regions in the normalized frequency domain in which arrays, of standard pressure transducers (with and without a conditioning plate) and of standard velocity transducers (without a conditioning plate), are both, viable and acceptable. A viable and acceptable region is designated a positive region. However, there are regions that are neither viable nor acceptable – these are negative regions. Positive and negative regions for one type of transducers do not necessarily completely overlap with those of another.

2. In details, the normalized outputs to (TBL) by arrays of transducers without the conditioning plate; see Figs. 31b and c, are about 20 dB higher in positive regions than the normalized output to (TBL) of an array of pressure transducers on a standard conditioning plate. This may be reason enough to consider the array of pressure transducers on a standard conditioning plate preferred. However and clearly, in the low normalized frequency range, where $\Omega < \Omega_o = 10$, the array of velocity transducers is acceptable whereas that of pressure transducers is not.

Encouraged by the results just analyzed, two questions may be posed: Can a compliant layer with a higher surface stiffness; e.g., thirty (30), or even one hundred (100), measures of surface stiffness instead of ten (10), improve the situation further in favor of dispensing with the conditioning plate? Can this dispensation be achieved without paying a significant penalty in increased normalized outputs to (TBL)?

X. Normalized Outputs to (TBL) Introducing a Compliant Layer of Thirty (30) and One Hundred (100) Measures of Surface Stiffness

When the compliant layer is stiffened from ten (10) measures of surface stiffness to thirty (30) measures, the results displayed in Figs. 27a, 28a, 30a and 31 are changed to those displayed in Figs. 27b, 28b, 30b and 32, respectively. With respect to dispensing of the conditioning plate the situations is, indeed, improved. By and large, the modification to the first set of figures, which generate the second, can be accounted for largely by the change in the normalized resonance frequency (Ω_o) from (10) to (30). Except for a minor reversal in the normalized frequency range defined by $25 \lesssim \Omega \lesssim 40$ the array incorporating velocity transducers (without a conditioning plate) is as good or better than the array incorporating pressure transducers on a standard conditioning plate. Moreover, in this normalized frequency range and in the immediate margins of this range; i.e., in the range defined by $10 \lesssim \Omega \lesssim 80$, an array incorporating pressure transducers with and without the conditioning plate are essentially on par with respect to the noise due to (TBL). Be that so, one may dispense with the conditioning plate and use an array of pressure transducers to supplement an array of velocity transducers in this limited range. In any case, supporting an array incorporating pressure transducers as well as velocity transducers, both without a conditioning plate may be advantageous; a well conceived duplication of this kind may be advised. In this way *intensity* measurements, in which the pressure and the velocity are combined to yield an output, may be afforded. This kind of signal processing, to minimize noise, may be promising. Clearly, this example indicated that design concepts and criteria are, thereby, emerging [8].

How far can one stiffen the compliant coating and derive further improvement? For this purpose results relating to a compliant layer that is given one hundred (100) measures of surface stiffness are displayed in Figs. 27c, 28c; 30c, and 33. These figures are to be compared with those displayed in Figs. 27a, 28a, 30a and 31 and in Figs. 27b, 28b, 30b and 32, respectively. If the displays in Figs. 27b, 28b, 30b and 32 show improvement over those in Figs. 27a, 28a, 30a and 31, then one may claim, although not with the same vigor, that Figs. 27c, 28c, 30c and 32

show improvement over those in Figs. 27b, 28b 30b and 32. However, the weakness in the normalized frequency range defined by $25 \lesssim \Omega \lesssim 40$ and exhibited for a surface stiffness of thirty (30) measures, is now shifted and broadened for a surface stiffness of one hundred (100) to the normalized frequency range defined by $70 \lesssim \Omega \lesssim 150$. In this frequency range the sensitivity of the velocity transducer (without the conditioning plate) is hardly acceptable. In this sense, some of the deterioration may be attributed to the excessive surface stiffness.

Again, an array comprised of velocity transducers and pressure transducers, without a conditioning plate, is suggested. In the low frequency range, now defined by $\Omega \lesssim 40$, an array of velocity transducer is superior by a significant amount. In the remaining range, defined by $\Omega \gtrsim 40$, the normalized outputs to (TBL) of an array of pressure transducers matches that of an array of velocity transducers. As already hinted in the range defined by $70 \lesssim \Omega \lesssim 150$, the sensitivity of an array incorporating velocity transducers may exhibit a serious weakness. This weakness is caused by the resonance in the parallel combinations of the surface impedance of the hull and the surface stiffness of the compliant layer. Figure 33 shows that this weakness can be covered by an array incorporating pressure transducers that are directly placed on the compliant layer; a conditioning plate is not necessary for this cover.

XI. Normalized Outputs to (TBL) with Compliant Layers Possessing Normalized Frequency Dependent Surface Stiffnesses

In the relevant normalized frequency range, defined by $10 \lesssim \Omega \lesssim 10^3$, most compliant layers exhibit dependence on this normalized frequency. Moreover, this dependence is usually of the type displayed in Fig. 24 and specified in Eqs. (67d) – (67f). These three different forms are artificially selected for demonstration purposes; there is no effort made to trace an actual form. Also, usually the loss factor in the compliant layer is normalized frequency dependent. Again, there is no effort made to trace an actual dependence of this kind with respect to this quantity.

Considerations in this report are limited to simple models; they are meant merely to serve as precursors for the design of practical planar arrays. In this aim, computations similar to those displayed in Figs. 27, 28 and 30 for the three cases stated in Eqs. 67a-c are now conducted for the three cases stated in Eqs. 67d-f. These computations are displayed in Figs. 34-36, respectively; i.e., in Figs 34a-36a, the case stated in Eq. (67d) is displayed, in Figs. 34b-36b, the case stated in Eq. (67e) is displayed and in Figs. 34c-36c, the case stated in Eq. (67f) is displayed. The normalized resonance frequency (Ω_o) for these three cases are stated in Eq. (67). As previously stated and deployed, the normalized resonance frequency (Ω_o) is pivotal to defining the lower normalized frequency range, the normalized frequency region and the higher normalized frequency range, respectively. In Figs. 37 and 38 variations on Fig. 36c are displayed analogously to Figs. 19 and 20 with respect to Fig. 17d, respectively. Thus, the mach number (M), that is the standard mach number (M_o); $M_o = (15/3)x10^{-3}$, in Fig. 36c, is changed to $M = (5/3)x10^{-3}$ and to $M = (25/3)x10^{-3}$ in Figs. 37 and 38, respectively. [cf. Fig. 17d and Figs. 19 and 20.] The positive-negative regions on the viability-acceptability plane for these three cases are depicted in Figs. 39-41, respectively, [cf. Figs 31-33.] The positive-negative regions on the viability-acceptability plane, based on Figs. 37 and 38, are depicted in Figs. 42 and 43, respectively. There are some variations from one case to another in the displayed data in Figs.

34-36. Indeed, these variations together with the data depicted in Figs. 27, 28 and 30 indicate how to design a more agreeable array by modifying the surface stiffness of the compliant layer. This rough-brush approach is meant to remind the reader that the rudimentary analysis employed herein may, at best, indicate trends rather than dictate precise design criteria. Some indication of speed dependence is also considered; e.g., in Figs. 37 and 38. In particular and again, if the conditioning plate is to be dispensed with, on the basis of Figs. 39-43, as on the basis of Figs. 31-33, support is given to the idea of designing an array comprised of velocity transducers as well as pressure transducers. This idea is proposed not only for supplemental and complemental uses, but also to bring to bear quadratic processings that may enhance considerably the signal-to-noise ratios issued by the planar arrays. Some aspects of these remarks are discussed briefly in the Appendix [8].

XII. Influence of Non-Ideal Boundaries on the Anti-Radiation, Reflections and Transmission from the Hull.

The filtering efficiencies on ideal boundaries relating to these properties are discussed and assessed in Section VIII. This assessment is reported in Figs. 21-23. How are these properties modified by the introduction of a standard conditioning plate and by assigning a surface stiffness to the compliant layer. The presence of the conditioning plate is indicated by subscript (or superscript) (1) and the absence of the conditioning plate is indicated by (2). [cf. Figs. 21-23.]

The filtering efficiencies on ideal boundaries, as assessed by Figs 21-23, indicated that the anti-radiation properties are excellent. The absolute square values of the reflection coefficients, as expected, are unity and the hull transfer functions are low so that very little is transferred from the hull to the boundary on which the array of transducers are placed. When the news under ideal conditions is too good to be true, deviations from these ideal conditions may spell bad news. The question is, how bad is the news? After all, the excellent isolation provided by a negligible surface stiffness is largely gone when the surface stiffness is made finite.

The standard conditioning plate is used and the compliant layer is assigned ten (10) measures of surface stiffness. How are Figs. 21-23 modified? The modification is depicted in Figs. 44-46, respectively. At the low range of the normalized frequency the news, depicted in Fig. 44, is not good. Not only are the anti-radiation properties significantly diminished, but a resonance amplification, by a few dBs, occurs in the normalized frequency region, where $\Omega = \Omega_o = 10$; e.g., throughout the relevant supersonic range, $A_h^{(1)}(x,0,10)$ and $A_h^{(2)}(x,0,10)$ are a factor equal to three (3). In the higher normalized frequency range, the news is better; e.g., for the normalized frequency (Ω) at (100), $A_h^{(1)}(x,0,100)$ and $A_h^{(2)}(x,0,100)$ are a factor better than (10^{-3}), which is an adequate reduction to be called "anti-radiation," i.e., the cladding is beneficial as an anti-radiation device. The news depicted in Fig. 45 is good on balance. In the low and high normalized frequency ranges, the absolute square values of the reflection

coefficients remain unchanged at unity. However, at the normalized resonance frequency region, where $\Omega \simeq \Omega_o = 10$, the absolute square values of the reflection coefficients is low by at least an order of magnitude from unity, indicating, thereby, that an absorption of the incident wave is taking place. This is a resonance absorption that occurs in the range of the normalized frequency where the radiation is amplified by the same resonance [5]. The news depicted in Fig. 46 is that the very low transferences depicted in Fig. 23 are no longer found in the former figure. Again, the news in the lower normalized frequency range; e.g., where $\Omega \lesssim \Omega_o = 10$, is worse than in the higher range; e.g., where $\Omega \gtrsim \Omega_o = 10$. Increasing the surface stiffness measures simply shifts the lower normalized frequency range higher, since the normalized resonance frequency (Ω_o) increases, as stated in Eq. (67). This is evidenced by comparing Figs. 44-46 with Figs. 47–49. In the latter set of figures, the surface stiffness measure is thirty (30). [cf. Eq. (67b).] These shifts are not good news if the array is meant to operate in the lower normalized frequency range defined by $\Omega \lesssim \Omega_o$. Can a normalized frequency dependent surface stiffness; e.g., as defined in Eqs. 67d and e and displayed in Fig. 24 help the situation by providing less surface stiffness at the lower normalized frequency range? The answer to this inquiry is presented, in part, in Figs. 50–52. In this set of figures the surface stiffness is as specified in Eq. (67e). Comparing these two sets of figures with those presented in Figs. 44-52 show some promise in preventing some of the resonance amplifications, but hardly providing beneficial qualities to the cladding. It should be mentioned that the introduction of a blanket, that is so effective in reducing the normalized outputs of the transducers to (TBL), is, within the context of the present analysis, of no use to the anti-radiation, the stealth and transference from the hull. These properties are hardly influenced by the presence of the type of a blanket herein considered. [The blanket, defined in the analysis pursued in this report, is the so called (ρc)-blanket, where (ρc) is the characteristic impedance of the fluid.]

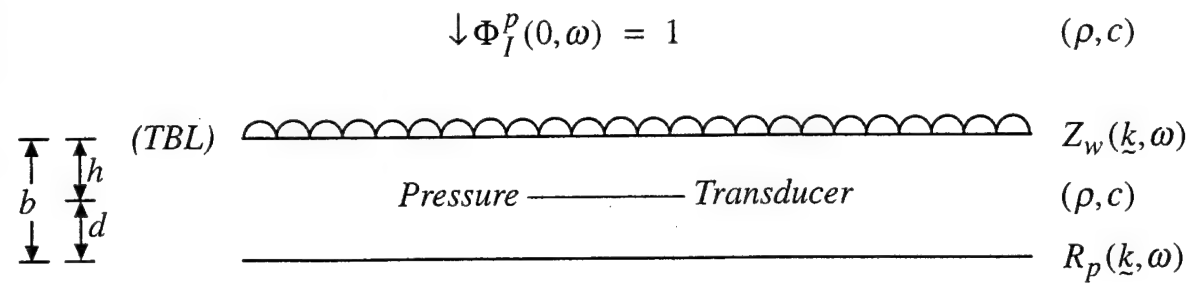

$$C_p(\underset{\sim}{k},\omega) = \left|\exp(-ihk_3)\ \{1+R_p(\underset{\sim}{k},\omega)\ \exp(-2idk_3)\}\right|^2$$

$$\Phi_{pI}(0,\omega) = \left|\{1+R_p(0,\omega)\ \exp(-2i\bar{d})\}\right|^2\ \Phi_p^I(0,\omega)\ ;\ \bar{d} = (\omega/c)d$$

a

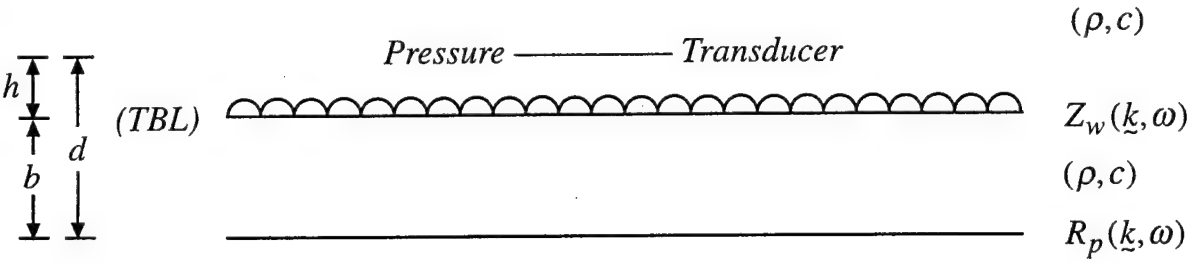

$$C_p(\underset{\sim}{k},\omega) = \left|\exp(-ihk_3)\ \{1+R_p(\underset{\sim}{k},\omega)\ \exp(-2ibk_3)\}\right|^2$$

$$\Phi_{pI}(0,\omega) = \left|\{1+R_p(0,\omega)\ \exp(-2i\bar{d})\}\right|^2\ \Phi_p^I(0,\omega)\ ;\ \bar{d} = (\omega/c)d$$

$$R_p(\underset{\sim}{k},\omega) = [Z_b(\underset{\sim}{k},\omega) - Z_w(\underset{\sim}{k},\omega)]\ [Z_b(\underset{\sim}{k},\omega) + Z_w(\underset{\sim}{k},\omega)]^{-1}$$

b

Fig 1. Cladding and configuration of a pressure transducer above the boundary which reflection coefficient $R_p(\underset{\sim}{k},\omega)$ is specified. $Z_b(\underset{\sim}{k},\omega)$ is the boundary surface impedance and $Z_w(\underset{\sim}{k},\omega)$ is the fluid surface impedance.

a. Pressure transducer is placed below the plane on which the (TBL) forms and the formalism thereof.

b. Pressure transducer is placed above the plane on which the (TBL) forms and the formalism thereof.

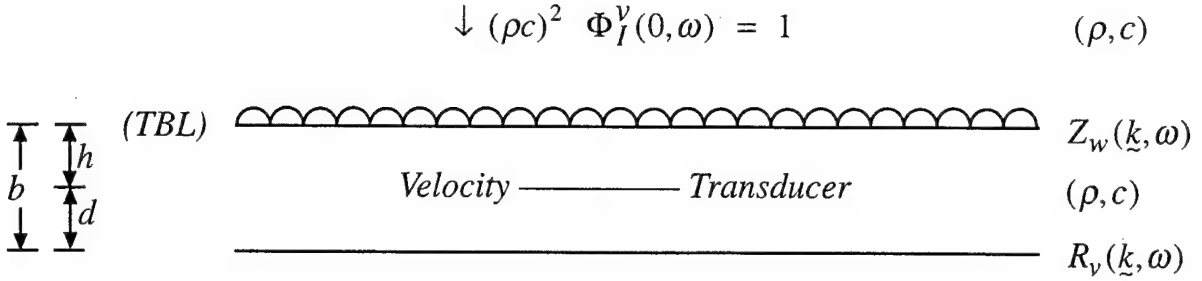

$$C_v(\underset{\sim}{k},\omega) = \left|\exp(-ihk_3)\ \{1+R_v(\underset{\sim}{k},\omega)\ \exp(-2idk_3)\}\right|^2$$

$$\Phi_{vI}(0,\omega) = \left|\{1+R_p(0,\omega)\ \exp(-2i\bar{d})\}\right|^2\ \Phi_I^v(0,\omega)\ ;\ \bar{d} = (\omega/c)d$$

$$\Phi_v(0,\omega) = C_v(\underset{\sim}{k},\omega)\left|\bar{k}_3\right|^2\ \Phi_I^v(0,\omega)$$

a

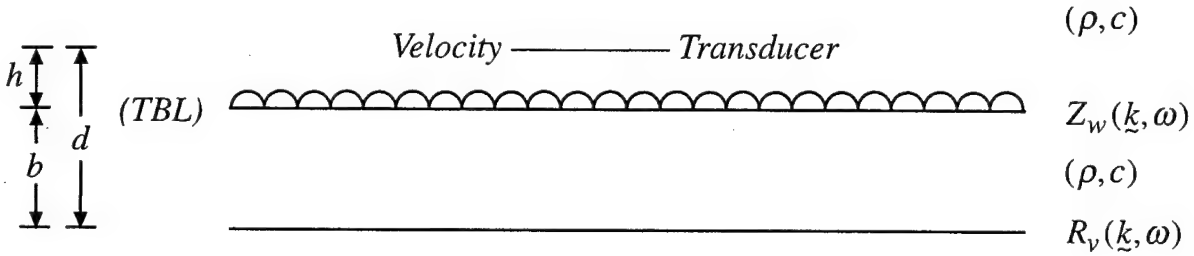

$$C_v(\underset{\sim}{k},\omega) = \left|\exp(-ihk_3)\ \{1+R_v(\underset{\sim}{k},\omega)\ \exp(-2ibk_3)\}\right|^2$$

$$\Phi_{vI}(0,\omega) = \left|\{1+R_p(0,\omega)\ \exp(-2i\bar{d})\}\right|^2\ \Phi_I^v(0,\omega)\ ;\ \bar{d} = (\omega/c)d$$

$$R_v(\underset{\sim}{k},\omega) = -R_p(\underset{\sim}{k},\omega)$$

$$\Phi_I^p(0,\omega) = (\rho c)^2\ \Phi_I^v(0,\omega)$$

b

Fig. 2. Cladding and configuration of a velocity transducer above the boundary which reflection coefficient $R_v(\underset{\sim}{k},\omega)$ is specified. $Z_b(\underset{\sim}{k},\omega)$ is the boundary surface impedance and $Z_w(\underset{\sim}{k},\omega)$ is the surface impedance of the fluid.

a. Velocity transducer is placed below the plane on which the (TBL) forms and the formalism thereof.

b. Velocity transducer is placed above the plane on which the (TBL) forms and the formalism thereof.

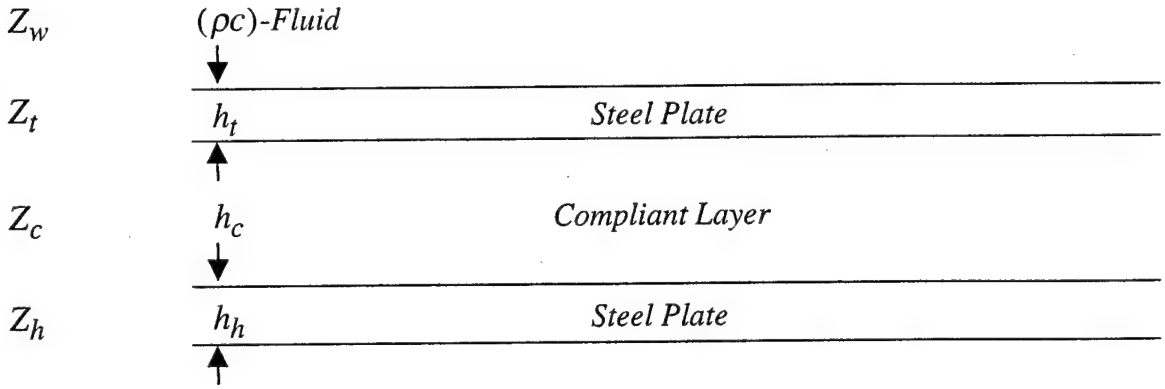

a

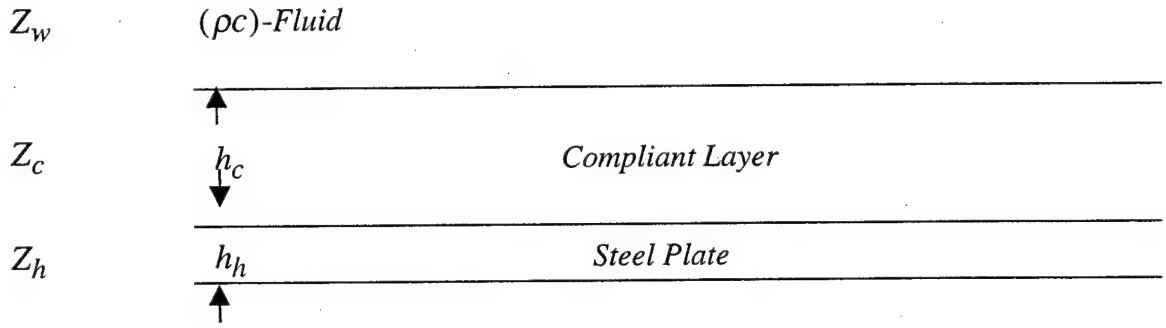

b

Fig. 3. The composition of the boundary: Z_h = surface impedance of hull, Z_c = surface stiffness of compliant layer, Z_t = surface impedance of conditioning plate and Z_w = surface impedance of fluid.

a. With a conditioning plate; $Z_t \neq 0$.

b. Without a conditioning plate; $Z_t \equiv 0$.

$V_b, = V_w \downarrow$

$Z_b = Z_t + Z_{ch}$

$Z_{ch} = Z_c Z_h (Z_c + Z_h)^{-1}$

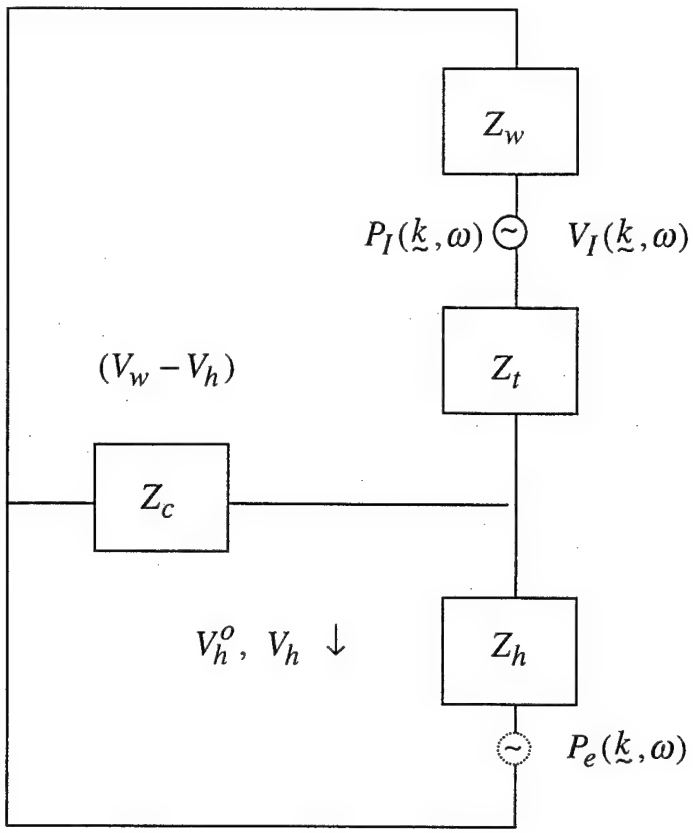

a

$Z_b = Z_{ch}$

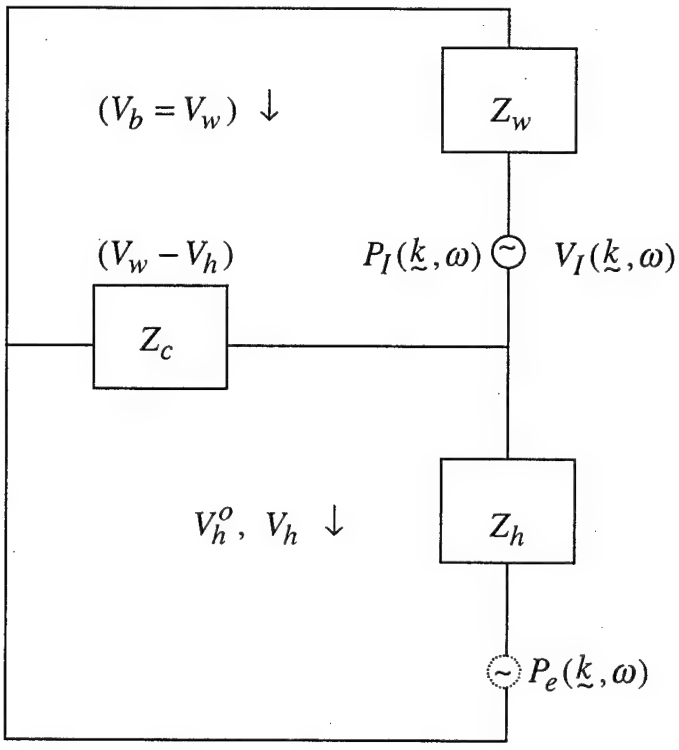

b

Fig 4. Equivalent circuit diagram of Fig. 3.

a. With a conditioning plate; $Z_t \neq 0$.

b. Without a condition plate; $Z_t \equiv 0$.

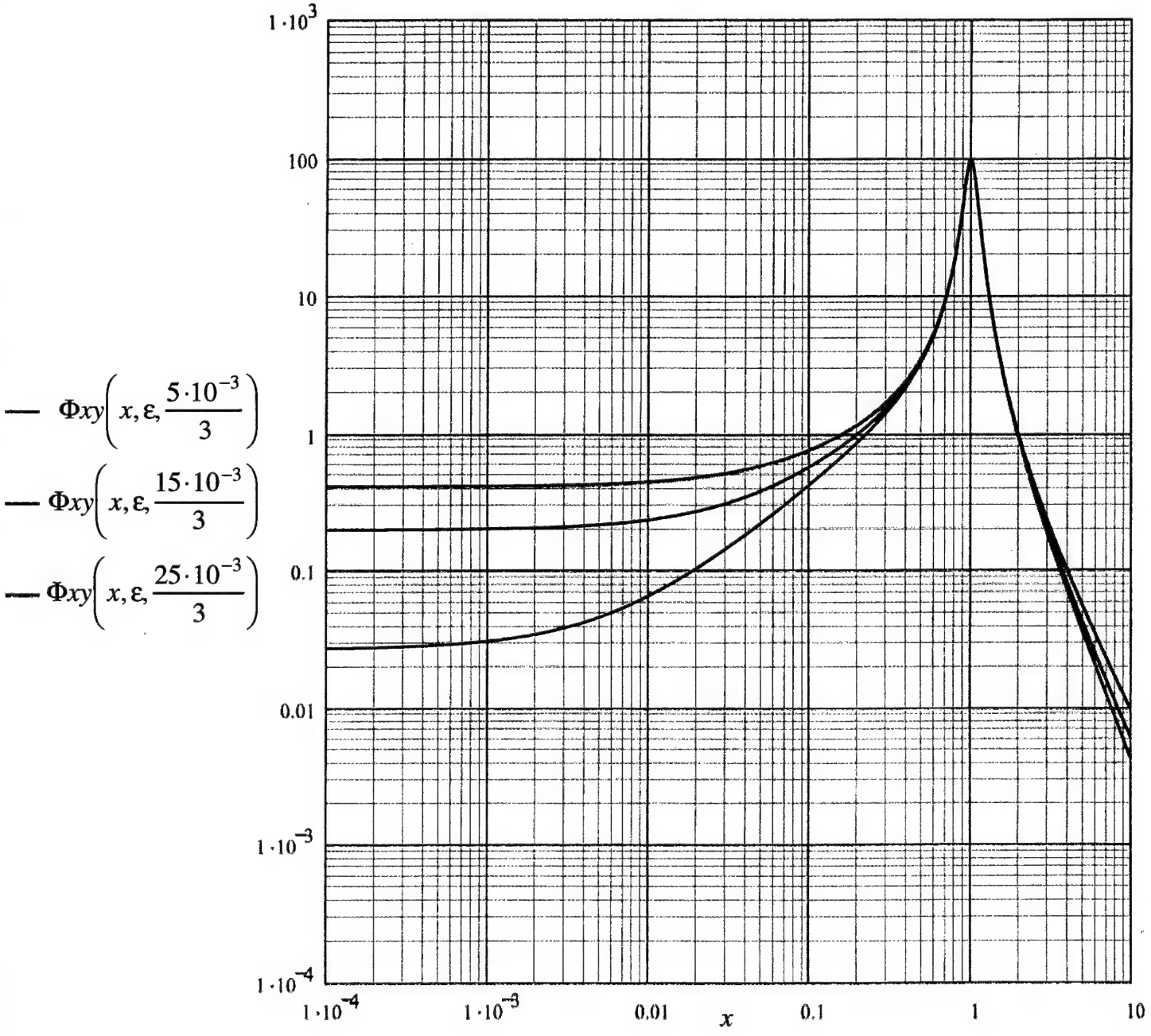

Fig 5. The spectral density $\Phi_{xy}(x, y, M)$ of the pressure generated by a turbulent boundary layer (TBL), as a function of the normalized wavenumber (x) in the stream-wise-direction, for a negligible value of the normalized wavenumber (y) in the cross-stream-wise-direction; $y \to 0$, and for three mach numbers (M); $M = (5/3)x10^{-3}$, $M = (15/3)x10^{-3}$ and $M = (25/3)x10^{-3}$. Of special interest are the peak at the convective position where $(x = 1)$ and the dependence of the intercept at $(x = 0)$.

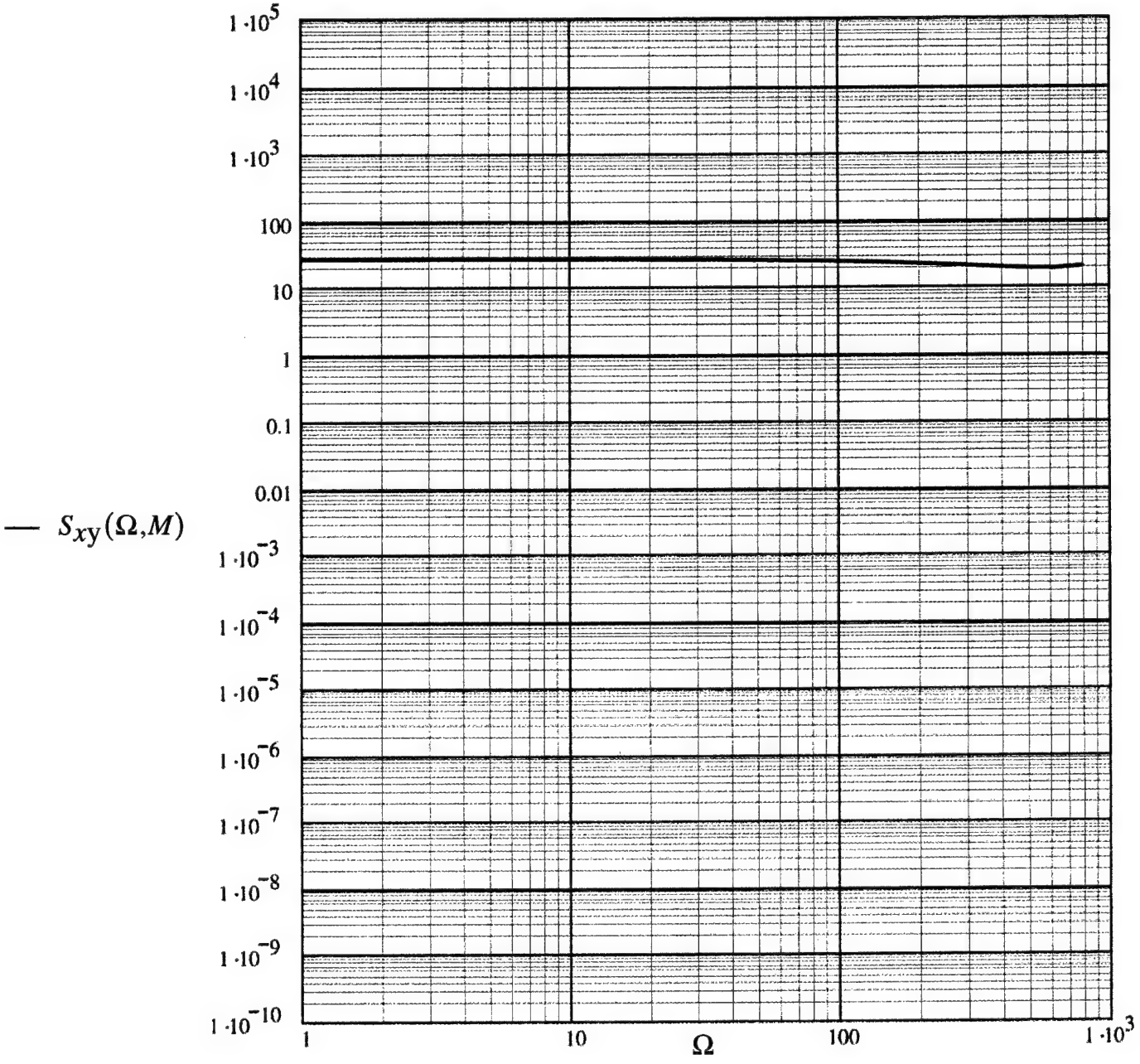

Fig 6. Determination of the frequency spectral density $S_{xy}(\omega, M) \equiv S_{xy}(\Omega, M)$, as a function of the normalized frequency (Ω), in the relevant range $1 \lesssim \Omega \lesssim 10^3$. This determination yields the value assigned in Eq. (47b).

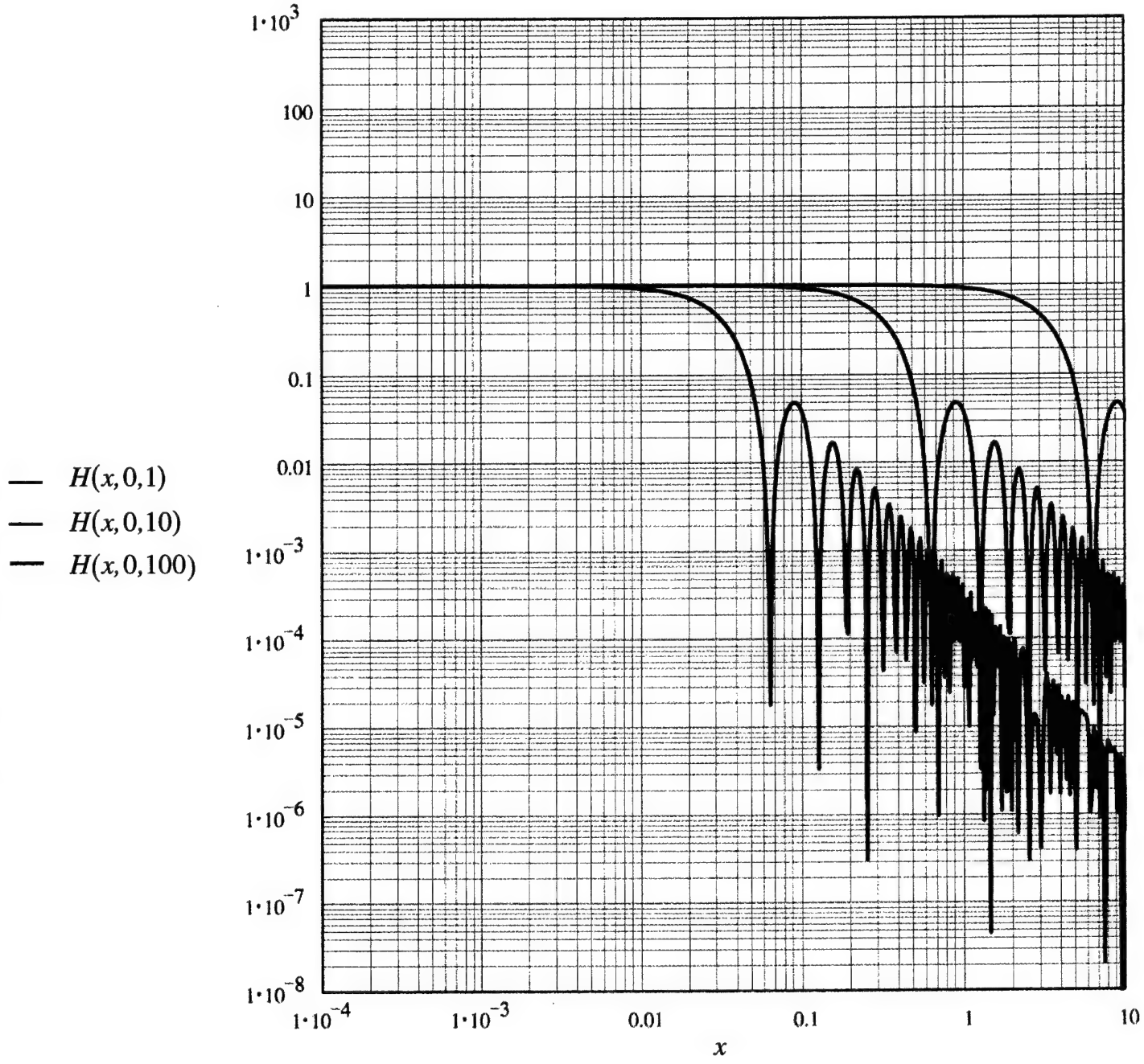

Fig 7. The filtering efficiency $H(x, y, \Omega)$ of a standard size transducer, as a function of the normalized wavenumber (x) with $y \to 0$ and for three values of the normalized frequency (Ω); $\Omega = 1$, 10 and 100. The standard transducer is a square transducer defined by $\gamma = \gamma_x = \gamma_y = (1/2)(M_o / M)$. [cf. Eqs. (52) and (54).]

a. A true representation. [cf. Eq. (51b).]

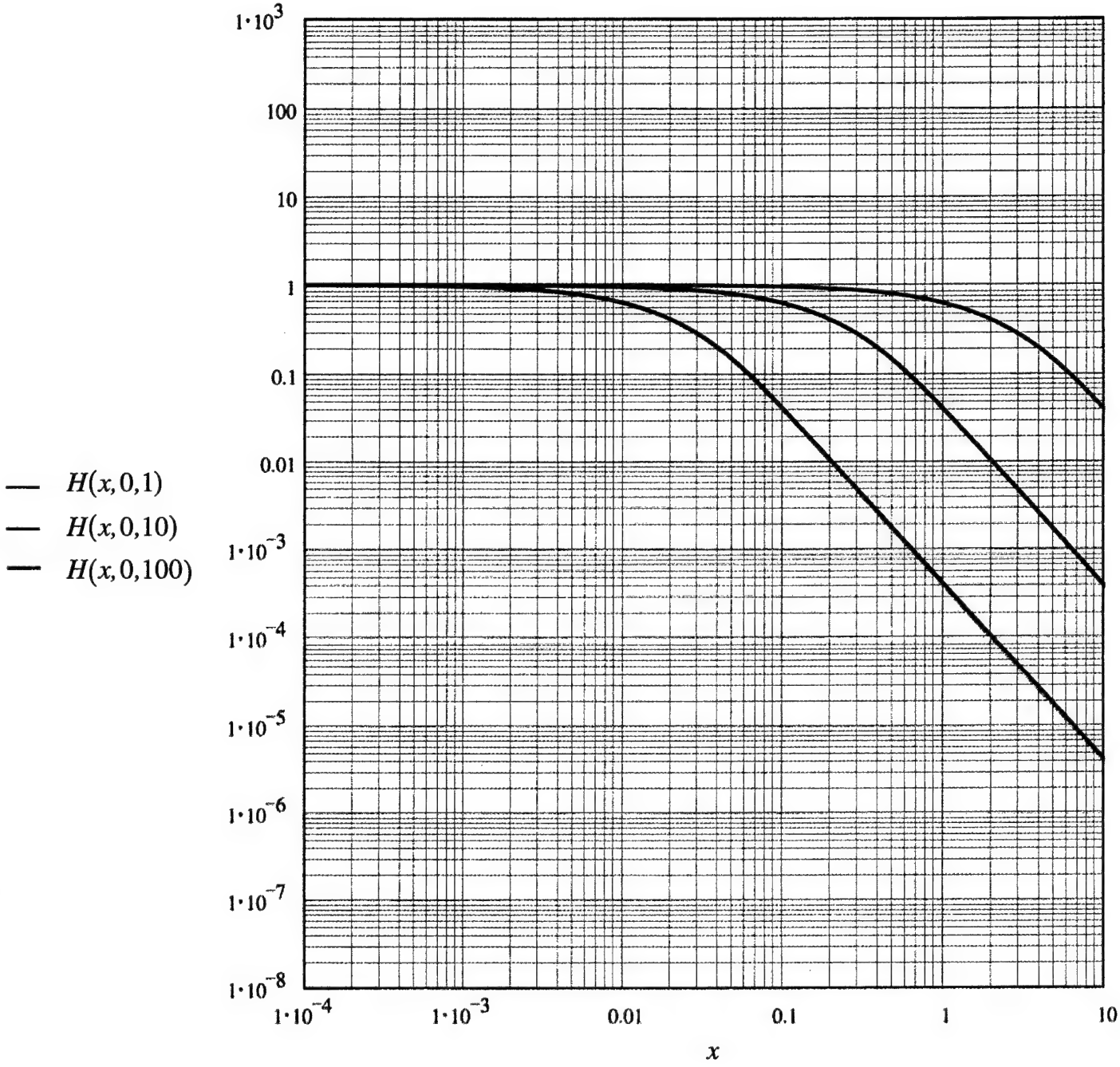

Fig 7. The filtering efficiency $H(x, y, \Omega)$ of a standard size transducer, as a function of the normalized wavenumber (x) with $y \to 0$ and for three values of the normalized frequency (Ω); $\Omega = 1$, 10 and 100. The standard transducer is a square transducer defined by $\gamma = \gamma_x = \gamma_y = (1/2)(M_o / M)$. [cf. Eqs. (52) and (54).]

b. An approximate representation in which the fluctuations are suppressed. [cf. Eq. (51c).]

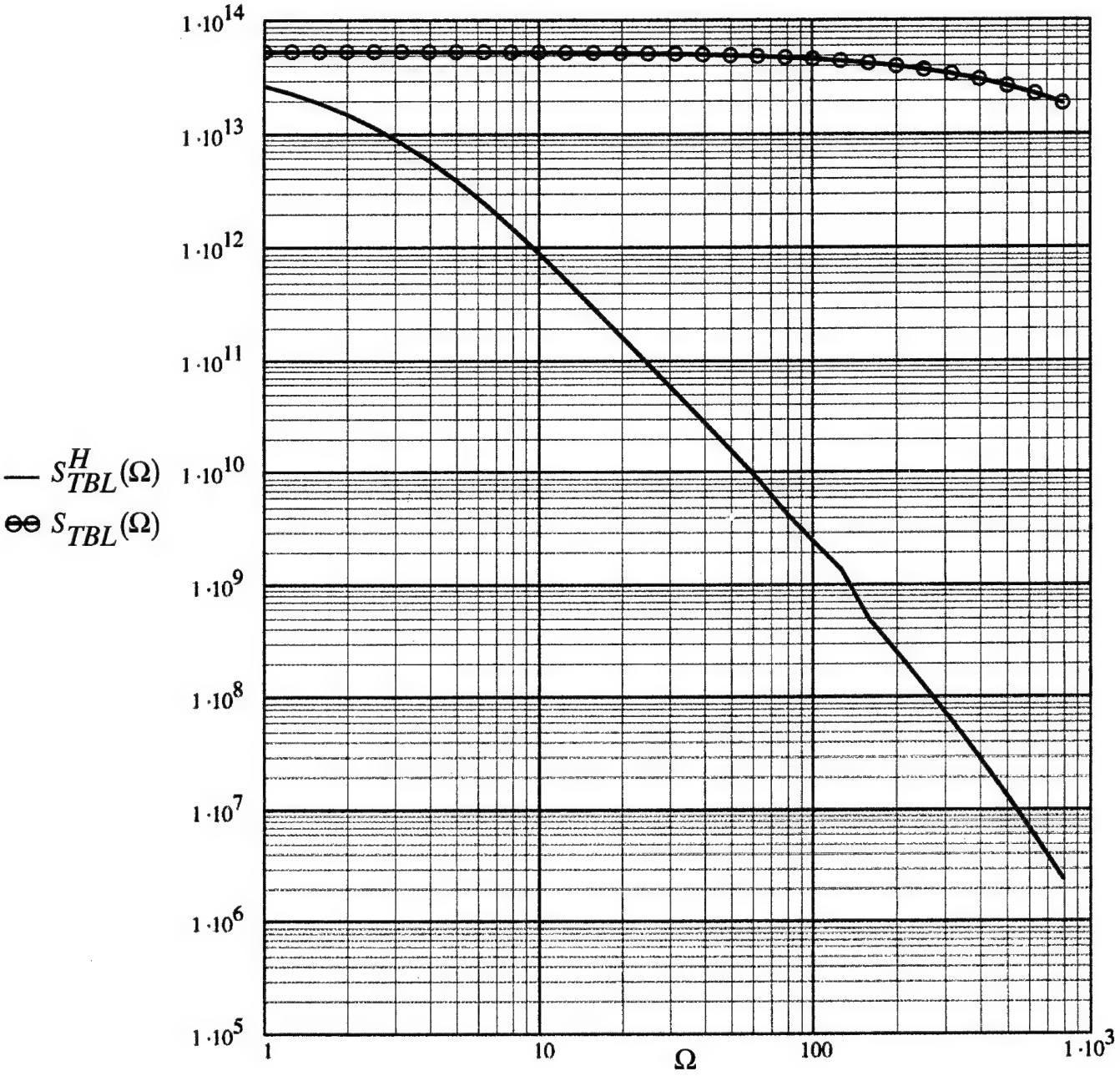

Fig 8. The normalized frequency spectral density $S_{TBL}(\Omega)$ of a point transducer and $S^{H}_{TBL}(\Omega)$ of a standard size transducer, as functions of the normalized frequency (Ω). The *averaging* due to the size of the transducer is clearly exhibited in this figure.

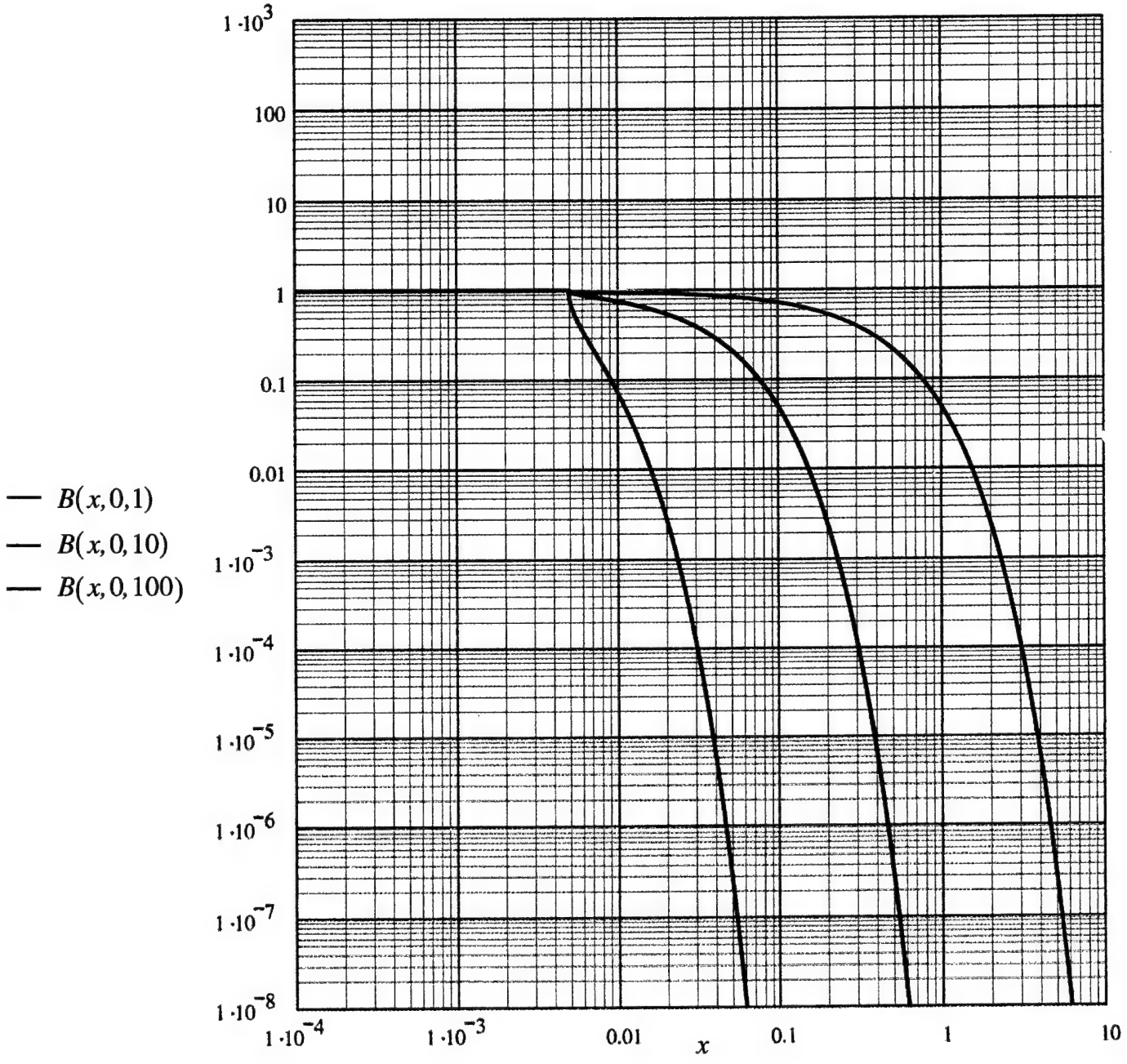

Fig 9. The filtering efficiency $B(x, y, \Omega)$ of a standard blanket, as a function of the normalized wavenumber (x) with $y \to 0$ and for three values of the normalized frequency (Ω); $\Omega = 1$, 10 and 100. The standard blanket is defined to be essentially of (ρc) characteristic impedance and of thickness $\gamma_b = (3/2)(M_o / M)$.

[cf. Eq (54).] $[B(x, y, \Omega) = |\exp(-i\gamma_b \Omega)[M^2 - (x^2 + y^2)^{1/2}]|^2 .]$

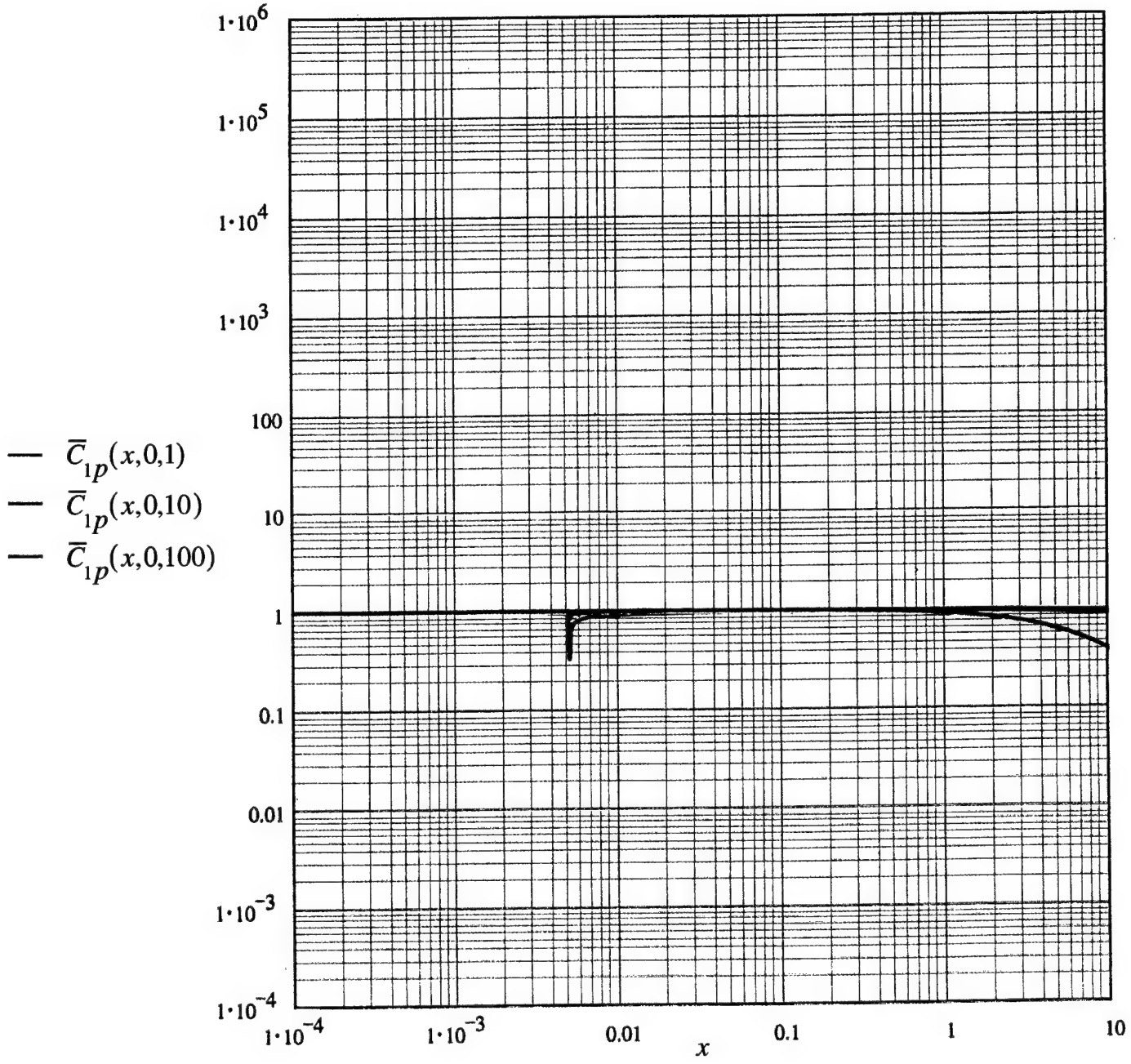

Fig 10. The filtering efficiency $\overline{C}_{1p}(x, y, \Omega)$ of a pressure transducer on an ideal (*rigid*) boundary, as a function of the normalized wavenumber (x) with $y \to 0$ and for three values of the normalized frequency (Ω); $\Omega = 1$, 10 and 100. [cf. Eq. (56a).]

a. A *point* pressure transducer and blanket-less.

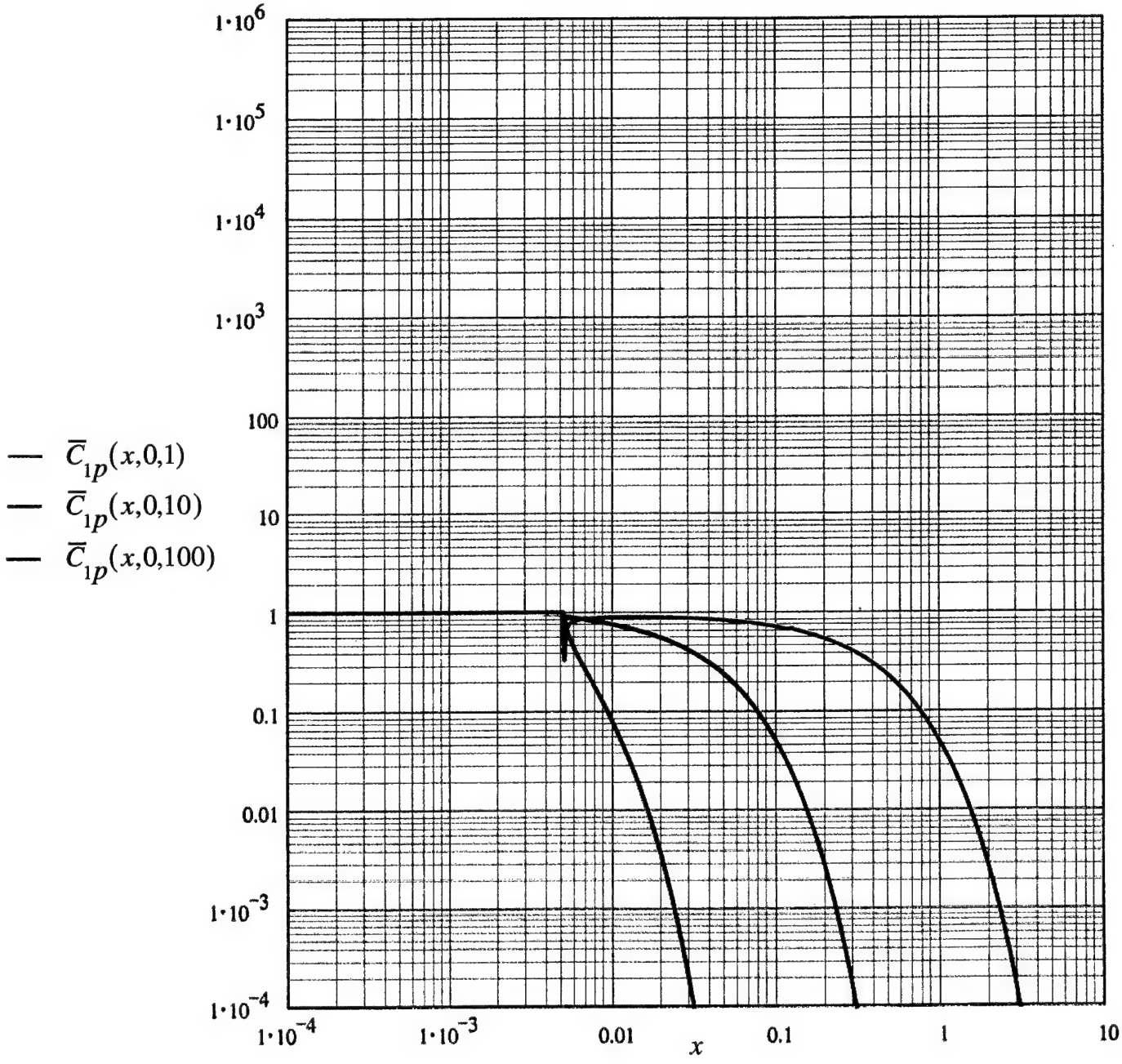

Fig 10. The filtering efficiency $\overline{C}_{1p}(x, y, \Omega)$ of a pressure transducer on an ideal (*rigid*) boundary, as a function of the normalized wavenumber (x) with $y \to 0$ and for three values of the normalized frequency (Ω); $\Omega = 1$, 10 and 100. [cf. Eq. (56a).]

b. A *point* pressure transducer under a standard blanket.

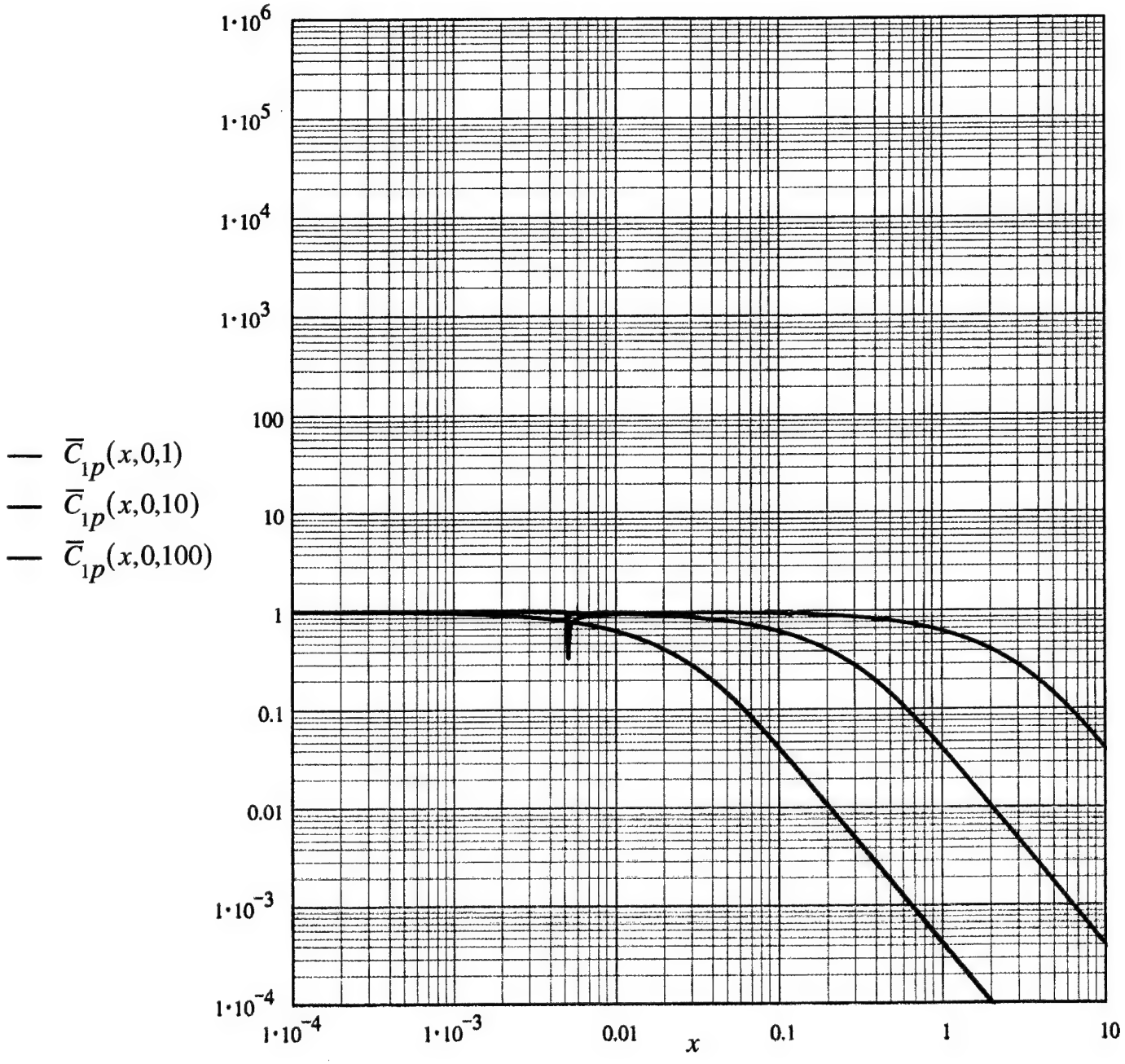

Fig 10. The filtering efficiency $\overline{C}_{1p}(x, y, \Omega)$ of a pressure transducer on an ideal (*rigid*) boundary, as a function of the normalized wavenumber (x) with $y \to 0$ and for three values of the normalized frequency (Ω); $\Omega = 1$, 10 and 100. [cf. Eq. (56a).]

c. A standard size pressure transducer and blanket-less.

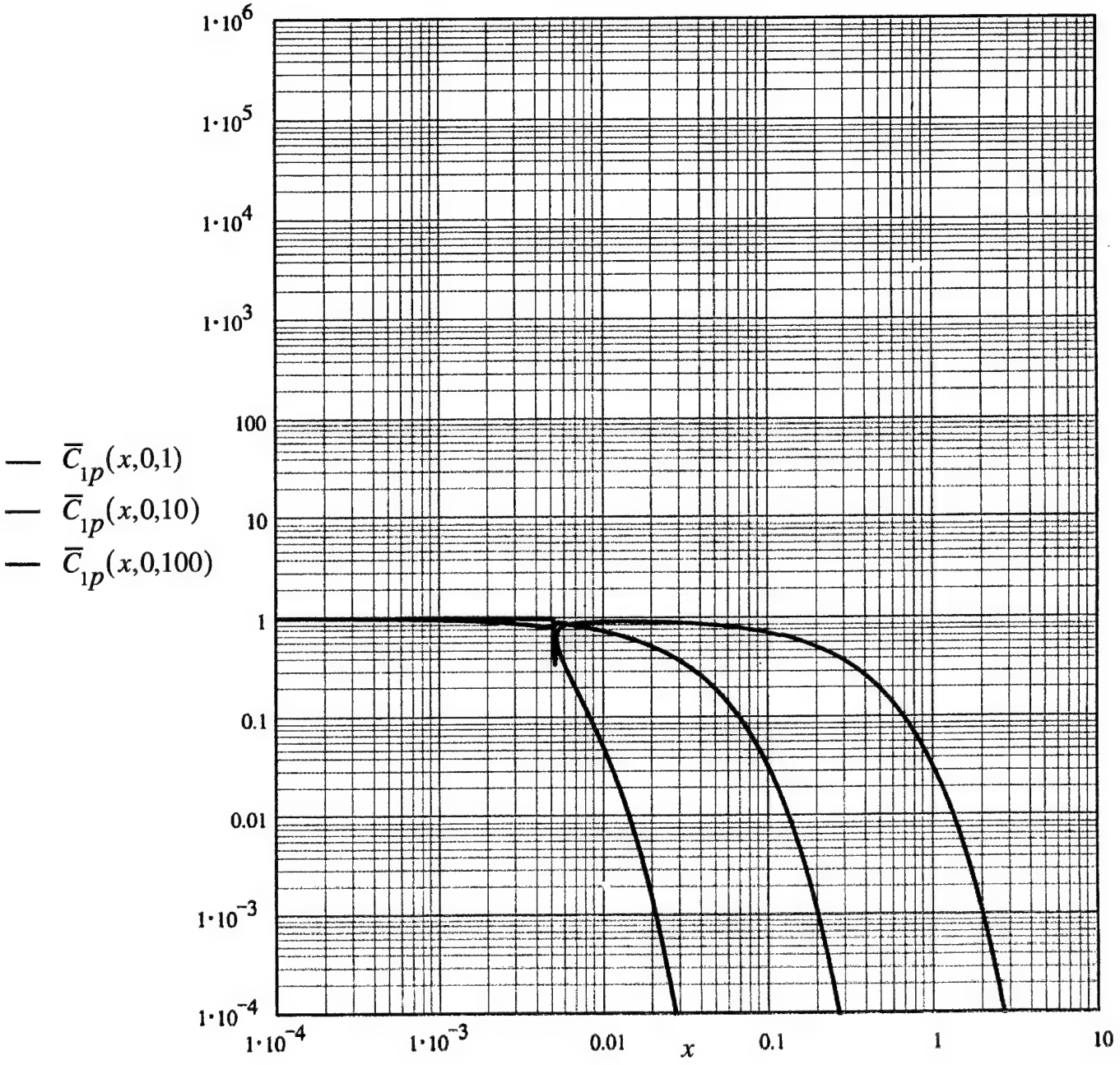

Fig 10. The filtering efficiency $\overline{C}_{1p}(x,y,\Omega)$ of a pressure transducer on an ideal (*rigid*) boundary, as a function of the normalized wavenumber (x) with $y \to 0$ and for three values of the normalized frequency (Ω); $\Omega = 1$, 10 and 100. [cf. Eq. (56a).]

d. A standard size pressure transducer under a standard blanket.

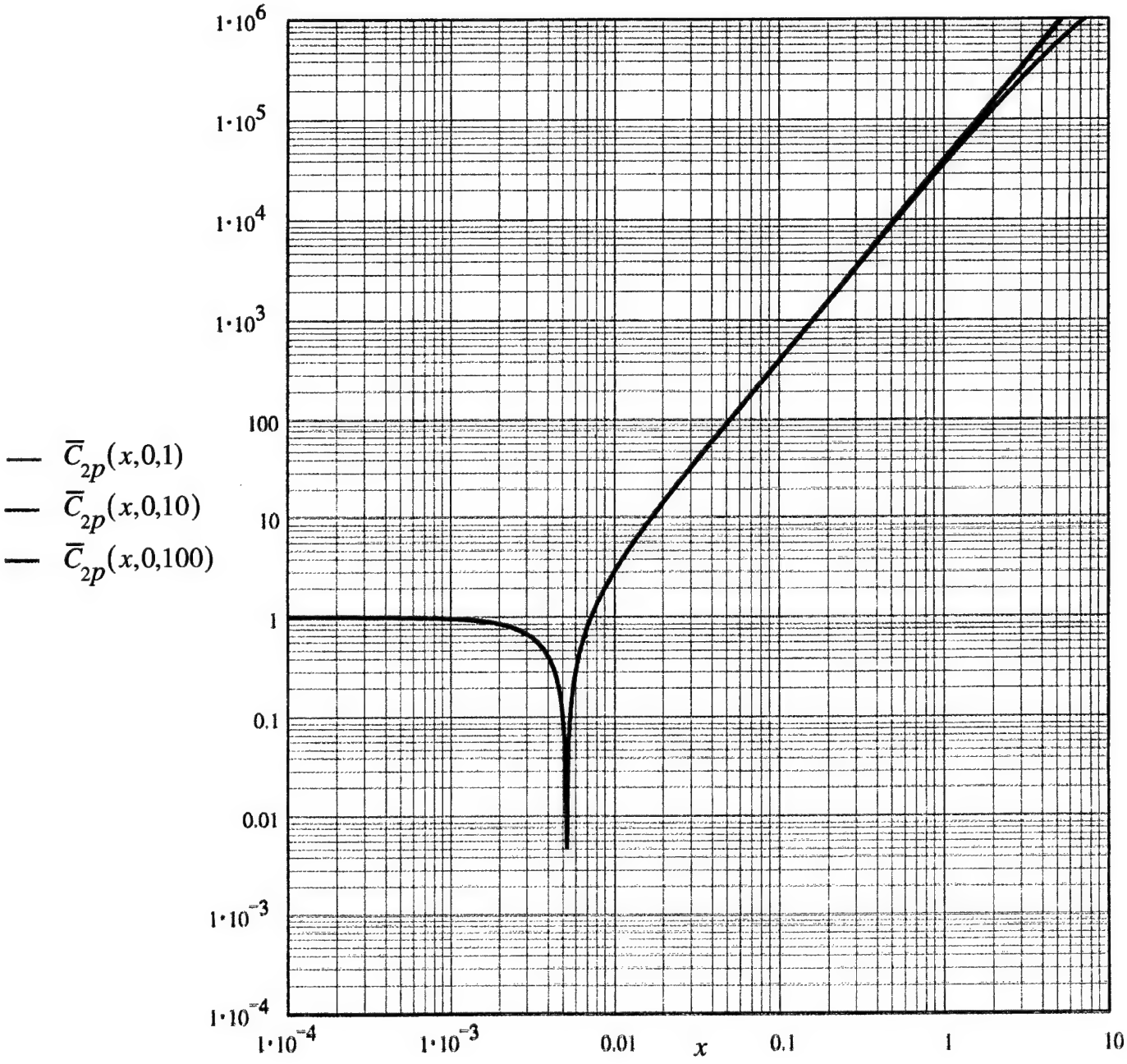

Fig 11. The filtering efficiency $\overline{C}_{2p}(x, y, \Omega)$ of a pressure transducer on an ideal *(pressure release)* boundary, as a function of the normalized wavenumber (x) with $y \to 0$ and for three values of the normalized frequency (Ω); $\Omega = 1$, 10 and 100. [cf. Eq. (56b).]

a. A *point* pressure transducer and blanket-less.

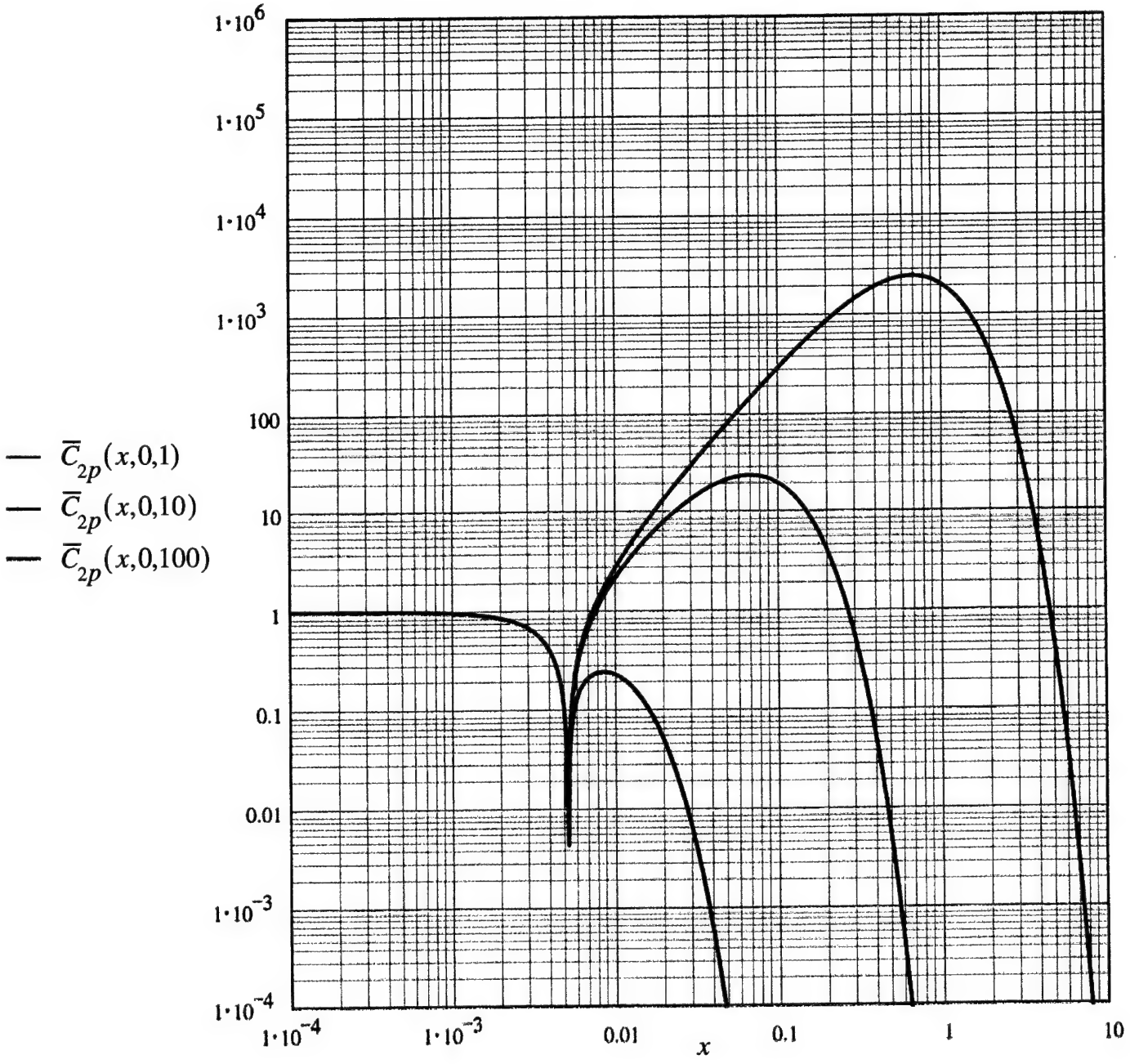

Fig 11. The filtering efficiency $\overline{C}_{2p}(x,y,\Omega)$ of a pressure transducer on an ideal *(pressure release)* boundary, as a function of the normalized wavenumber (x) with $y \to 0$ and for three values of the normalized frequency (Ω); $\Omega = 1$, 10 and 100. [cf. Eq. (56b).]

b. A *point* pressure transducer under a standard blanket.

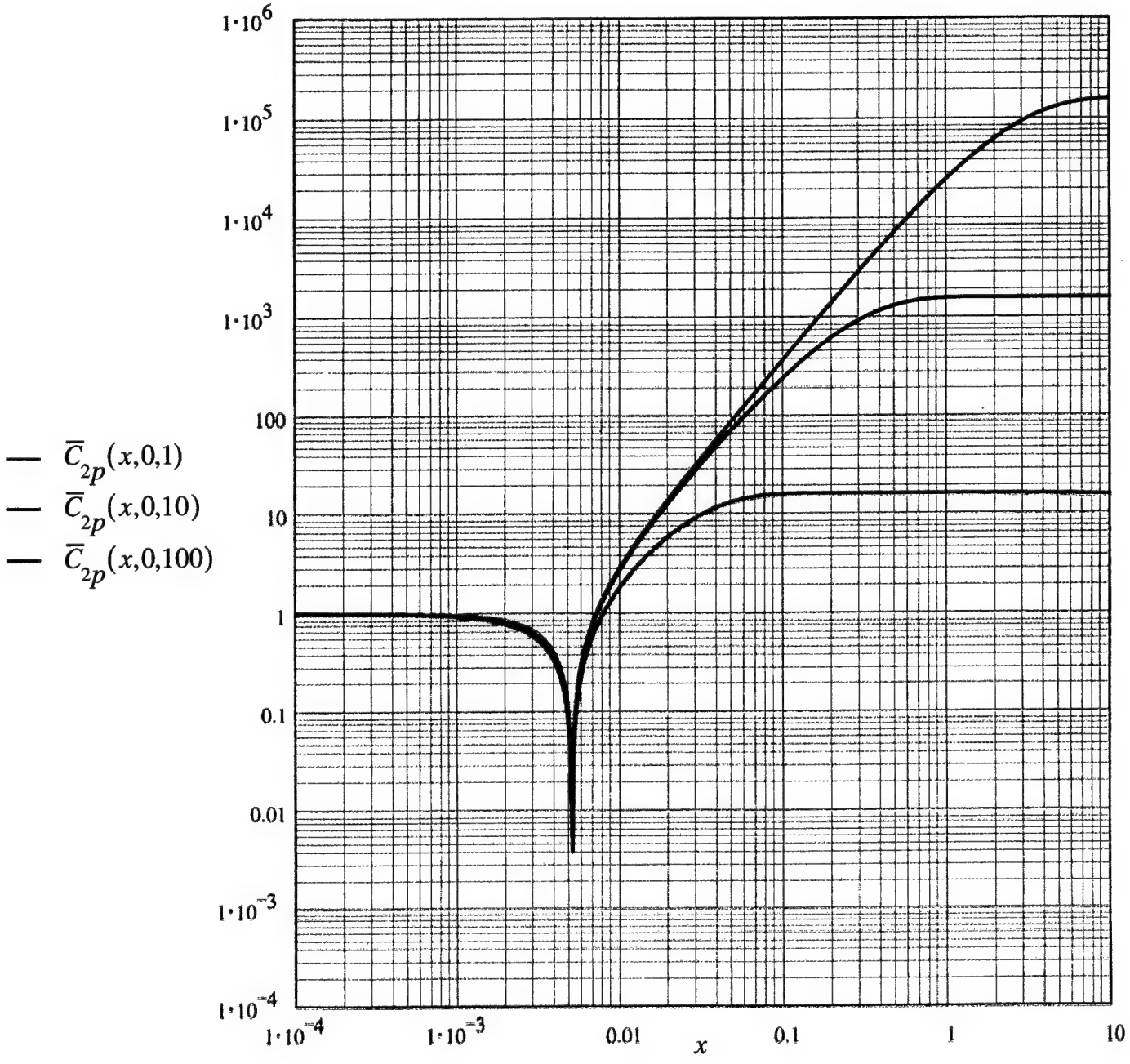

Fig 11. The filtering efficiency $\overline{C}_{2p}(x, y, \Omega)$ of a pressure transducer on an ideal *(pressure release)* boundary, as a function of the normalized wavenumber (x) with $y \to 0$ and for three values of the normalized frequency (Ω); $\Omega = 1$, 10 and 100. [cf. Eq. (56b).]

c. A standard size pressure transducer and blanket-less.

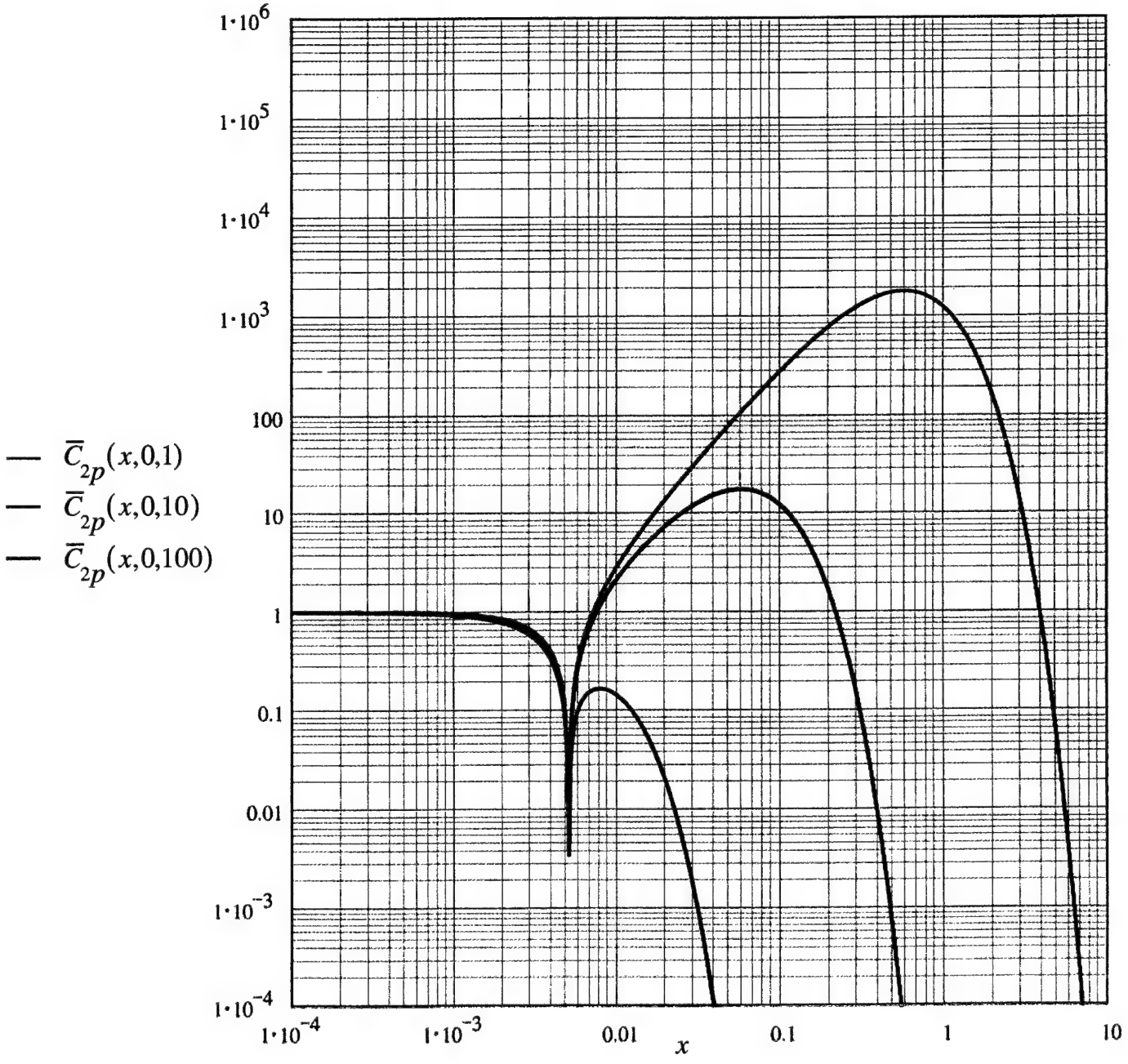

Fig 11. The filtering efficiency $\overline{C}_{2p}(x,y,\Omega)$ of a pressure transducer on an ideal *(pressure release)* boundary, as a function of the normalized wavenumber (x) with $y \to 0$ and for three values of the normalized frequency (Ω); $\Omega = 1$, 10 and 100. [cf. Eq. (56b).]

d. A standard size velocity transducer under a standard blanket.

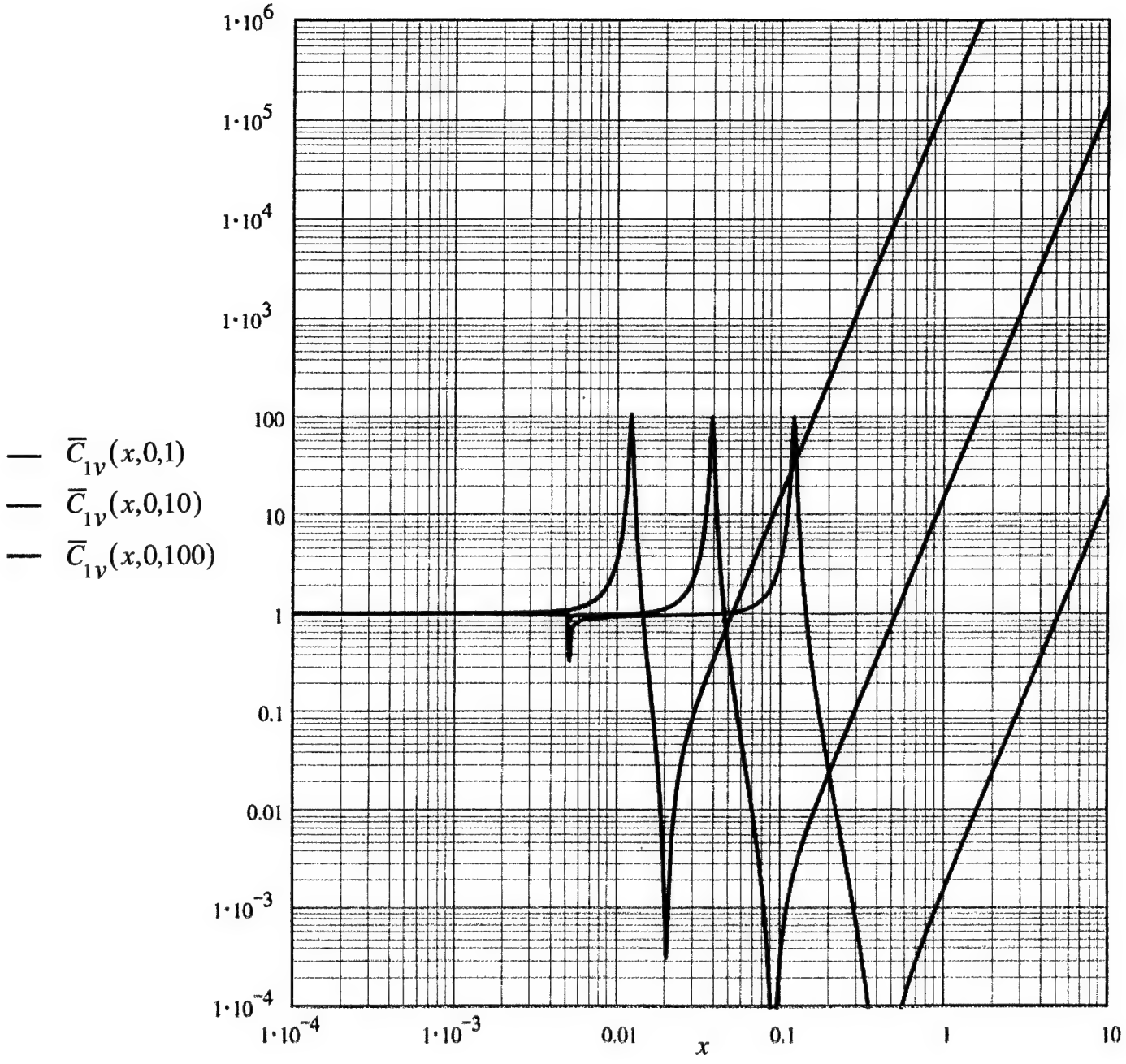

Fig 12. The filtering efficiency $\overline{C}_{1v}(x, y, \Omega)$ of a velocity transducer on an ideal (*rigid)* boundary as a function of the normalized wavenumber (x) with $y \to 0$ and for three values of the normalized frequency (Ω); $\Omega = 1$, 10 and 100. [cf. Eq. (57a).]

a. A *point* velocity transducer and blanket-less.

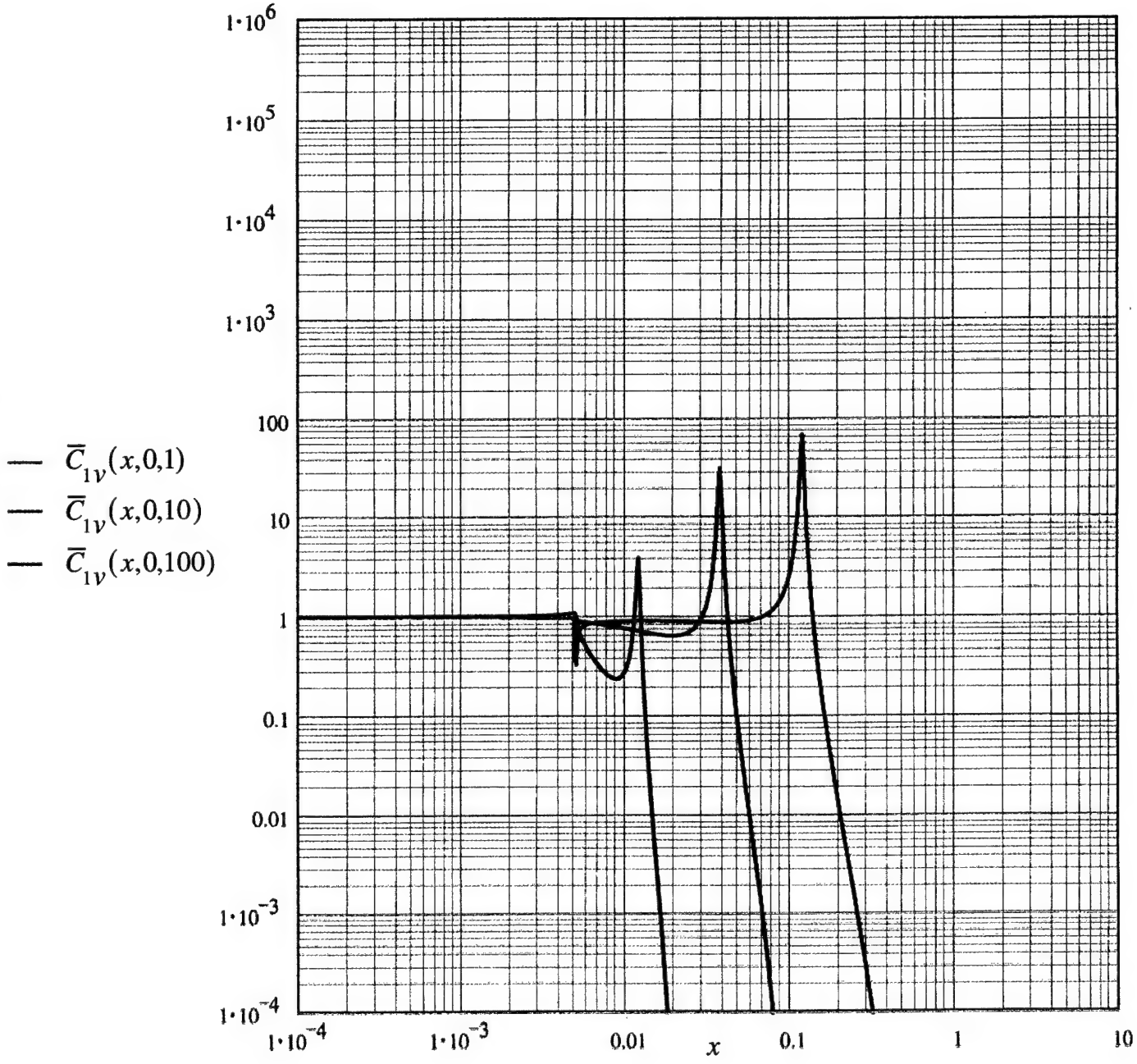

Fig 12. The filtering efficiency $\overline{C}_{1v}(x, y, \Omega)$ of a velocity transducer on an ideal *(rigid)* boundary as a function of the normalized wavenumber (x) with $y \to 0$ and for three values of the normalized frequency (Ω); $\Omega = 1$, 10 and 100. [cf. Eq. (57a).]

b. A *point* velocity transducer under a standard blanket.

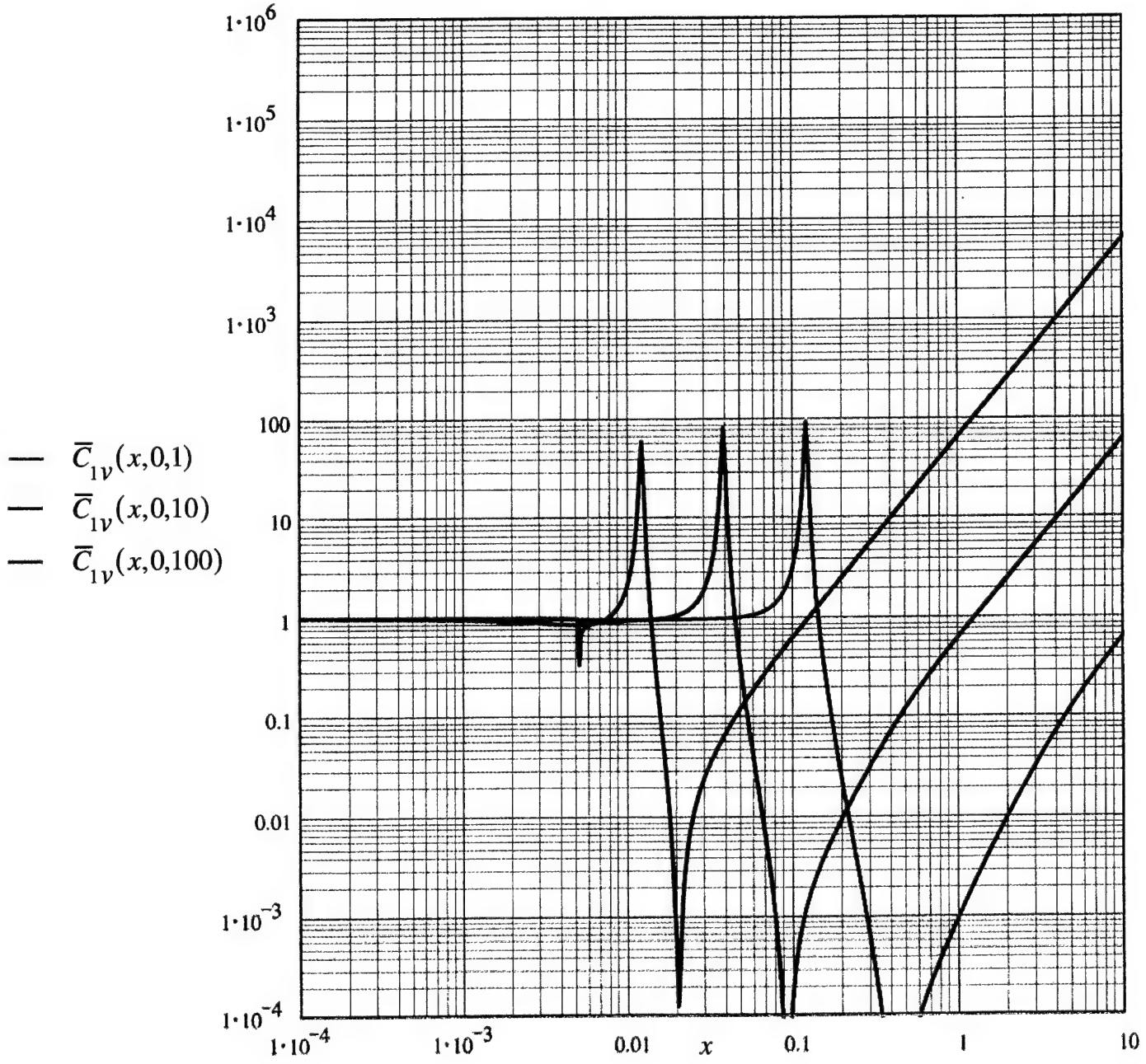

Fig 12. The filtering efficiency $\overline{C}_{1v}(x, y, \Omega)$ of a velocity transducer on an ideal *(rigid)* boundary as a function of the normalized wavenumber (x) with $y \to 0$ and for three values of the normalized frequency (Ω); $\Omega = 1$, 10 and 100. [cf. Eq. (57a).]

c. A standard size velocity transducer and blanket-less.

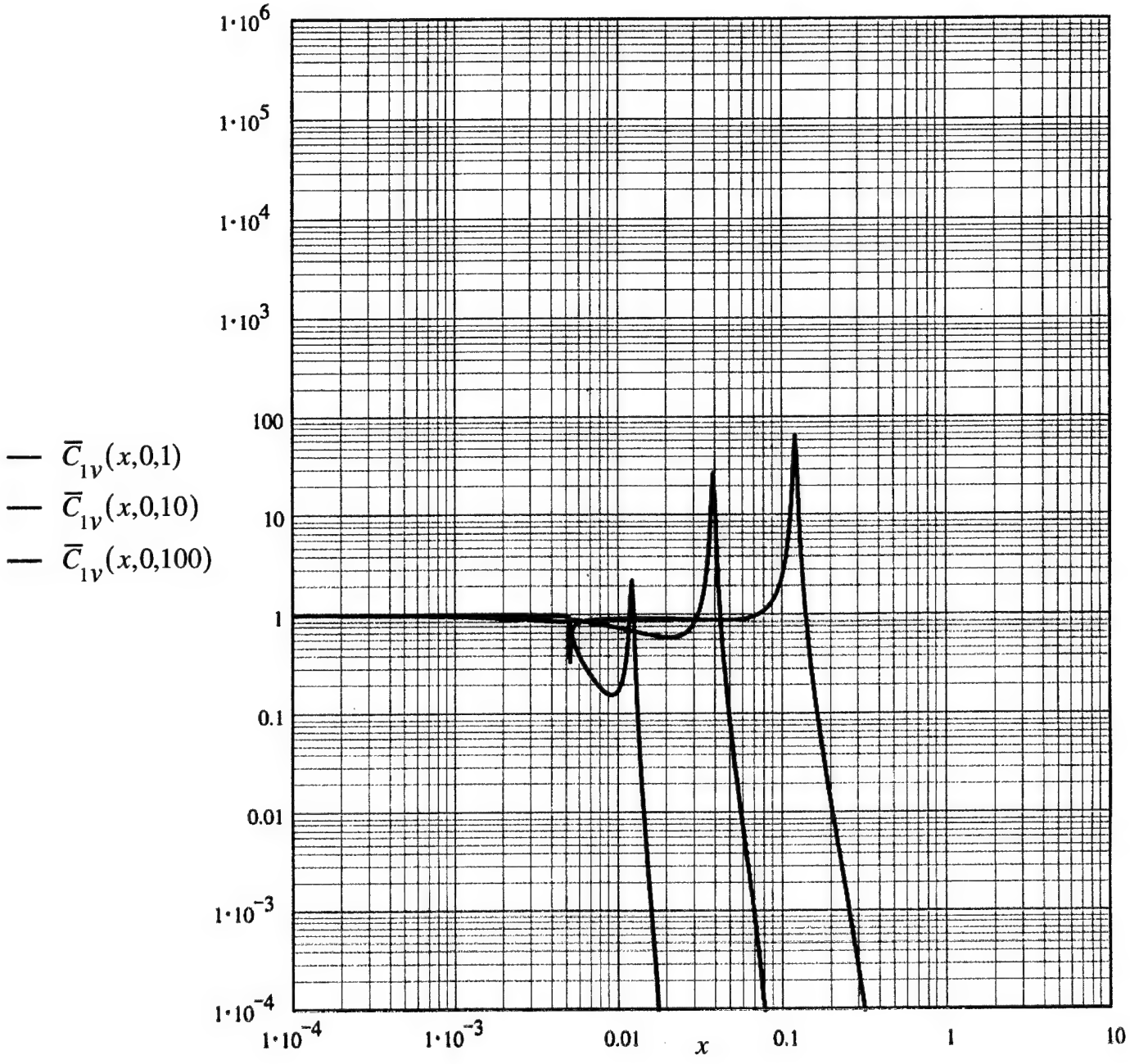

Fig 12. The filtering efficiency $\overline{C}_{1v}(x, y, \Omega)$ of a velocity transducer on an ideal *(rigid)* boundary as a function of the normalized wavenumber (x) with $y \to 0$ and for three values of the normalized frequency (Ω); $\Omega = 1$, 10 and 100. [cf. Eq. (57a).]

d. A standard size velocity transducer under a standard blanket.

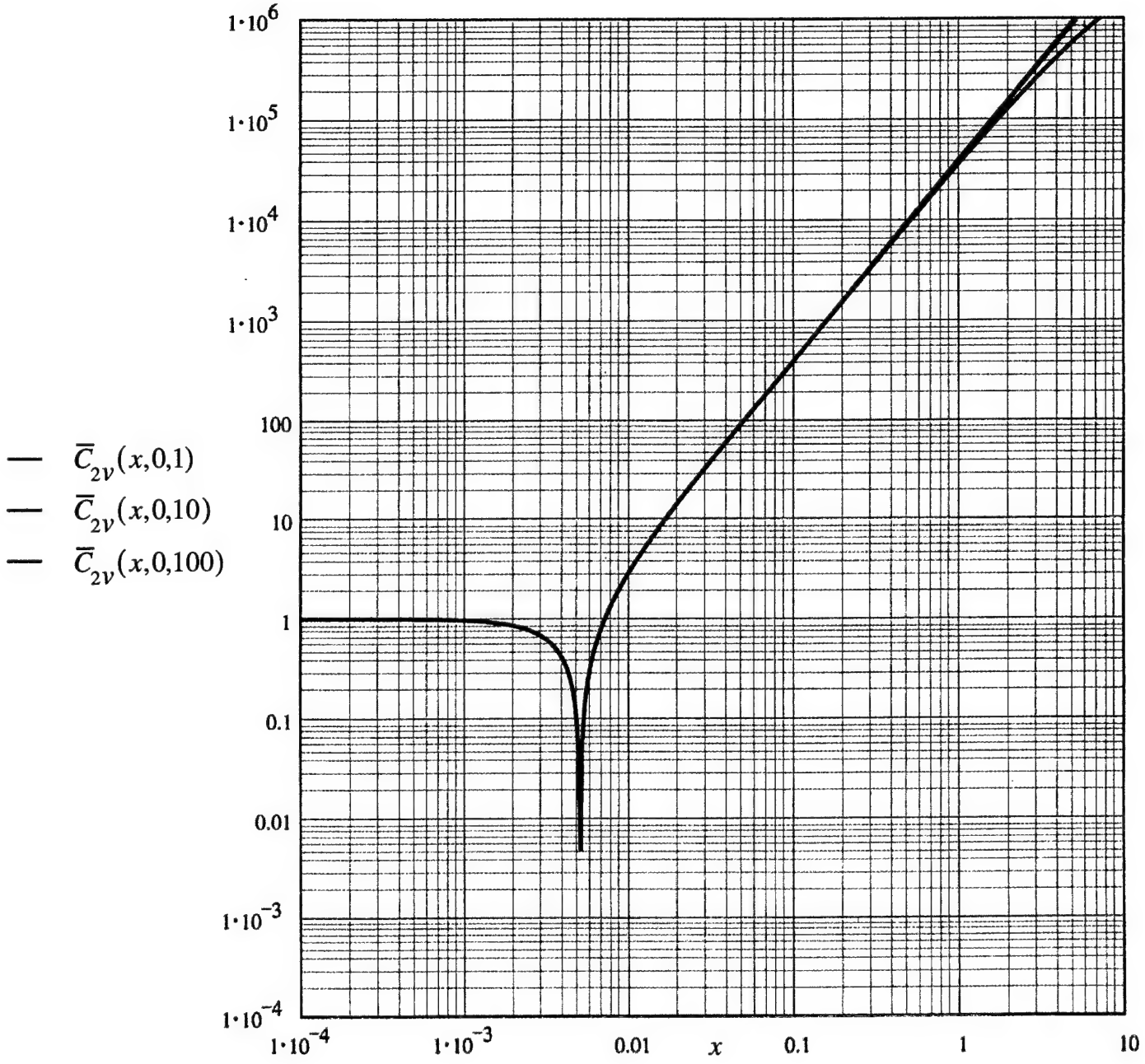

Fig 13. The filtering efficiency $\overline{C}_{2v}(x, y, \Omega)$ of a velocity transducer on an ideal (*pressure release*) boundary, as a function of the normalized wavenumber (x) with $y \to 0$ and for three values of the normalized frequency (Ω); $\Omega = 1$, 10 and 100. [cf. Eq. (57b).]

a. A *point* velocity transducer and blanket-less.

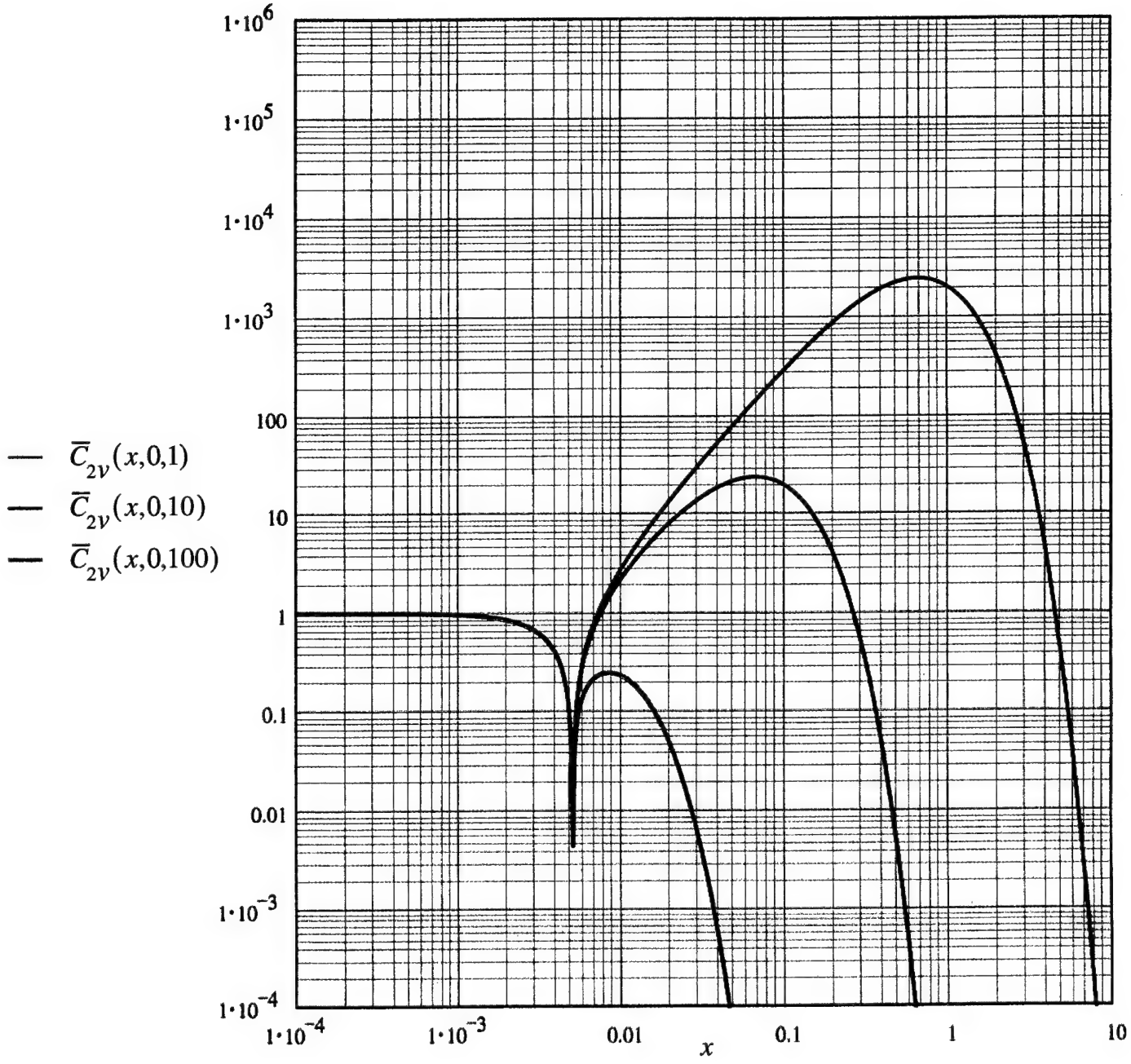

Fig 13. The filtering efficiency $\overline{C}_{2v}(x,y,\Omega)$ of a velocity transducer on an ideal (*pressure release*) boundary, as a function of the normalized wavenumber (x) with $y \to 0$ and for three values of the normalized frequency (Ω); $\Omega = 1$, 10 and 100. [cf. Eq. (57b).]

b. A *point* velocity transducer under a standard blanket.

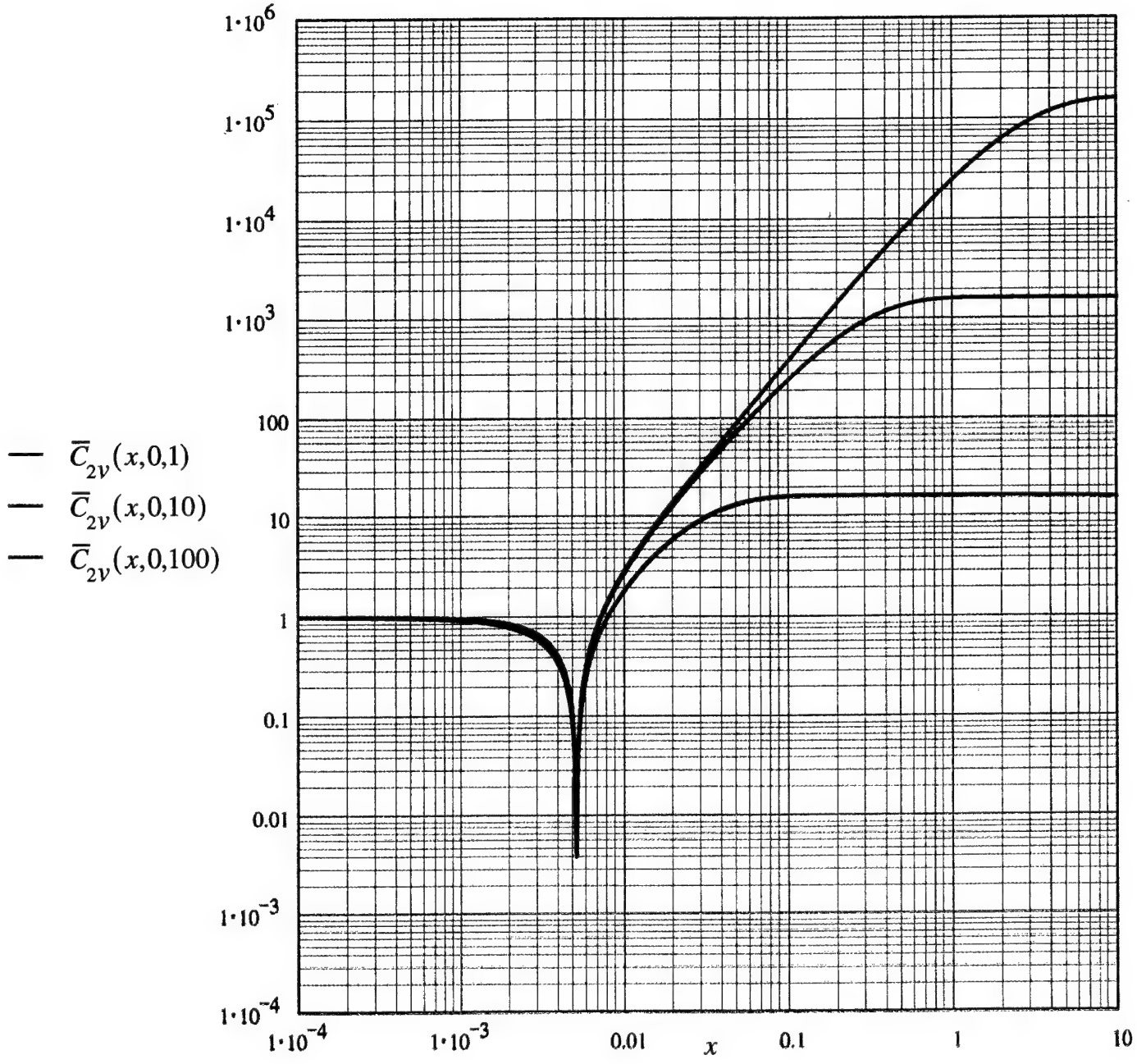

Fig 13. The filtering efficiency $\overline{C}_{2v}(x,y,\Omega)$ of a velocity transducer on an ideal (*pressure release*) boundary, as a function of the normalized wavenumber (x) with $y \to 0$ and for three values of the normalized frequency (Ω); $\Omega = 1$, 10 and 100. [cf. Eq. (57b).]

c. A standard size velocity transducer and blanket-less.

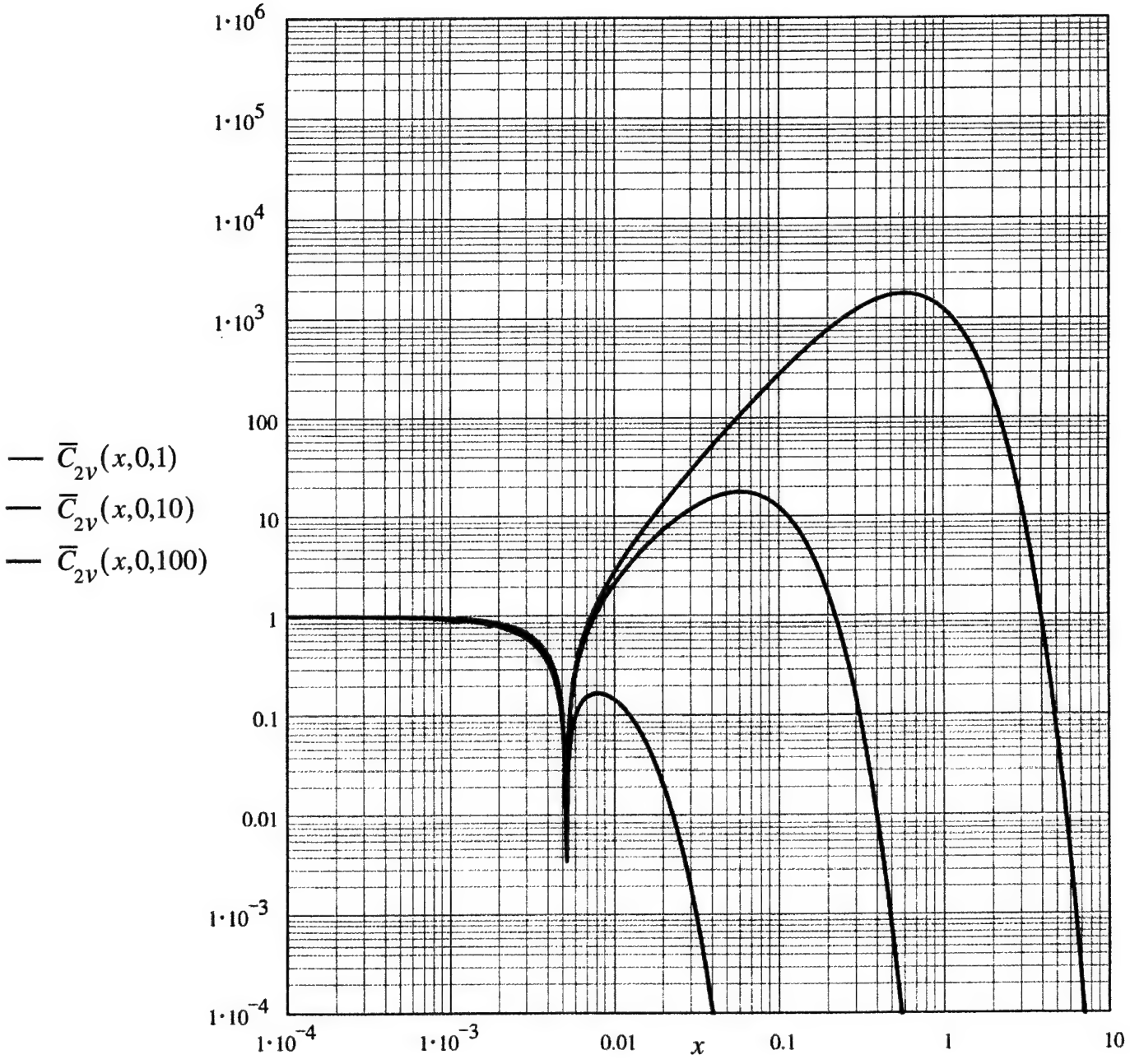

Fig 13. The filtering efficiency $\overline{C}_{2v}(x, y, \Omega)$ of a velocity transducer on an ideal (*pressure release*) boundary, as a function of the normalized wavenumber (x) with $y \to 0$ and for three values of the normalized frequency (Ω); $\Omega = 1$, 10 and 100. [cf. Eq. (57b).]

d. A standard size velocity transducer under a standard blanket.

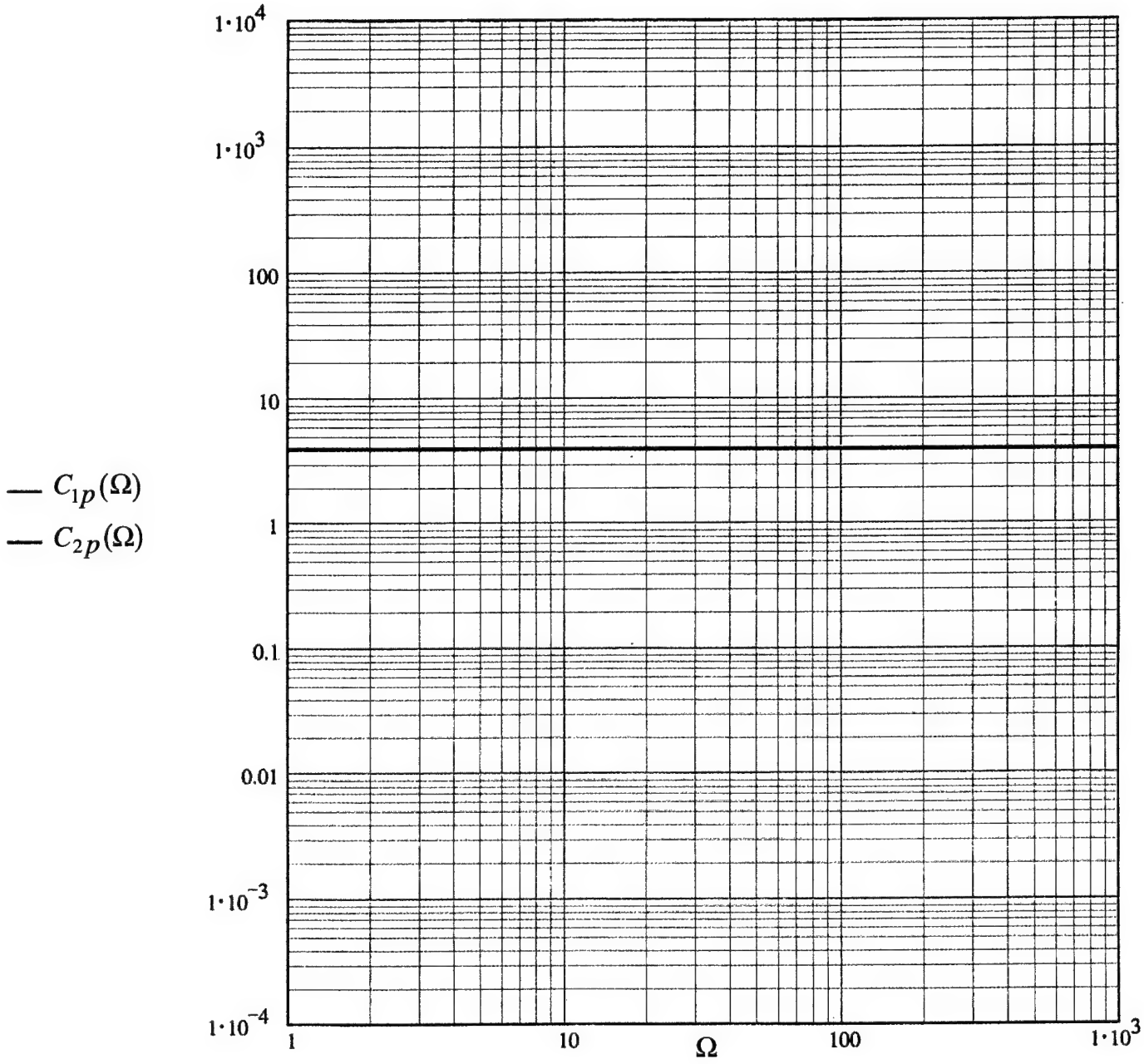

Fig 14. The sensitivities $C_{1p}(\Omega)$ and $C_{2p}(\Omega)$ of a pressure transducer with and without an ideal *(rigid)* conditioning plate, respectively, as functions of the normalized frequency (Ω); in the displayed range $1 \leq \Omega \leq 10^3$. [cf. Eq. (59).] In the absence of a conditioning plate the ideal boundary is *pressure release*.

a. Normal ordinate.

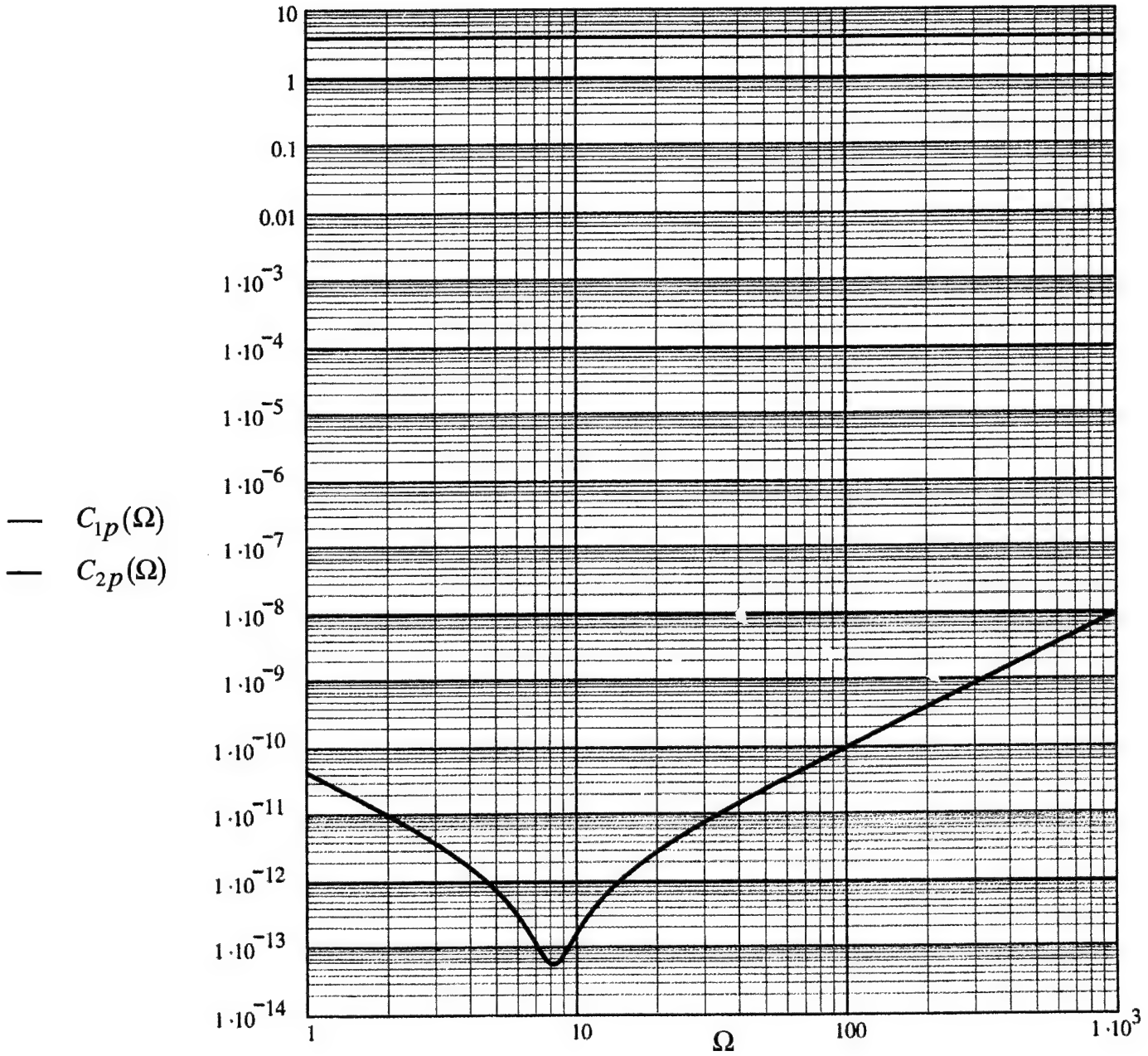

Fig 14. The sensitivities $C_{1p}(\Omega)$ and $C_{2p}(\Omega)$ of a pressure transducer with and without an ideal *(rigid)* conditioning plate, respectively, as functions of the normalized frequency (Ω); in the displayed range $1 \leq \Omega \leq 10^3$. [cf. Eq. (59).] In the absence of a conditioning plate the ideal boundary is *pressure release*.

b. Expanded ordinate.

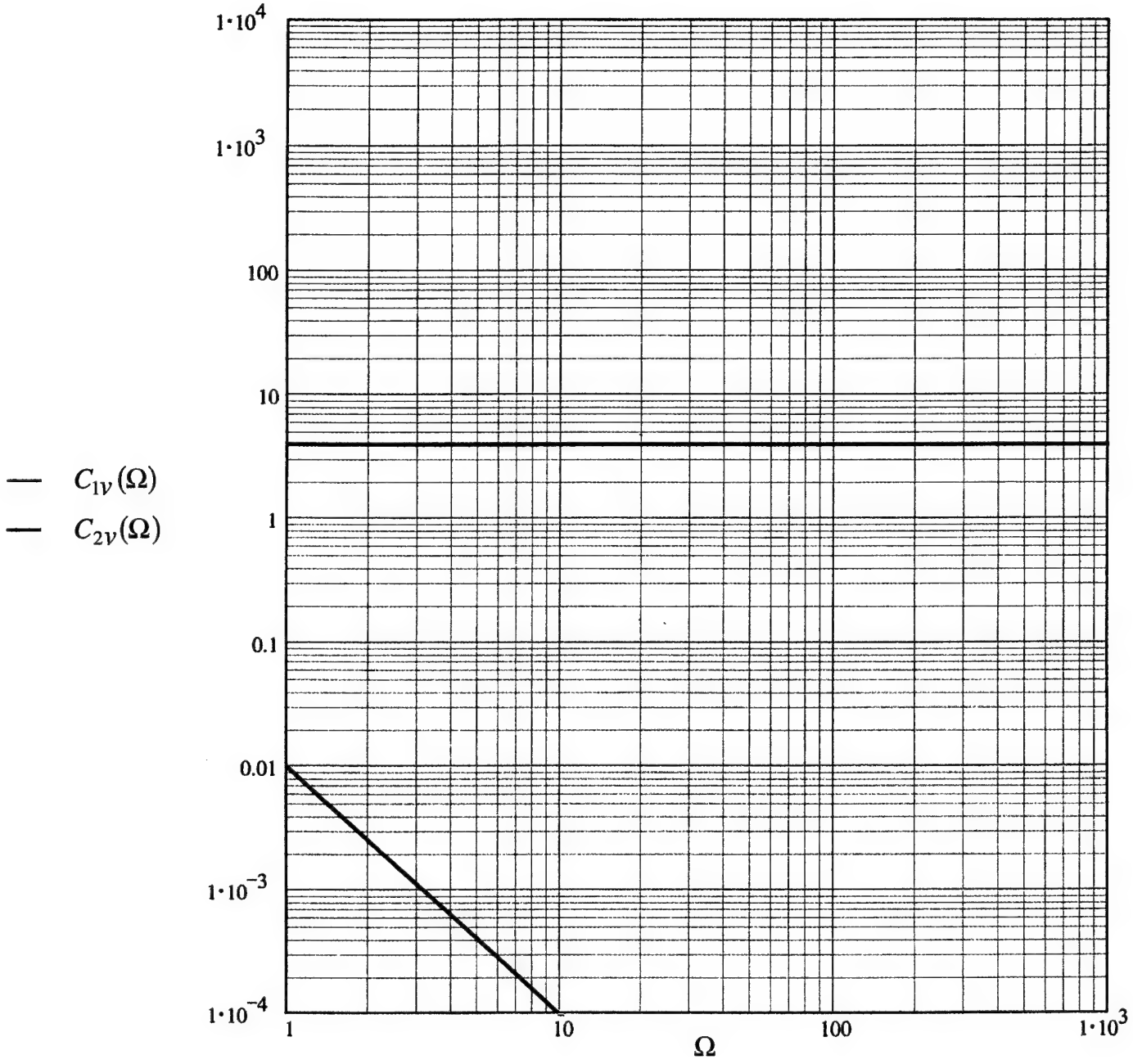

Fig 15. The sensitivities $C_{1v}(\Omega)$ and $C_{2v}(\Omega)$ of a velocity transducer with and without an ideal *(rigid)* conditioning plate, respectively, as functions of the normalized frequency (Ω); in the displayed range $1 \leq \Omega \leq 10^3$. [cf. Eq. (60).] In the absence of a conditioning plate the ideal boundary is *pressure release*.

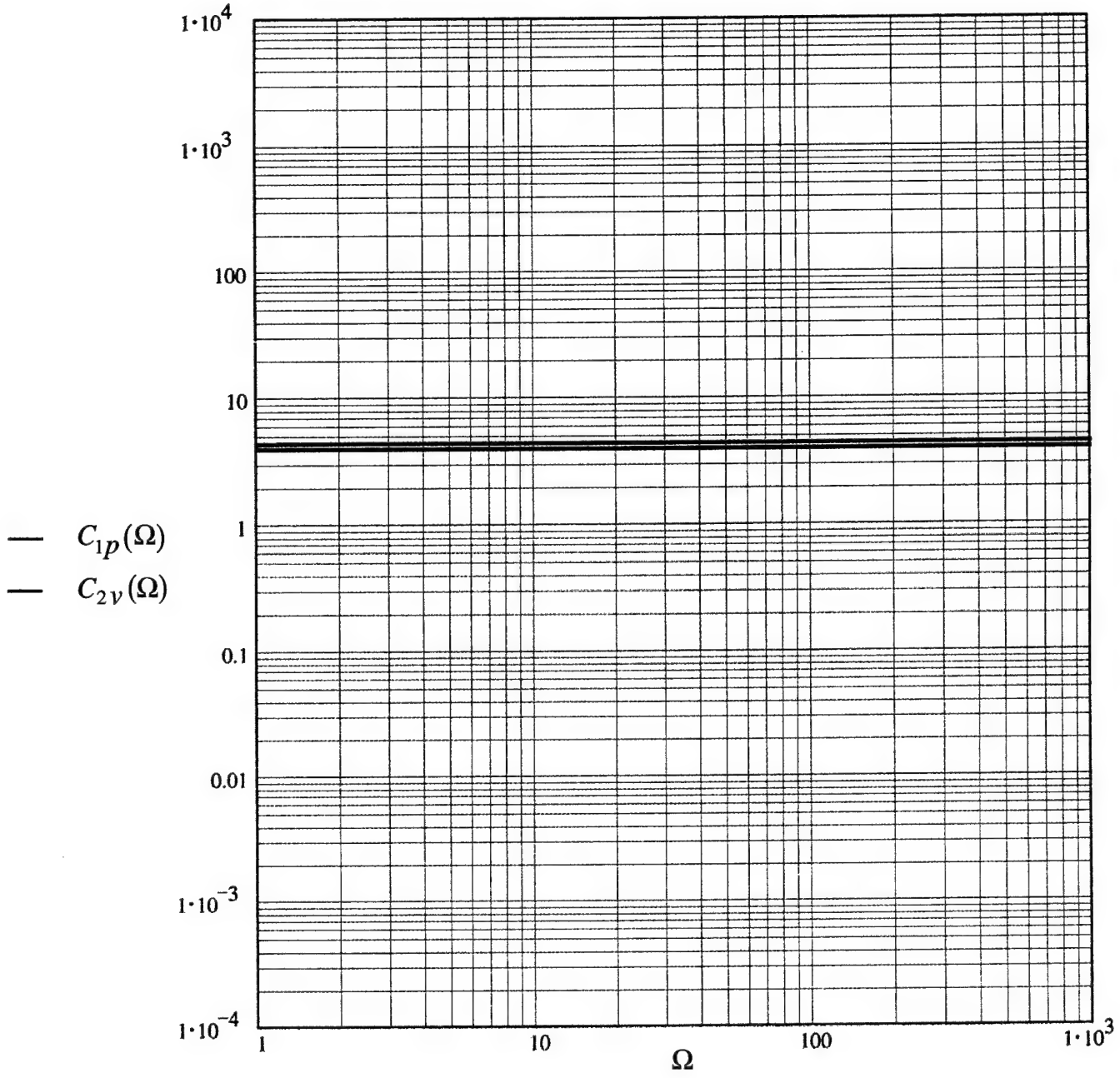

Fig 16. The sensitivities $C_{1p}(\Omega)$ and $C_{2v}(\Omega)$ of a pressure transducer with an ideal *(rigid)* conditioning plate and of a velocity transducer on an ideal *(pressure release)* boundary, respectively, as functions of the normalized frequency (Ω); in the displayed range $1 \leq \Omega \leq 10^3$. [cf. Eqs. (59a) and (60b).] The two curves overlap and both show sensitivities that are equal to (4) throughout the depicted range.

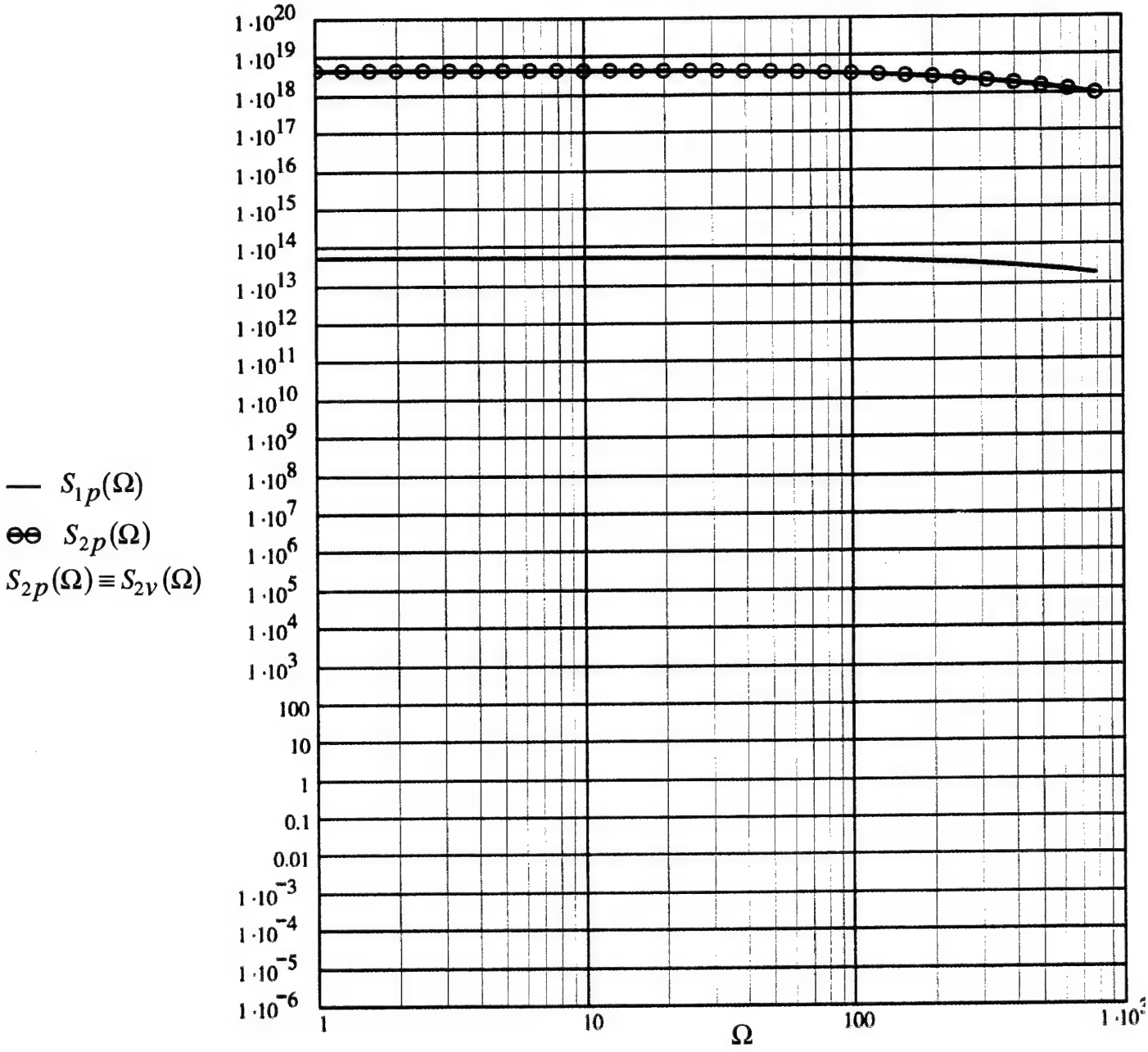

Fig. 17. The normalized outputs to (TBL) $S_{1p}(\Omega)$ and $S_{2p}(\Omega)$ of a pressure transducer on an ideal *rigid* boundary and on an ideal *pressure release* boundary, respectively, as functions of the normalized frequency (Ω); in the displayed range $1 \leq \Omega \leq 10^3$. [cf. Eqs. (62a) and 62d), respectively.] It is noted that $S_{2p}(\Omega)$ is identical to $S_{2v}(\Omega)$; $S_{2p}(\Omega) \equiv S_{2v}(\Omega)$

a. *Point* transducer and blanket-less.

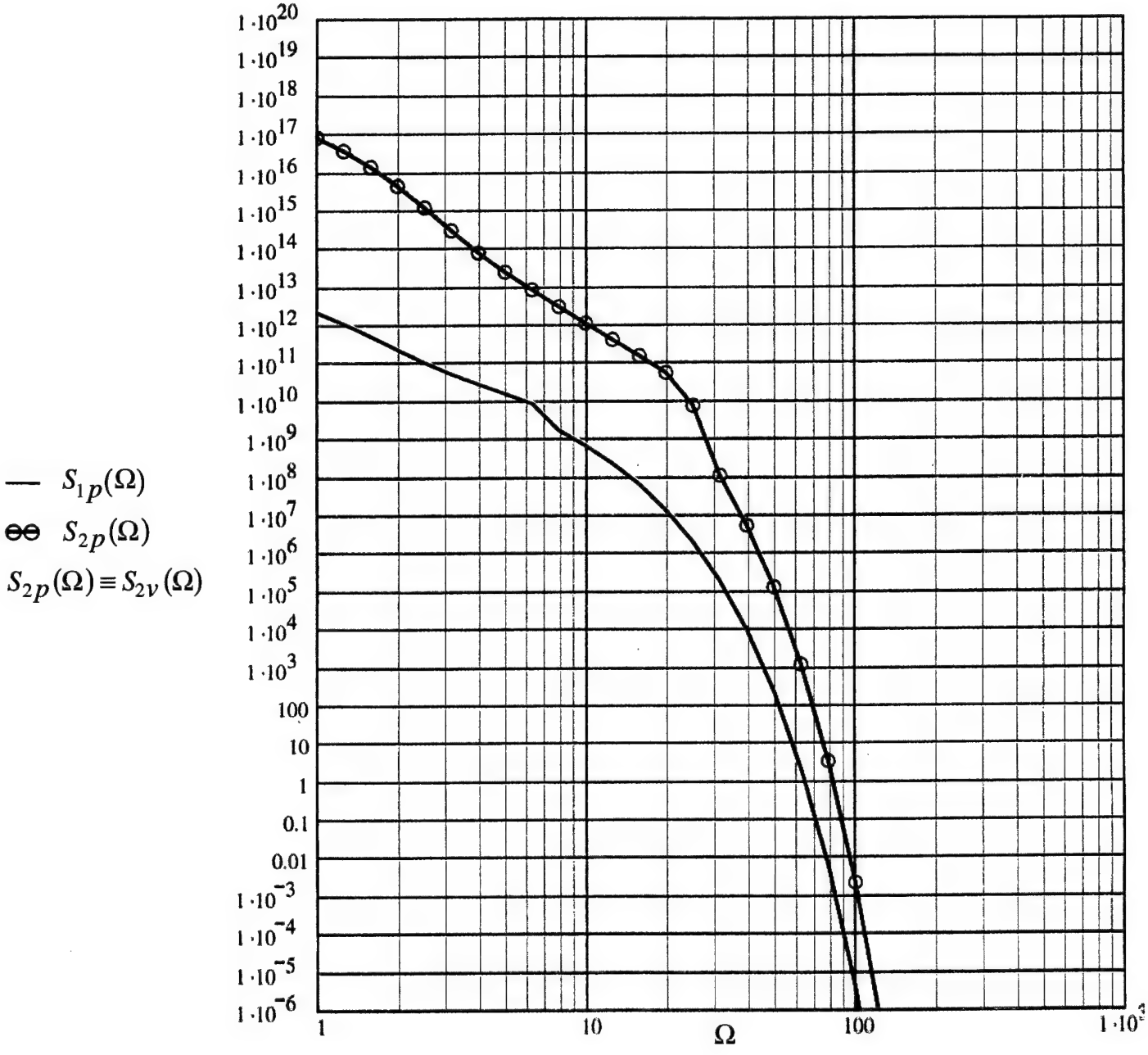

Fig. 17. The normalized outputs to (TBL) $S_{1p}(\Omega)$ and $S_{2p}(\Omega)$ of a pressure transducer on an ideal *rigid* boundary and on an ideal *pressure release* boundary, respectively, as functions of the normalized frequency (Ω); in the displayed range $1 \leq \Omega \leq 10^3$. [cf. Eqs. (62a) and 62d), respectively.] It is noted that $S_{2p}(\Omega)$ is identical to $S_{2v}(\Omega)$; $S_{2p}(\Omega) \equiv S_{2v}(\Omega)$

b. *Point* transducers under a blanket.

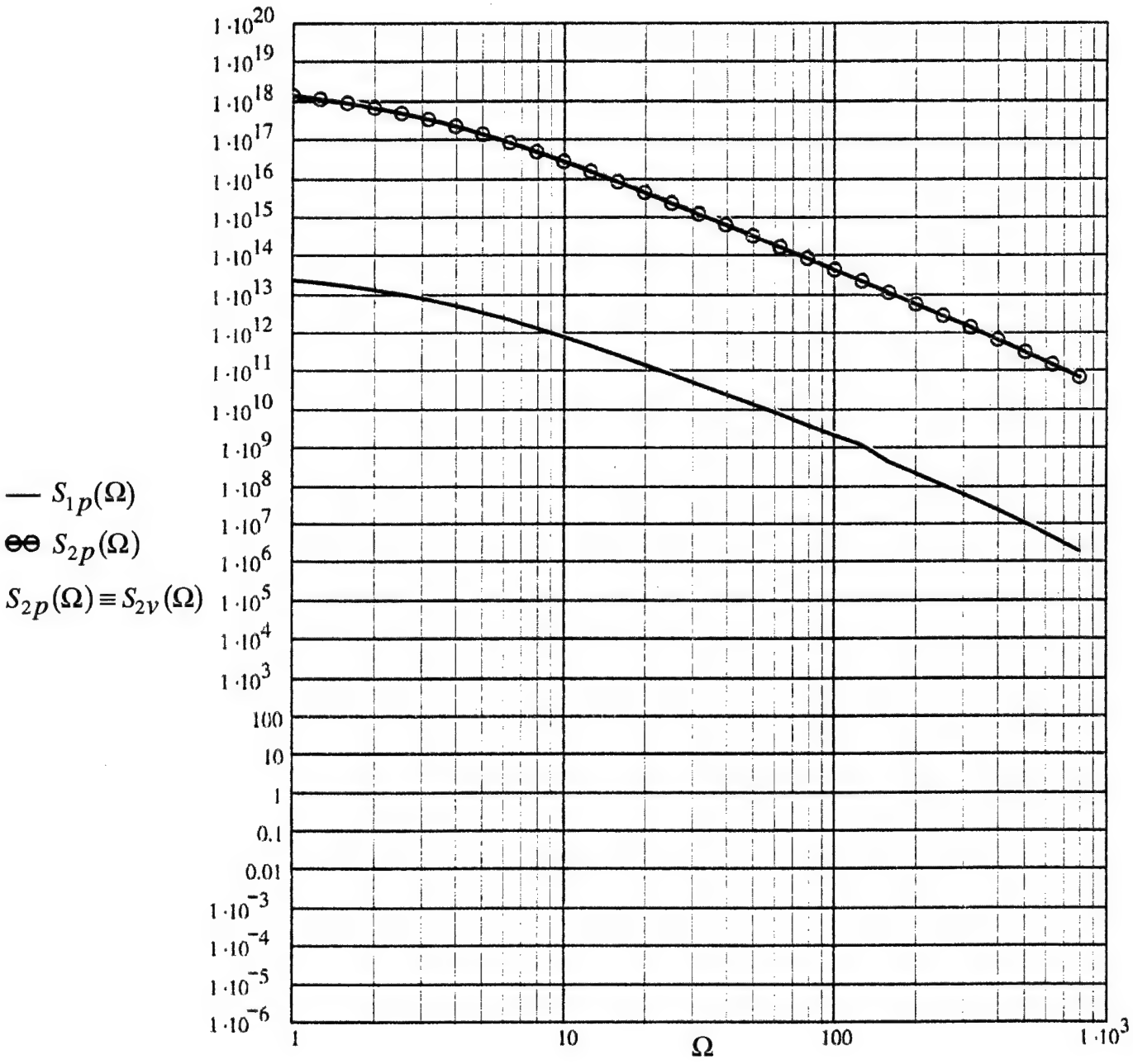

Fig. 17. The normalized outputs to (TBL) $S_{1p}(\Omega)$ and $S_{2p}(\Omega)$ of a pressure transducer on an ideal *rigid* boundary and on an ideal *pressure release* boundary, respectively, as functions of the normalized frequency (Ω); in the displayed range $1 \leq \Omega \leq 10^3$. [cf. Eqs. (62a) and 62d), respectively.] It is noted that $S_{2p}(\Omega)$ is identical to $S_{2v}(\Omega)$; $S_{2p}(\Omega) \equiv S_{2v}(\Omega)$

c. Standard size transducers and blanket-less.

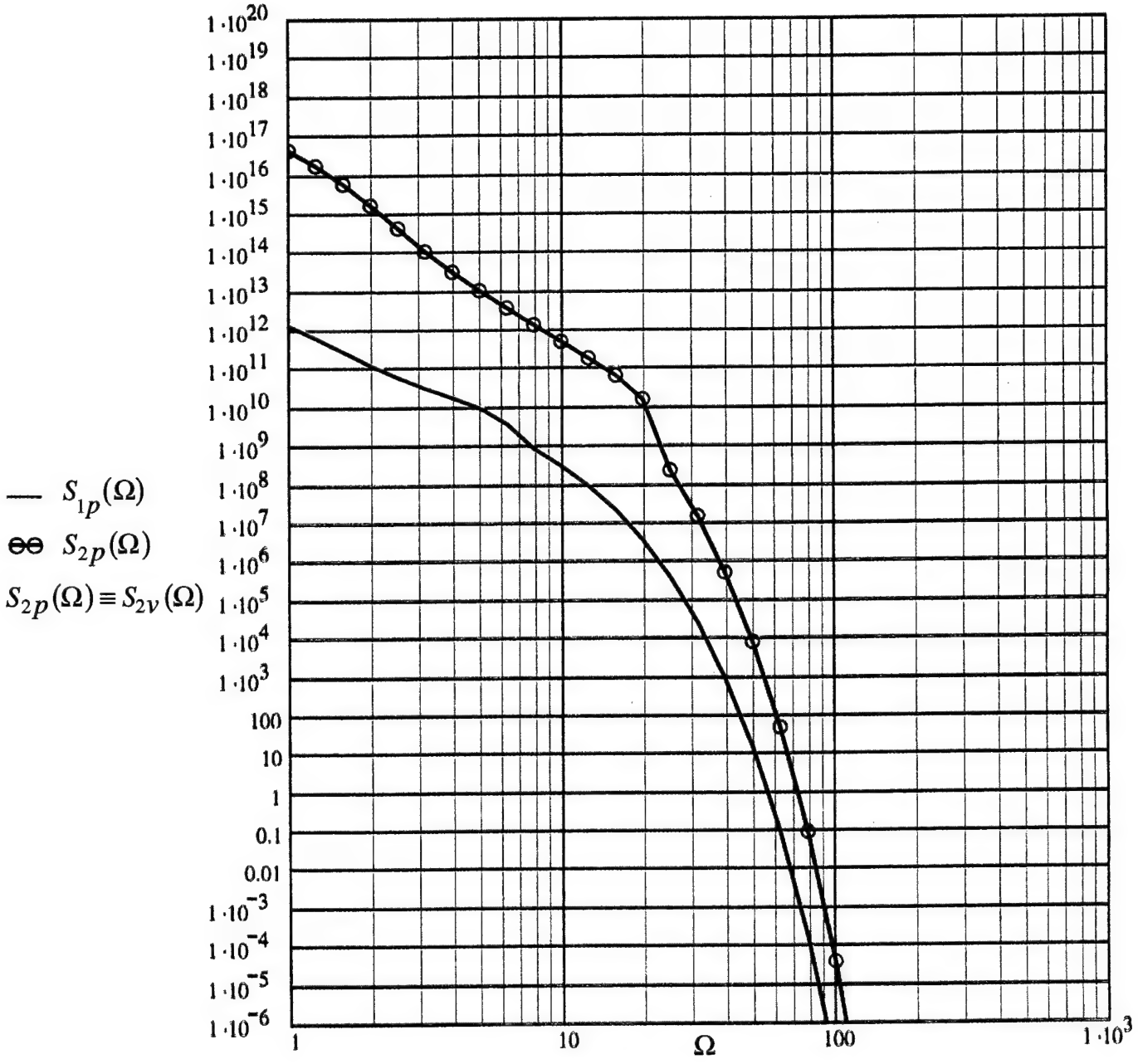

Fig. 17. The normalized outputs to (TBL) $S_{1p}(\Omega)$ and $S_{2p}(\Omega)$ of a pressure transducer on an ideal *rigid* boundary and on an ideal *pressure release* boundary, respectively, as functions of the normalized frequency (Ω); in the displayed range $1 \leq \Omega \leq 10^3$. [cf. Eqs. (62a) and 62d), respectively.] It is noted that $S_{2p}(\Omega)$ is identical to $S_{2v}(\Omega)$; $S_{2p}(\Omega) \equiv S_{2v}(\Omega)$

d. Standard size transducers under a standard blanket.

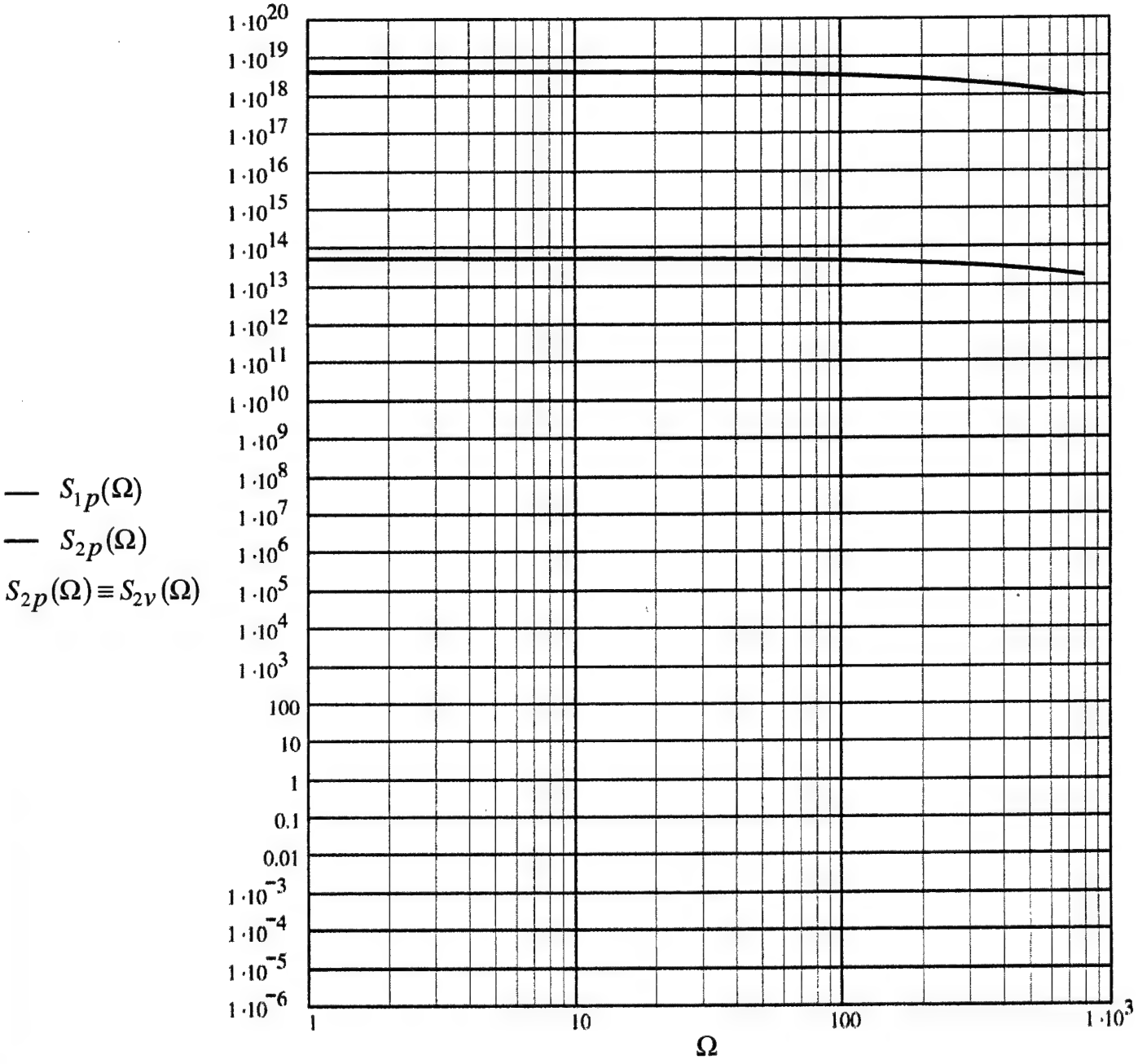

Fig 18a. The normalized outputs to (TBL) $S_{1p}(\Omega)$ and $S_{2v}(\Omega)$of a pressure transducer on an ideal *rigid* conditioning plate and a velocity transducer on an ideal *pressure release* boundary, respectively, as functions of the normalized frequency (Ω); in the displayed range $1 \leq \Omega \leq 10^3$. [cf. Eqs. (61a).] This figure when compared with Fig. 17a, establishes the identity of $S_{2p}(\Omega)$ and $S_{2v}(\Omega)$ for an ideal *pressure release* boundary.

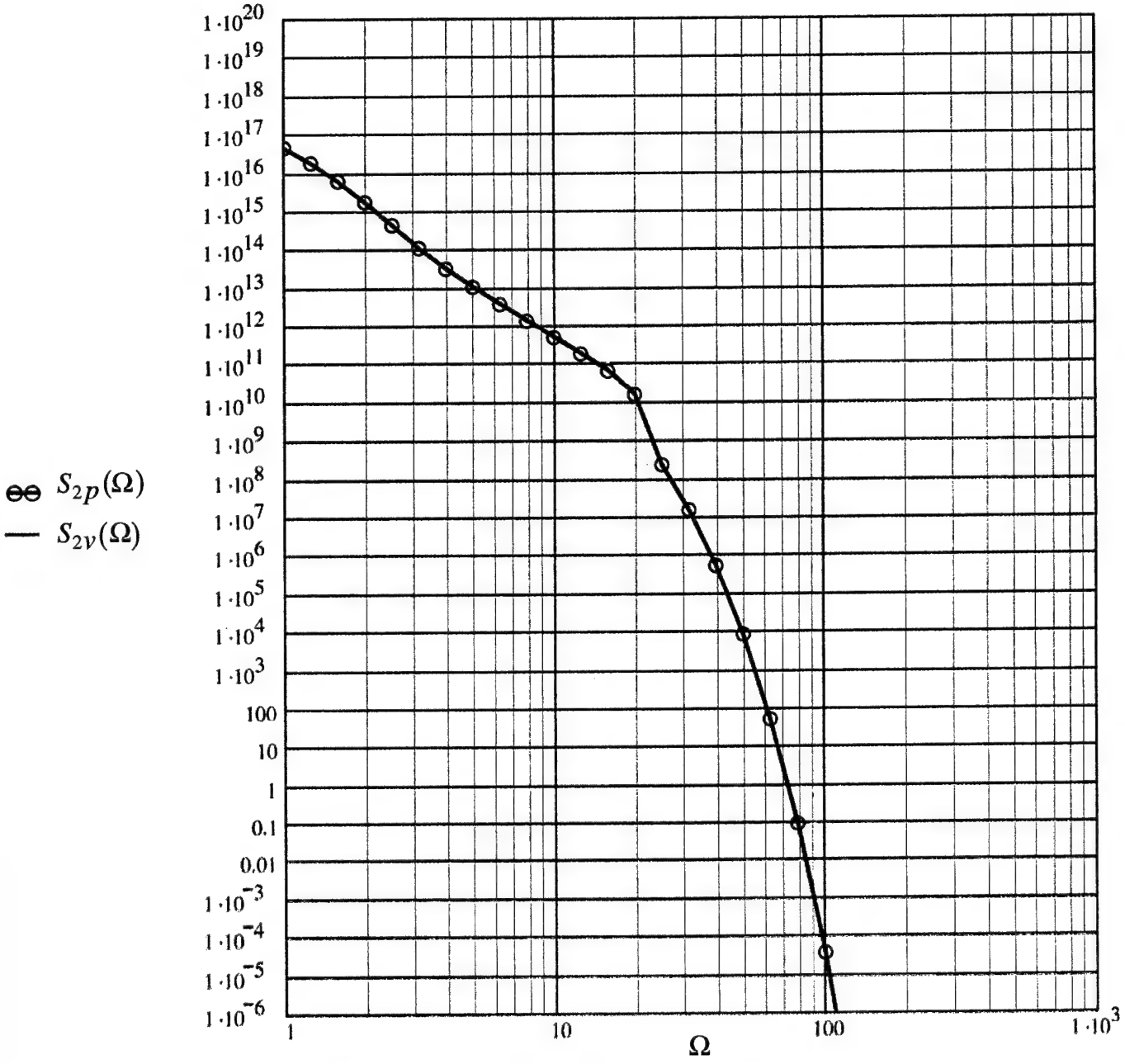

Fig 18b. The normalized outputs to (TBL) $S_{2p}(\Omega)$ and $S_{2v}(\Omega)$ of a pressure transducer and a velocity transducer, respectively, both on an ideal *pressure release* boundary, as functions of the normalized frequency (Ω); in the displayed range $1 \lesssim \Omega \lesssim 10^3$. [cf. Eqs. (61d)]. The identity of $S_{2p}(\Omega)$ and $S_{2v}(\Omega)$ for an ideal *pressure release* boundary is directly established.

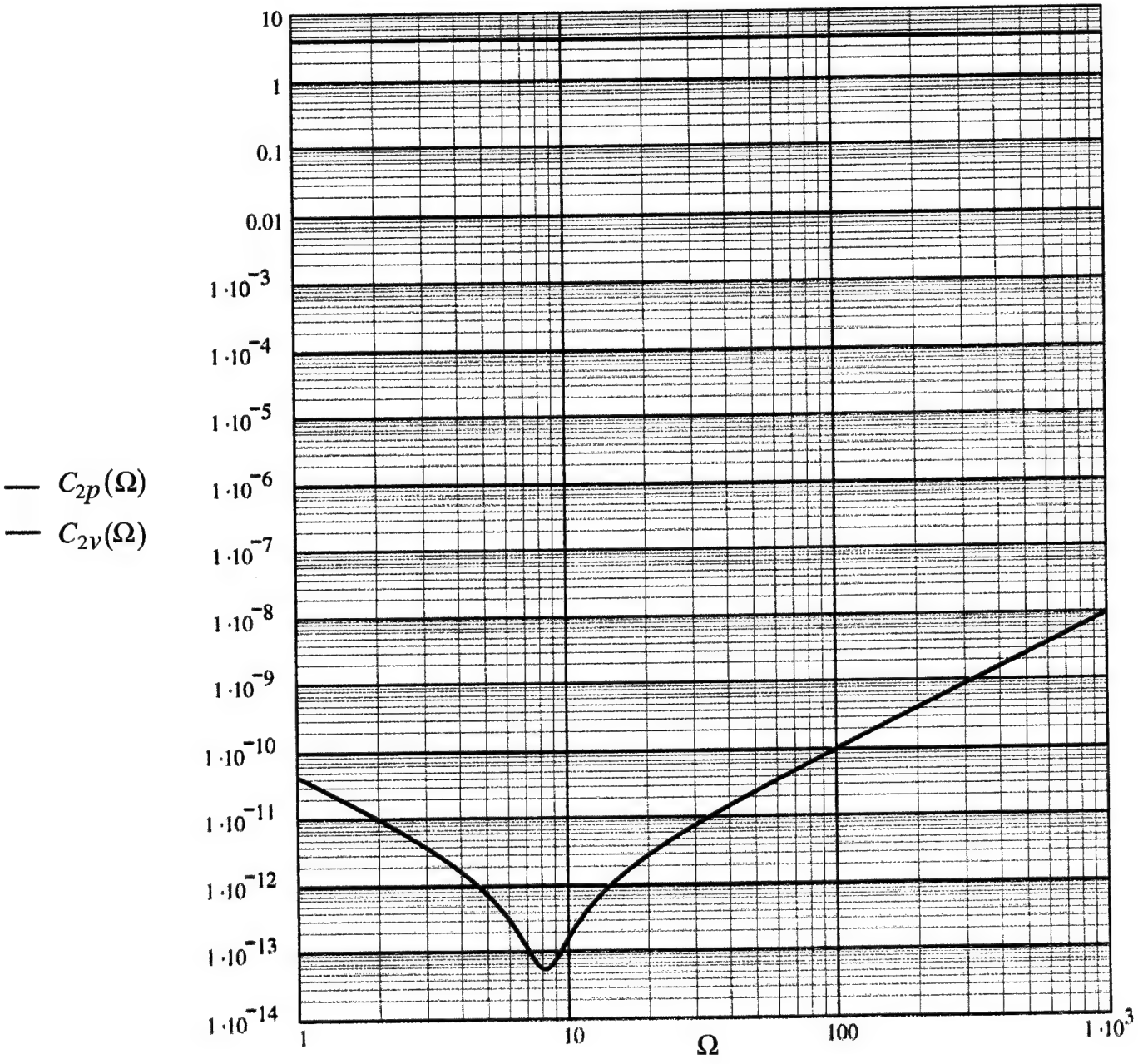

Fig 18c. The sensitivities $C_{2p}(\Omega)$ and $C_{2v}(\Omega)$ of a pressure transducer and a velocity transducer, respectively, both on an ideal *pressure release* boundary, as functions of the normalized frequency (Ω); in the displayed range $1 \leq \Omega \leq 10^3$. [cf. Eqs. (62b) and (62d), respectively, and Fig. 14b.]

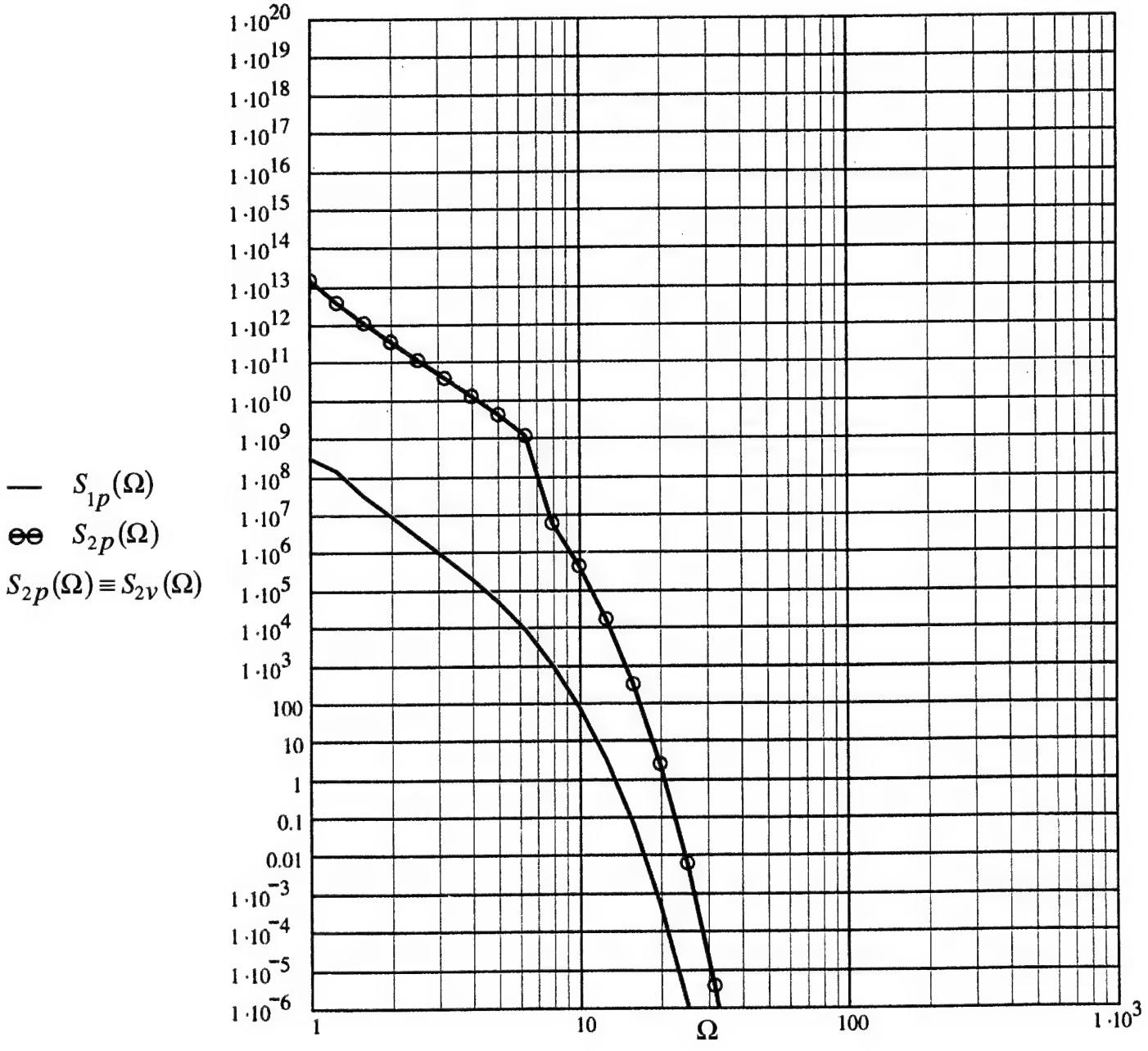

Fig 19. Repeats Fig. 17d, except that (M) is changed from its standard value of $M_o = (15/3)x10^{-3}$ to $M = (5/3)x10^{-3}$.

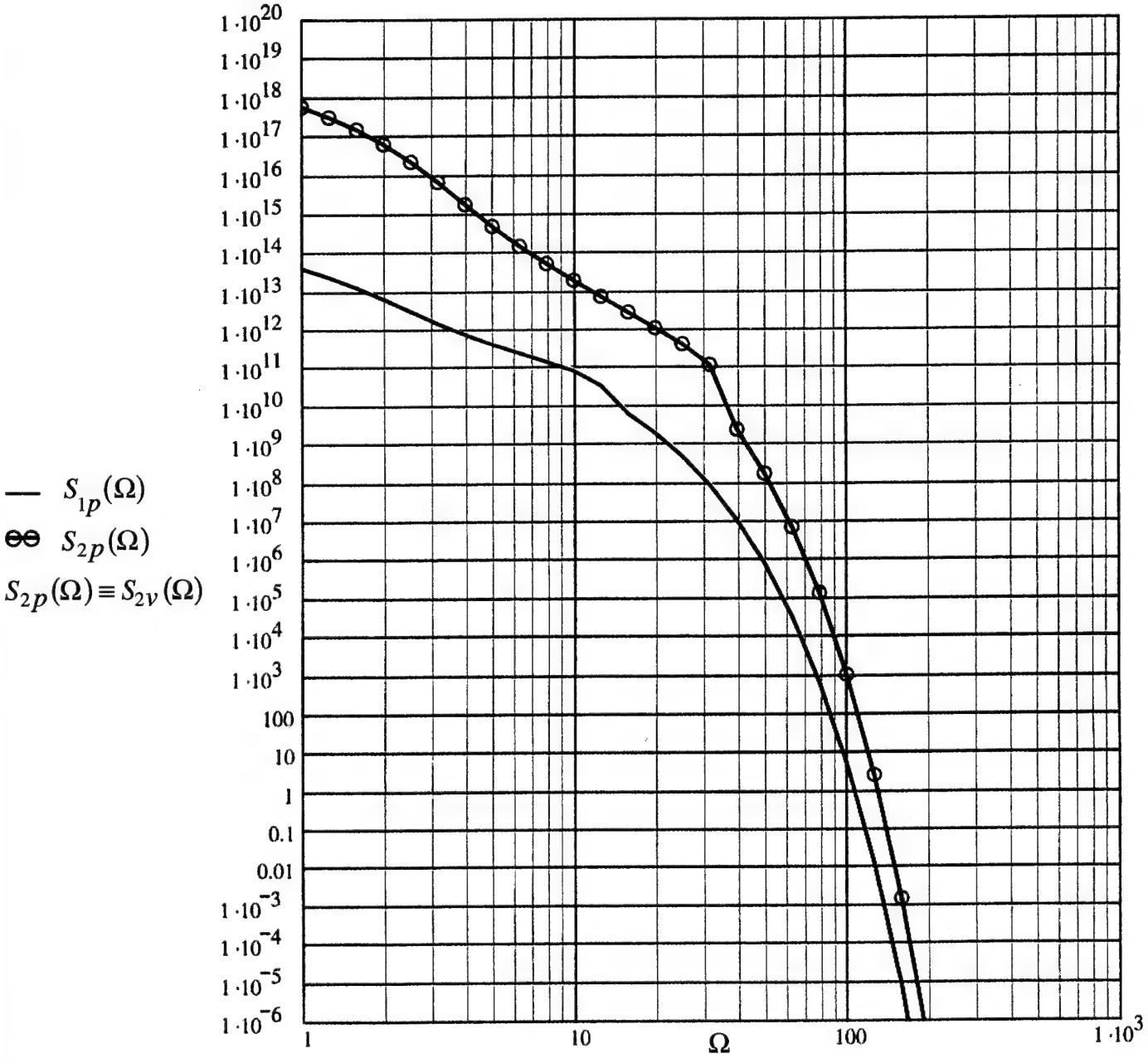

Fig 20. Repeats Fig.17d, except that (M) is changed from its standard value of $M_o = (15/3)x10^{-3}$ to $M = (25/3)x10^{-3}$.

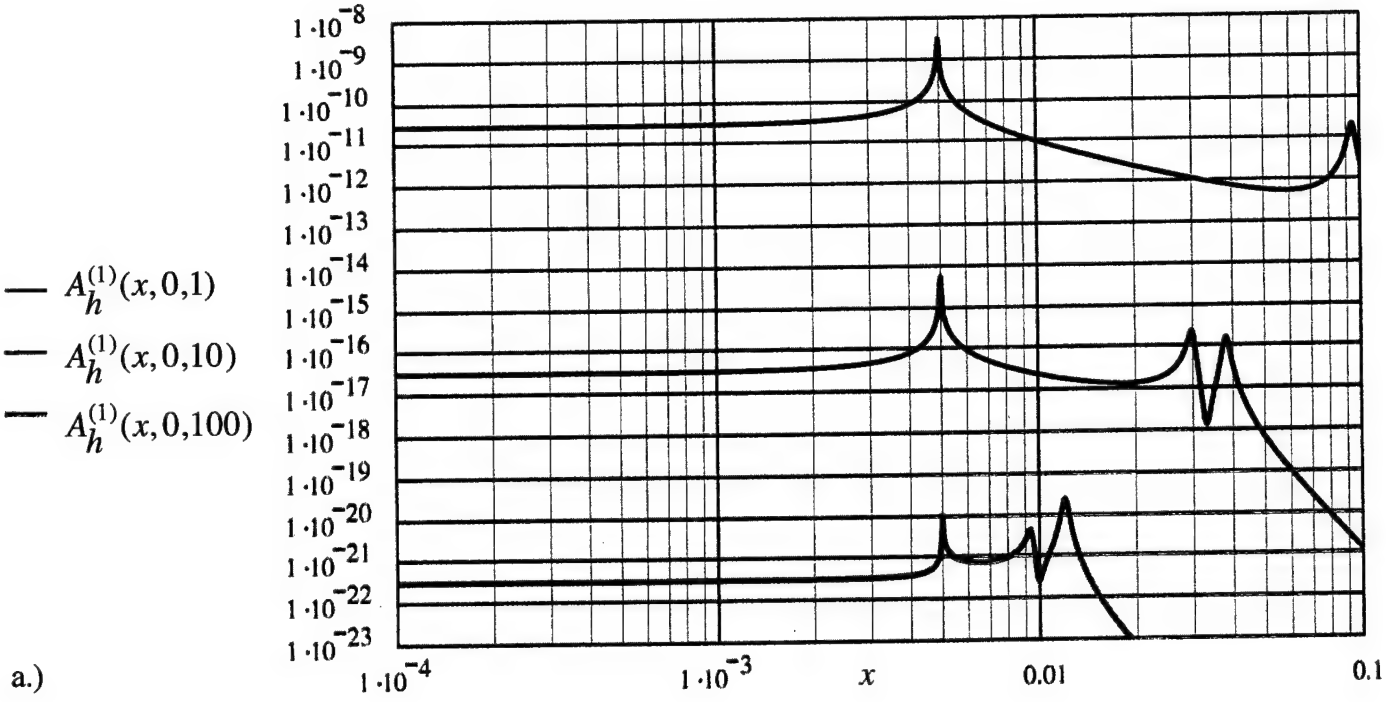

a.)

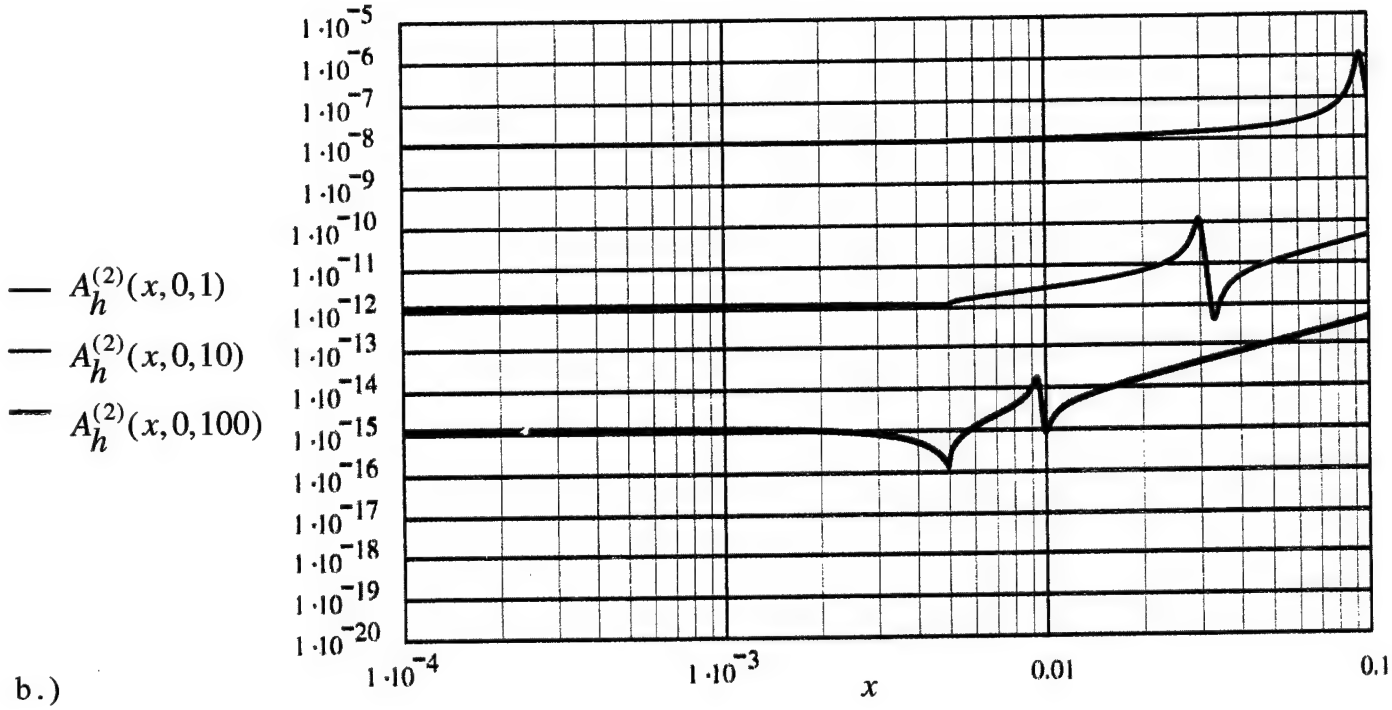

b.)

Fig 21. The anti-radiation properties of the cladding on the hull, in terms of the filtering efficiency $A_h(x,y,\Omega)$ as a function of the normalized wavenumber (x) with $y\to 0$ and for three values of the normalized frequency (Ω); $\Omega=1$, 10 and 100. [The relevant data confined to the supersonic region where $(x<M)$.]

a. With an ideal *rigid* conditioning plate; $A_h^{(1)}(x,y,\Omega)$.

b. With and ideal *pressure release* boundary; $A_h^{(2)}(x,y,\Omega)$.

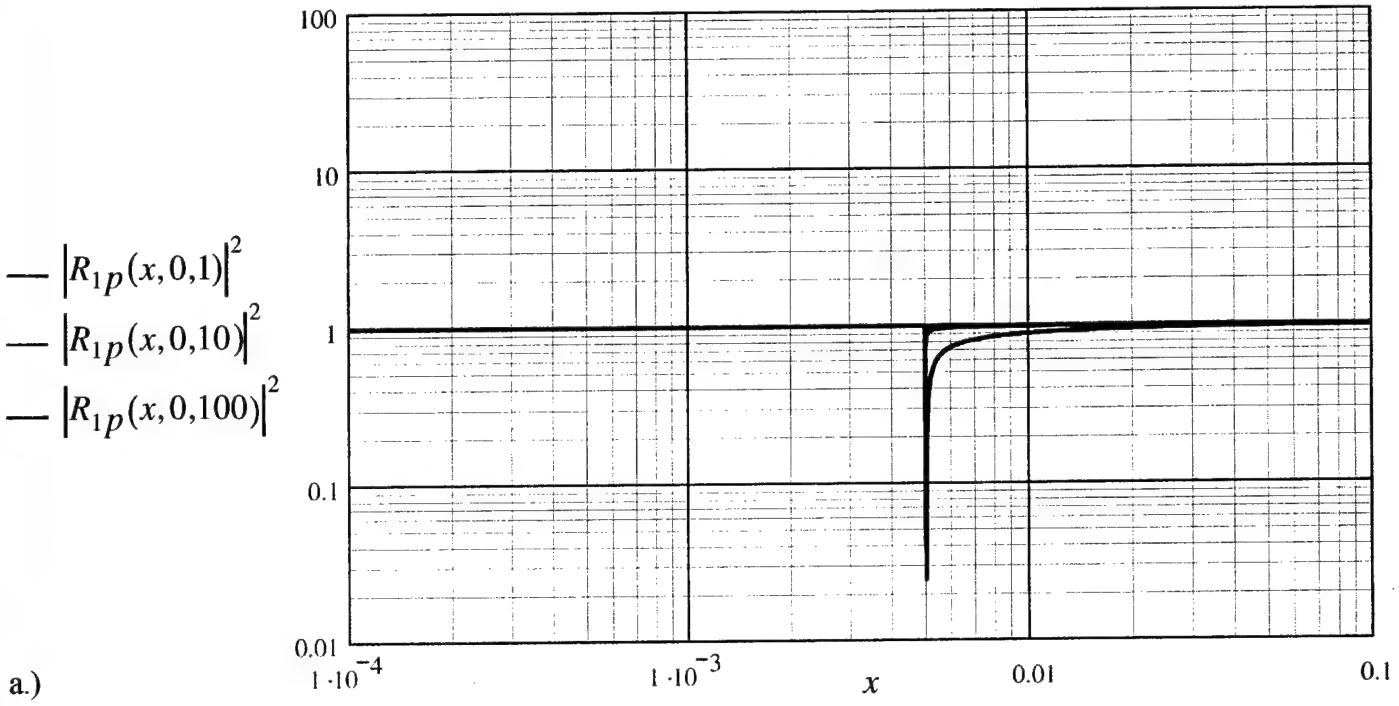

a.)

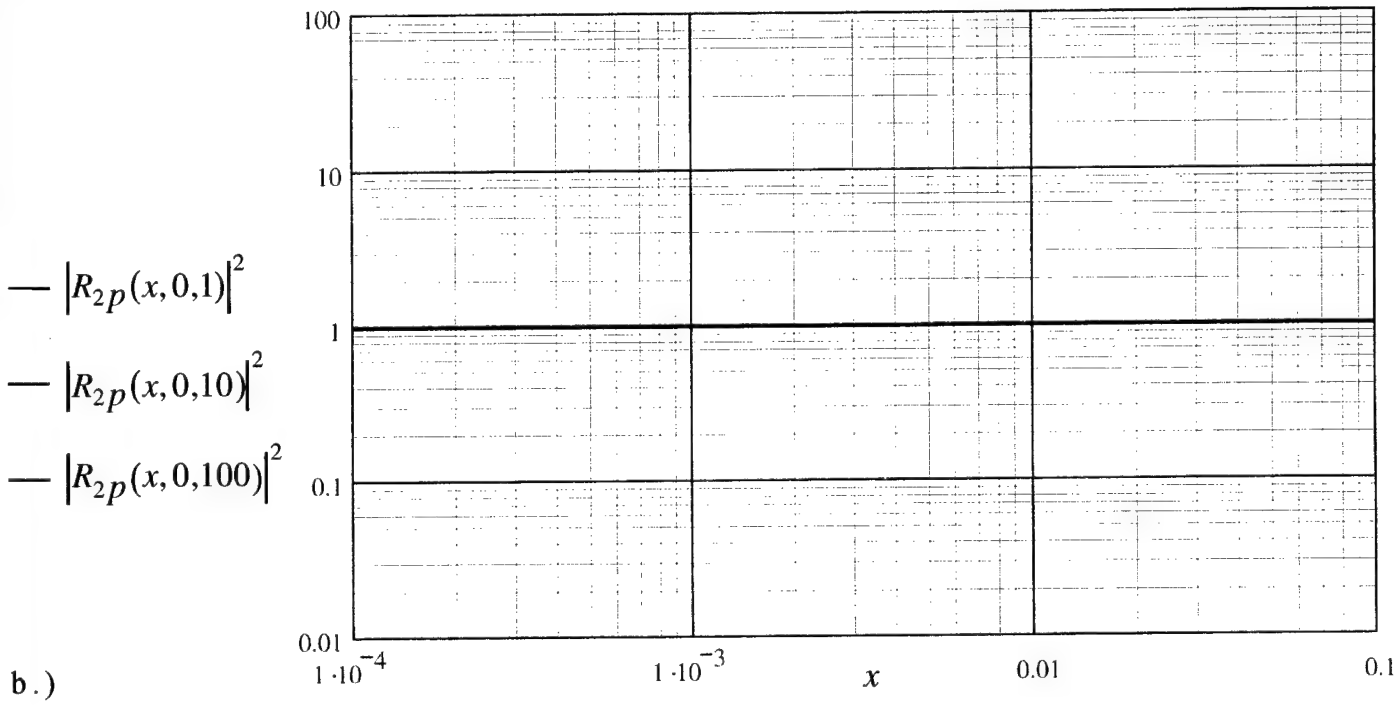

b.)

Fig 22. The specular reflection efficiency $|R(x,y,\Omega)|^2$ of the cladded hull, as a function of the normalized wavenumber (x) with $y \to 0$ and for three values of the normalized frequency (Ω); $\Omega = 1$, 10 and 100. [The relevant data are confined to supersonic region where $(x < M)$.]

a. With an ideal *rigid* conditioning plate; $|R_{1p}(x,y,\Omega)|^2$.

b. With and ideal *pressure release* boundary; $|R_{2p}(x,y,\Omega)|^2$.

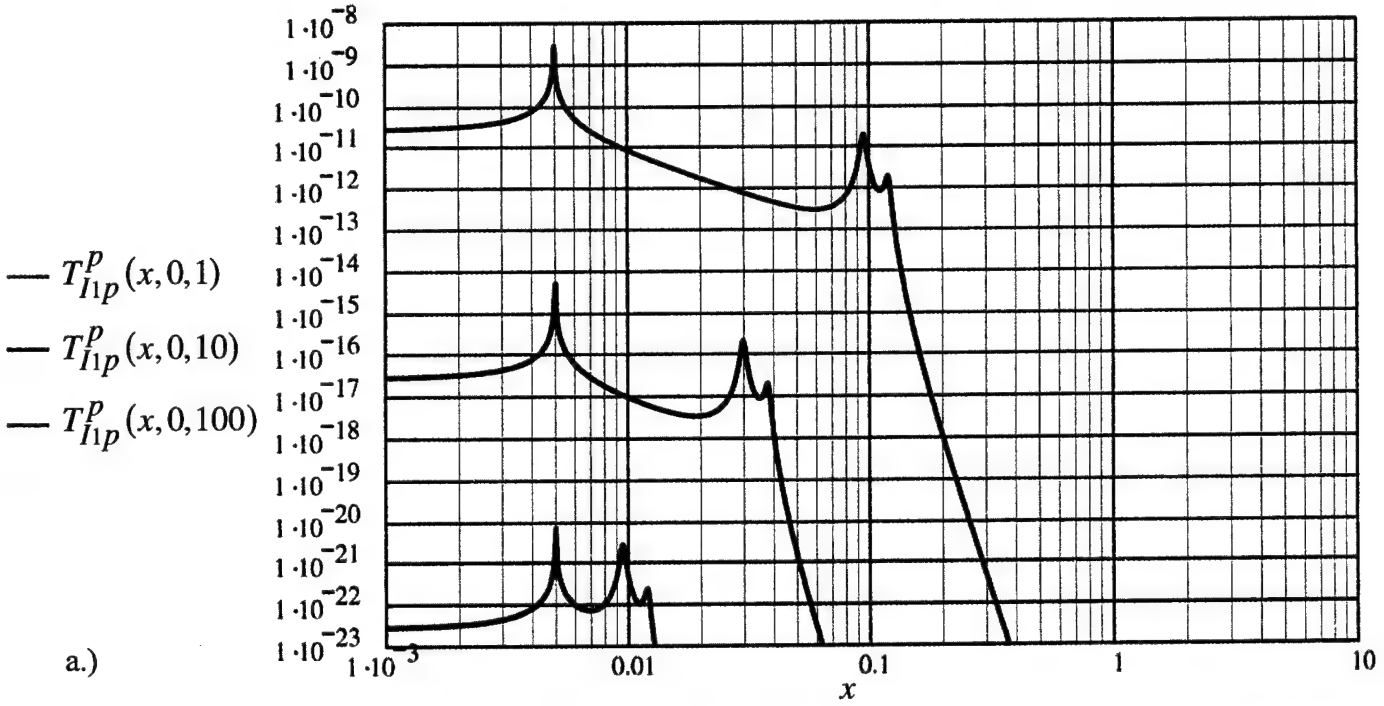

a.)

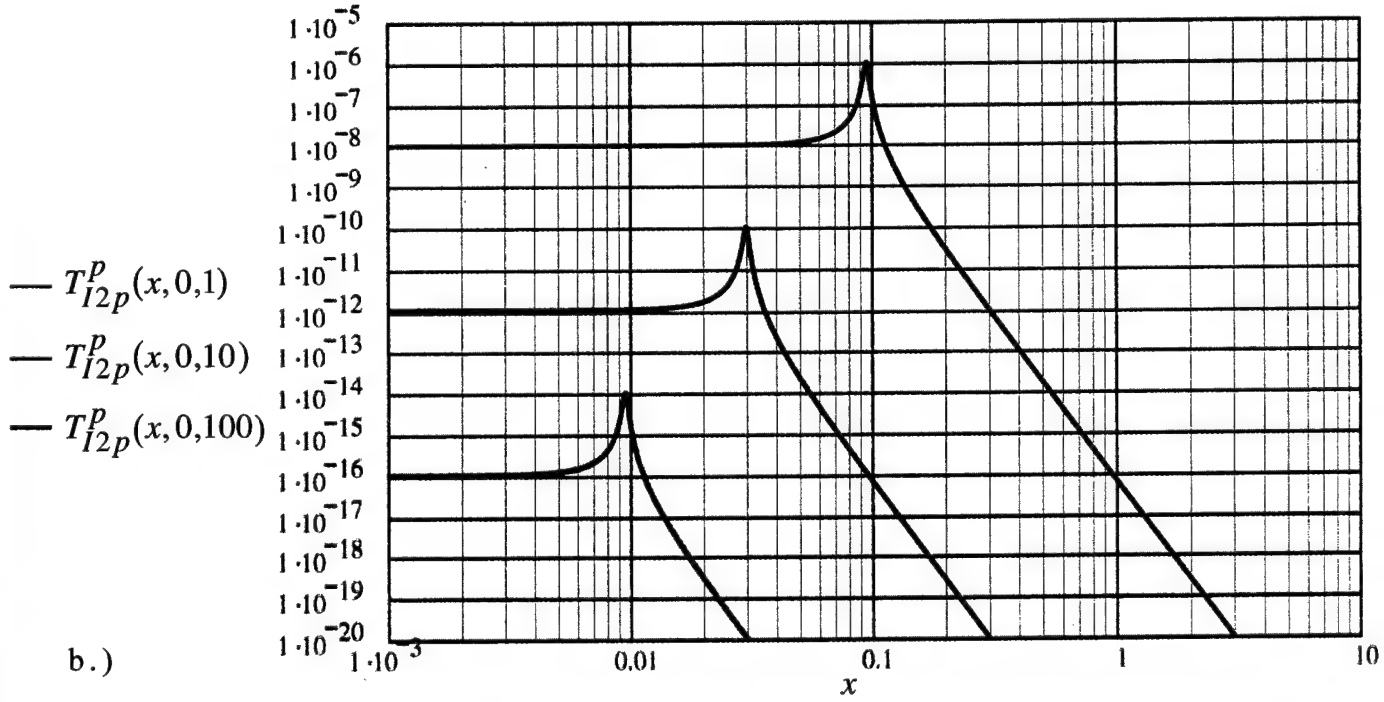

b.)

Fig 23. The transference $T(x,y,\Omega)$ from the hull to the boundary on which the transducers are flush-mounted, as a function of the normalized wavenumber (x) with $y \to 0$ and for three values of the normalized frequency (Ω); $\Omega = 1$, 10 and 100.

a. $T^p_{I1p}(x,y,\Omega)$ is the transference of a drive on the hull to a pressure on the boundary. The ideal *rigid* conditioning plate is present.

b. $T^p_{I2p}(x,y,\Omega)$ as in (a), except that the conditioning plate is removed, thereby exposing a *pressure release* boundary.

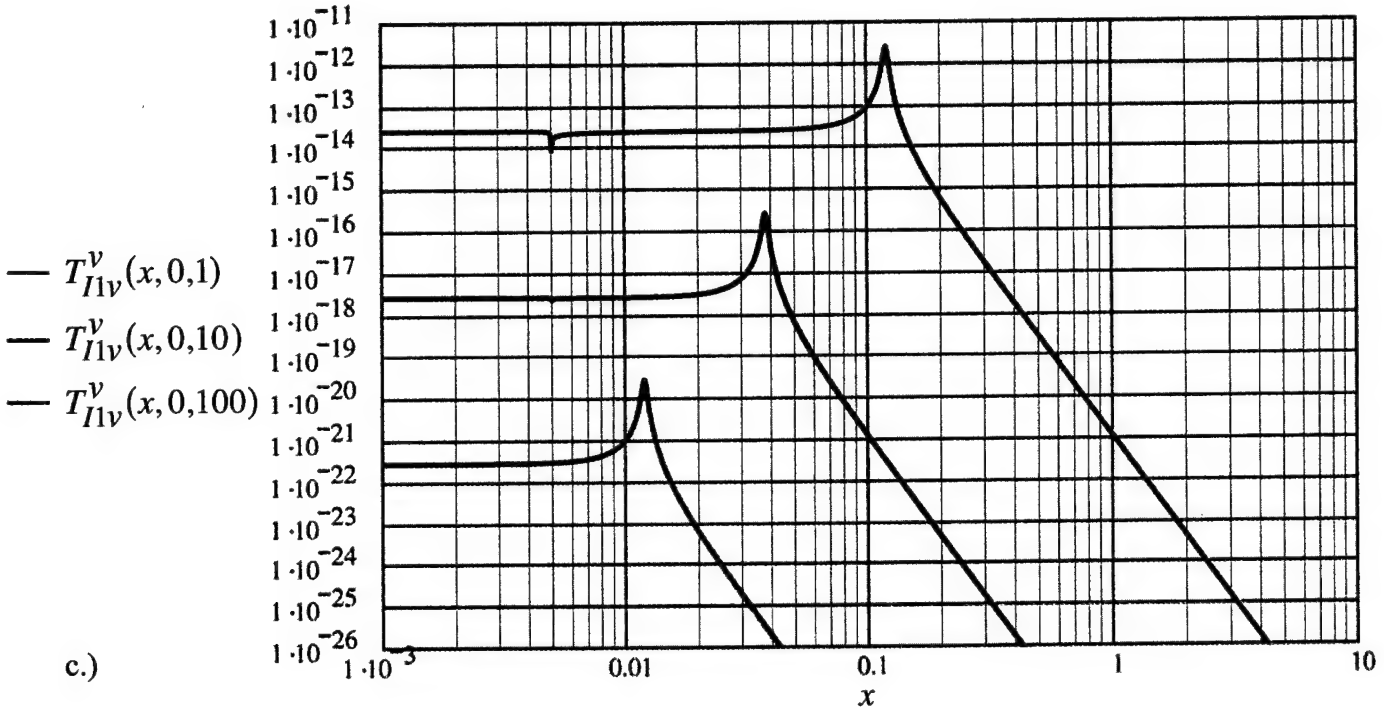

c.)

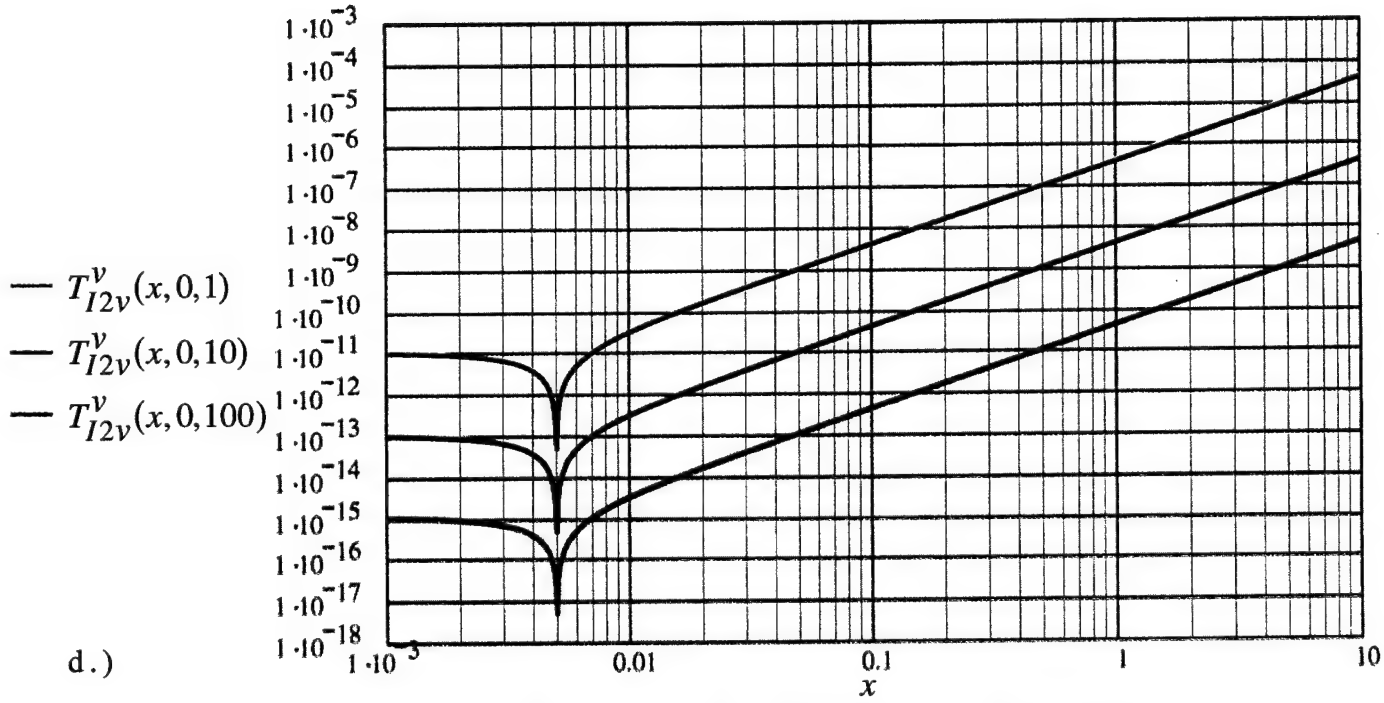

d.)

Fig 23. The transference $T(x,y,\Omega)$ from the hull to the boundary on which the transducers are flush-mounted, as a function of the normalized wavenumber (x) with $y \to 0$ and for three values of the normalized frequency (Ω); $\Omega = 1$, 10 and 100.

c. $T^v_{I1v}(x,y,\Omega)$ is the transference of a velocity on the hull to a velocity on the boundary. The ideal *rigid* conditioning plate is present.

d. $T^v_{I2v}(x,y,\Omega)$ as in (c), except that the conditioning plate is removed, thereby, exposing a *pressure release* boundary.

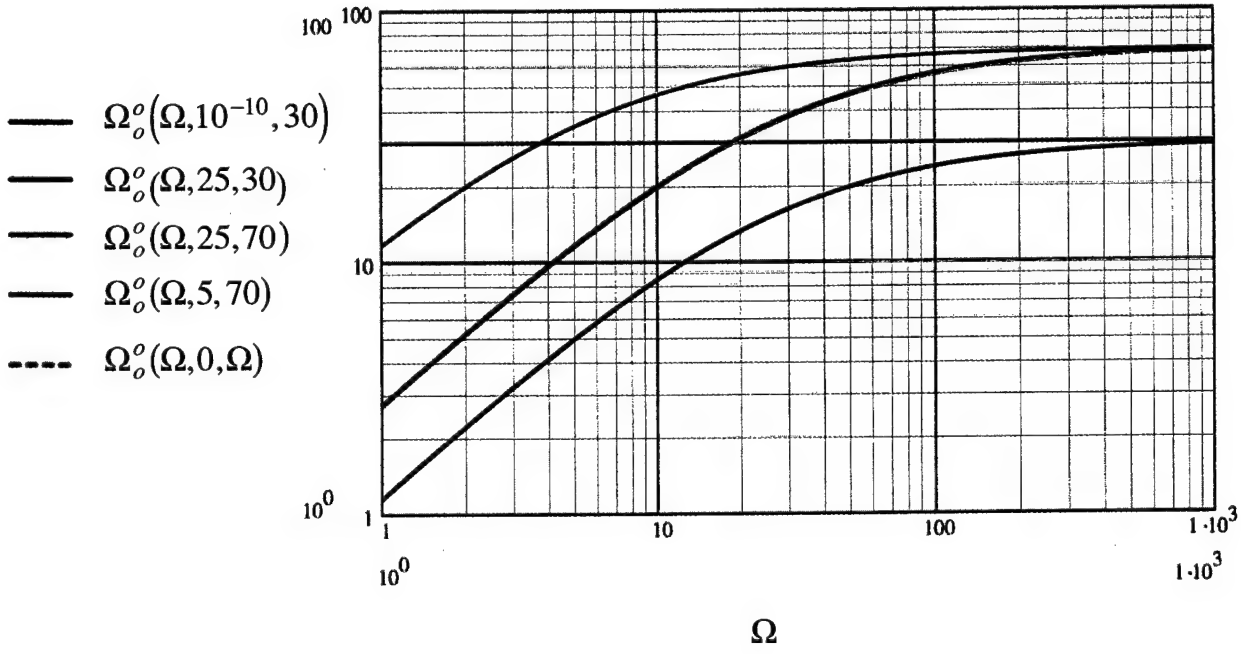

Fig 24. The measures of the surface stiffness of the compliant layer in terms of the normalized resonance frequency (Ω_o^o), as a function of the normalized frequency (Ω); $\Omega_o^o\ (\Omega,\Omega_s\Omega^o) = \Omega^o[\Omega(\Omega+\Omega_s)^{-1}]$, in the displayed range $1 \leq \Omega \leq 10^3$. [cf. Eq. (66).] The different curves are represented by different pairs of (Ω_s,Ω_o). The normalized resonance frequency is with respect to the surface mass of the hull. [cf. Eqs. (67b), (67d), (67e) and (67f).] Dashed curve is derived by $\Omega_s = 0$ and $\Omega^o = \Omega$.

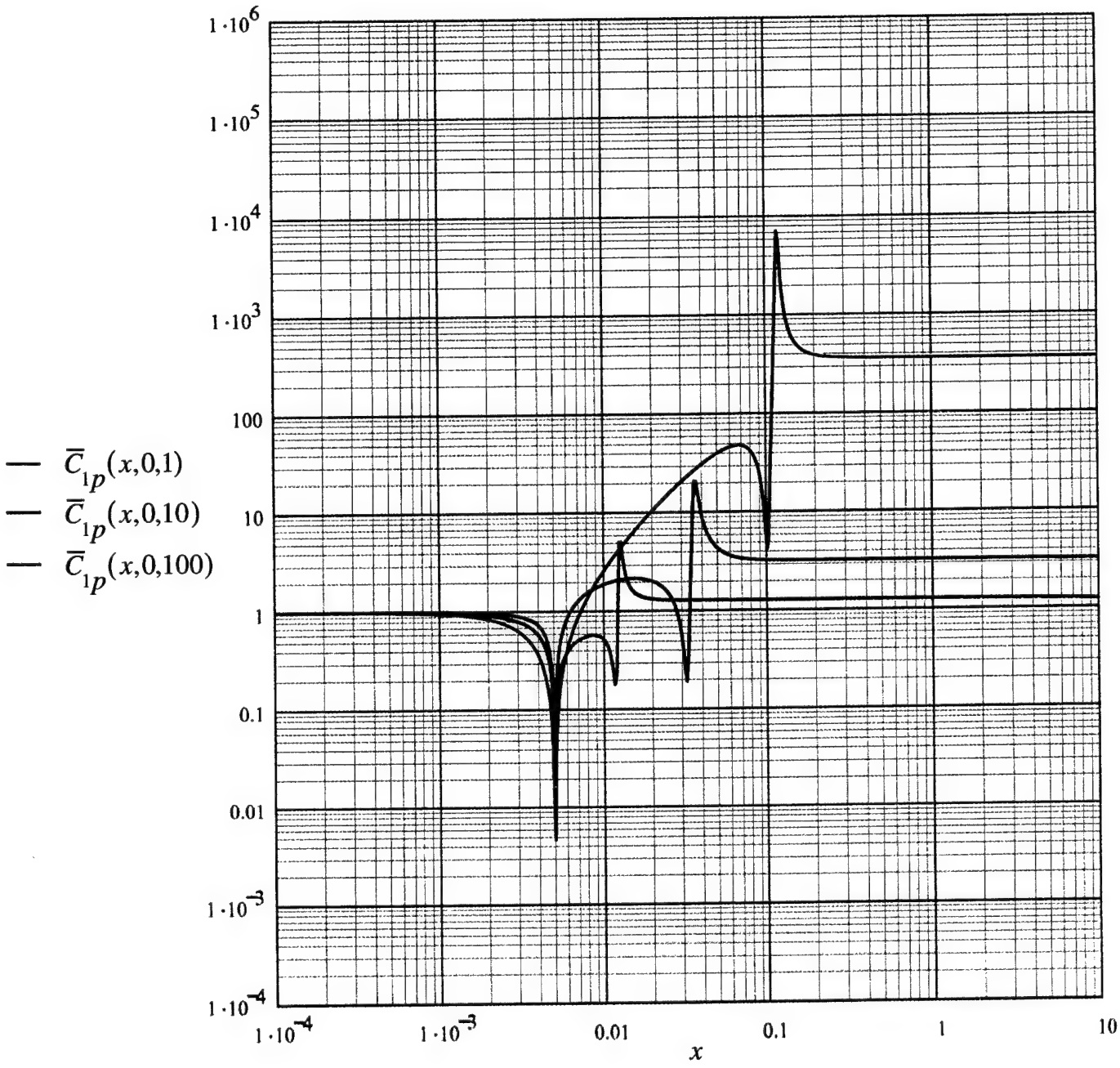

Fig 25. The filtering efficiencies, as functions of the normalized wavenumber (x) with $y \to 0$ and for three values of the normalized frequency (Ω); $\Omega = 1$, 10 and 100, of uncladded point transducers on a boundary composed of a compliant layer that is given ten (10) measures of surface stiffness.

a. A pressure transducer with a standard conditioning plate. [cf. Eq. (56a).]

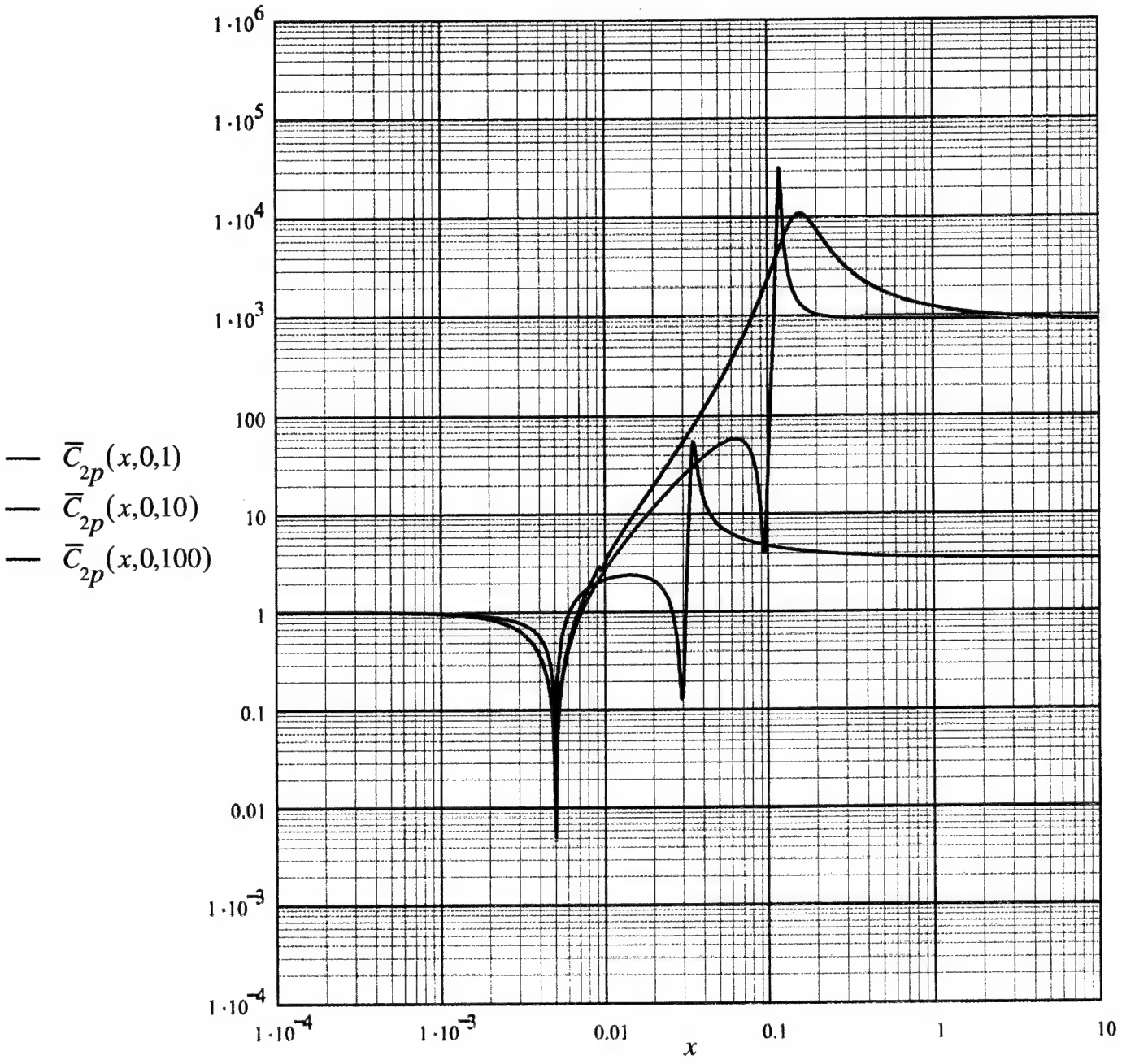

Fig 25. The filtering efficiencies, as functions of the normalized wavenumber (x) with $y \to 0$ and for three values of the normalized frequency (Ω); $\Omega = 1$, 10 and 100, of uncladded point transducers on a boundary composed of a compliant layer that is given ten (10) measures of surface stiffness.

b. A pressure transducer without a conditioning plate. [cf. Eq. (56b).]

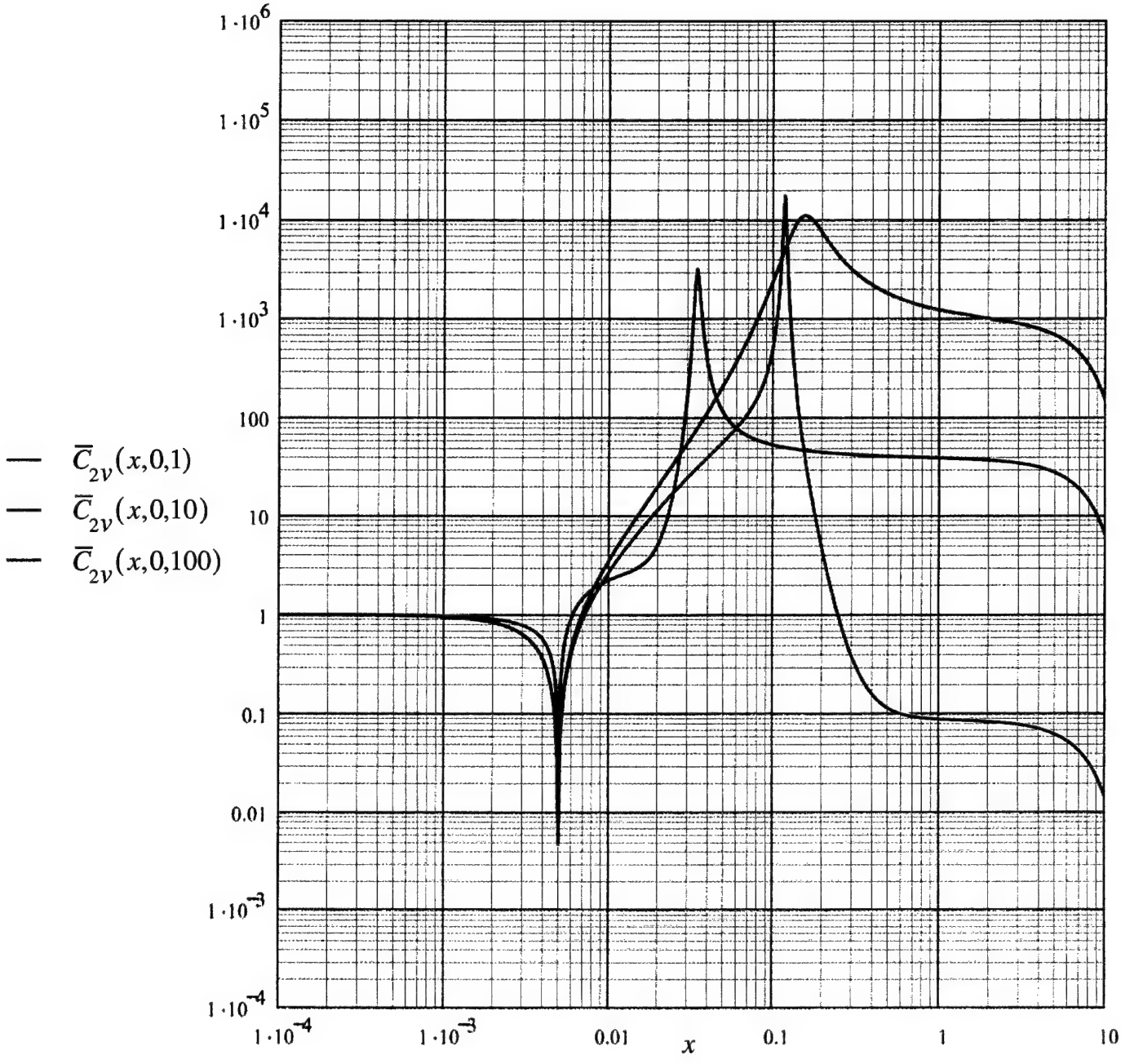

Fig 25. The filtering efficiencies, as functions of the normalized wavenumber (x) with $y \to 0$ and for three values of the normalized frequency (Ω); $\Omega = 1$, 10 and 100, of uncladded point transducers on a boundary composed of a compliant layer that is given ten (10) measures of surface stiffness.

c. A velocity transducer without a condition plate. [cf. Eq. (57b).]

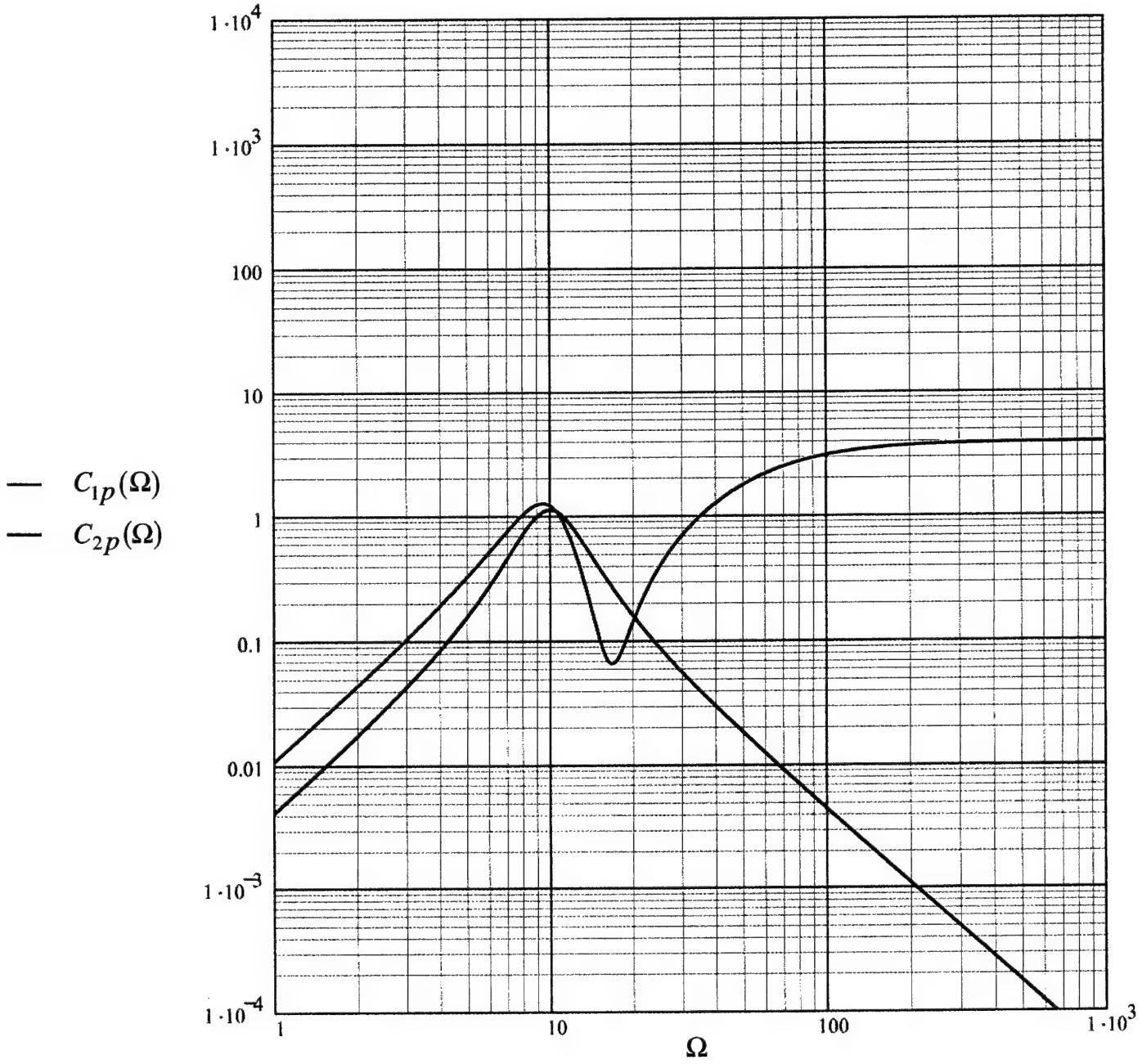

Fig 26. The sensitivities, as functions of the normalized frequency (Ω), of point transducers on a boundary composed of a compliant layer that is given ten (10) measures of surface stiffness.

a. Comparison between a pressure transducer with and without a standard conditioning plate. [cf. Eqs. (59a) and (59b).]

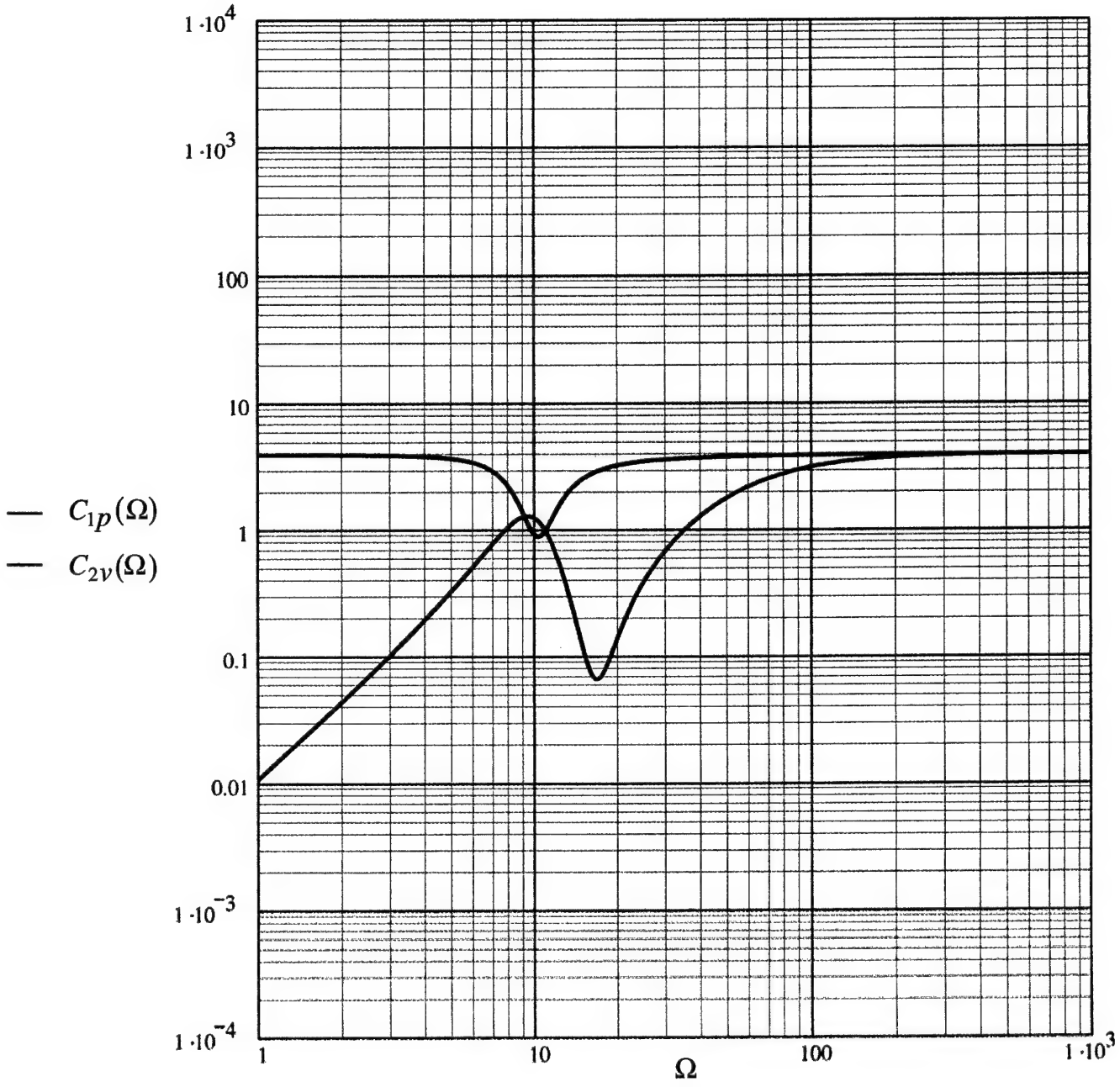

Fig 26. The sensitivities, as functions of the normalized frequency (Ω), of point transducers on a boundary composed of a compliant layer that is given ten (10) measures of surface stiffness.

b. Comparison between a pressure transducer with a standard conditioning plate and a velocity transducer (without conditioning plate). [cf. Eqs. (59a) and (60b).]

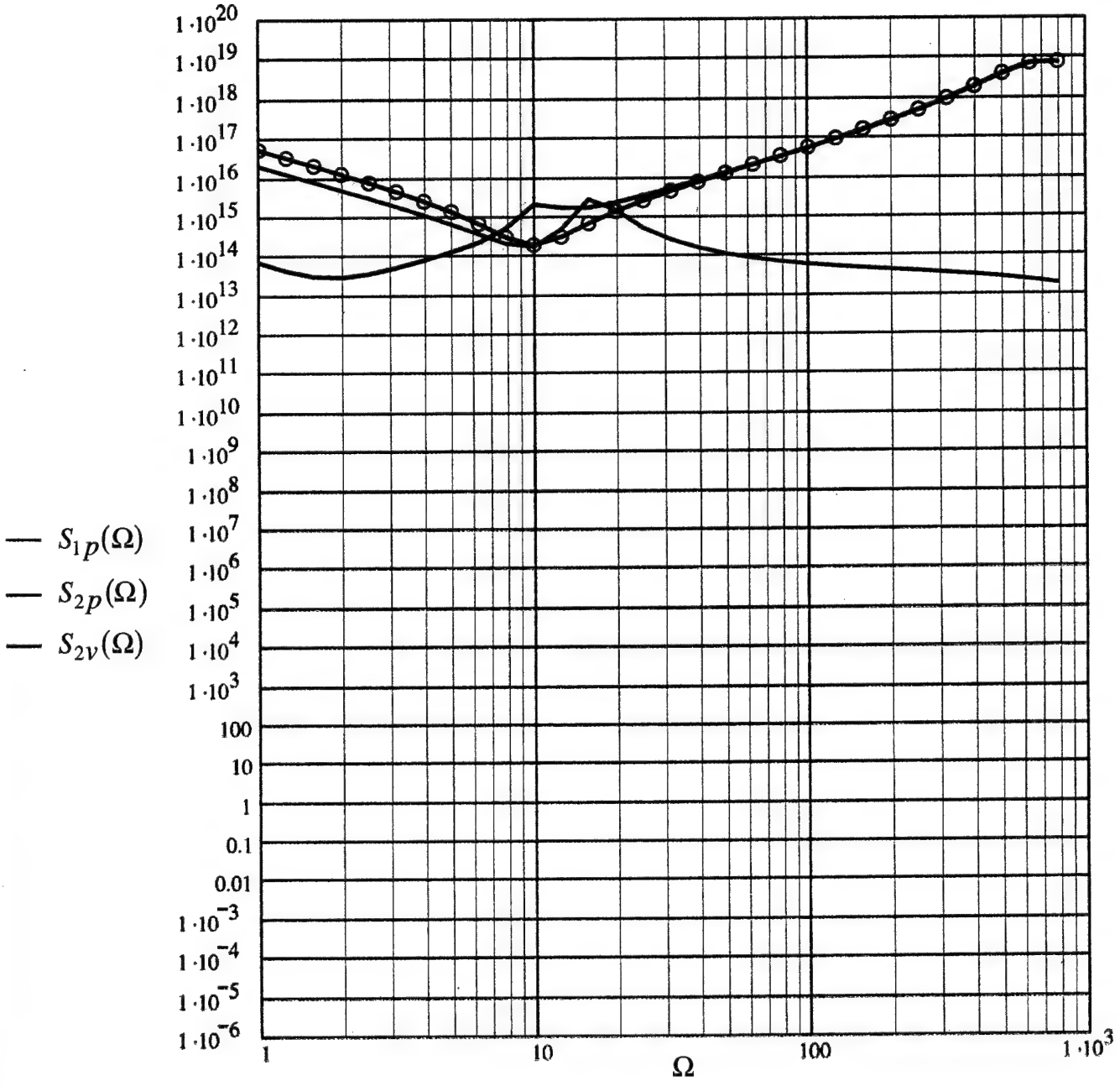

Fig 27. The normalized outputs to (TBL) $S_{1p}(\Omega)$, $S_{2p}(\Omega)$ and $S_{2v}(\Omega)$, as functions of the normalized frequency (Ω), for uncladded point transducers. [cf. Eqs. (62a), (62b) and (62d).]

a. A boundary composed of a compliant layer that is given ten (10) measures of surface stiffness. [cf. Eq. (67a).]

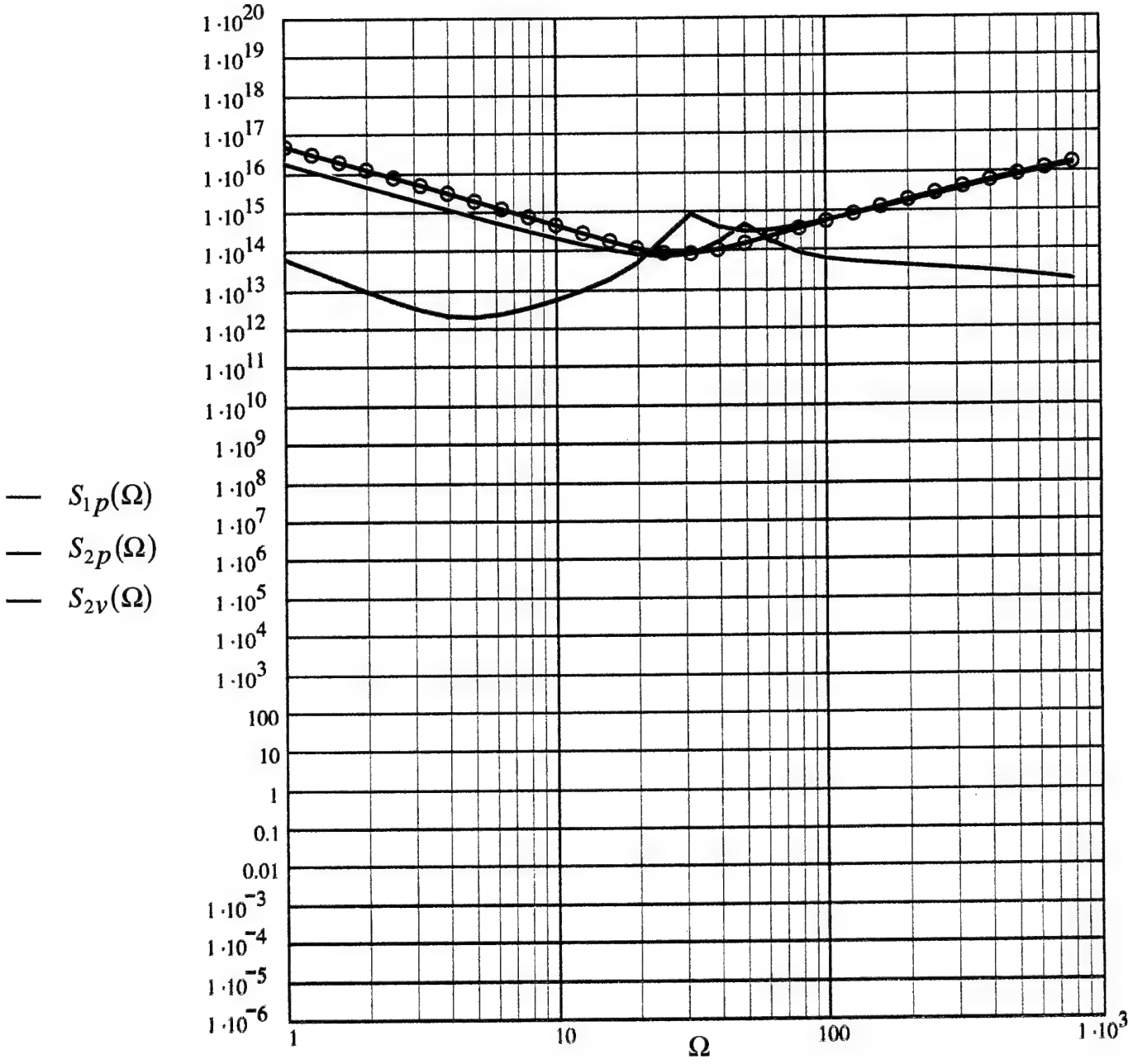

Fig 27. The normalized outputs to (TBL) $S_{1p}(\Omega)$, $S_{2p}(\Omega)$ and $S_{2v}(\Omega)$, as functions of the normalized frequency (Ω), for uncladded point transducers. [cf. Eqs. (62a), (62b) and (62d).]

b. A boundary composed of a compliant layer that is given thirty (30) measures of surface stiffness. [cf. Eq. (67b).]

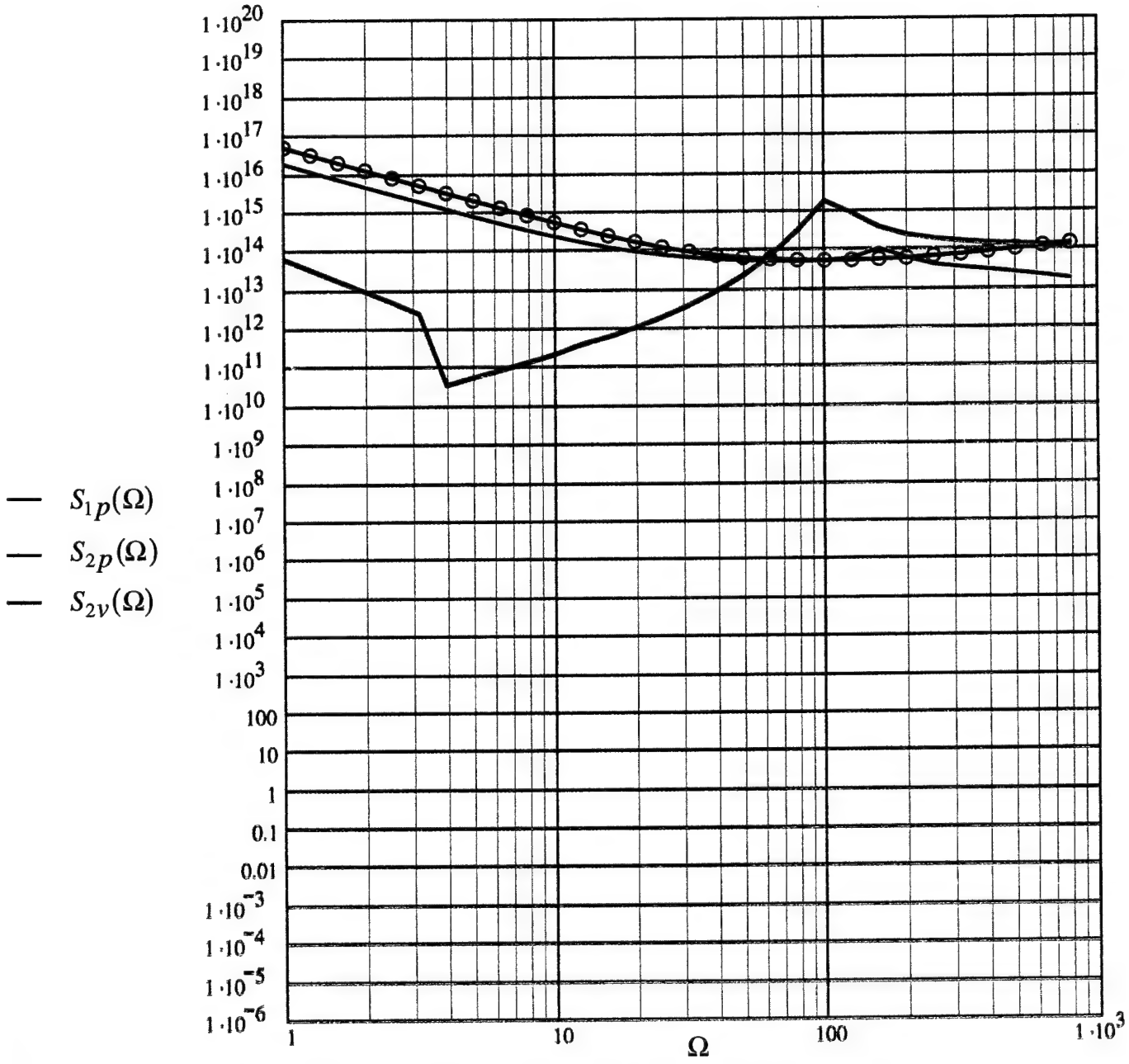

Fig 27. The normalized outputs to (TBL) $S_{1p}(\Omega)$, $S_{2p}(\Omega)$ and $S_{2v}(\Omega)$, as functions of the normalized frequency (Ω), for uncladded point transducers. [cf. Eqs. (62a), (62b) and (62d).]

c. A boundary composed of a compliant layer that is given one hundred (100) measures of surface stiffness. [cf. Eq. (67c).]

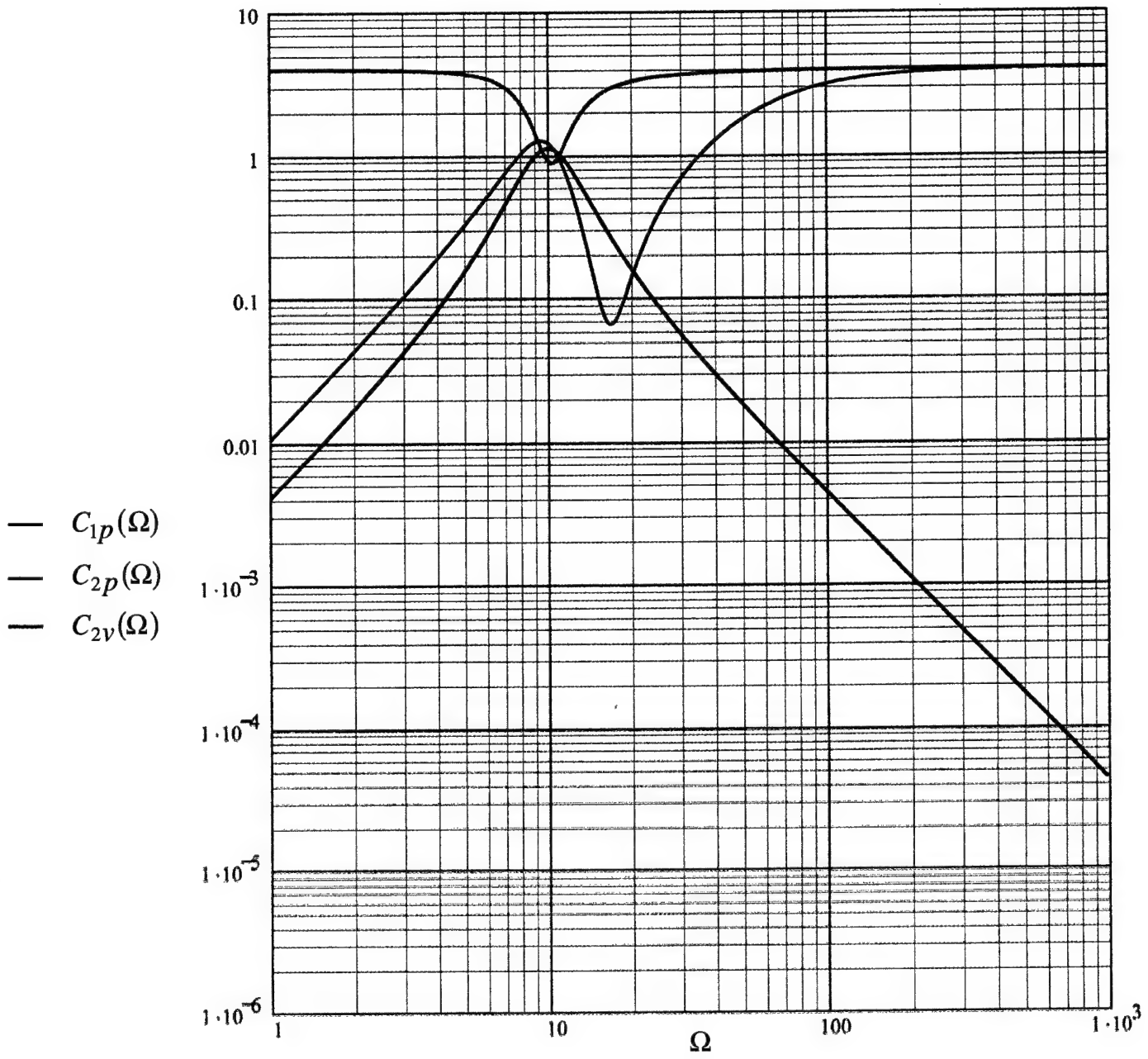

Fig 28. The sensitivities $C_{1p}(\Omega)$, $C_{2p}(\Omega)$ and $C_{2v}(\Omega)$ of a pressure transducer with and without a standard conditioning plate and a velocity transducer without a conditioning plate, respectively, as functions of the normalized frequency (Ω). [cf. Eqs. (59a), (59b), and (60b).]

a. A boundary composed of a compliant layer that is given ten (10) measures of surface stiffness. [cf. Eq. (67a) and Fig. 27a.]

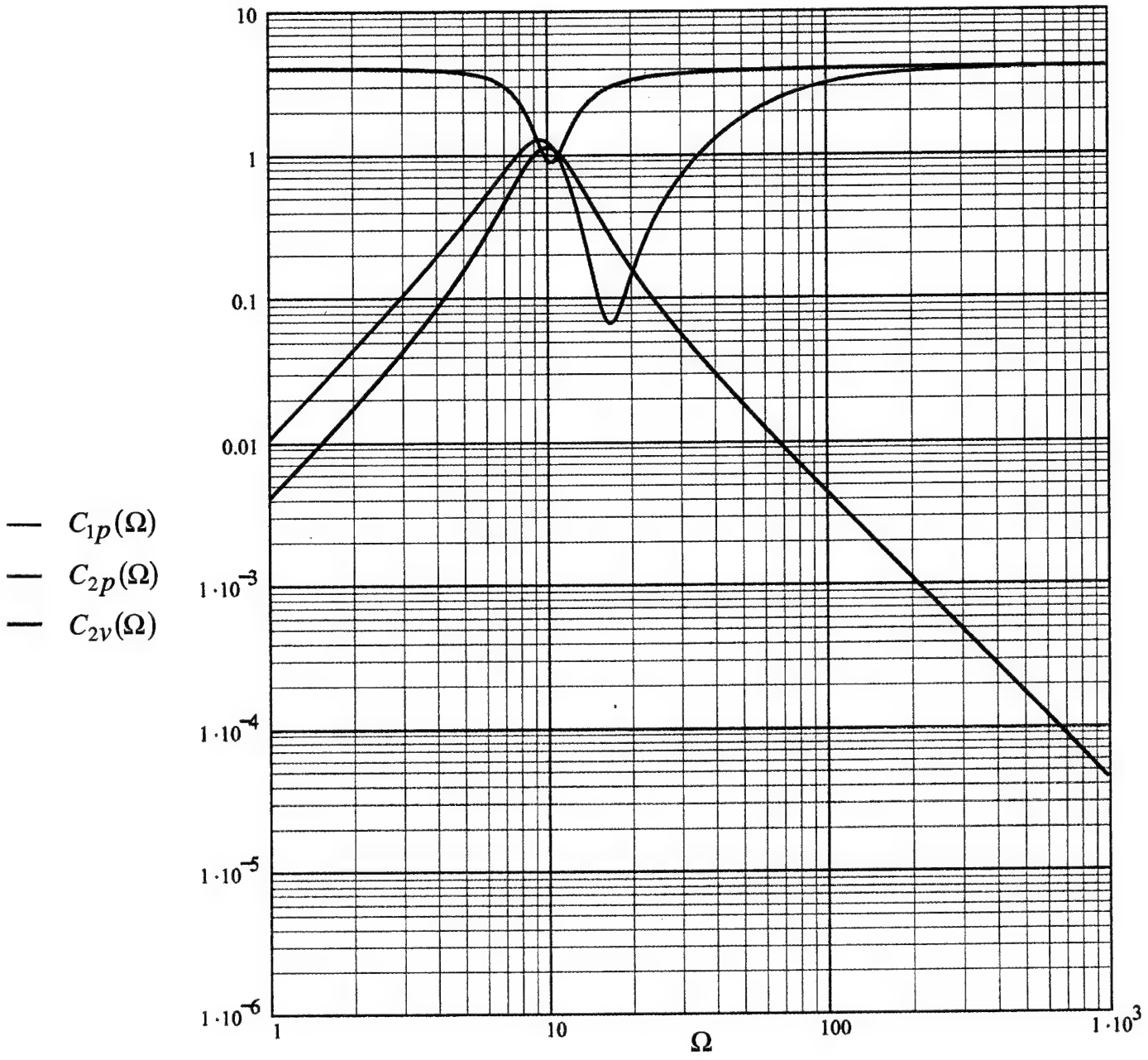

Fig 28. The sensitivities $C_{1p}(\Omega)$, $C_{2p}(\Omega)$ and $C_{2v}(\Omega)$ of a pressure transducer with and without a standard conditioning plate and a velocity transducer without a conditioning plate, respectively, as functions of the normalized frequency (Ω). [cf. Eqs. (59a), (59b), and (60b).]

b. A boundary composed of a compliant layer that is given thirty (30) measures of surface stiffness. [cf. Eq. (67b) and Fig. 27b.]

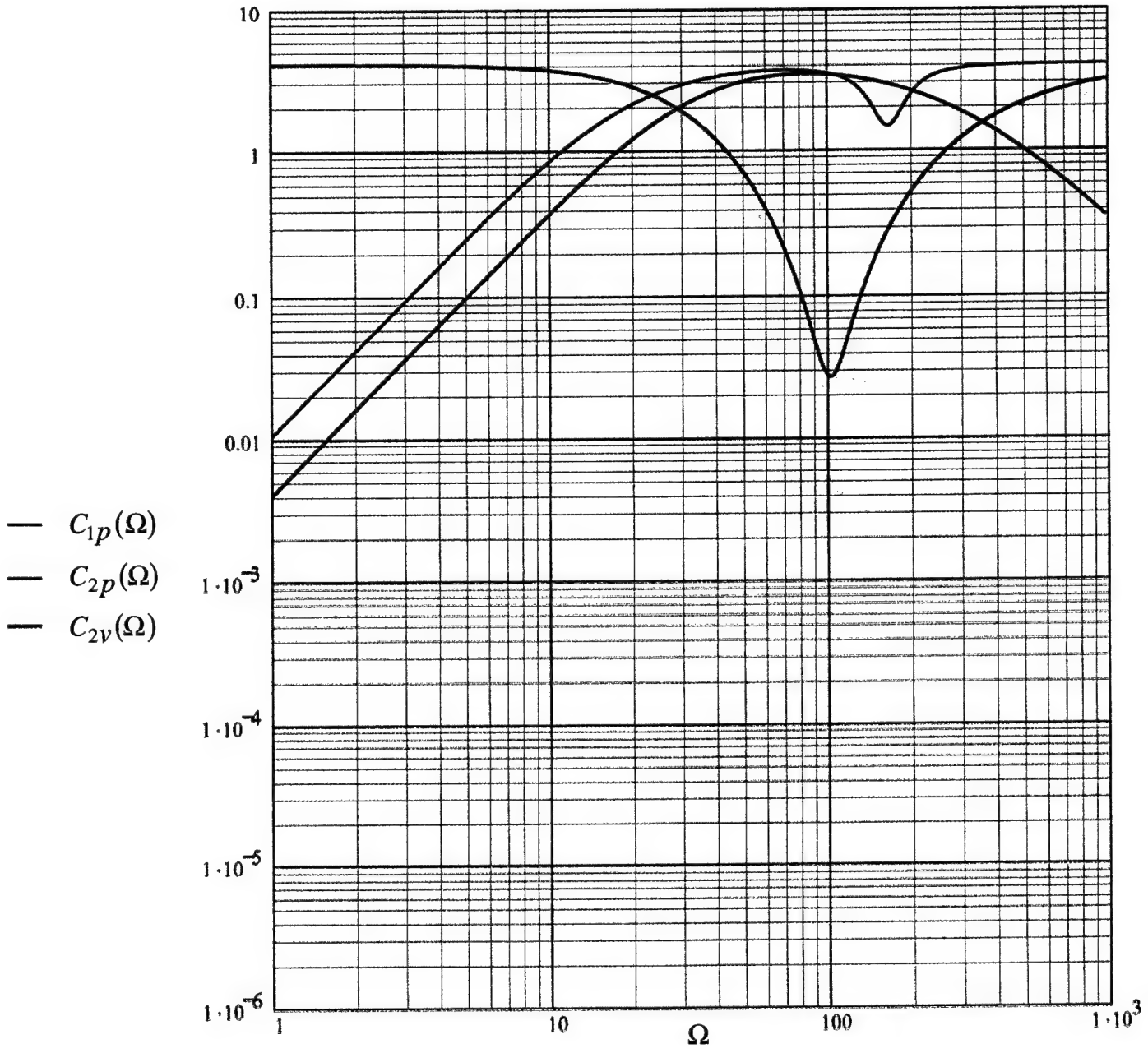

Fig 28. The sensitivities $C_{1p}(\Omega)$, $C_{2p}(\Omega)$ and $C_{2v}(\Omega)$ of a pressure transducer with and without a standard conditioning plate and a velocity transducer without a conditioning plate, respectively, as functions of the normalized frequency (Ω). [cf. Eqs. (59a), (59b), and (60b).]

c. A boundary composed of a compliant layer that is given one hundred (100) measures of surface stiffness. [cf. Eq. (67c) and Fig. 27c.]

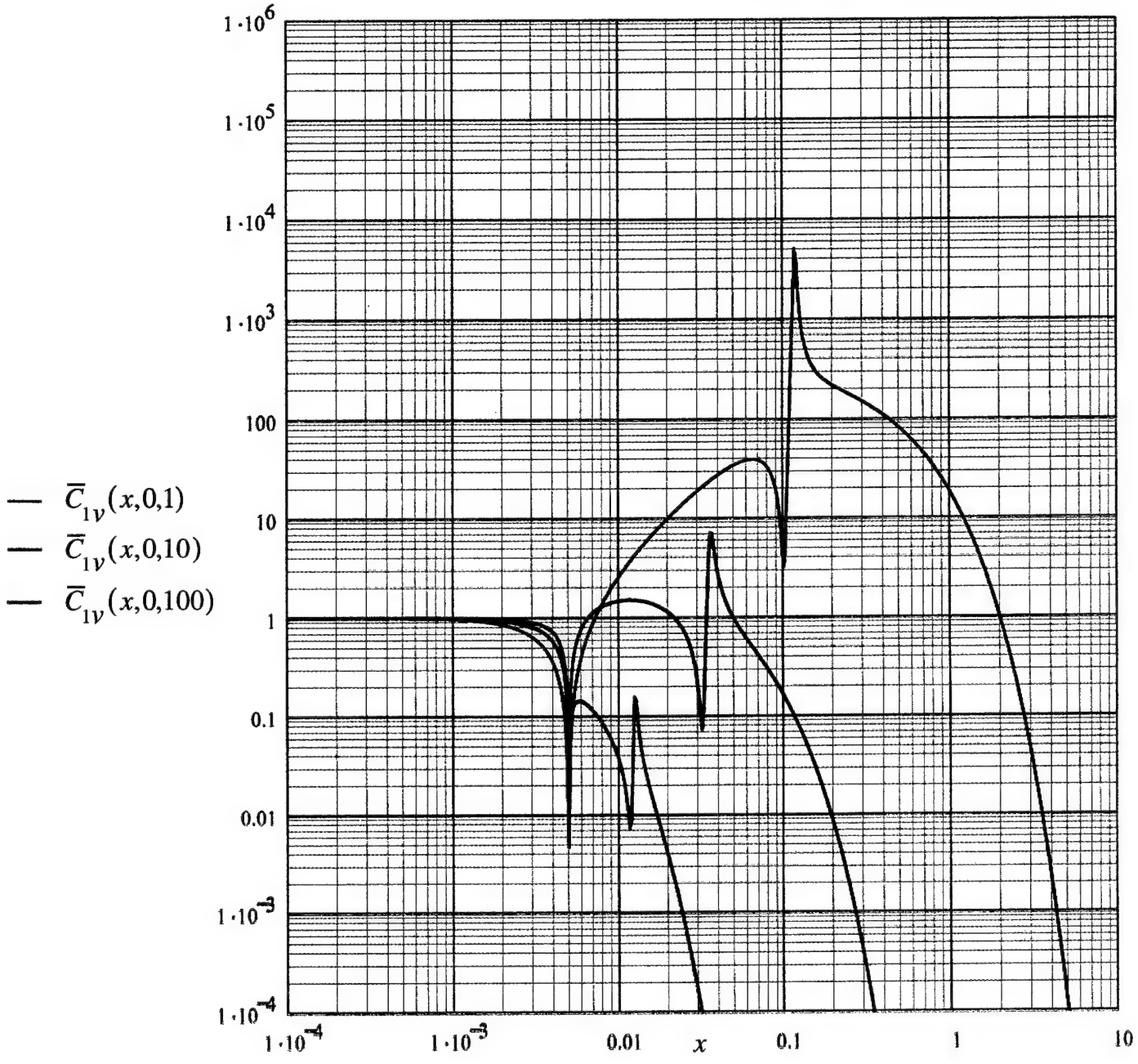

Fig 29. As in Figs. 25, except that the transducer are cladded by a standard blanket.

a. A pressure transducer on a standard conditioning plate. [cf. Eq. (56a).]

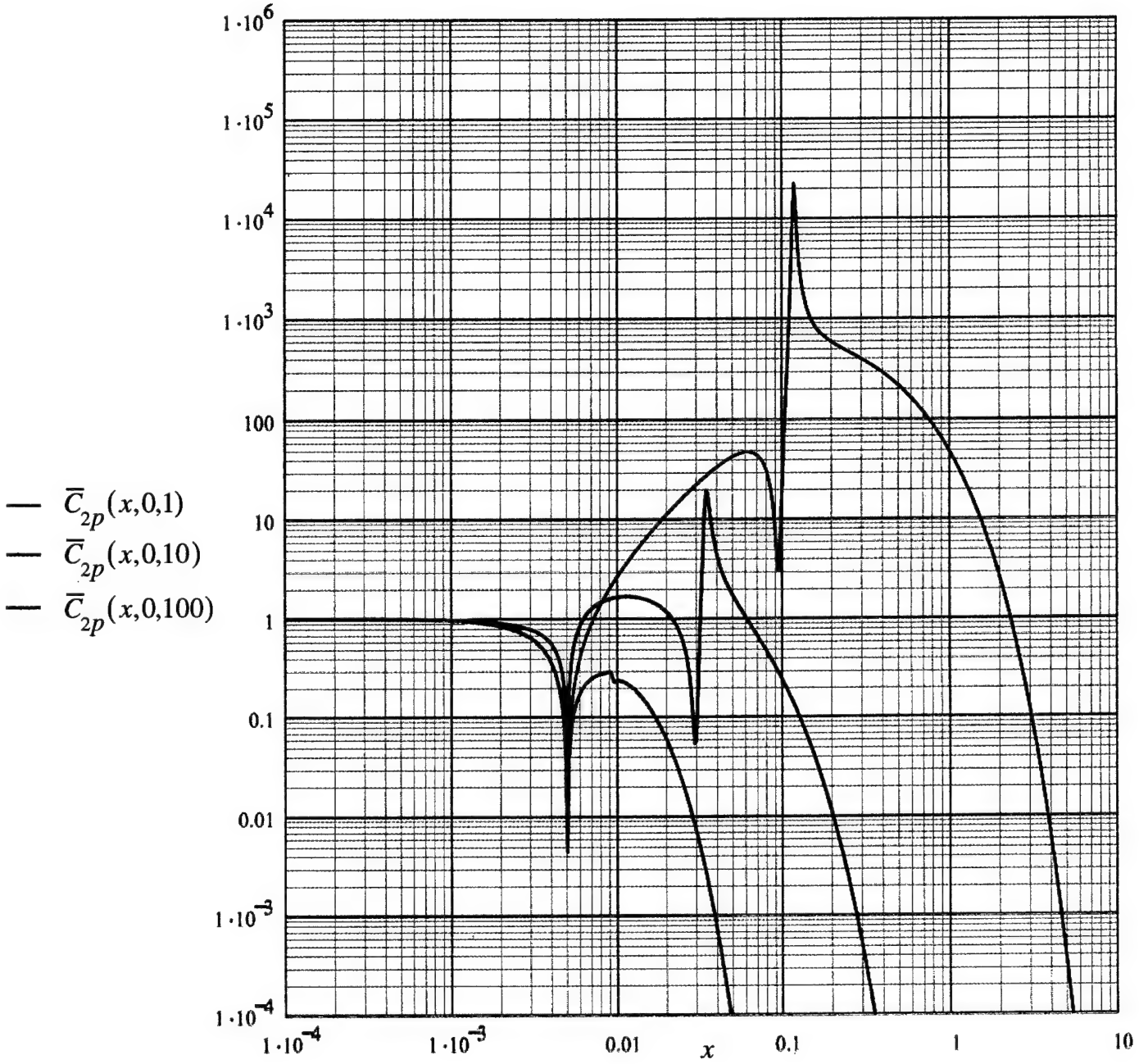

Fig 29. As in Figs. 25, except that the transducer are cladded by a standard blanket.

b. A pressure transducer without a conditioning plate. [cf. Eq. (56b).]

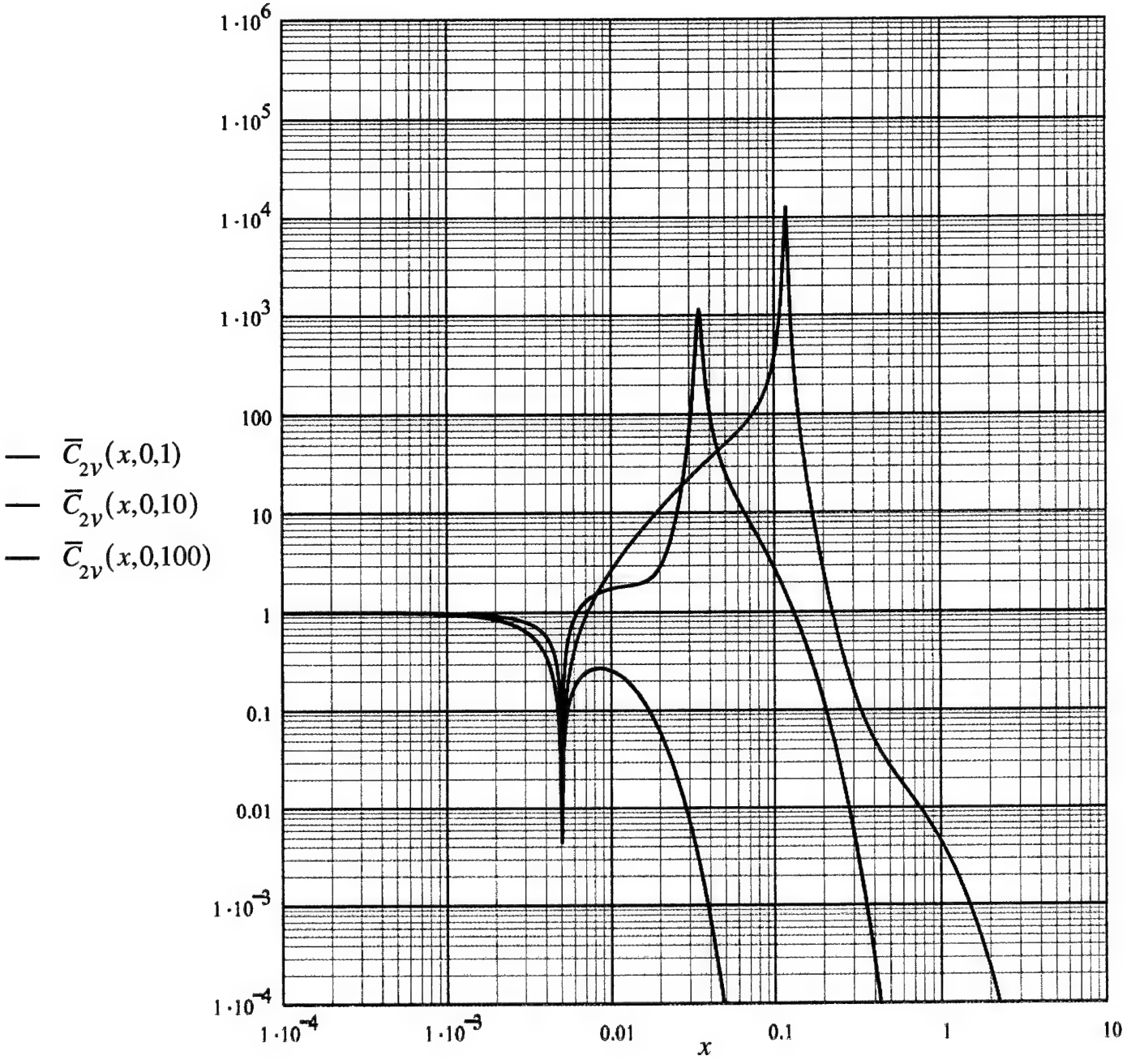

Fig 29. As in Figs. 25, except that the transducer are cladded by a standard blanket.

c. A velocity transducer (without a conditioning plate). [cf. Eq. (57b).]

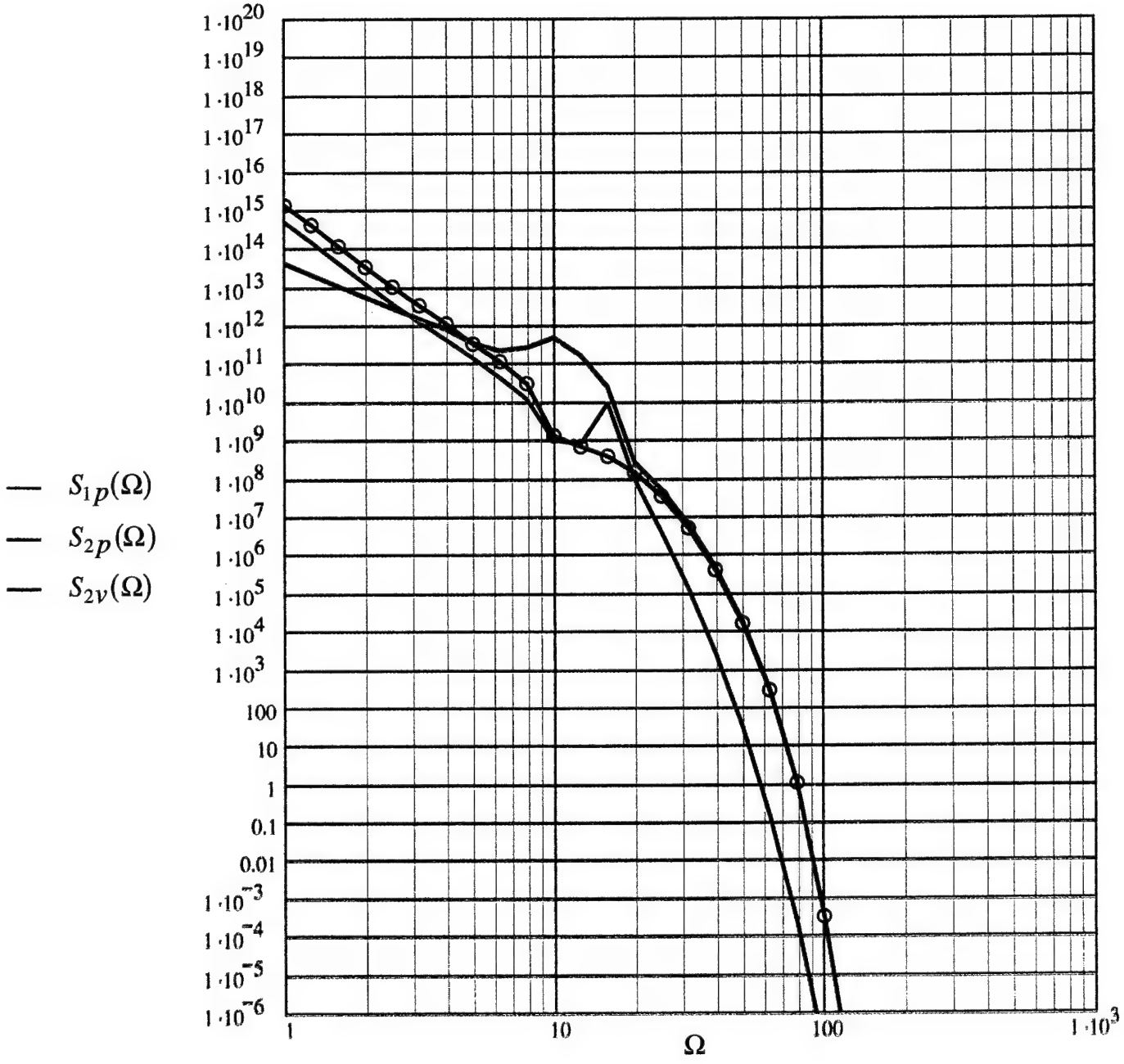

Fig 30. The normalized outputs to (TBL) $S_{1p}(\Omega)$, $S_{2p}(\Omega)$ and $S_{2v}(\Omega)$, as functions of the normalized frequency (Ω), for standard cladding and standard size transducers. [cf. Eqs. (62a), (62b) and (62d) and Fig. 27.]

a. A boundary composed of a compliant layer that is given ten (10) measures of surface stiffness. [cf. Eq. (67a).]

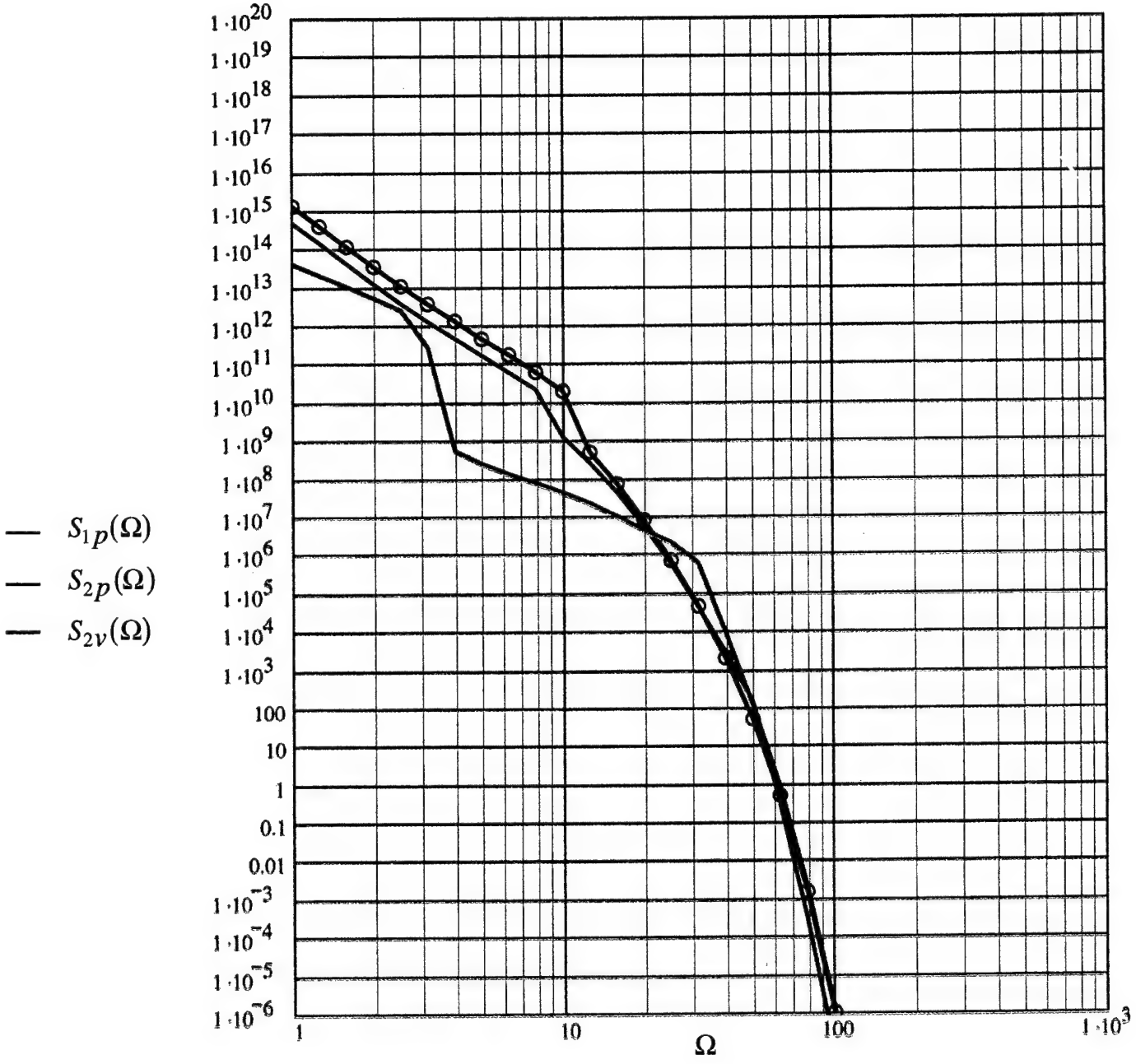

Fig 30. The normalized outputs to (TBL) $S_{1p}(\Omega)$, $S_{2p}(\Omega)$ and $S_{2v}(\Omega)$, as functions of the normalized frequency (Ω), for standard cladding and standard size transducers. [cf. Eqs. (62a), (62b) and (62d) and Fig. 27.]

b. A boundary composed of a compliant layer that is given thirty (30) measures of surface stiffness [cf. Eq. (67b).]

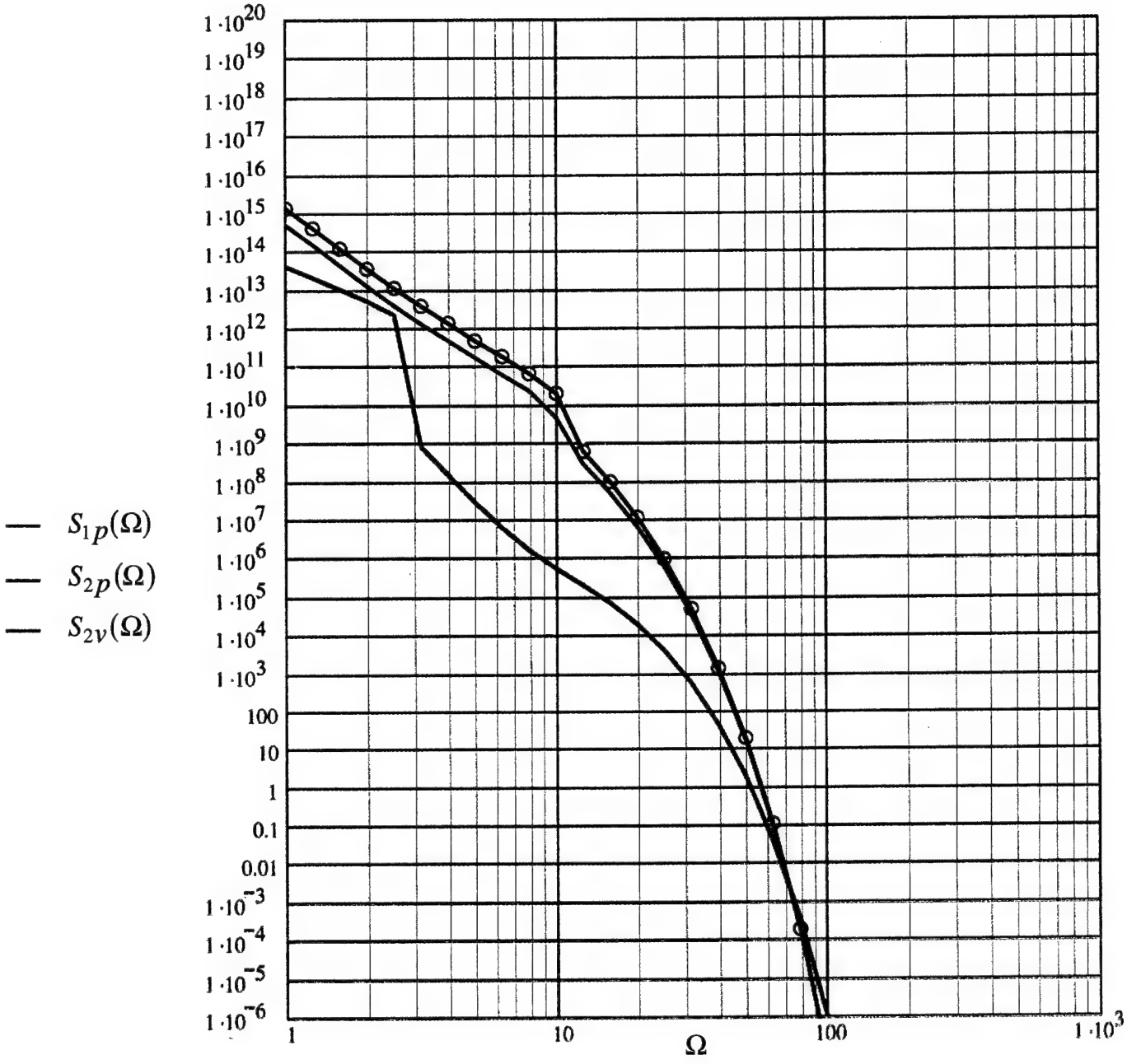

Fig 30. The normalized outputs to (TBL) $S_{1p}(\Omega)$, $S_{2p}(\Omega)$ and $S_{2v}(\Omega)$, as functions of the normalized frequency (Ω), for standard cladding and standard size transducers. [cf. Eqs. (62a), (62b) and (62d) and Fig. 27.]

c. A boundary composed of a compliant layer that is given one hundred (100) measures of surface stiffness. [cf. Eq. (67c).]

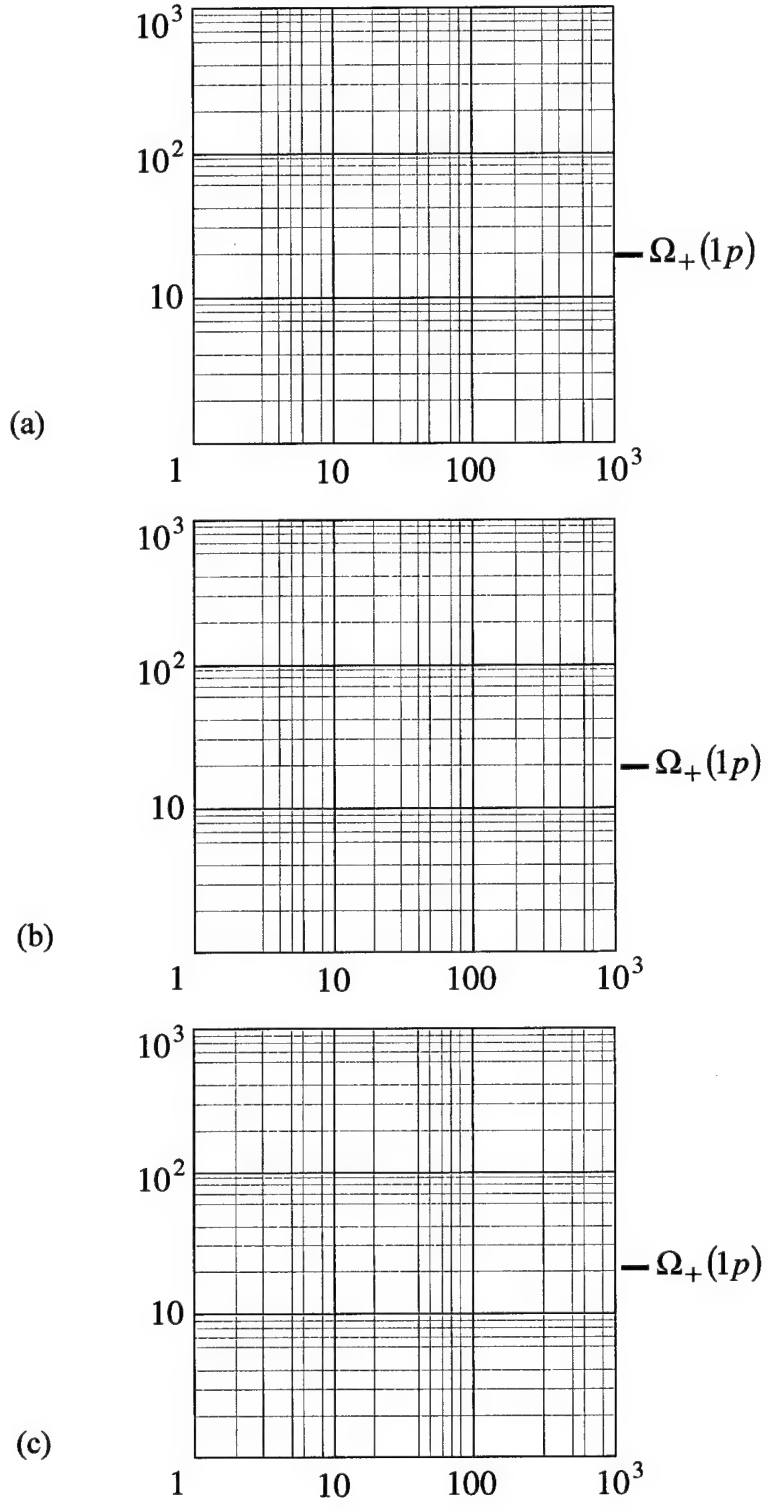

Fig 31. Regions of viability and acceptability, as functions of the normalized frequency (Ω), for the conditions specified in Figs. 28a and 30a.

a. A pressure transducer with a standard conditioning plate.

b. A pressure transducer without a conditioning plate.

c. A velocity transducer without a conditioning plate.

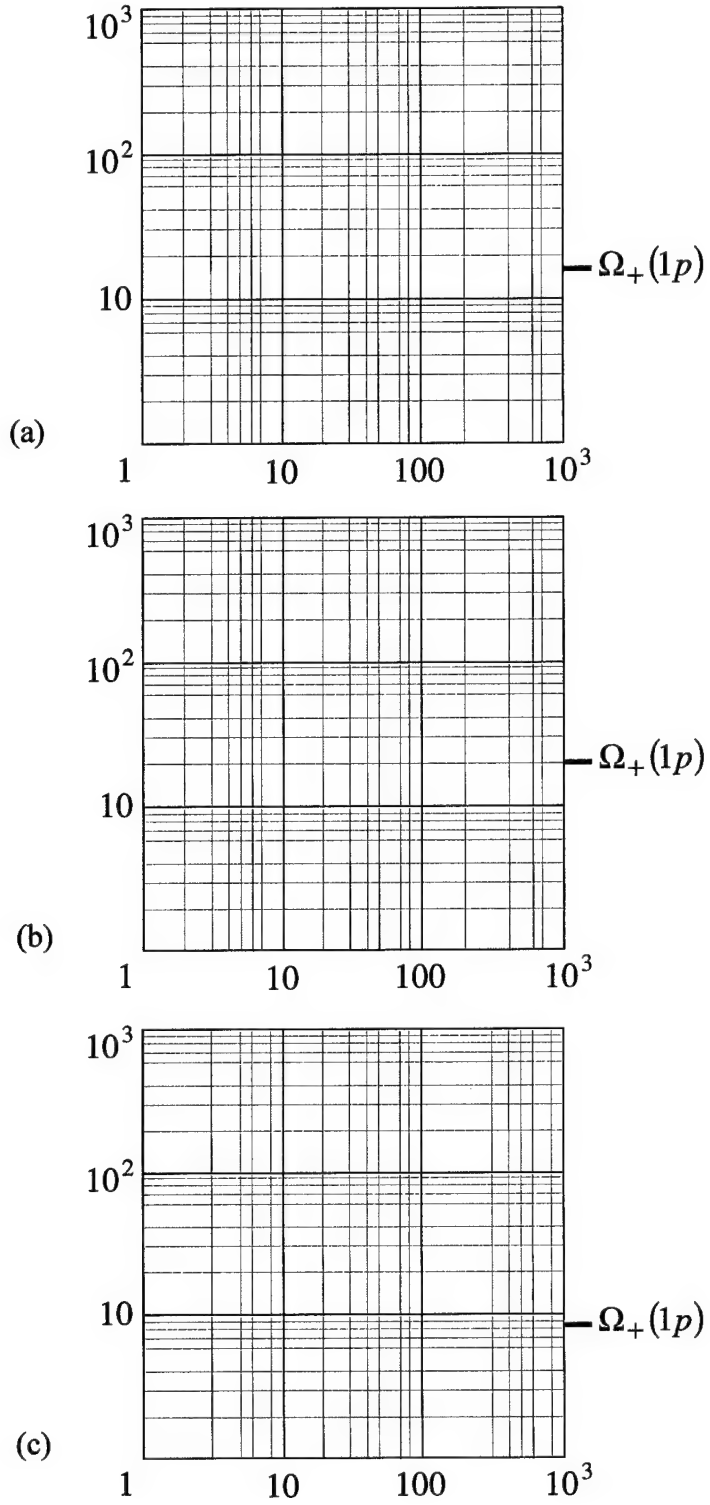

Fig 32. Regions of viability and acceptability, as functions of the normalized frequency (Ω), for the conditions specified in Figs. 28b and 30b.

a. A pressure transducer with a standard conditioning plate.

b. A pressure transducer without a conditioning plate.

c. A velocity transducer without a conditioning plate.

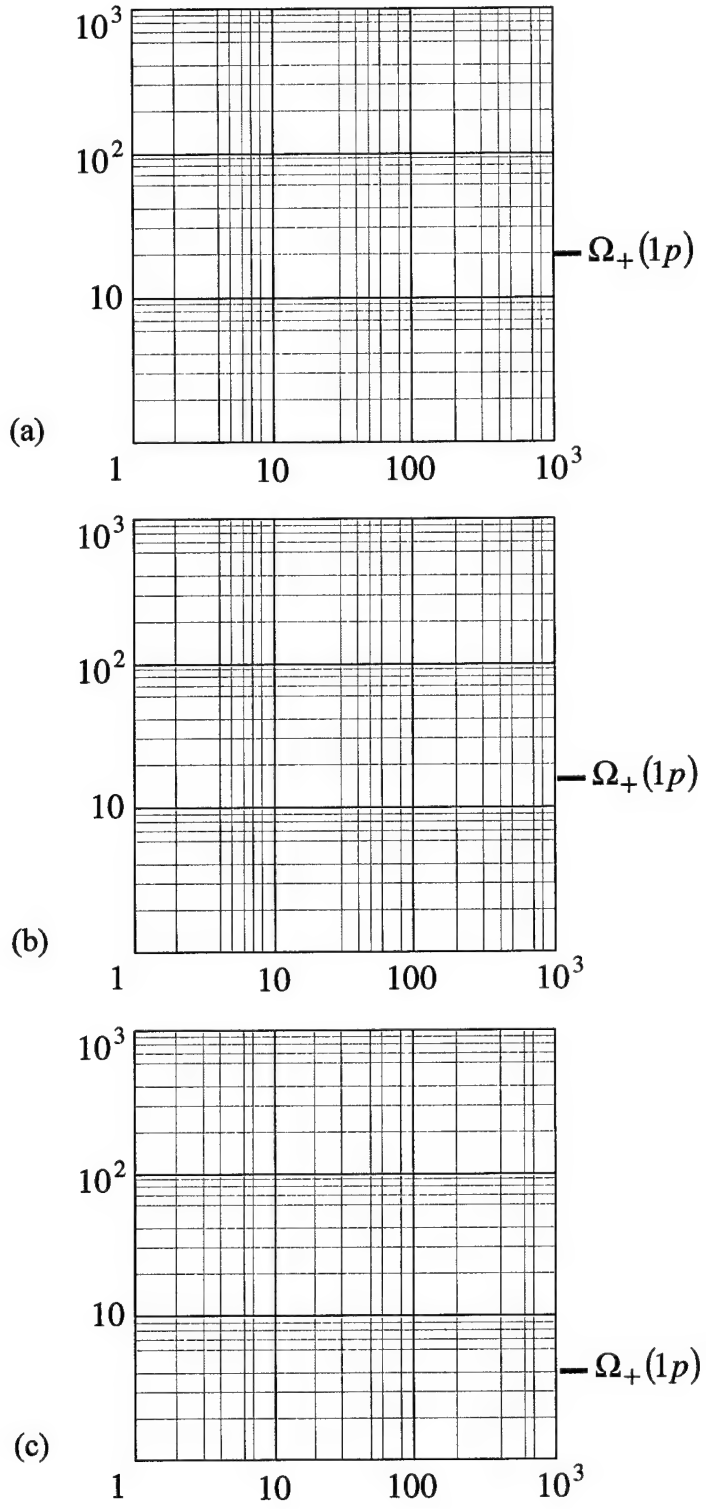

Fig 33. Regions of viability and acceptability, as functions of the normalized frequency (Ω), for the conditions specified in Figs. 28c and 30c.

a. A pressure transducer with a standard conditioning plate.

b. A pressure transducer without a conditioning plate.

c. A velocity transducer without a conditioning plate.

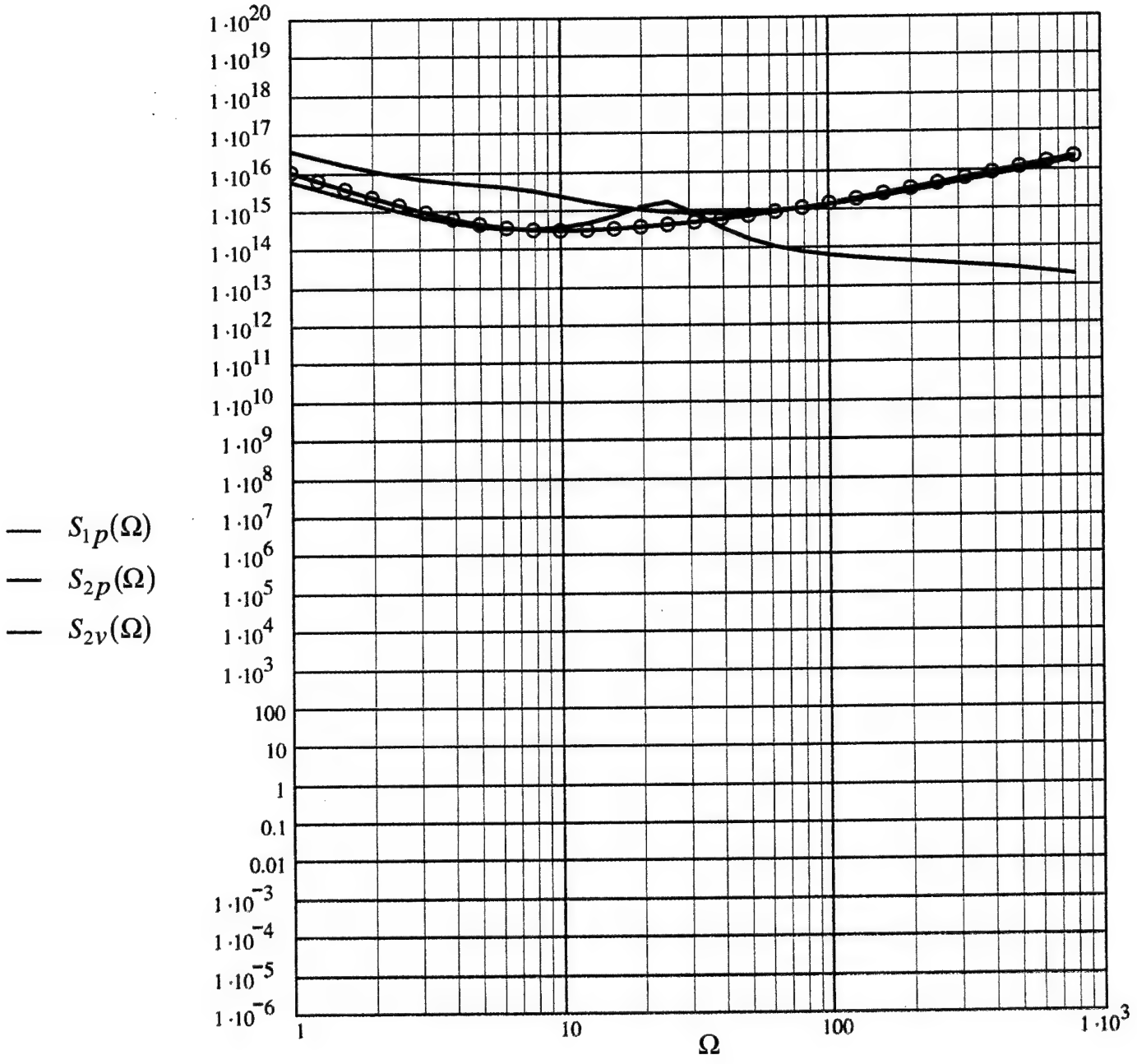

Fig. 34. The normalized outputs to (TBL) $S_{1p}(\Omega)$, $S_{2p}(\Omega)$ and $S_{2v}(\Omega)$, as functions of the normalized frequency (Ω), for uncladded point transducers. [cf. Eqs. (62a), (62b) and (62d).]

a. A boundary composed of a compliant layer for which the surface stiffness is defined by $\{25,30\}$. [cf. Eq. (67d).]

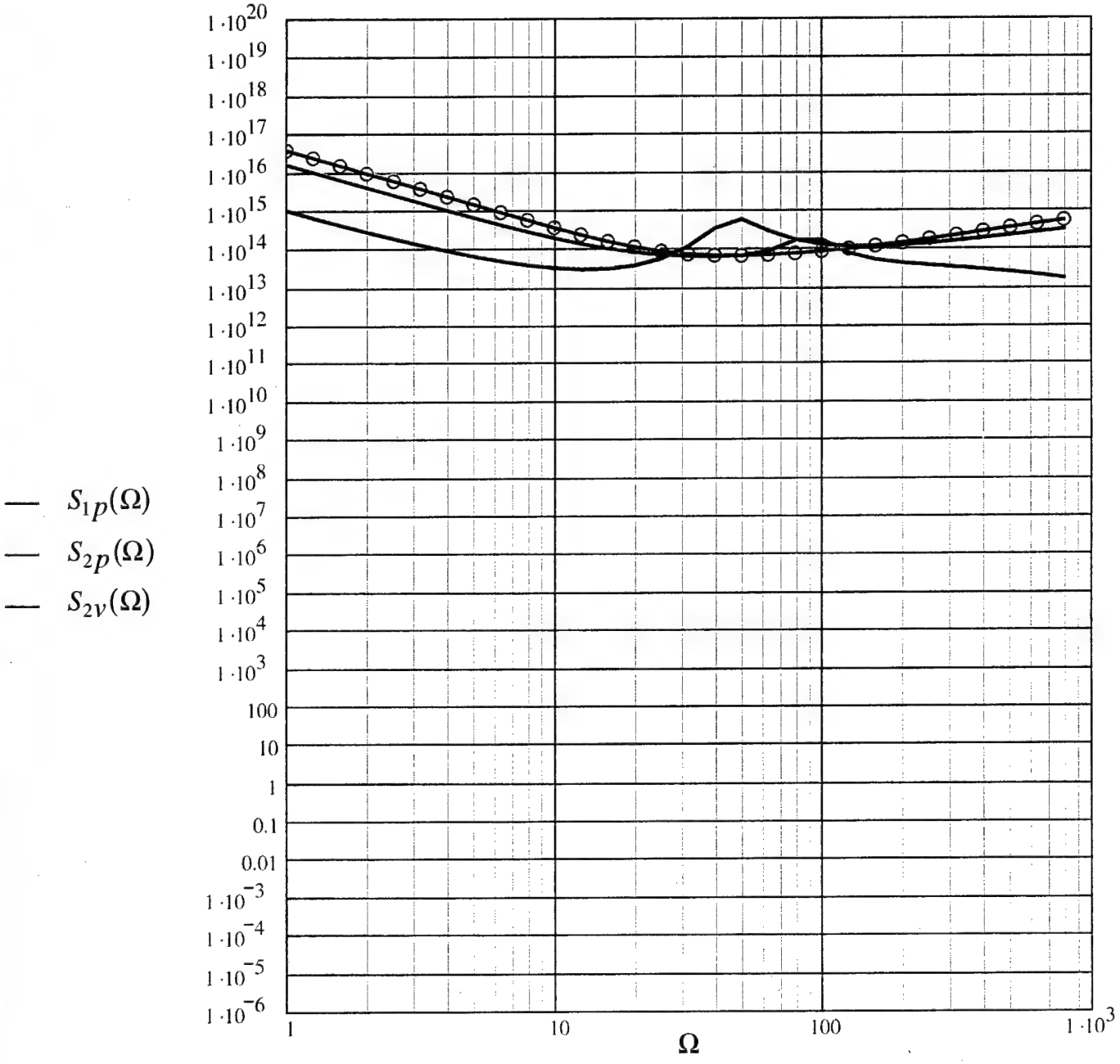

Fig. 34. The normalized outputs to (TBL) $S_{1p}(\Omega)$, $S_{2p}(\Omega)$ and $S_{2v}(\Omega)$, as functions of the normalized frequency (Ω), for uncladded point transducers. [cf. Eqs. (62a), (62b) and (62d).]

b. A boundary composed of a compliant layer for which the surface stiffness is defined by $\{25, 70\}$. [cf. Eq;. (67e).]

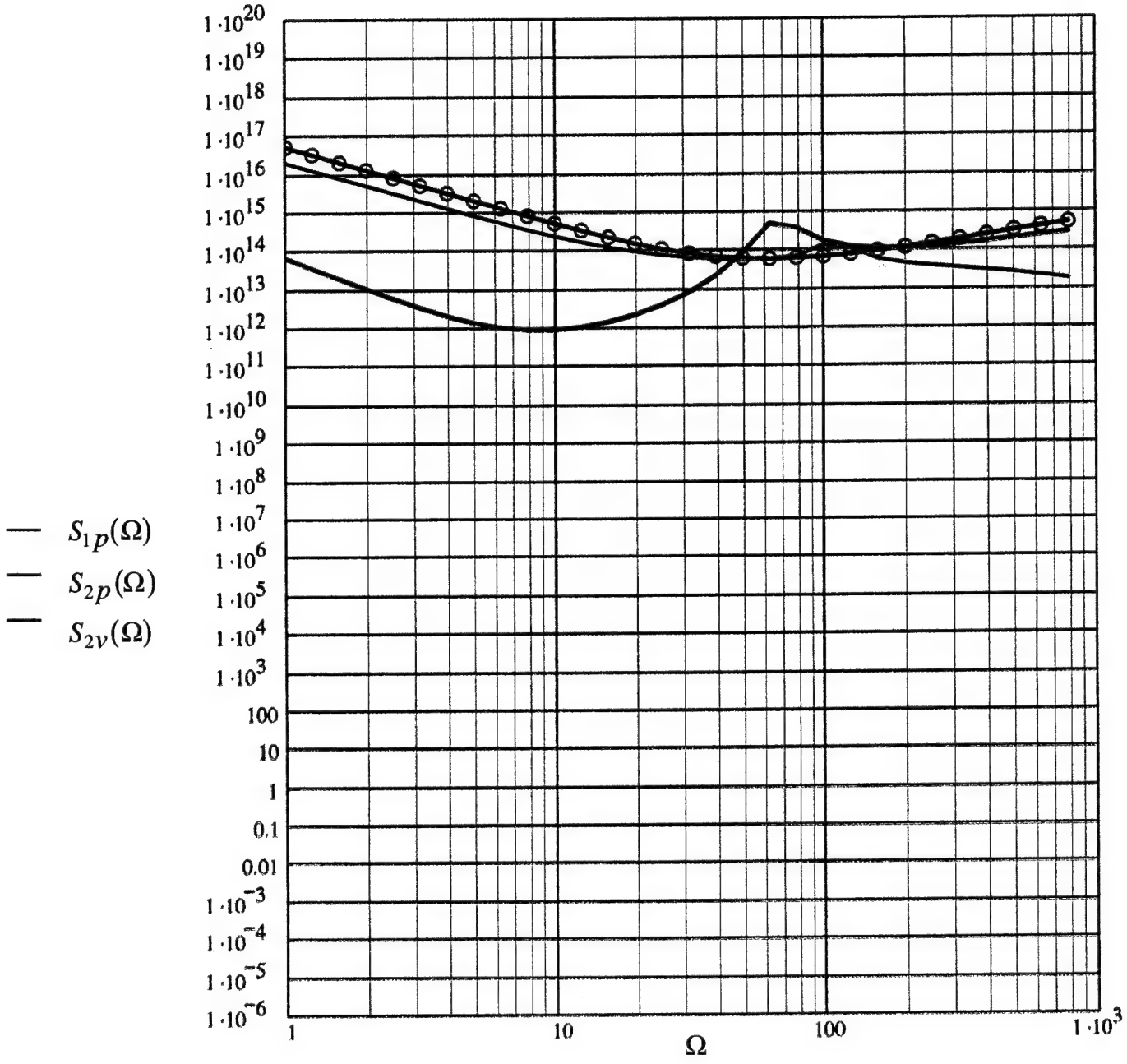

Fig. 34. The normalized outputs to (TBL) $S_{1p}(\Omega)$, $S_{2p}(\Omega)$ and $S_{2v}(\Omega)$, as functions of the normalized frequency (Ω), for uncladded point transducers. [cf. Eqs. (62a), (62b) and (62d).]

c. A boundary composed of a compliant layer for which the surface stiffness is defined by $\{5, 70\}$. [cf. Eq. (67f).]

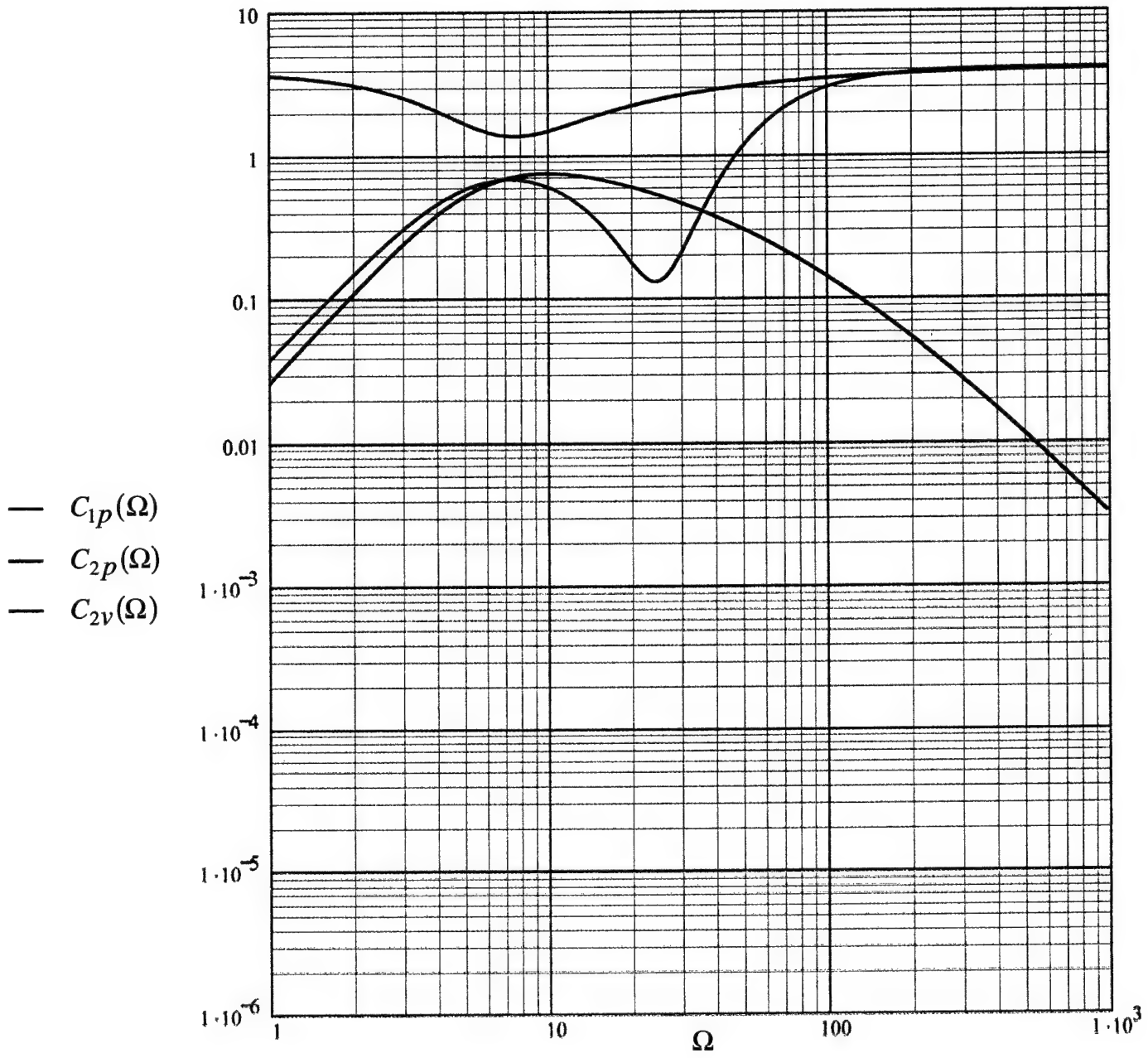

Fig. 35. The sensitivities $C_{1p}(\Omega)$, $C_{2p}(\Omega)$ and $C_{2v}(\Omega)$ of a pressure transducer transducer with and without a standard conditioning plate and a velocity transducer without a conditioning plate, respectively, as functions of the normalized frequency (Ω). [cf. Eqs. (59a), (59b), and (60b).]

a. A boundary composed of a compliant layer for which the surface stiffness is defined by $\{25,30\}$. [cf. Eq. (67d).]

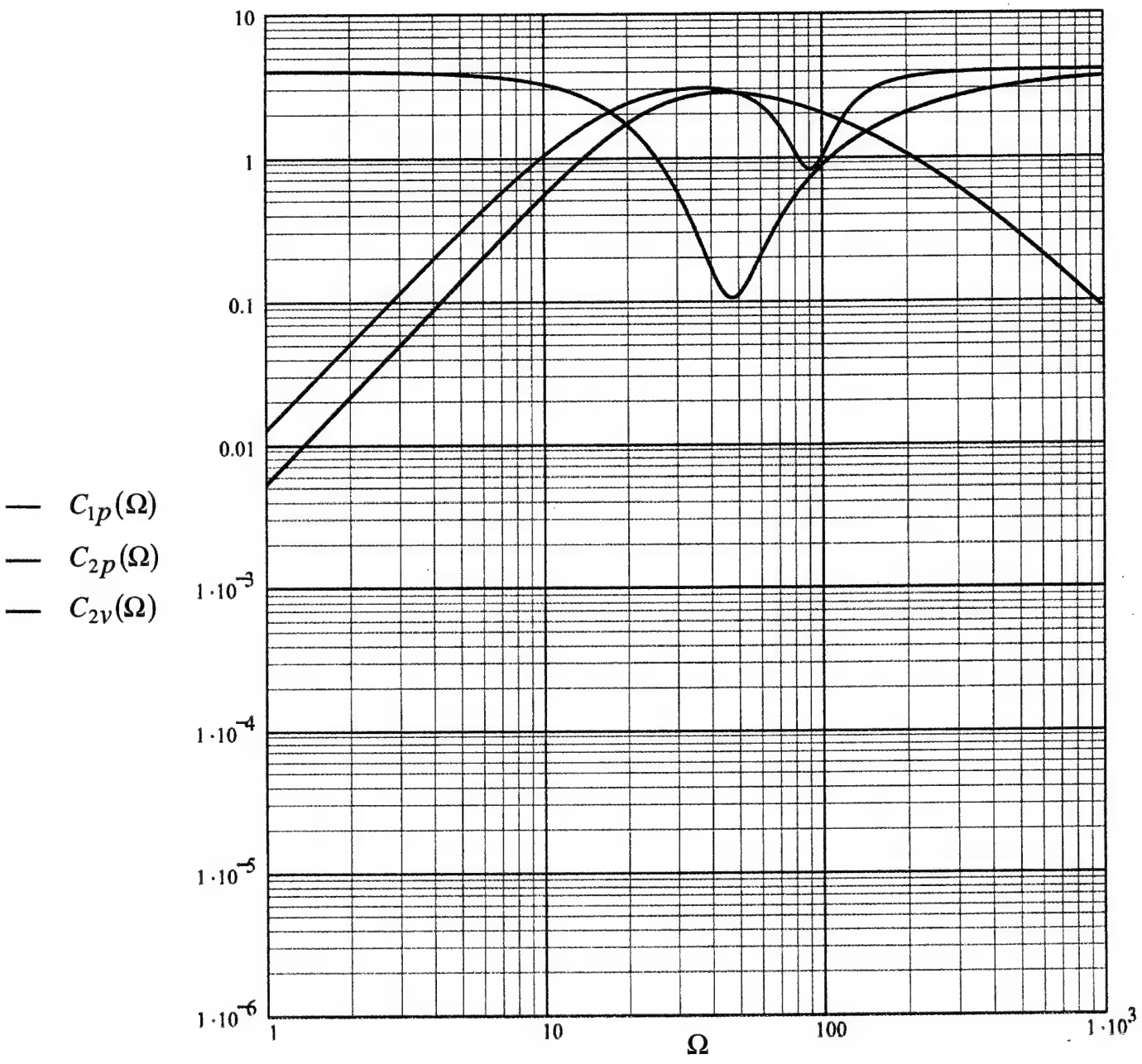

Fig. 35. The sensitivities $C_{1p}(\Omega)$, $C_{2p}(\Omega)$ and $C_{2v}(\Omega)$ of a pressure transducer transducer with and without a standard conditioning plate and a velocity transducer without a conditioning plate, respectively, as functions of the normalized frequency (Ω). [cf. Eqs. (59a), (59b), and (60b).]

b. A boundary composed of a compliant layer for which the surface stiffness is defined by $\{25, 70\}$. [cf. Eq. (67e).]

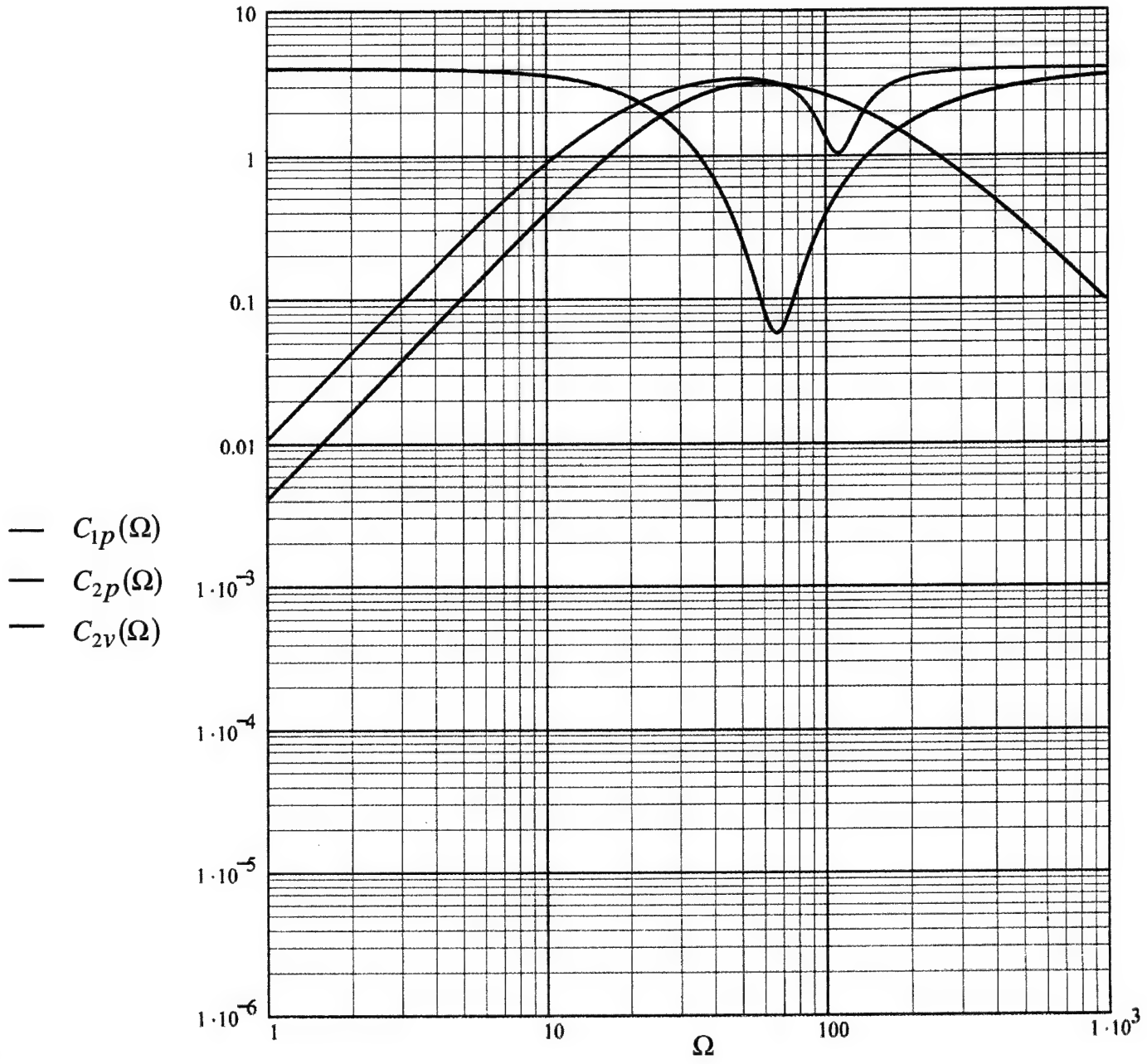

Fig. 35. The sensitivities $C_{1p}(\Omega)$, $C_{2p}(\Omega)$ and $C_{2v}(\Omega)$ of a pressure transducer transducer with and without a standard conditioning plate and a velocity transducer without a conditioning plate, respectively, as functions of the normalized frequency (Ω). [cf. Eqs. (59a), (59b), and (60b).]

c. A boundary composed of a compliant layer for which the surface stiffness is defined by $\{5, 70\}$. [cf. Eq. (67f).]

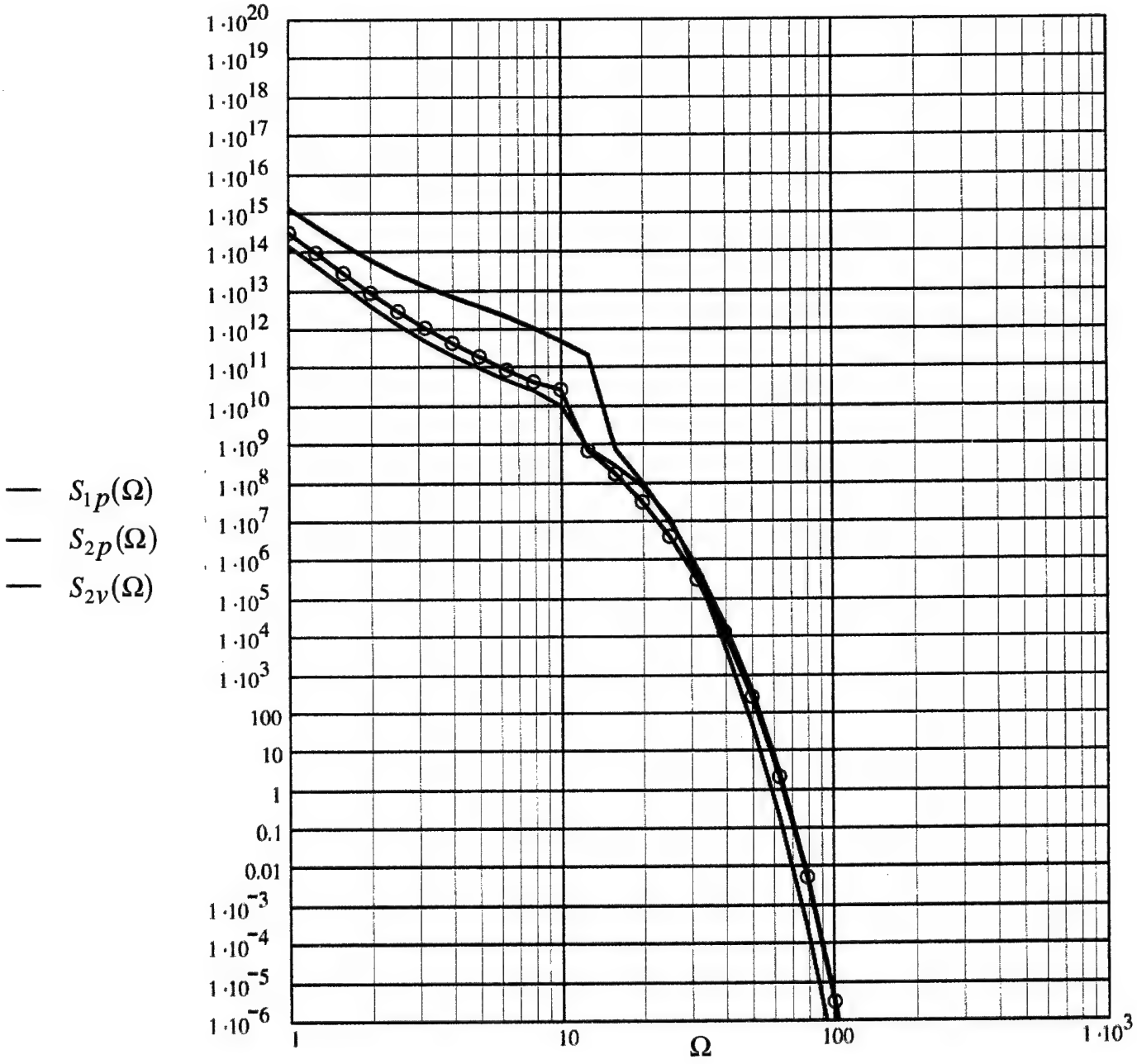

Fig. 36. The normalized outputs to (TBL) $S_{1p}(\Omega)$, $S_{2p}(\Omega)$ and $S_{2v}(\Omega)$, as functions of the normalized frequency (Ω), for a standard blanket and standard size transducers. [cf. Fig. 34.]

a. A boundary composed of a compliant layer for which the surface stiffness is defined by {25,30}. [cf. Eq. (67d) and Fig. 34a.]

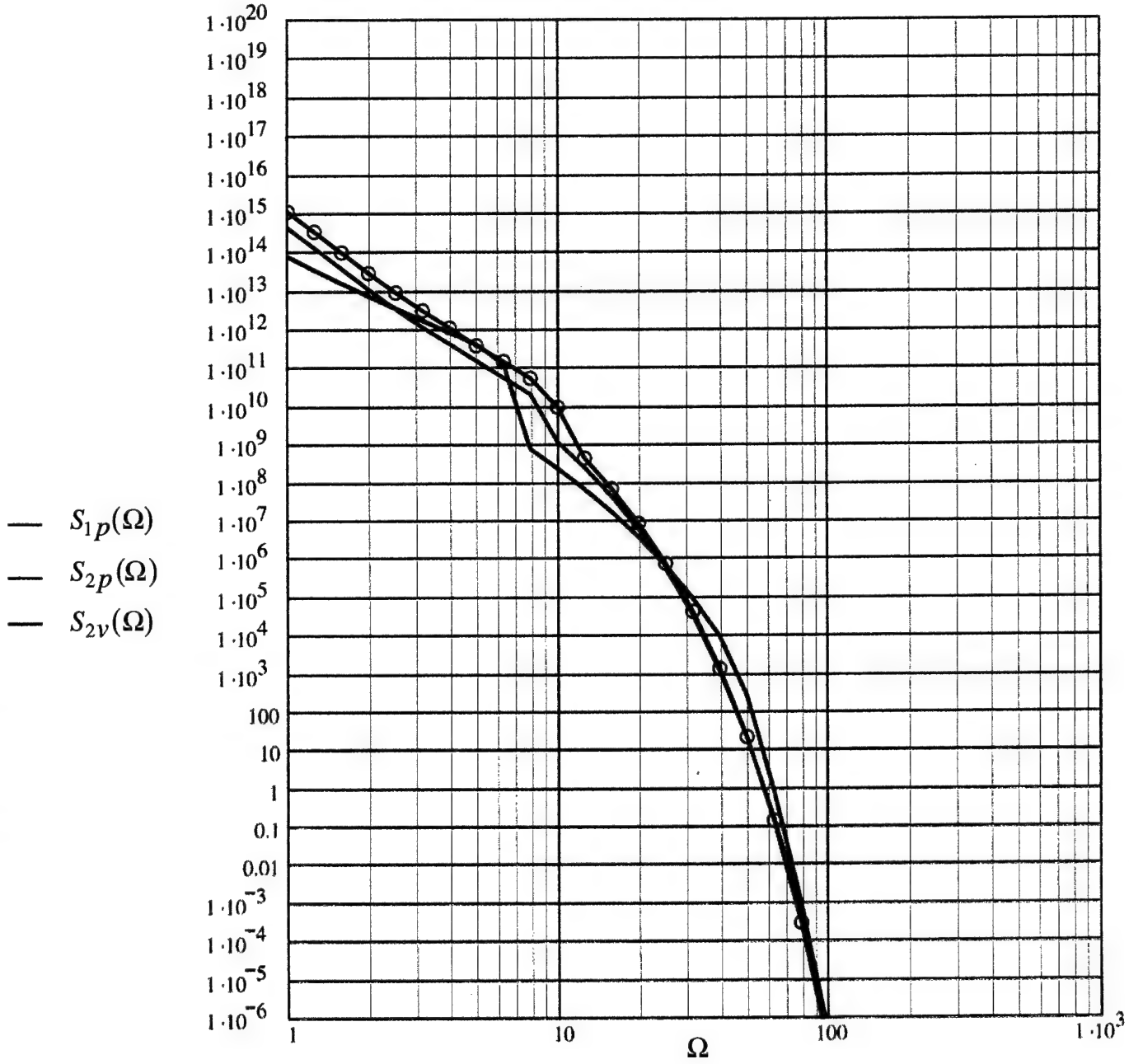

Fig. 36. The normalized outputs to (TBL) $S_{1p}(\Omega)$, $S_{2p}(\Omega)$ and $S_{2v}(\Omega)$, as functions of the normalized frequency (Ω), for a standard blanket and standard size transducers. [cf. Fig. 34.]

b. A boundary composed of a compliant layer for which the surface stiffness is defined by $\{25, 70\}$. [cf. Eq. (67e) and Fig. 34b.]

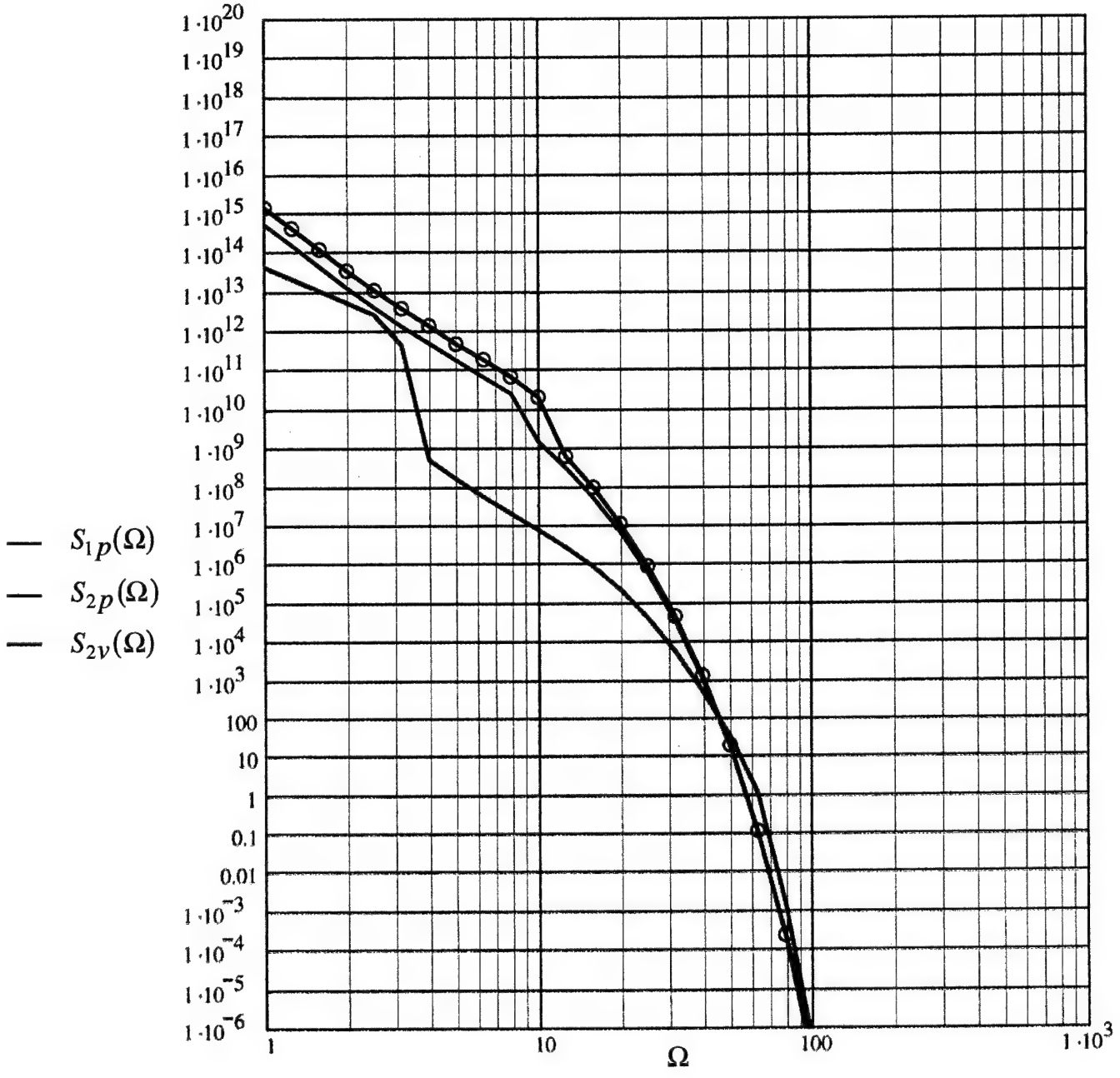

Fig. 36. The normalized outputs to (TBL) $S_{1p}(\Omega)$, $S_{2p}(\Omega)$ and $S_{2v}(\Omega)$, as functions of the normalized frequency (Ω), for a standard blanket and standard size transducers. [cf. Fig. 34.]

c. A boundary composed of a compliant layer for which the surface stiffness is defined by $\{5, 70\}$. [cf. Eq. (67f) and Fig. 34c.]

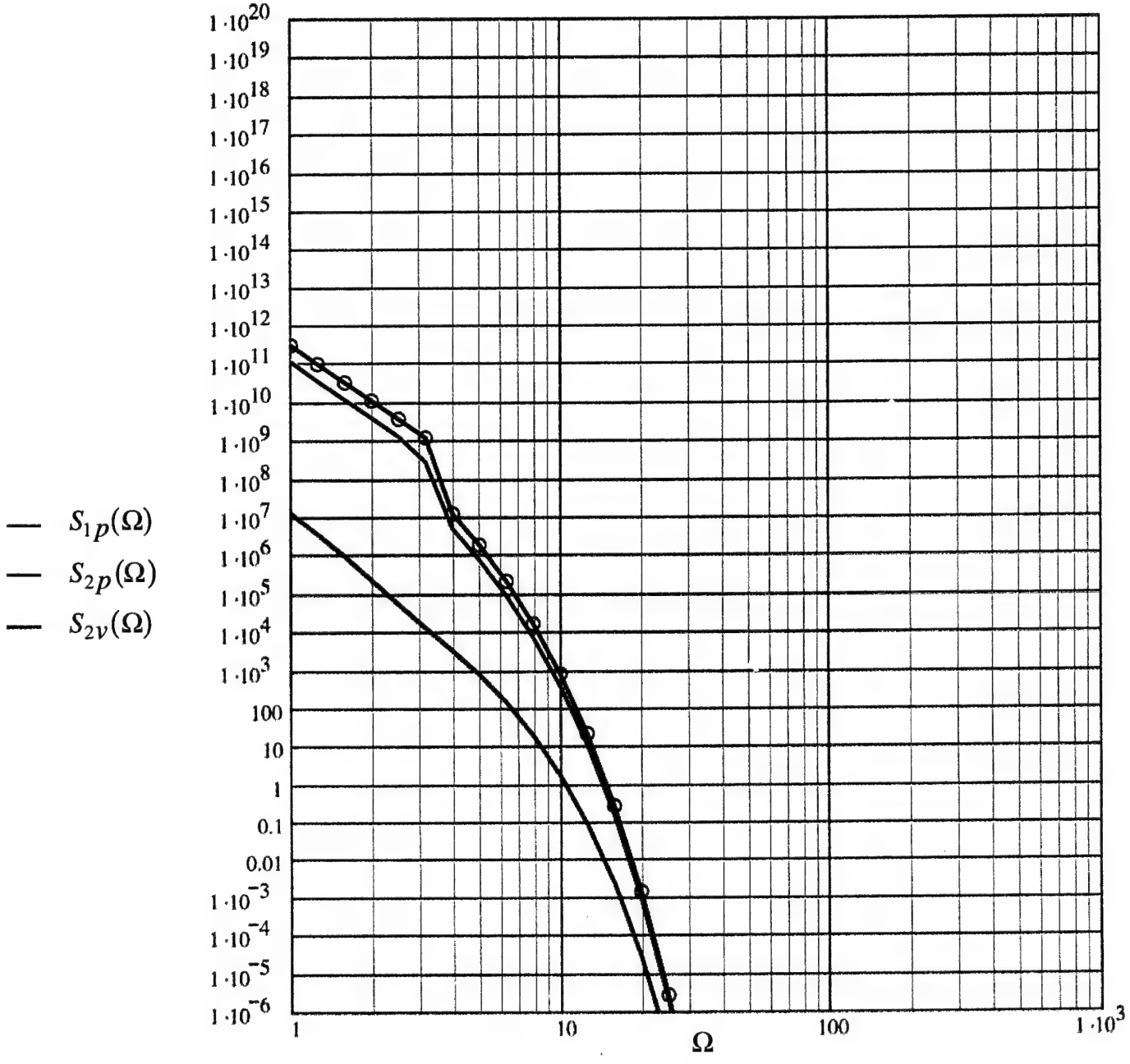

Fig. 37. Repeats Fig. 36c, except that (M) is changed from its standard value of $M_o = (15/3)x10^{-3}$ to $M = (5/3)x10^{-3}$.

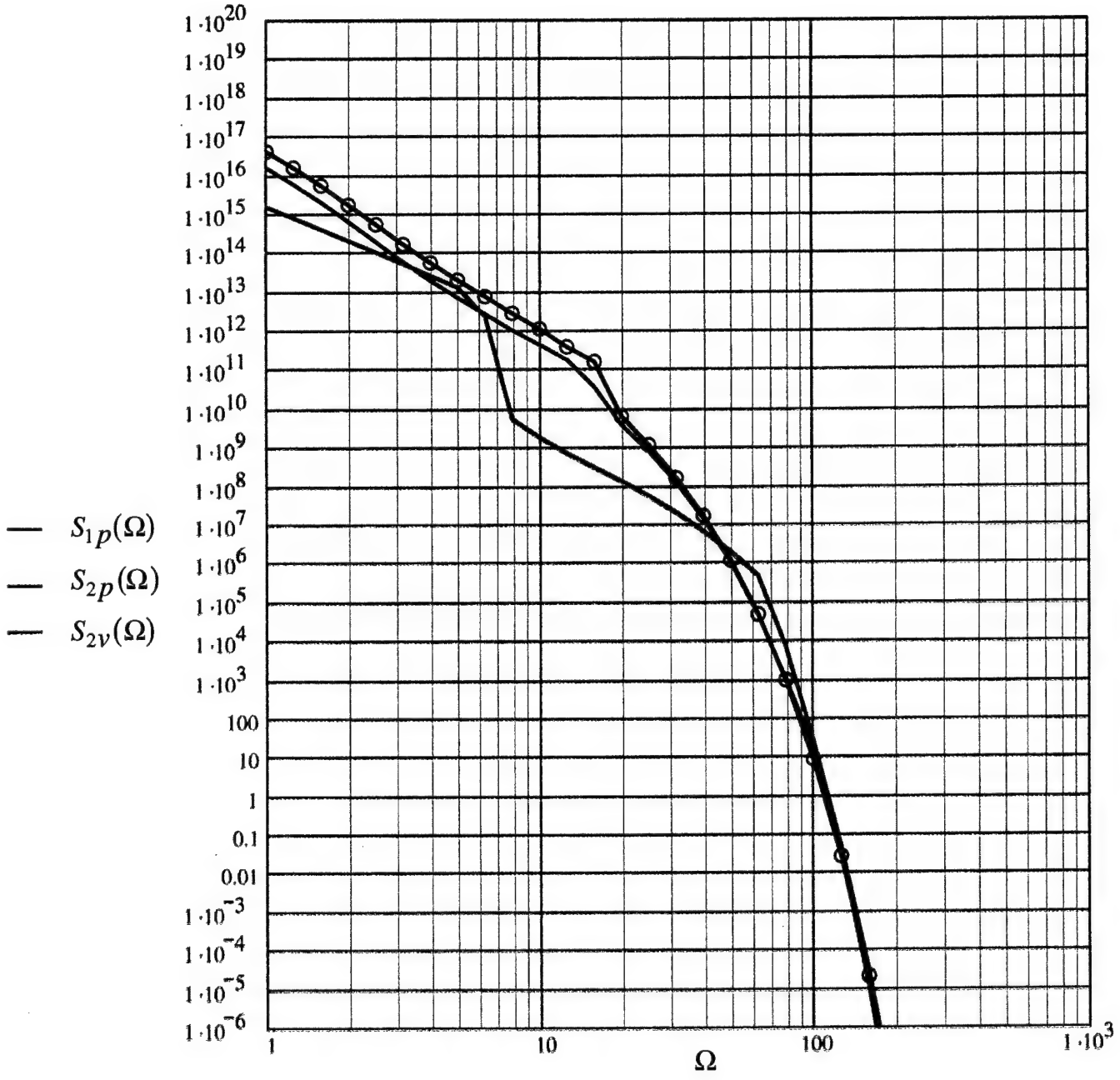

Fig. 38. Repeats Fig. 36c, except that (M) is changed from its standard value of $M_o = (15/3)x10^{-3}$ to $M = (25/3)x10^{-3}$. **[SAME AS FIG. 37.]**

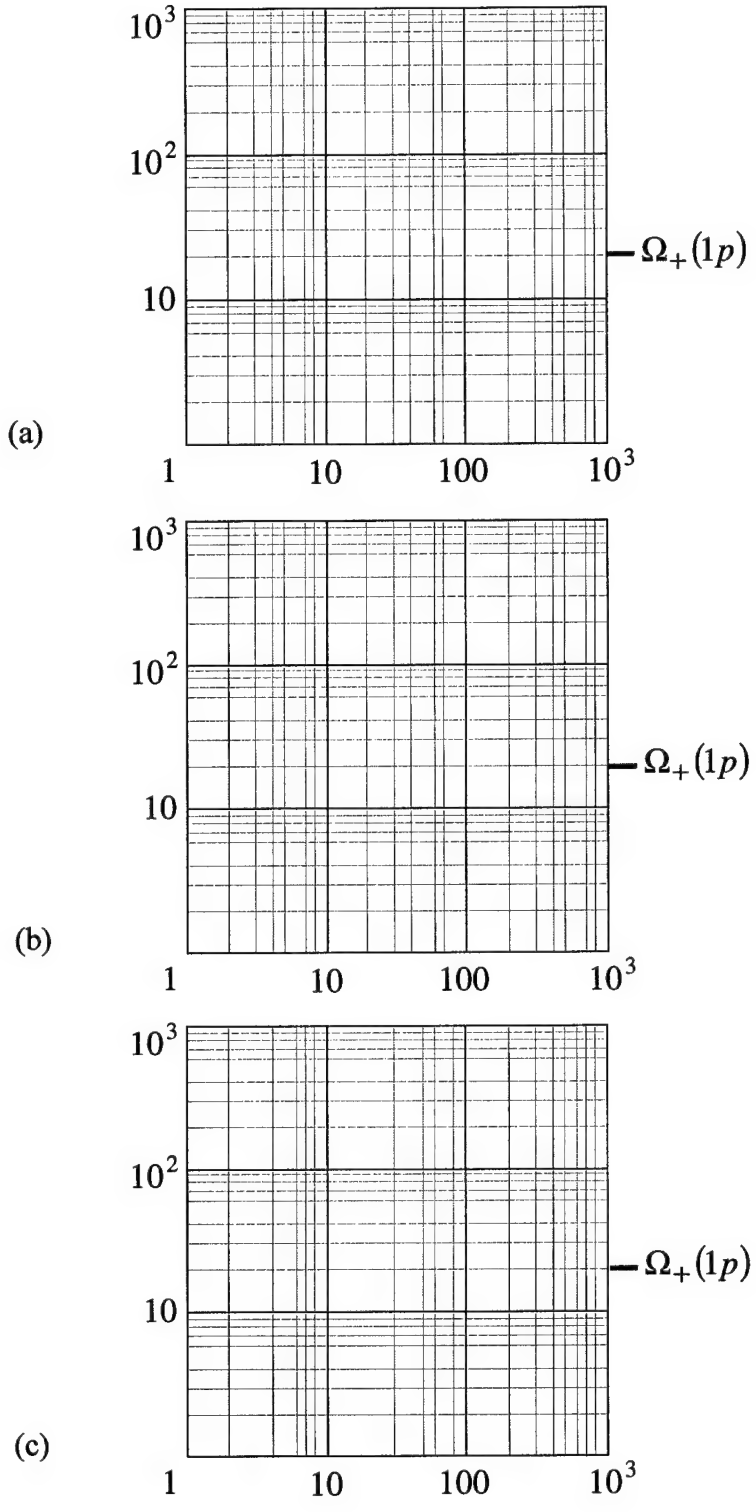

Fig. 39. Regions of viability and acceptability, as functions of the normalized frequency (Ω), for the conditions specified in Figs. 35a and 36a.

a. A pressure transducer with a standard conditioning plate.

b. A pressure transducer without a conditioning plate.

c. A velocity transducer without a conditioning plate.

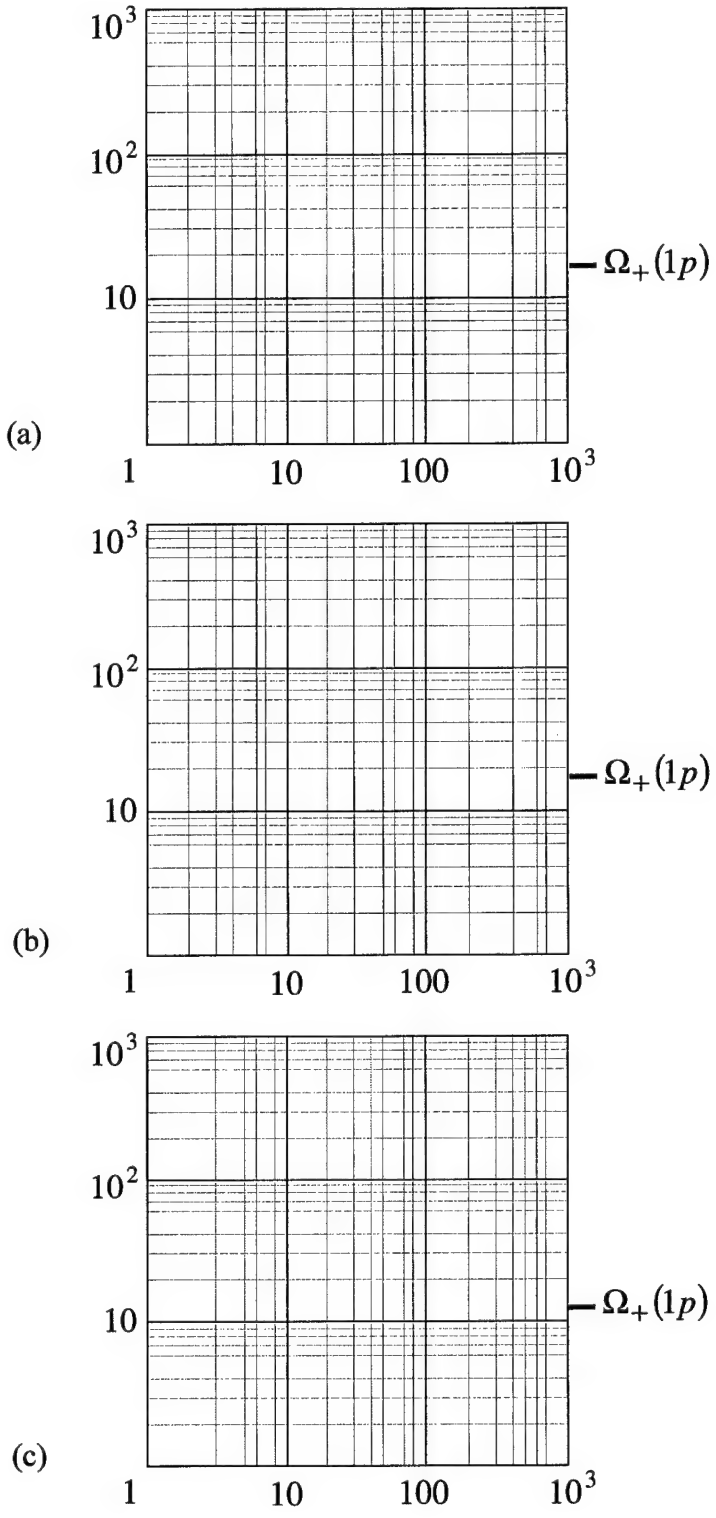

Fig. 40. Regions of viability and acceptability, as functions of the normalized frequency (Ω), for the conditions specified in Figs. 35b and 36b.

a. A pressure transducer with a standard conditioning plate.

b. A pressure transducer without a conditioning plate.

c. A velocity transducer without a conditioning plate.

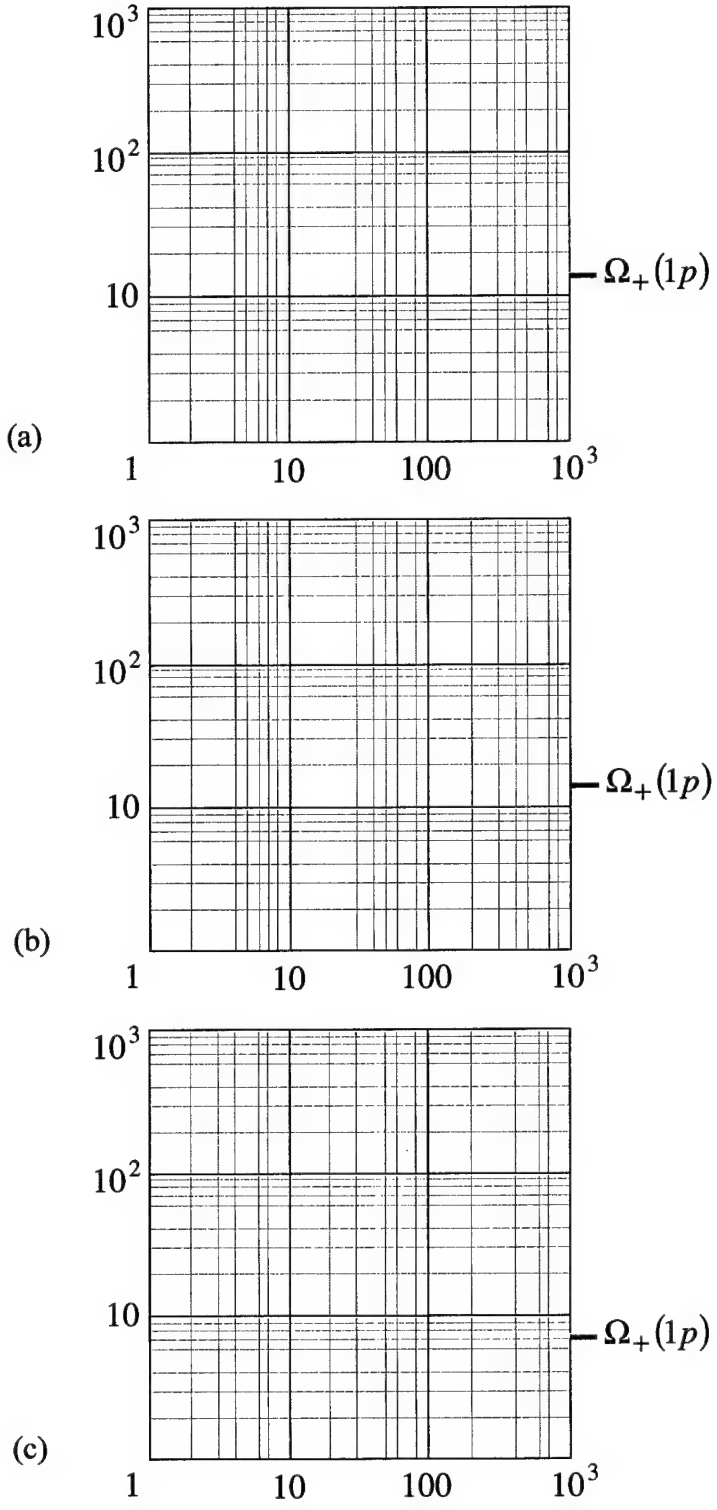

Fig. 41. Regions of viability and acceptability, as functions of the normalized frequency (Ω), for the conditions specified in Figs. 35c and 36c.

a. A pressure transducer with a standard conditioning plate.

b. A pressure transducer without a conditioning plate.

c. A velocity transducer without a conditioning plate.

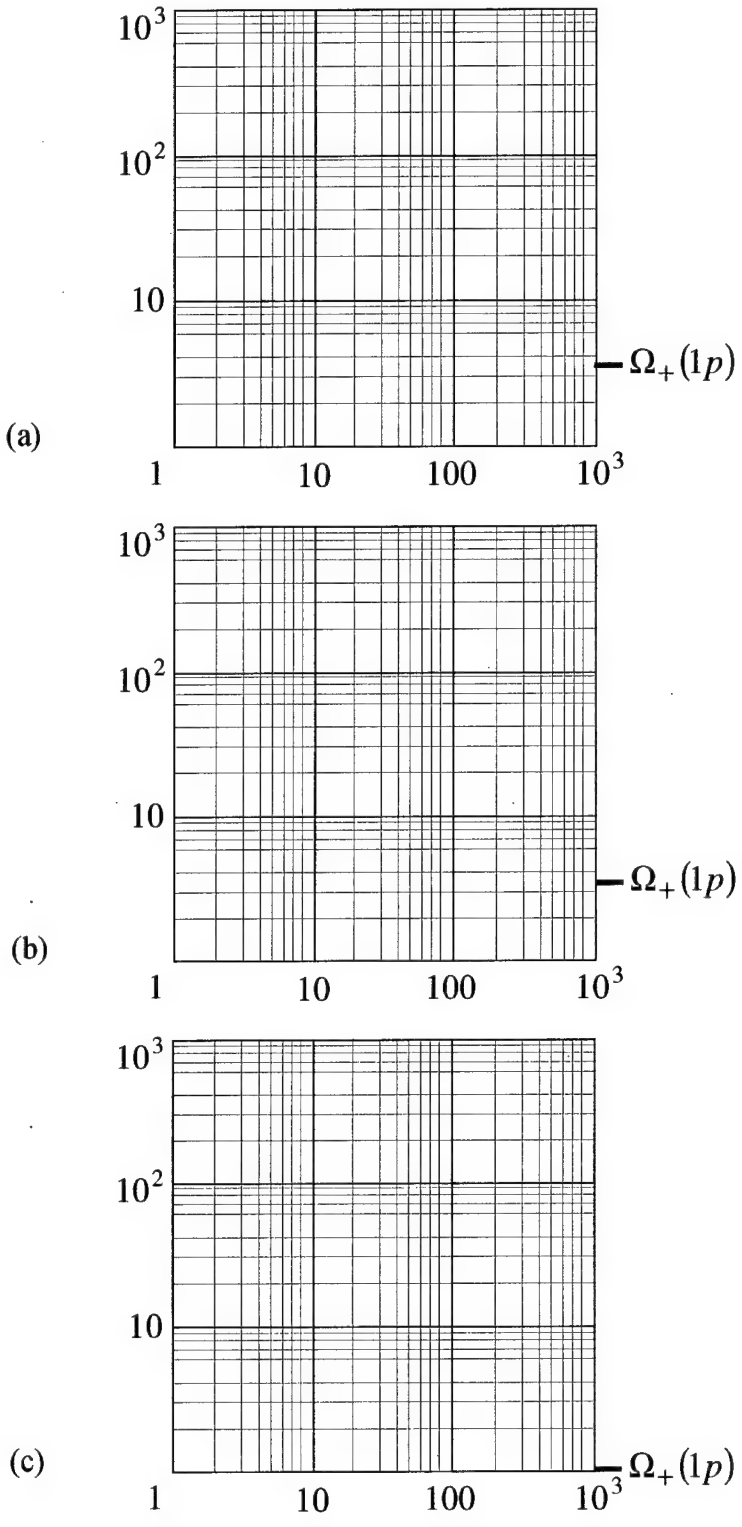

Fig. 42. Regions of viability and acceptability, as functions of the normalized frequency (Ω), for the conditions specified in Figs. 35c and 37.

a. A pressure transducer with a standard conditioning plate.

b. A pressure transducer without a conditioning plate.

c. A velocity transducer without a conditioning plate.

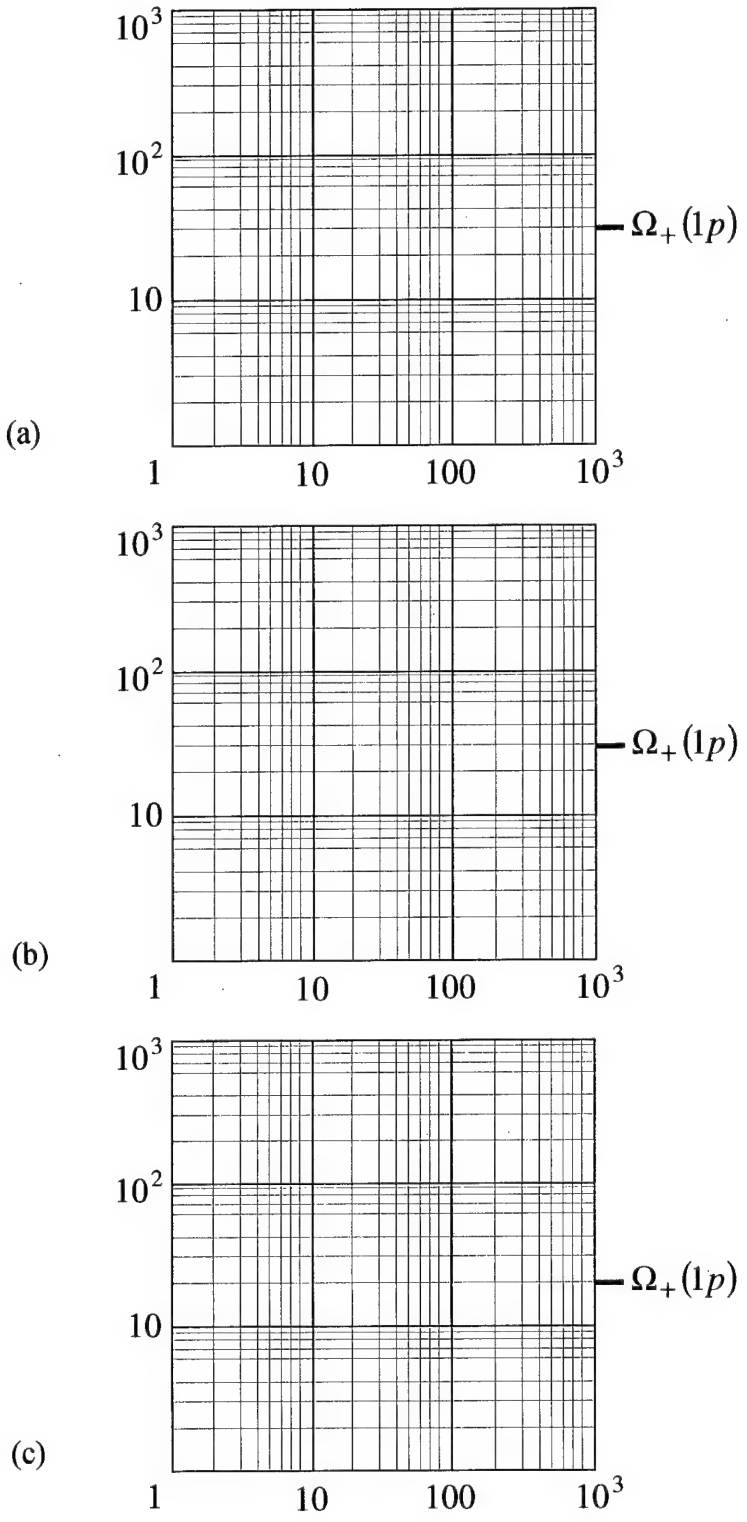

Fig. 43. Regions of viability and acceptability, as functions of the normalized frequency (Ω), for the conditions specified in Figs. 35c and 38.

a. A pressure transducer with a standard conditioning plate.

b. A pressure transducer without a conditioning plate.

c. A velocity transducer without a conditioning plate.

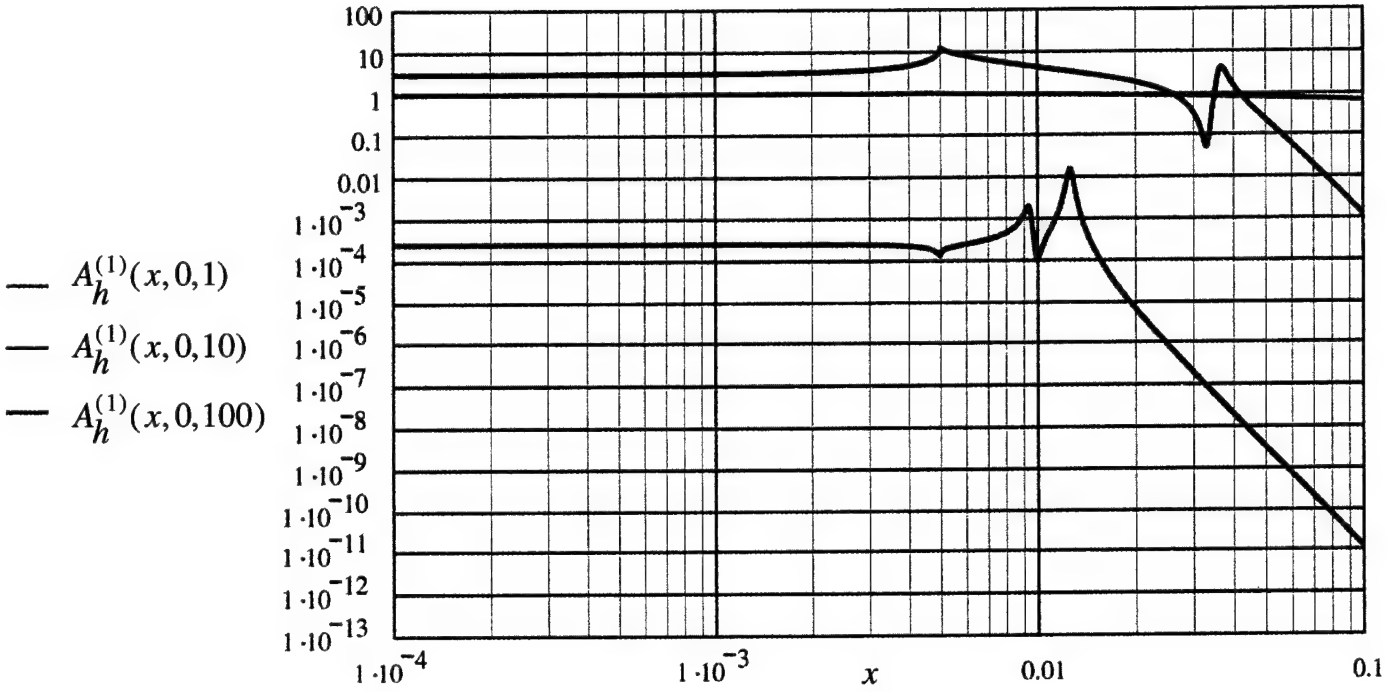

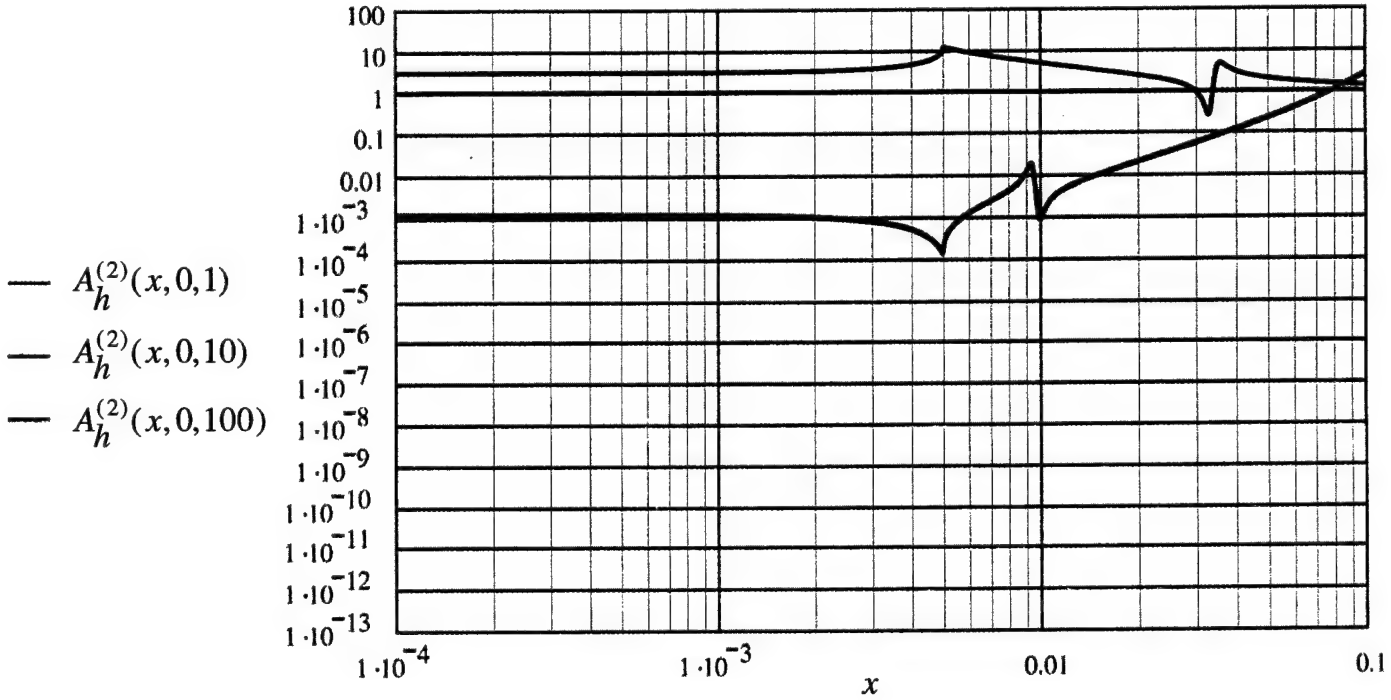

Fig. 44. The anti-radiation properties of the cladding on the hull, in terms of the filtering efficiency $A_h(x,y,\Omega)$ as a function of the normalized wavenumber (x) with $y \to 0$ and for three values of the normalized frequency (Ω); $\Omega = 1$, 10 and 100. [cf. Fig. 21.] The surface stiffness of the compliant layer is ten (10) measures.

a. With a standard conditioning plate; $A_h^{(1)}(x,y,\Omega)$

b. Without a conditioning plate; $A_h^{(2)}(x,y,\Omega)$.

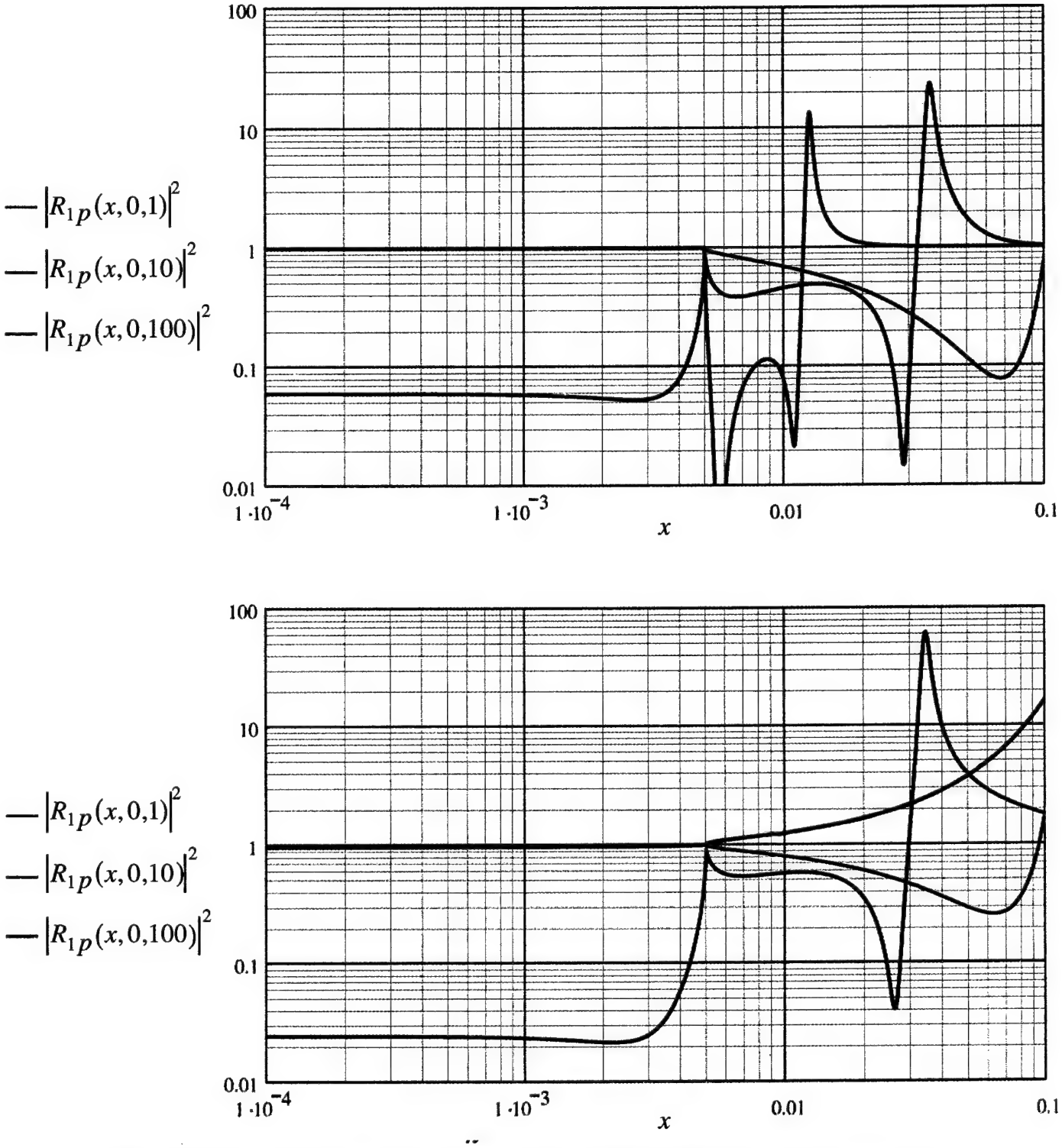

Fig. 45. The specular reflection efficiency $|R(x,y,\Omega)|^2$ of the cladded hull, as a function of the normalized wavenumber (x) with $y \to 0$ and for three values of the normalized frequency (Ω); $\Omega = 1$, 10 and 100. [cf. Fig. 22.] The surface stiffness of the compliant layer is ten (10) measures. [cf. Eq. (67a).]

a. With a standard conditioning plate; $|R_{1p}(x,y,\Omega)|^2$.

b. Without a conditioning plate; $|R_{2p}(x,y,\Omega)|^2$.

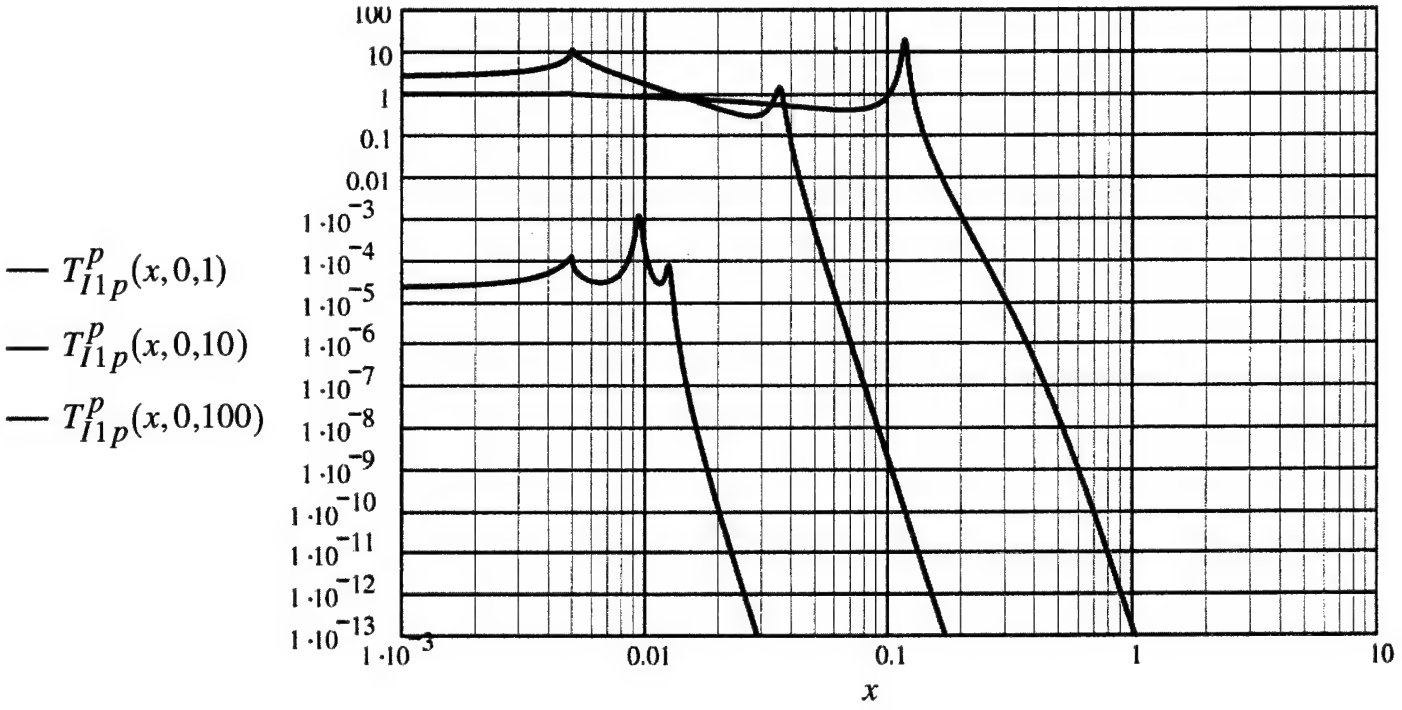

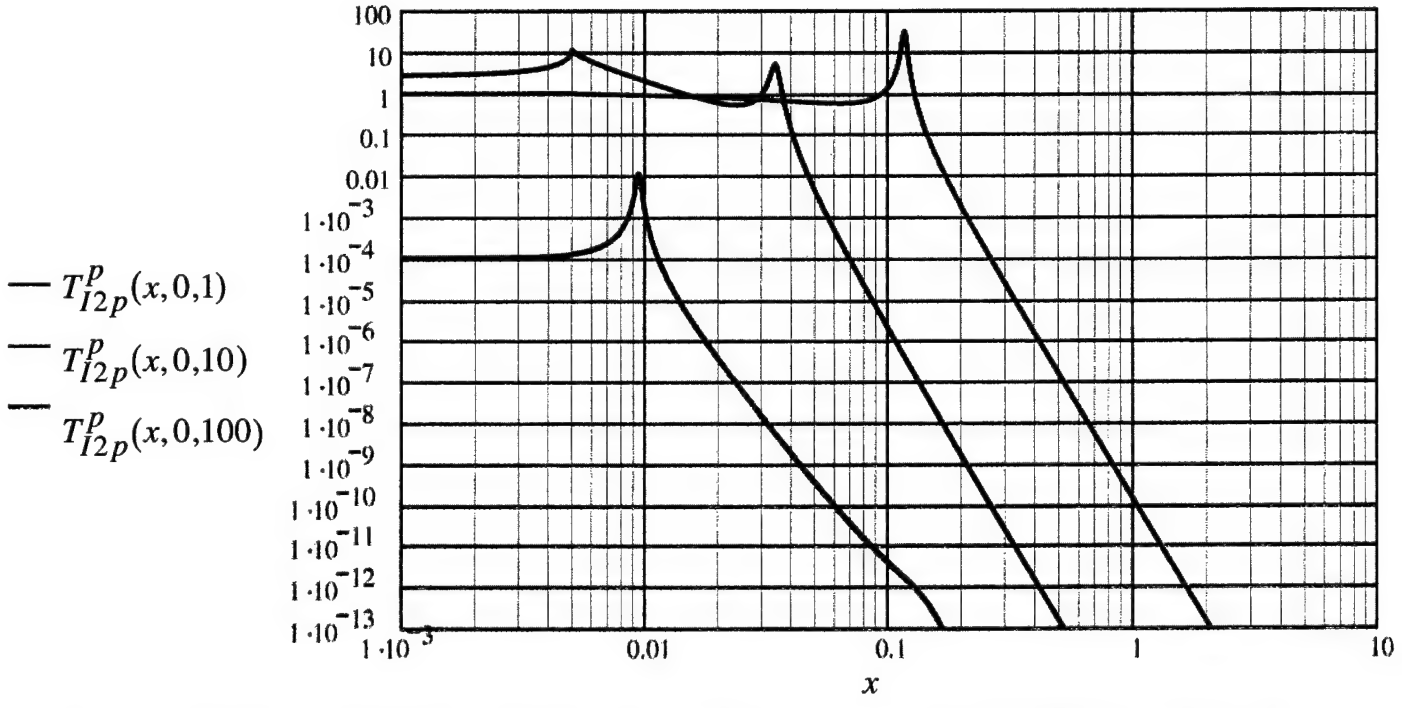

Fig. 46. The transference $T(x,y,\Omega)$ from the hull to the boundary on which the transducer are flush-mounted, as a function of the normalized wavenumber (x) with $y \to 0$ and for three values of the normalized frequency (Ω); $\Omega = 1$, 10 and 100. [cf. Fig. 23.] The surface stiffness of the compliant layer is ten (10) measures. [cf. Eq. (67a).]

a. $T^p_{I1p}(x,y,\Omega)$ is the transference of a drive on the hull to a pressure on the boundary. A standard conditioning plate is in place.

b. $T^p_{I2p}(x,y,\Omega)$ as in (a) except that the condition plate is removed.

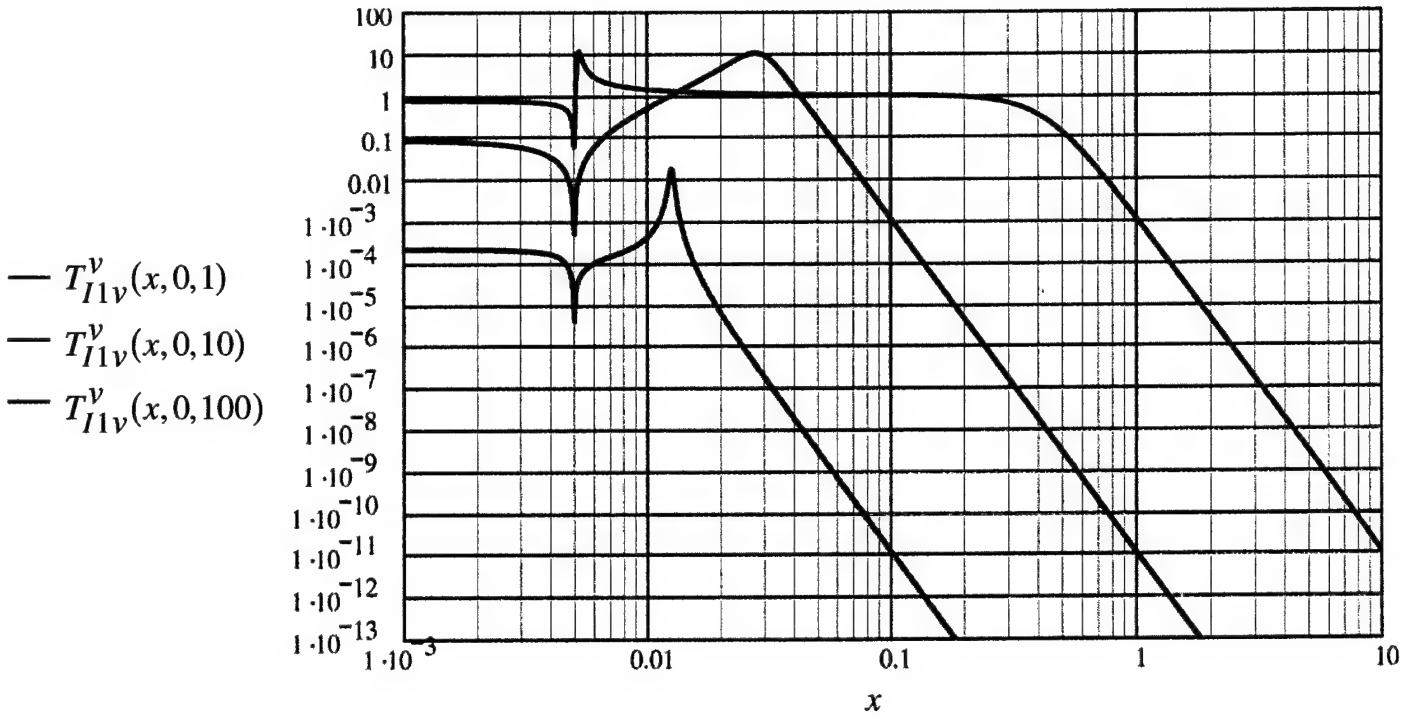

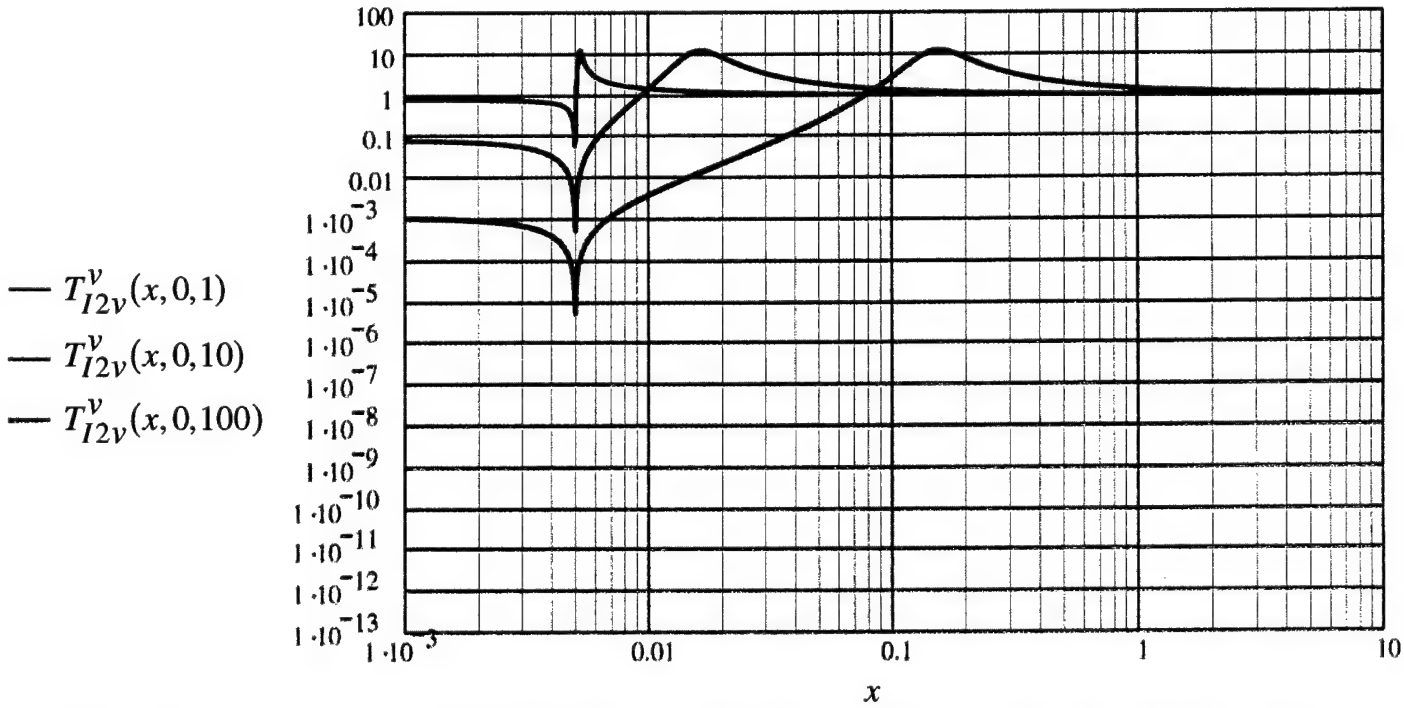

Fig. 46. The transference $T(x,y,\Omega)$ from the hull to the boundary on which the transducer are flush-mounted, as a function of the normalized wavenumber (x) with $y \to 0$ and for three values of the normalized frequency (Ω); $\Omega = 1$, 10 and 100. [cf. Fig. 23.] The surface stiffness of the compliant layer is ten (10) measures. [cf. Eq. (67a).]

c. $T^{v}_{I1v}(x,y,\Omega)$ is the transference of a velocity on the hull to a velocity on the boundary. A standard conditioning plate is in place.

d. $T^{v}_{I2v}(x,y,\Omega)$ as in (c), except that the condition plate is removed.

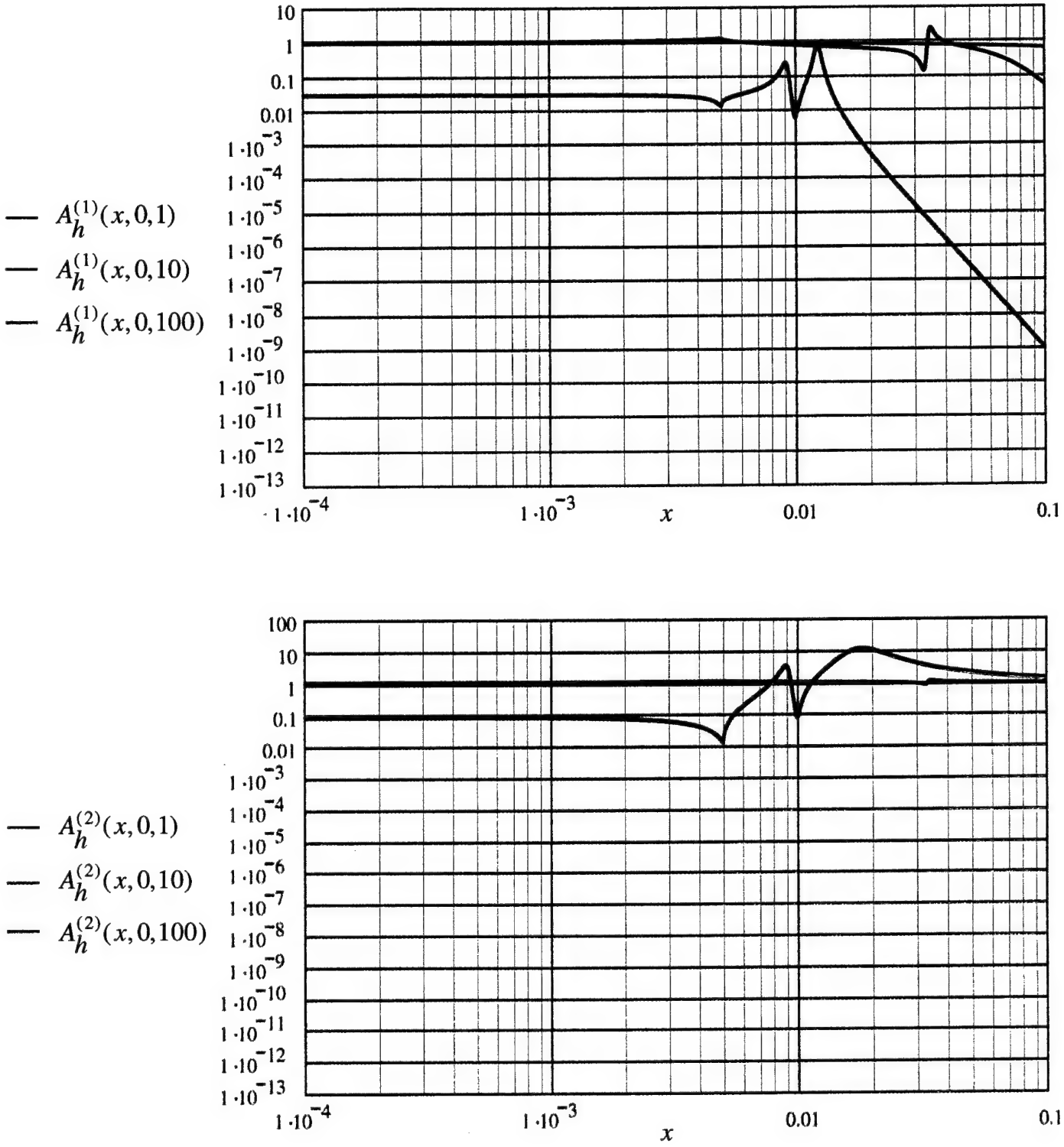

Fig. 47. Repeats Fig. 44, except that the surface stiffness of the compliant layer is thirty (30) measures, as specified in Eq. (67b).

a. With a standard conditioning plate; $A_h^{(1)}(x,y,\Omega)$

b. Without a conditioning plate; $A_h^{(2)}(x,y,\Omega)$.

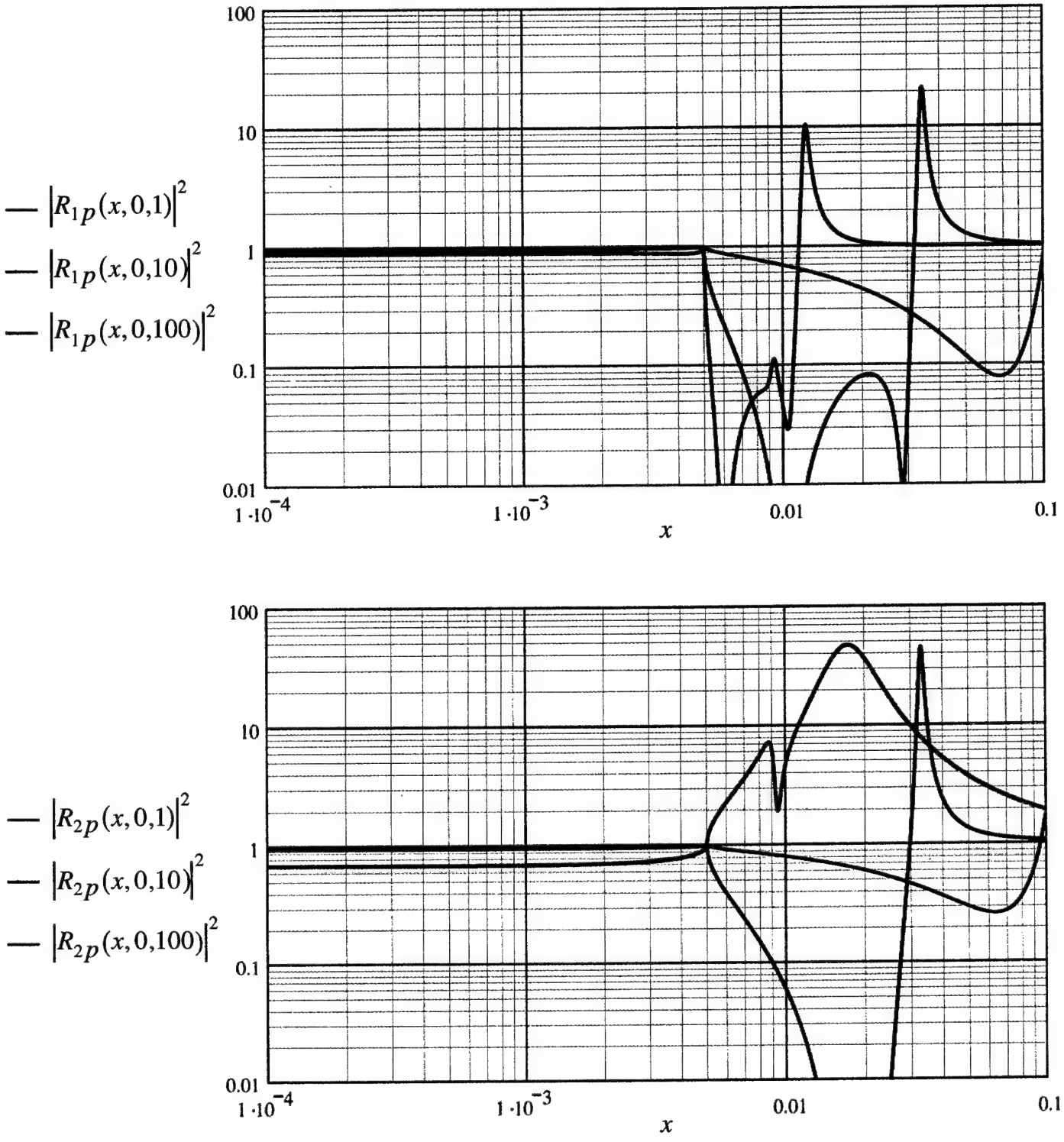

Fig. 48. Repeats Fig. 45, except that the surface stiffness of the compliant layer is thirty (30) measures, as specified in Eq. (67b).

a. With a standard conditioning plate; $|R_{1p}(x,y,\Omega)|^2$.

b. Without a conditioning plate; $|R_{2p}(x,y,\Omega)|^2$.

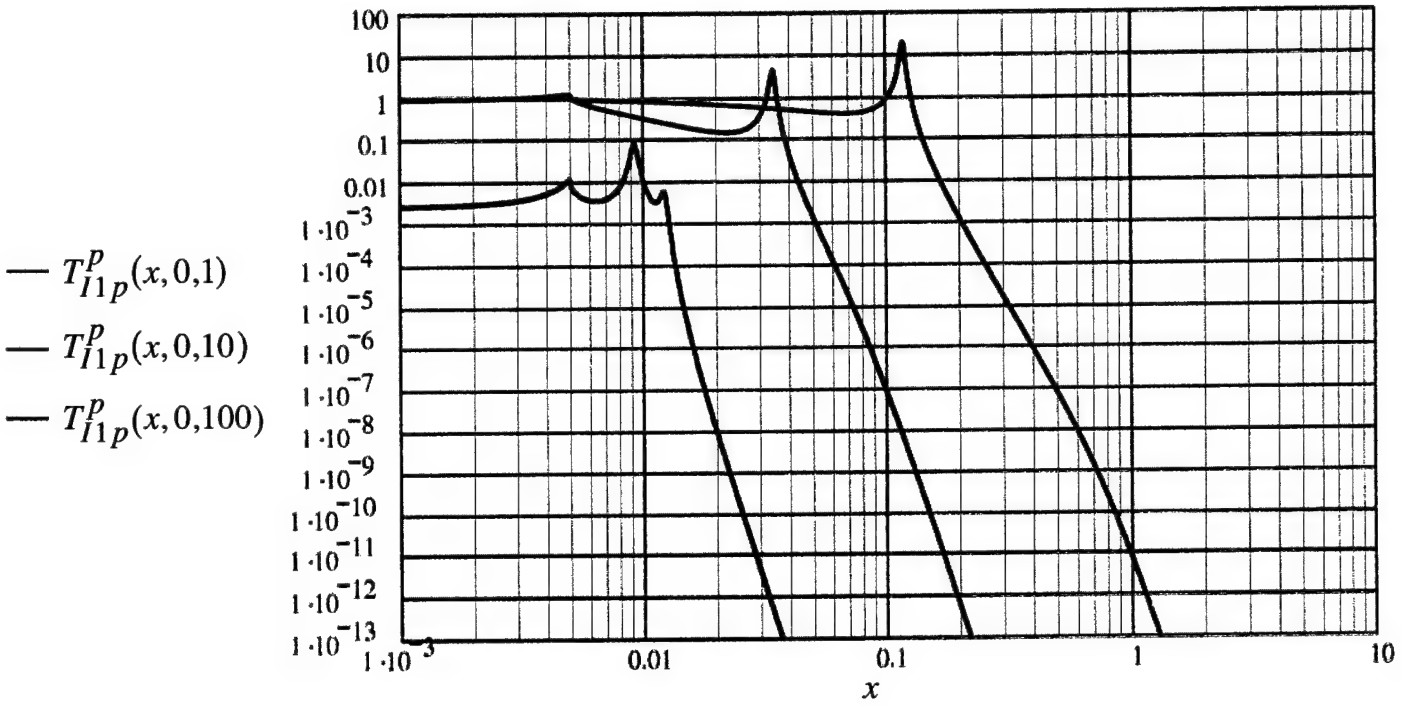

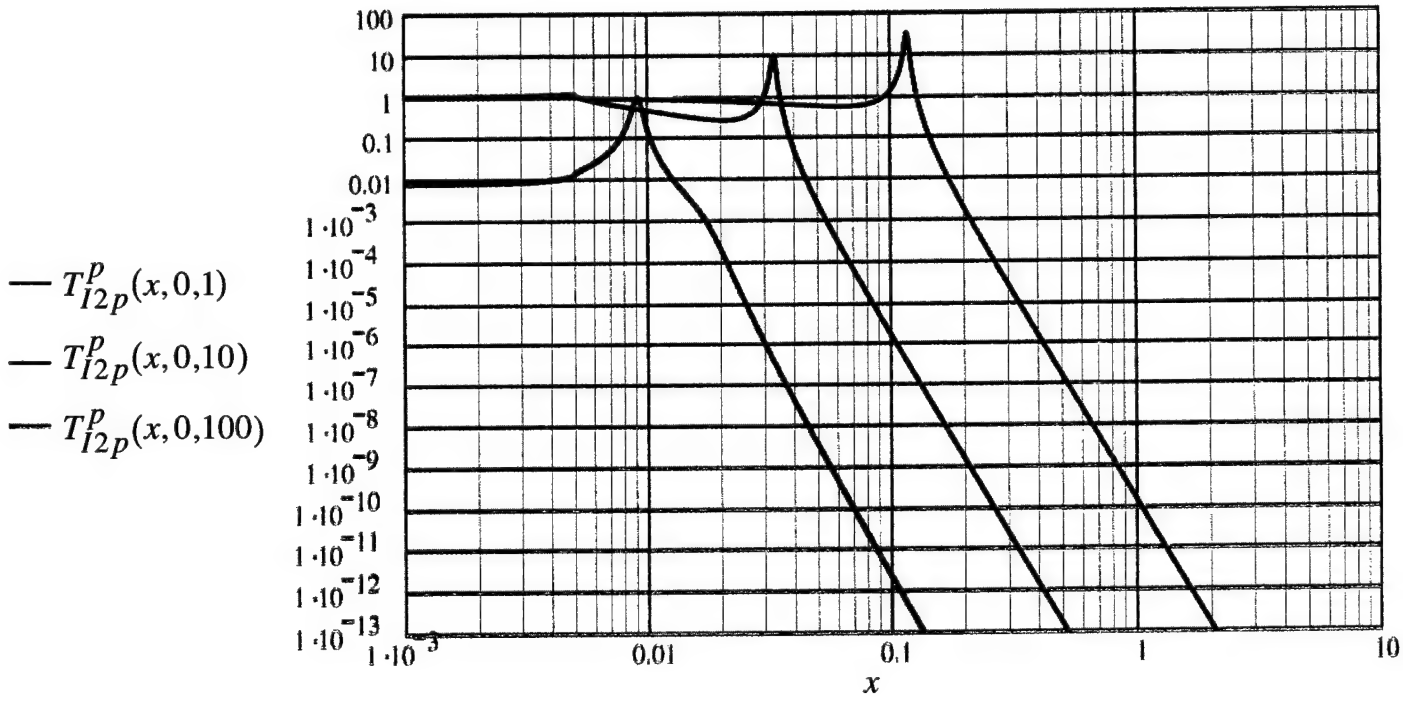

Fig. 49. Repeats Fig. 46, except that the surface stiffness of the compliant layer is thirty (30) measures, as specified in Eq. (67b).

a. $T^p_{I1p}(x,y,\Omega)$ is the transference of a drive on the hull to a pressure on the boundary. A standard conditioning plate is in place.

b. $T^p_{I2p}(x,y,\Omega)$ as in (a) except that the condition plate is removed.

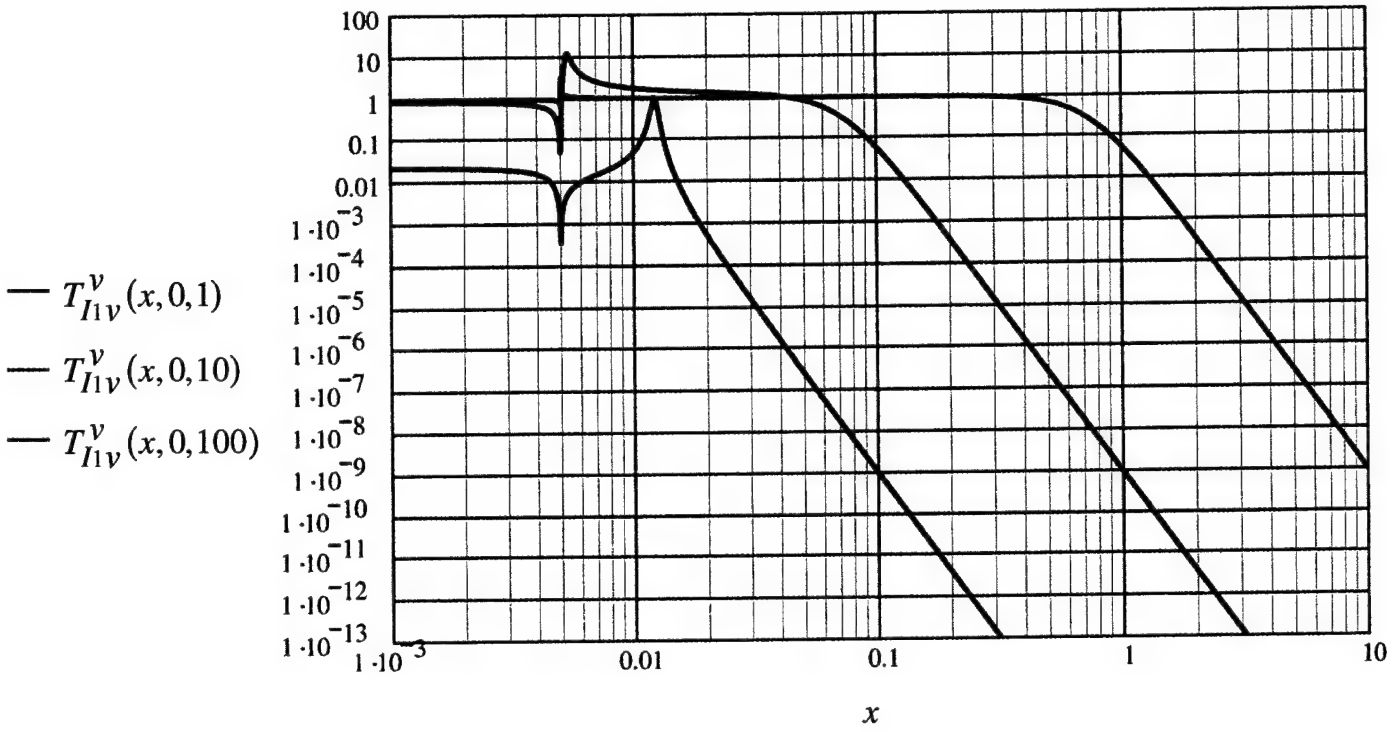

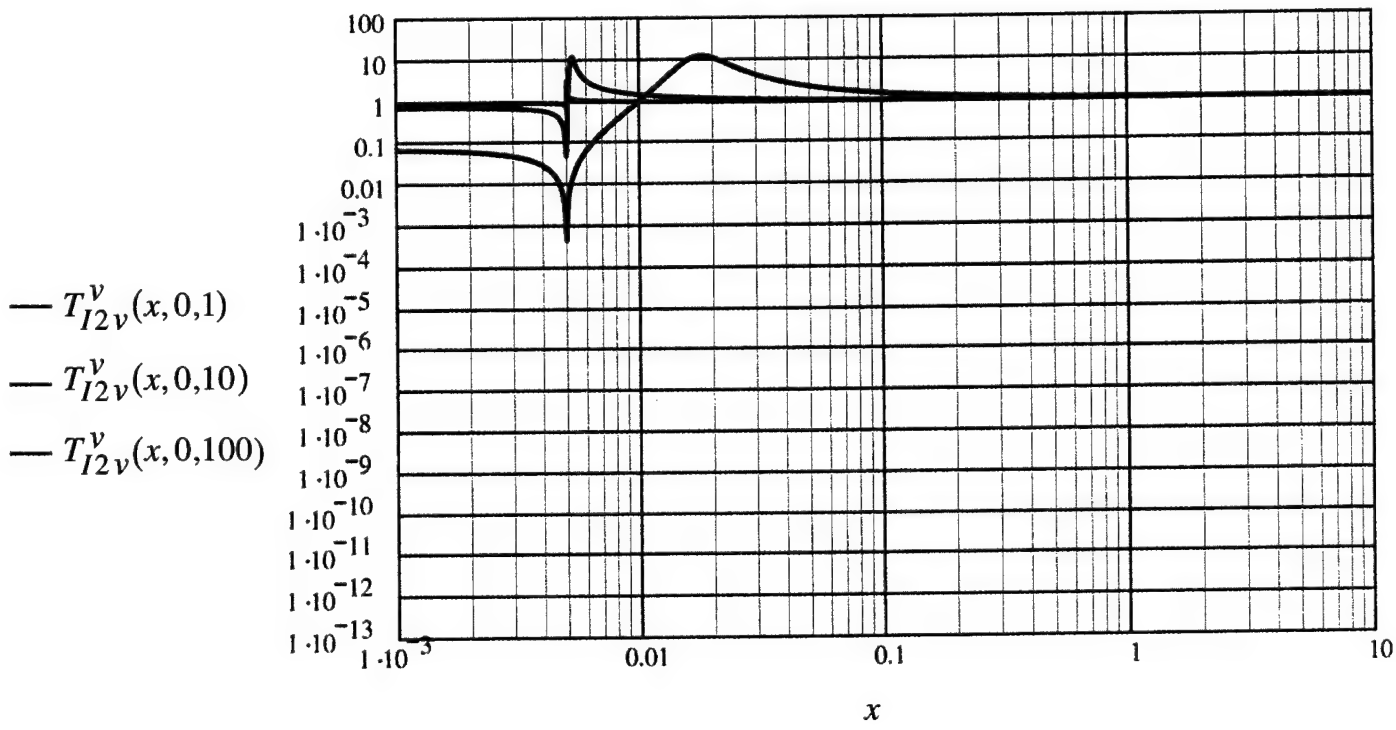

Fig. 49. Repeats Fig. 46, except that the surface stiffness of the compliant layer is thirty (30) measures, as specified in Eq. (67b).

c. $T^{v}_{I1v}(x,y,\Omega)$ is the transference of a velocity on the hull to a velocity on the boundary. A standard conditioning plate is in place.

d. $T^{v}_{I2v}(x,y,\Omega)$ as in (c), except that the condition plate is removed.

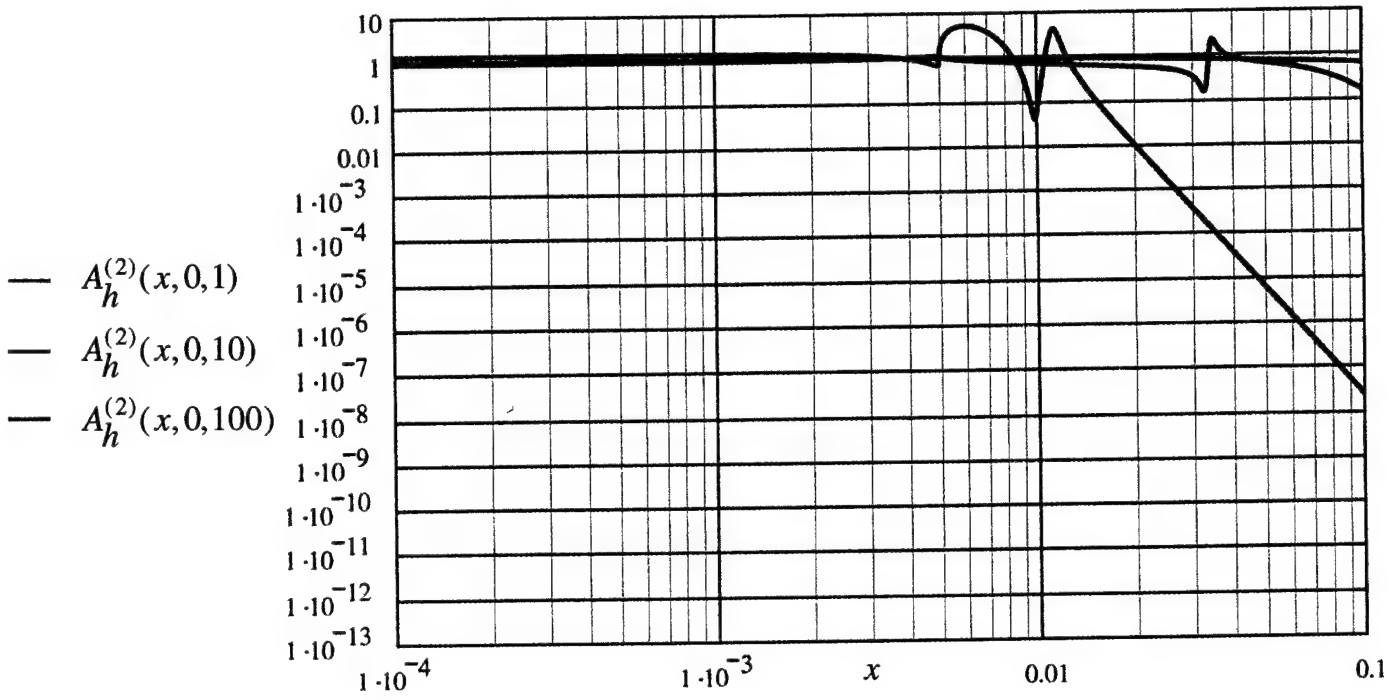

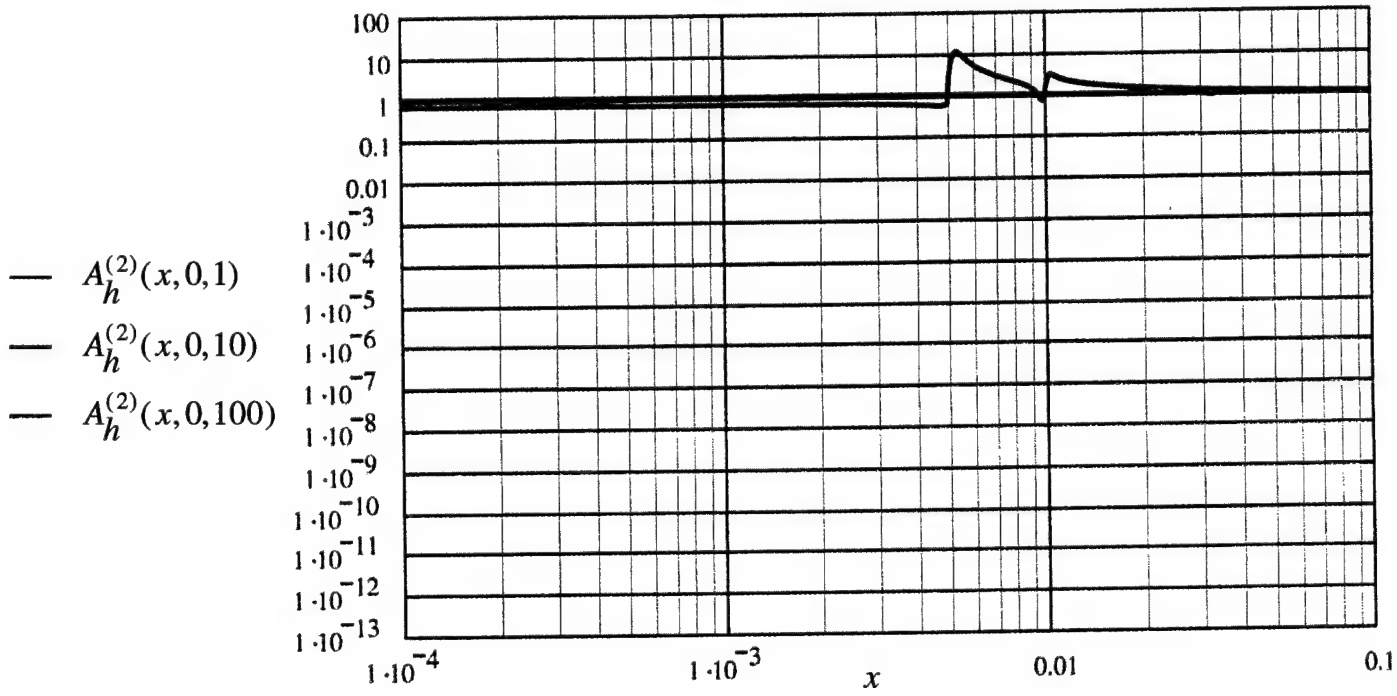

Fig. 50. Repeats Fig. 44, except that the surface stiffness of the compliant layer is specified by $\{5, 70\}$, as stated in Eq. (67f).

a. With a standard conditioning plate; $A_h^{(1)}(x, y, \Omega)$

b. Without a conditioning plate; $A_h^{(2)}(x, y, \Omega)$.

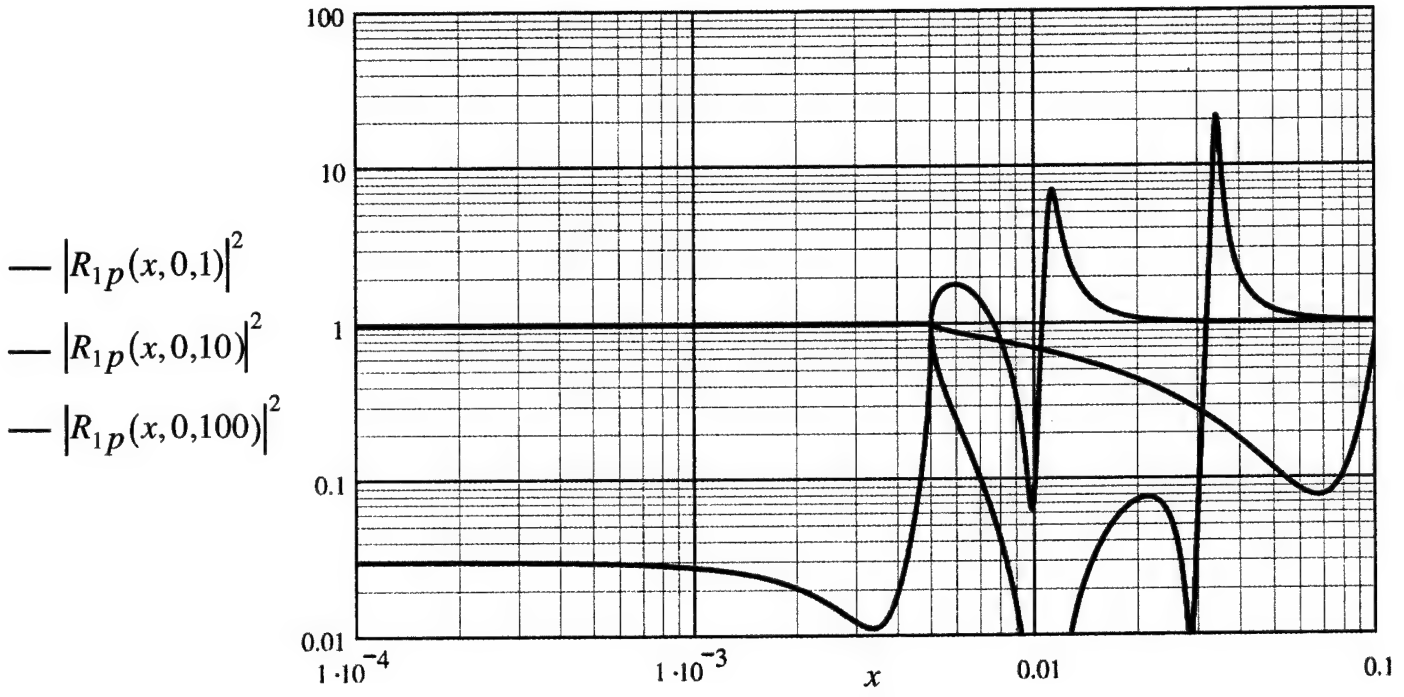

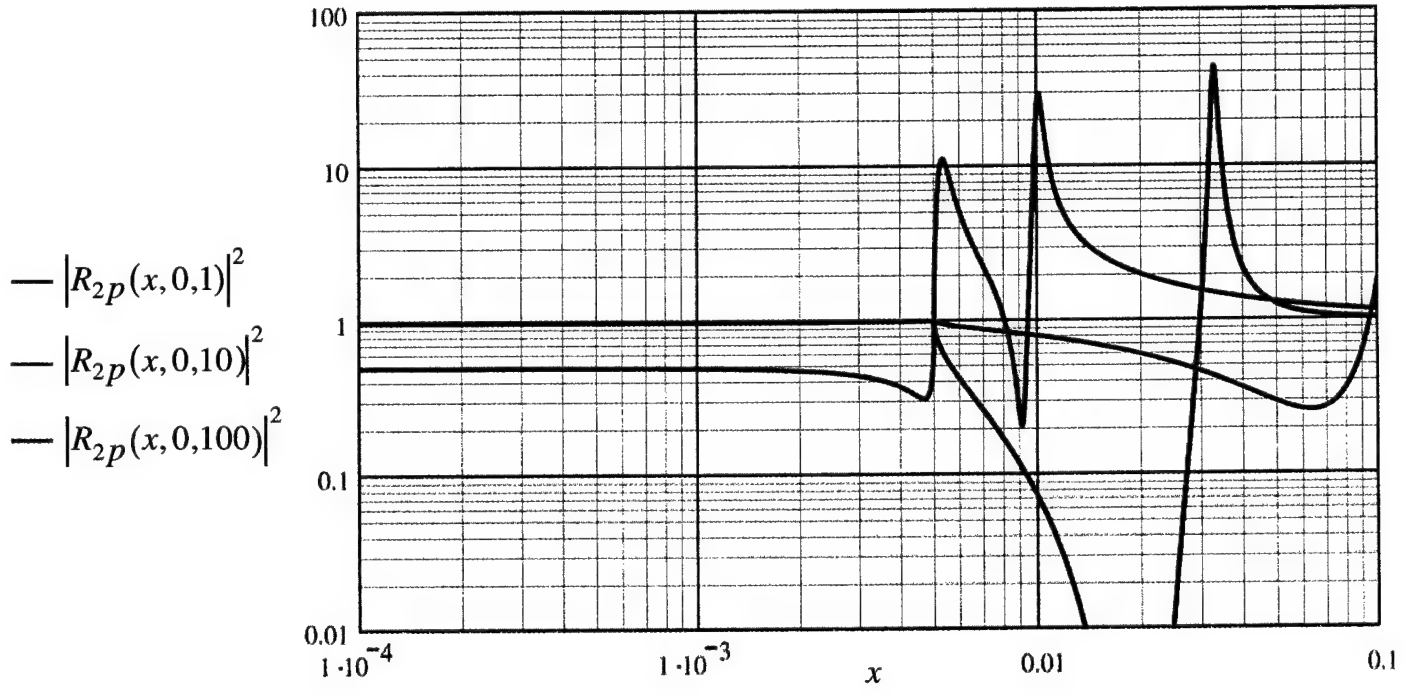

Fig. 51. Repeats Fig. 45, except that the surface stiffness of the compliant layer is specified by $\{5, 70\}$, as stated in Eq. (67f).

a. With a standard conditioning plate; $|R_{1p}(x, y, \Omega)|^2$.

b. Without a conditioning plate; $|R_{2p}(x, y, \Omega)|^2$.

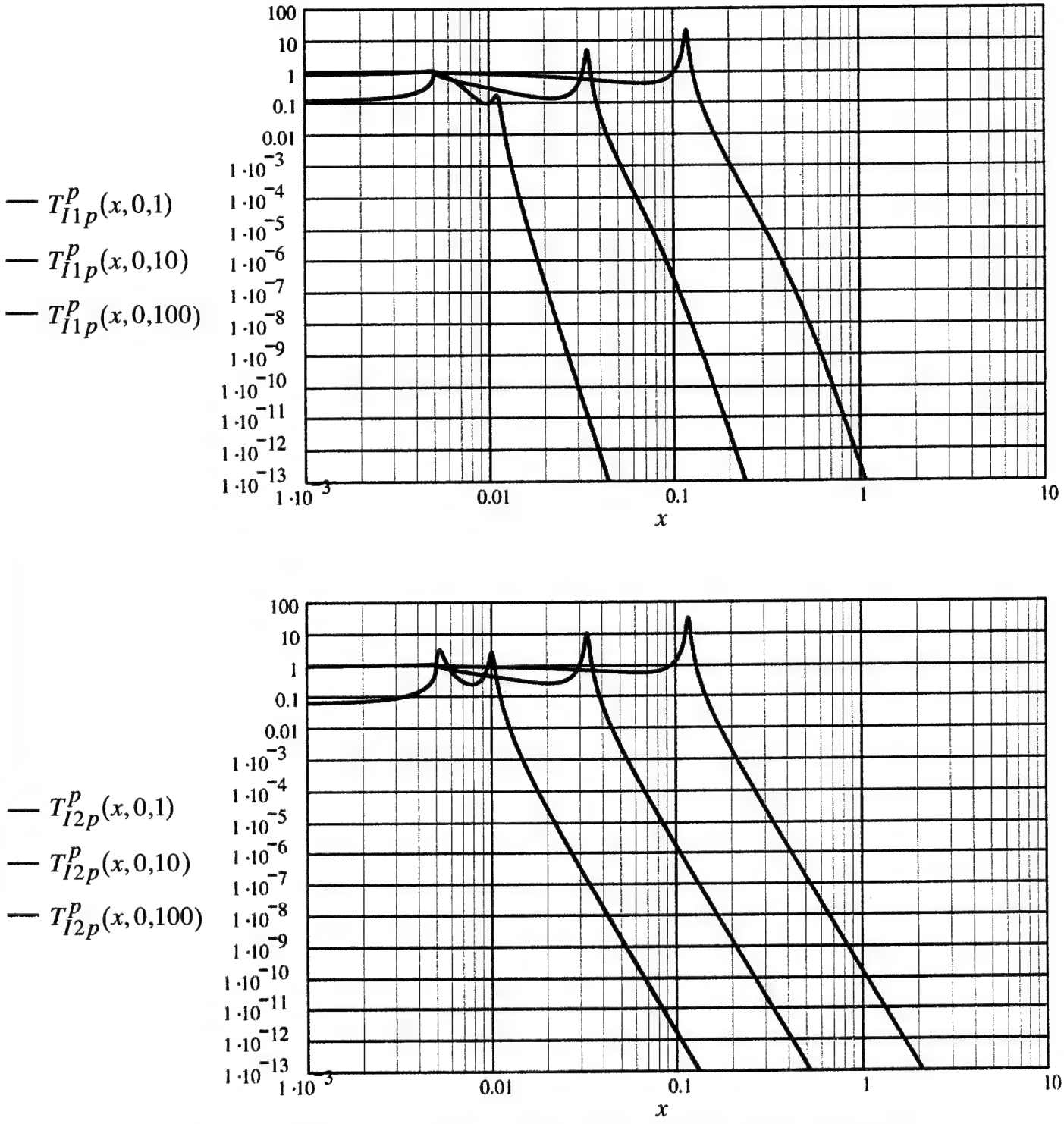

Fig. 52. Repeats Fig. 46, except that the surface stiffness of the compliant layer is specified by $\{5,70\}$, as stated in Eq. (67f).

a. $T^p_{I1p}(x,y,\Omega)$ is the transference of a drive on the hull to a pressure on the boundary. A standard conditioning plate is in place.

b. $T^p_{I2p}(x,y,\Omega)$ as in (a) except that the condition plate is removed.

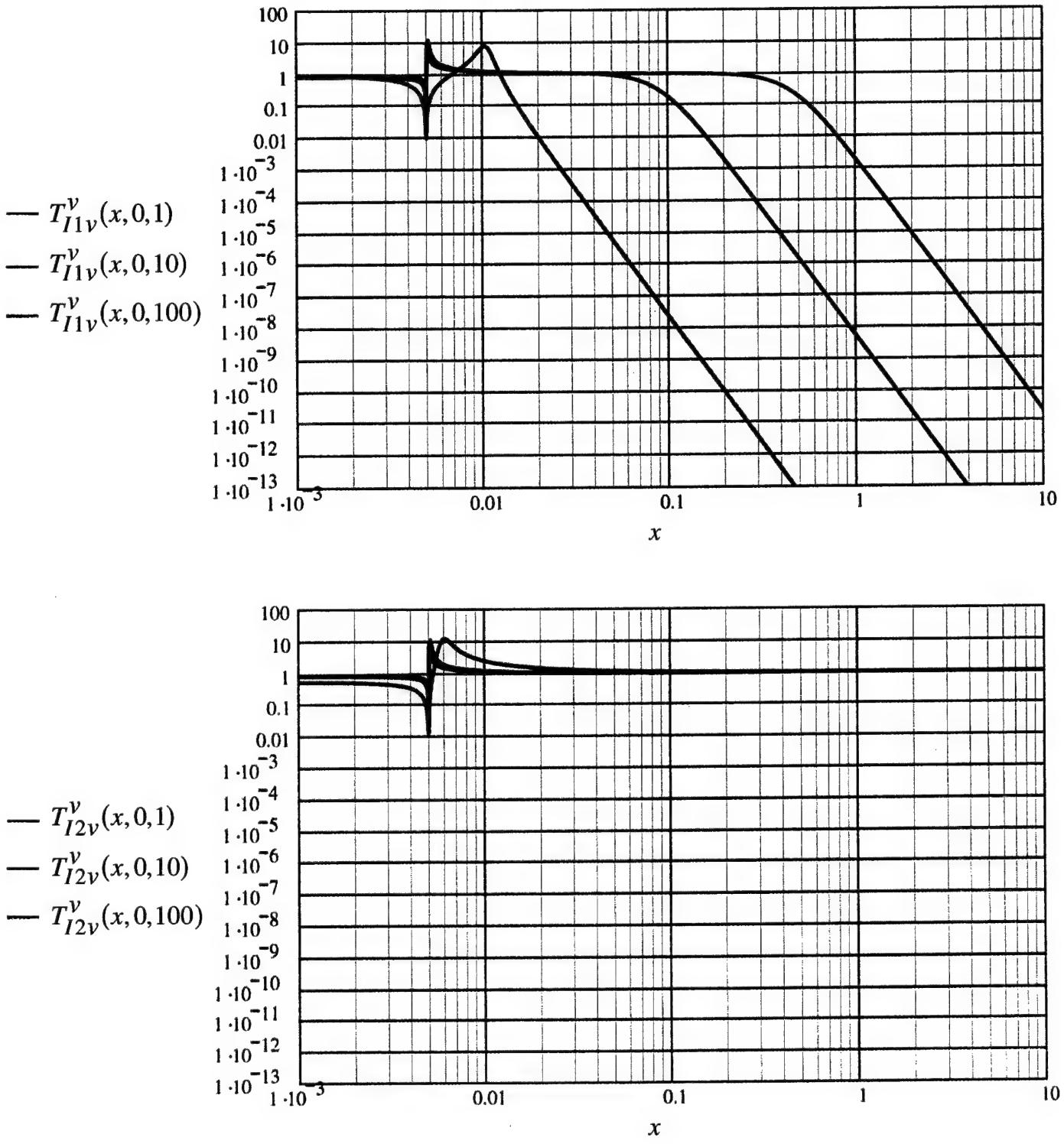

Fig. 52. Repeats Fig. 46, except that the surface stiffness of the compliant layer is specified by $\{5,70\}$, as stated in Eq. (67f).

c. $T^{v}_{I1v}(x,y,\Omega)$ is the transference of a velocity on the hull to a velocity on the boundary. A standard conditioning plate is in place.

d. $T^{v}_{I2v}(x,y,\Omega)$ as in (c), except that the condition plate is removed.

Appendix: What are some of the Alternatives?

Can the properties of the compliant layer; if called for, be artificially designed to improve the results just stated in the text? Indeed, these results seem to suggest a way to achieve an improvement: If $\Omega_o^o(\Omega)$ can be kept at least linear with respect to the normalized frequency through out the displayed or, at least, the relevant range, the results just related in the text will undergo changes. These changes may not, however, spell improvements. Nonetheless, the attempt to account for these changes may gain physical insights into the processes that are taking place in determining the performance of an array. Armed with such insights may help develop design guidelines that will improve the performance of the arrays. For this purpose the normalized frequency $\Omega_o^o(\Omega)$, that measures the surface stiffness of the compliant layer, is assigned a linear form; $\Omega_o^o(\Omega) = (\Omega / a)$, where (a) is a constant independent of (Ω). Then, for a normally incident pressure wave, the normalized surface impedance resulting from the parallel combination of the surface impedance of the compliant layer and surface impedance of the hull remains, for $a < 1$, mass control, for $a \cong 1$, resistance control and for $a > 1$, stiffness control, throughout the displayed normalized frequency range. [The resistance control surface impedance is equal to the surface impedance of the surface mass of the hull divided by $(i\eta_c)$, where (η_c) is the loss factor associated with the surface stiffness of the compliant layer. This surface impedance is, therefore, higher for smaller values of (η_c). In this report (η_c) is given the standard value of $3x10^{-1}$]. The normalized frequencies $\Omega_o^o(\Omega)$ for the three values of (a); $a = (1/2)$, (1) and $(5/2)$, are depicted, as a function of the normalized frequency (Ω); in Fig A1. The curves for $a = (1/2)$ and $a = (5/2)$ do not intersect, by definition, the curve for $a = (1)$ or, for that matter, each

other. [cf. Fig. 24.] Thus, the sensitivity curves exhibit only monotonic changes, as functions of the normalized frequency. The sensitivity curves are depicted in Figs. 2A-4A. Each figure exhibits three curves, which belong to the three types of arrays, with $a=(1/2)$, (1) and $(5/2)$, respectively. The sensitivities $C_{1p}(\Omega)$ and $C_{2p}(\Omega)$, both of pressure transducers, increase monotonically with increase in (Ω), indicating that these sensitivities are commensurate with corresponding increases in the surface impedance of the boundary, as can be verified from Eq. (36). Moreover, one may expect and observe that $C_{1p}(\Omega)$, that includes the conditioning plate, exceeds $C_{2p}(\Omega)$ in these figures. The latter sensitivity excludes the conditioning plate. However, for a standard conditioning plate, the difference between these two sensitivities should be rather insignificant. On the other hand, the sensitivity $C_{2v}(\Omega)$ of the velocity transducers decrease monotonically with increase in (Ω), indicating, again, that this sensitivity is commensurate with corresponding increases in the surface impedance of the boundary. Due to this monotonic behavior of the sensitivities, for a reasonable range of (a); $(1/5)\le a\le 5$, say, intersections of $C_{1p}(\Omega)$ and $C_{2p}(\Omega)$ with $C_{2v}(\Omega)$ occur. The intersections between $C_{2p}(\Omega)$ and $C_{2v}(\Omega)$ defines a normalized intersection frequency (Ω_c) that can be readily determined to be

$$\Omega_c=\Omega_\beta[(1-a^2)^2+\ \eta_c^2]^{1/2}\ /\ (1+\eta_c^2)^{1/2}\quad , \tag{A1}$$

where

$$\Omega_\beta\ =\ (\beta\Omega_h)\ ;\ \beta\ =\ [(\rho c)\ /\ (\omega_h m_h)]\quad . \tag{A2}$$

This normalized intersection frequency (Ω_c) supercedes the normalized resonance frequency (Ω_o), which, by definition, is lacking in the customized examples. [cf. Eqs (66) and (67), and Fig. 24 in the text.] In Eq. (A2), (ρc) is the characteristic impedance of the fluid, (ω_h) is the critical frequency and (m_h) is the surface mass of the hull, (β) is the fluid loading parameter and $\Omega_h = (\omega_h \delta / U)$. In the computations $\beta = 10^{-1}$, $\Omega_h = 360$ and η_c, as mentioned, is set equal to $3x10^{-1}$. Thus, (Ω_β) is approximately equal to (36) and from Eq. (A1), for $a = (1/2)$, $\Omega_c \cong 26$, for $a = (1)$, $\Omega_c \cong 10$ and for $a = (5/2)$, $\Omega_c \cong 190$. Moreover, an approximate evaluation of the sensitivities $C_{2p}(\Omega)$ and $C_{2v}(\Omega)$ may be derived in the forms

$$C_{2p}(\Omega/\Omega_c) = 4(\Omega/\Omega_c)^2 \ [(\Omega/\Omega_c)^2 + b]^{-1} \quad , \qquad \text{(A3a)}$$

$$C_{2v}(\Omega/\Omega_c) = 4(\Omega_c/\Omega)^2 \ [(\Omega_c/\Omega)^2 + b]^{-1} \equiv C_{2p}(\Omega_c/\Omega) \quad , \qquad \text{(A3b)}$$

where (b) is a constant of the order of unity. The sensitivities $C_{1p}(\Omega)$, $C_{2p}(\Omega)$ and $C_{2v}(\Omega)$ are computed and displayed in Figs. A2-A4 which pertain to $a = (1/2), (1)$ and $(5/2)$, respectively. These figures largely conform with Eqs. (A1)-(A3). In particular, in the lower normalized frequency range defined here by $\Omega < \Omega_c$, the sensitivity of the velocity transducers in array $(2v)$ lies largely at its maximum value of four (4), whereas the sensitivities of the pressure transducers, with and without the standard conditioning plate, in array $(1p)$ and array $(2p)$ are monotonically increasing toward such a maximum value at about the quadratic rate of $(\Omega < \Omega_c)^2$. It follows that in this lower normalized frequency range the velocity transducers in array $(2v)$ are, well nigh, acceptable, whereas the pressure transducers in array $(1p)$ and array $(2p)$ are hardly acceptable an octave or two below the normalized intersection frequency (Ω_c).

One is reminded that an array is defined, herein, to be *acceptable* if its sensitivity exceeds the value of (10^{-1}). [cf. Eq. (65).] The value is arbitrarily chosen, for certain purposes a higher or a lower value may be more judicially selected. A normalized frequency region, defined here by $\Omega \simeq \Omega_c$, spans from about an octave or two below (Ω_c) to about an octave or two above (Ω_c). In this region the sensitivities of the velocity transducers $C_{2v}(\Omega)$, of array $(2v)$, and of the pressure transducers $C_{1p}(\Omega)$ and $C_{2v}(\Omega)$, of array $(1p)$ and array $(2v)$, respectively, are, by definition, largely the same and approximately equal to two (2). It follows that in this region the velocity transducers in array $(2v)$ and the pressure transducers in array $(1p)$ and array $(2p)$ all meet the acceptability criterion. In the higher normalized frequency range defined here by $\Omega > \Omega_c$, the sensitivities $C_{1p}(\Omega)$ and $C_{2p}(\Omega)$ of the pressure transducers, of array $(1p)$ and array $(2p)$, respectively, rapidly reach, from the value of about two (2), the maximum value of four (4), whereas the sensitivity $C_{2v}(\Omega)$, of the velocity transducers, of array $(2v)$, monotonically diminishes, from the value of about two (2), at about the inverse quadratic rate of $(\Omega_c / \Omega)^2$. Therefore, in this higher normalized frequency range, array $(2v)$, incorporating velocity transducers, becomes unacceptable an octave or two above the normalized intersection frequency (Ω_c). Throughout the displayed normalized frequency range, array $(1p)$ is largely comparable in sensitivity to array $(2p)$; on the basis of sensitivity, these two arrays are twins, with possibly the former insignificantly superior to the later. Therefore, as far as sensitivity is concerned, under the conditions imposed in the Appendix, the dispensation of the conditioning plate is no longer at issue; the pressure transducers, with and without the conditioning plate, are, by and large, equally acceptable. It remains to examine the viability of the normalized outputs to (TBL) of the three arrays in contention.

The outputs to (TBL) $S_{1p}(\Omega)$, $S_{2p}(\Omega)$ and $S_{2v}(\Omega)$ are displayed, as functions of the normalized frequency (Ω); for $a=(1/2)$ in Fig. A5, for $a=(1)$ in Fig. A6 and for $a=(5/2)$ in A7. [cf. Figs. 17b, 30 and 36.]

When the surface stiffness is high enough; e.g., when $a=(1/2)$, and the levels are viable i.e., $S(\Omega) < 10^8$ re[$(\mu\text{Pa})^2$ / Hz]), the normalized output to (TBL) $S_{2v}(\Omega)$ is marginally better than the normalized outputs to (TBL) $S_{1p}(\Omega)$ and $S_{2p}(\Omega)$. The latter two exhibits largely identical normalized outputs to (TBL). [cf. Figs. 17b, 30 and 36.] In the light of Figs. A2 and A5, the performance of array $(1p)$ and array $(2p)$ are largely identical throughout. Again, with respect to these arrays, the use of the standard conditioning plate ceases to be an issue; the conditioning plate may be simply dispensed without a penalty. In the lower normalized frequency range, defined by $\Omega<\Omega_c\approx 26$, the performance of array $(2v)$ is superior to that of array $(1p)$ and array $(2p)$, largely, but not exclusively, on account of the sensitivity. In the region of the normalized frequency that spans an octave or two below (Ω_c) to an octave or two above (Ω_c); and is defined by $\Omega\approx\Omega_c\approx 26$, array $(2v)$ performs marginally better than array $(1p)$ and array $(2p)$, largely on the basis of a lower normalized output to (TBL). In the higher normalized frequency range defined by $\Omega>\Omega_c\approx 26$, the performance of array $(2v)$ is inferior to that of array $(1p)$ and array $(2p)$, largely on the basis of failing sensitivity an octave or two above (Ω_c). Since the viability of the normalized outputs to (TBL) commences only above the normalized frequency at $\Omega=10$, the utility of array $(2v)$ is cast in doubt except for conjunctive employment with array $(2p)$ and then only in the region defined by $\Omega\approx\Omega_c=26$. [cf. Section VII.]

When the surface stiffness is kept in resonance; i.e., when $a=1$, and the levels are to be viable, the normalized output to (TBL) $S_{2v}(\Omega)$ is only marginally worse than

the normalized outputs to (TBL) $S_{1p}(\Omega)$ and $S_{2p}(\Omega)$. The latter two exhibit identical normalized outputs to (TBL). [cf. Figs. 17a, 30 and 36.] Consulting Figs. A3 and A6, one infers, that the performance of array $(1p)$ and array $(2p)$ are largely identical throughout, and therefore, with respect to these arrays, the dispensation of the standard conditioning plate, again, ceases to be an issue. Since for $a = 1$, the normalized intersection frequency (Ω_c) is less than ten (10) and since the viability of the normalized outputs to (TBL) commences only above this normalized frequency, there is little incentive to bring in the employment of array $(2v)$, the exclusive employment of array $(2p)$ and not of CAVES is then recommended.

When the surface stiffness is kept low enough; e.g., when $a = (5/2)$, the normalized outputs to (TBL) $S_{2p}(\Omega)$ and $S_{2v}(\Omega)$ of array $(2p)$ and array $(2v)$, respectively, are largely identical and are marginally higher than the normalized output to (TBL) $S_{1p}(\Omega)$ of array $(1p)$, throughout the displayed normalized frequency range. The difference is more marginal, the more the viable range is penetrated. In light of Figs. A4 and A7, the performance of array $(1p)$ and array $(2p)$ are largely unacceptable in the normalized frequency range that lies an octave or two below the normalized intersection frequency (Ω_c). In this example (Ω_c) is high and is equal to about 190. On the other hand, array $(1p)$and array $(2p)$ become acceptable, with improving sensitivities, in the complementary range defined by $\Omega \geq (\Omega_c / 3) \cong 60$, whereas array $(2v)$ becomes largely unacceptable an octave or two beyond the normalized intersection frequency where $\Omega \geq 600$. In the region defined by $\Omega \approx \Omega_c = 190$, the performances of array $(2v)$ and array $(2p)$ are, by and large, identical. In this region, the performance of array $(1p)$ is marginally superior. Taking into account that the viabilities of the normalized outputs to (TBL) commence above the normalized frequency at $\Omega\Omega_t \approx 10$,

the employment of array $(2v)$ is thus demanded at the lower normalized frequency range defined by $\Omega \leq 60$. [cf. Eq. (64) in the text.] In this range neither array $(1p)$ nor array $(2p)$ are acceptable alternatives; the slight viability advantage of array $(1p)$ is not enough to compensate for the deficiency in its sensitivity. The low surface impedance of the surface mass control boundary, in this case, cannot sufficiently shore up the surface impedance of the boundary to satisfy the sensitivities of pressure transducers at this low normalized frequency range. At the higher normalized frequency region, where $60 \leq \Omega \leq 190$, all three arrays in contention are viable and acceptable, notwithstanding that array $(1p)$ is marginally a better performer in this range. For the still higher range, where $\Omega > 190$, array $(1p)$ and array $(2p)$ increase their performances with increase in the normalized frequency, with the former array maintaining the performance lead. On the other hand, in this range the performance of array $(2v)$ deteriorates with increase in the normalized frequency, becoming unacceptable when $\Omega \geq 500$. In this normalized frequency range and in the absence of a standard conditioning plate, the conjunctive utilization of array $(2p)$ is, thereby, demanded. Nonetheless, as is evidenced in Figs. A4 and A7, for $a = (5/2)$, the performance of array $(2p)$ falls marginally short of the performance of array $(1p)$ throughout the normalized frequency range including that just quoted.

Taking a composite of Figs. 5 and A1 and Figs. A2-A7, many features in Figs. 28 and 35 and 17a, 30 and 36 may be readily explained and physically accounted for. A composite of this sort may also be employed with regard to auxiliary functions of the cladding; e.g., those relating to anti-radiation, stealth and transference from the hull to the array. In this manner design guidelines may be developed to decipher means to improve the performances of the arrays and minimize their affects on auxiliary functions that may

be crucial to the successful operation of the vehicle as a whole. In this sense one finds the justification for including the Appendix in this report.

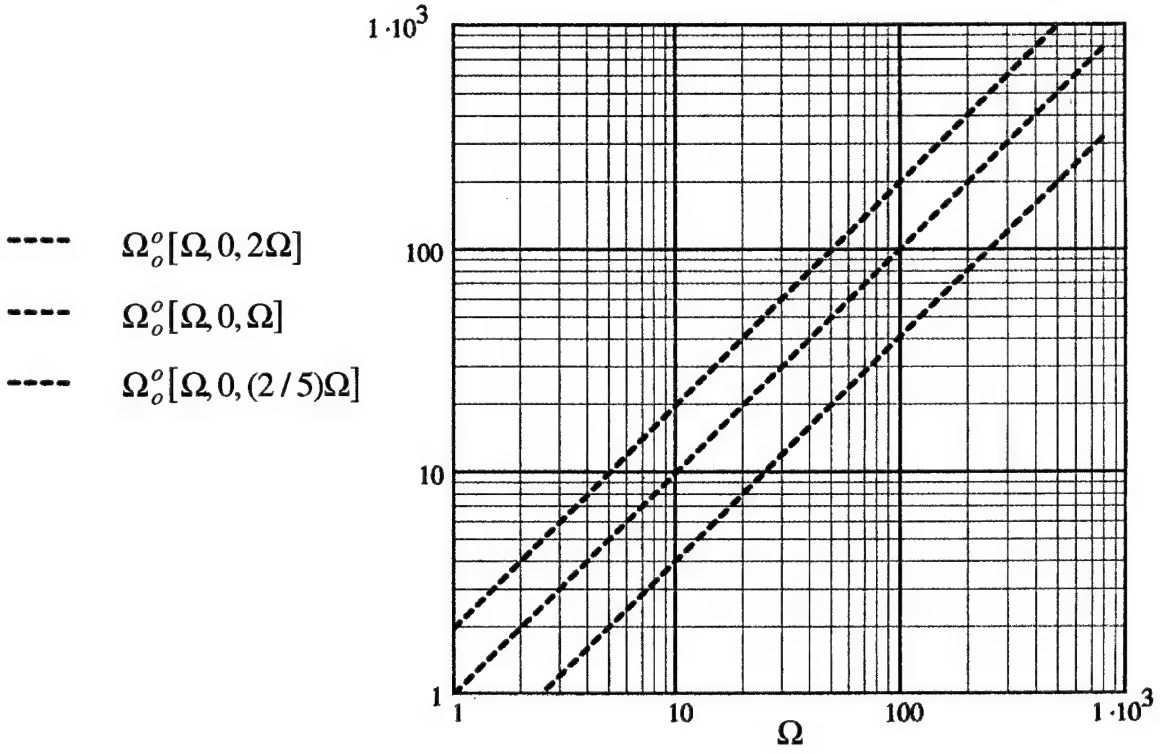

Fig. A1. Three (artificial) forms for the linear measure of the surface stiffness of the compliant layer: $\Omega_o^o(\Omega) = (\Omega/a)$; $a = (1/2), (1)$ and $(5/2)$; $\Omega_o^o(\Omega, \Omega_s, \Omega^o) = \Omega^o\{(\Omega)(\Omega_s + \Omega)^{-1}\}$. [cf. Fig. 5.]

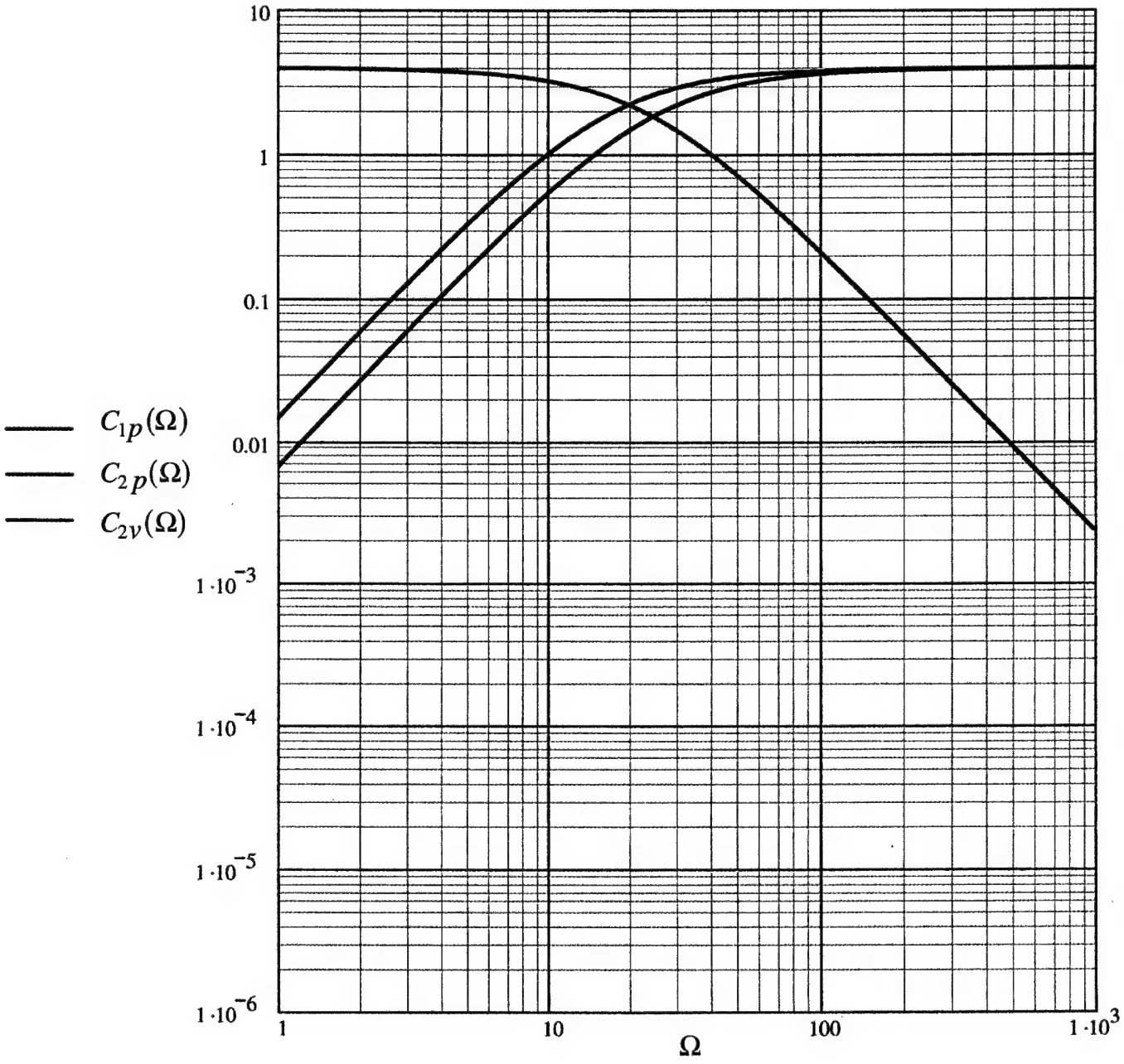

Fig. A2. Sensitivities $C_{1p}(\Omega)$, $C_{2p}(\Omega)$ and $C_{2v}(\Omega)$, as functions of the normalized frequency (Ω) of array $(1p)$, array $(2p)$ and array $(2v)$, respectively, with the measure of the surface stiffness set to $\Omega_o^o(\Omega) = 2\Omega$.

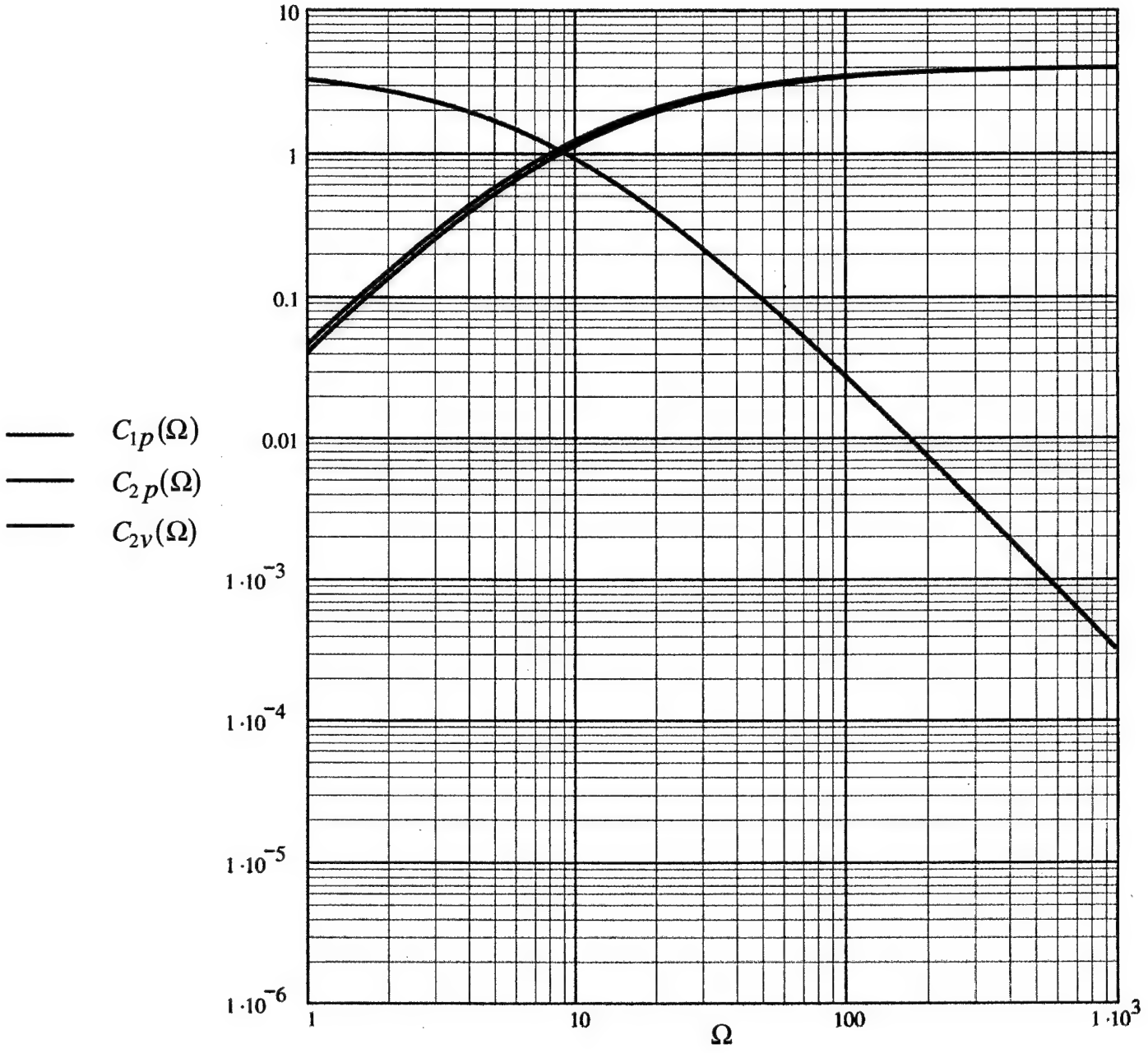

Fig. A3. Repeats Fig. A2, except that $\Omega_o^o(\Omega) = \Omega$. [cf. Fig. A1.]

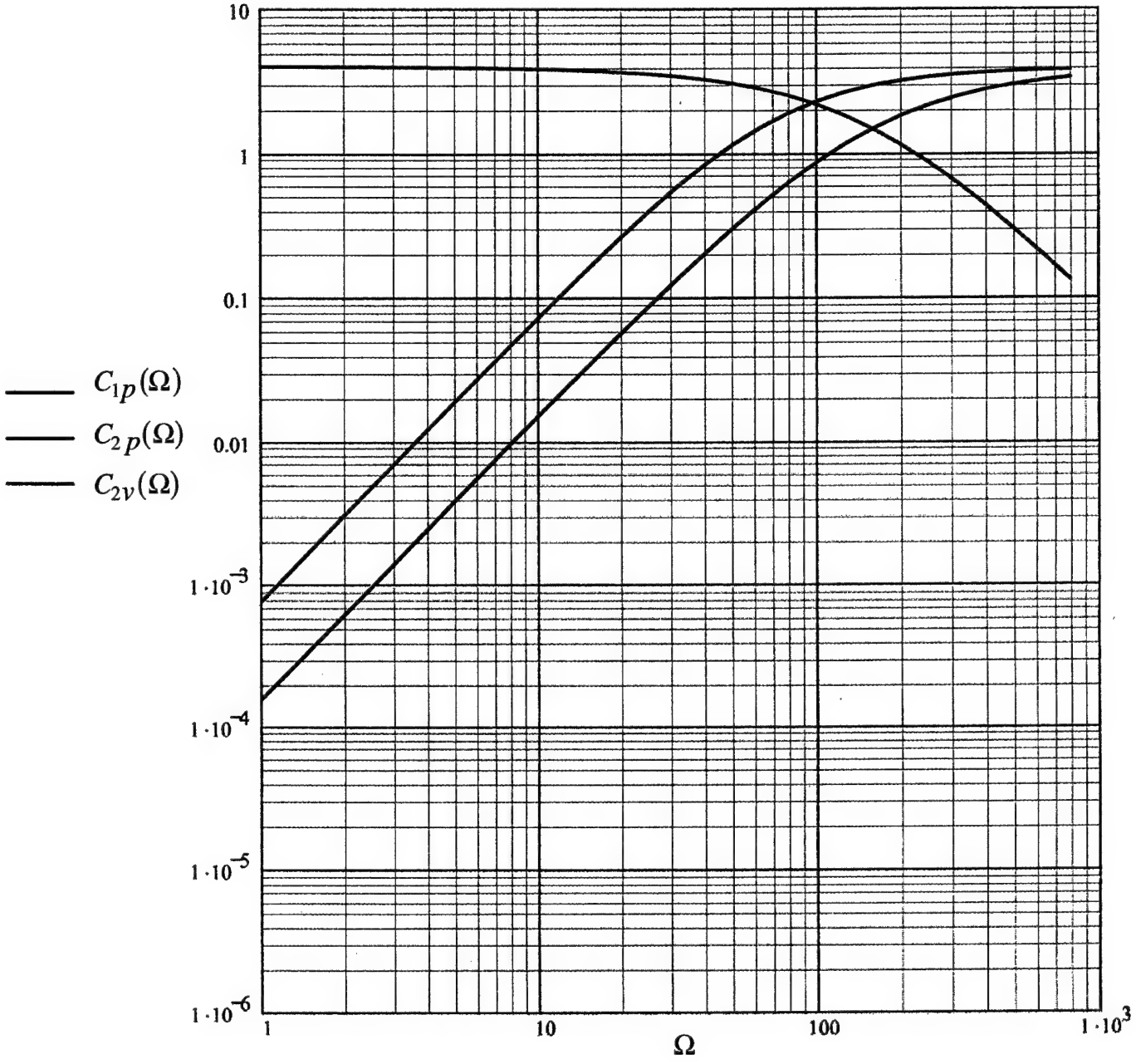

Fig. A4. Repeats Fig. A2, except that $\tilde{\Omega}_o^o(\Omega) = (2/5)\Omega$. [cf. Fig. A1.]

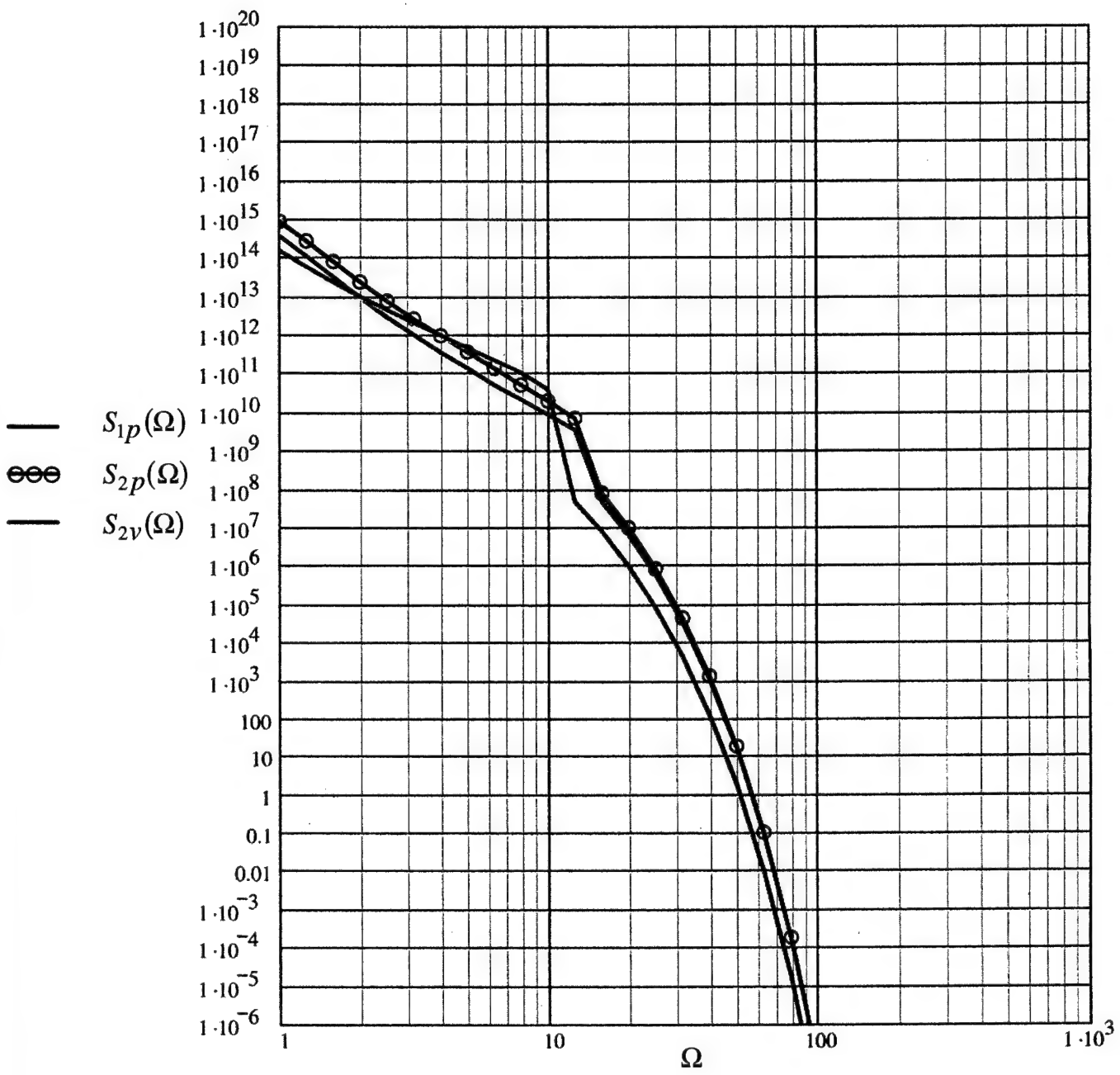

Fig. A5. Normalized outputs to (TBL) $S_{1p}(\Omega)$, $S_{2p}(\Omega)$ and $S_{2v}(\Omega)$, as functions of the normalized frequency (Ω) for the three arrays; array $(1p)$, array $(2p)$ and array $(2v)$, respectively. In this figure the measure of the surface stiffness is set to $\Omega_o^o(\Omega) = 2\Omega$. [cf. Figs. 2 and A1.]

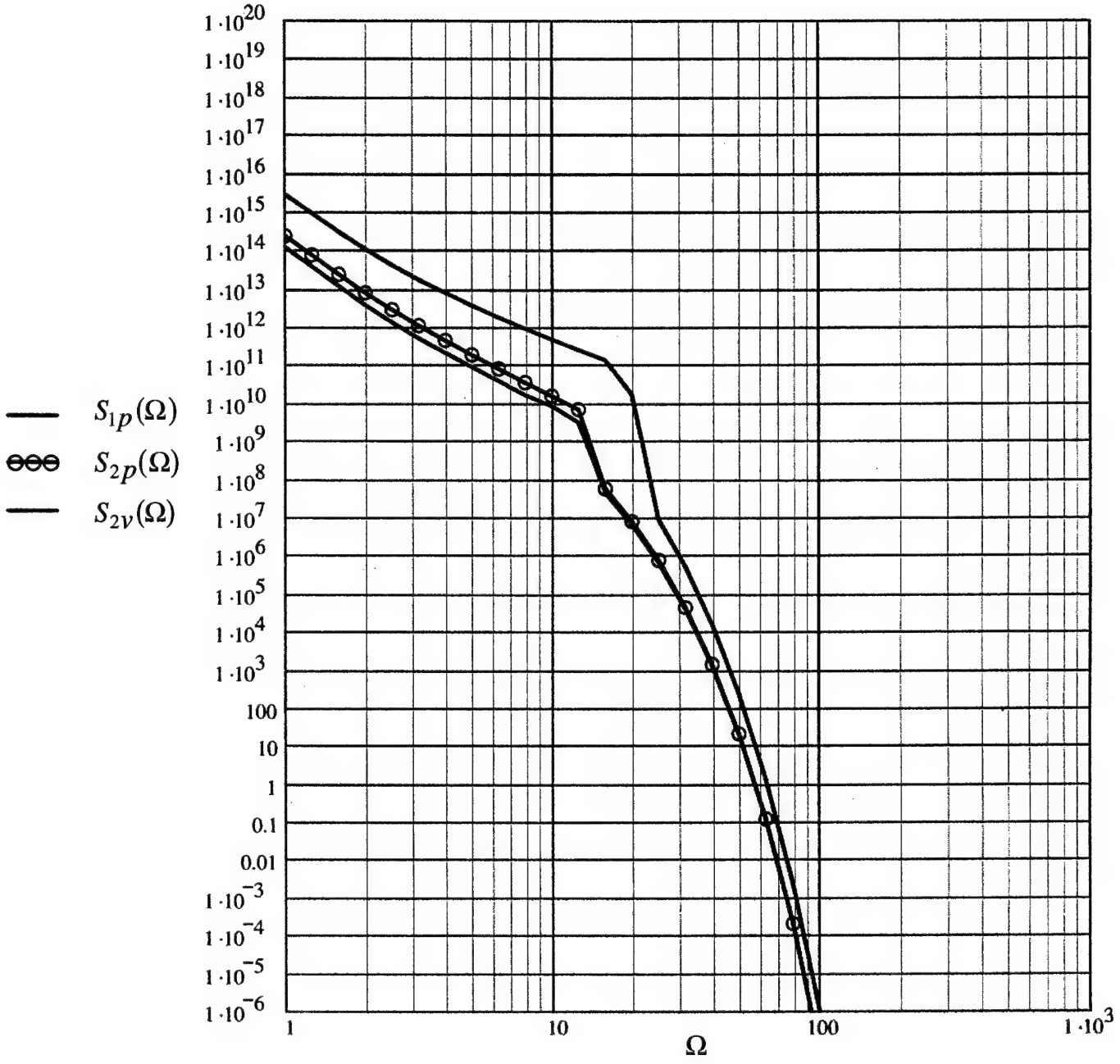

Fig. A6. Repeats Fig. A5, except that $\Omega_o^o(\Omega) = \Omega$.

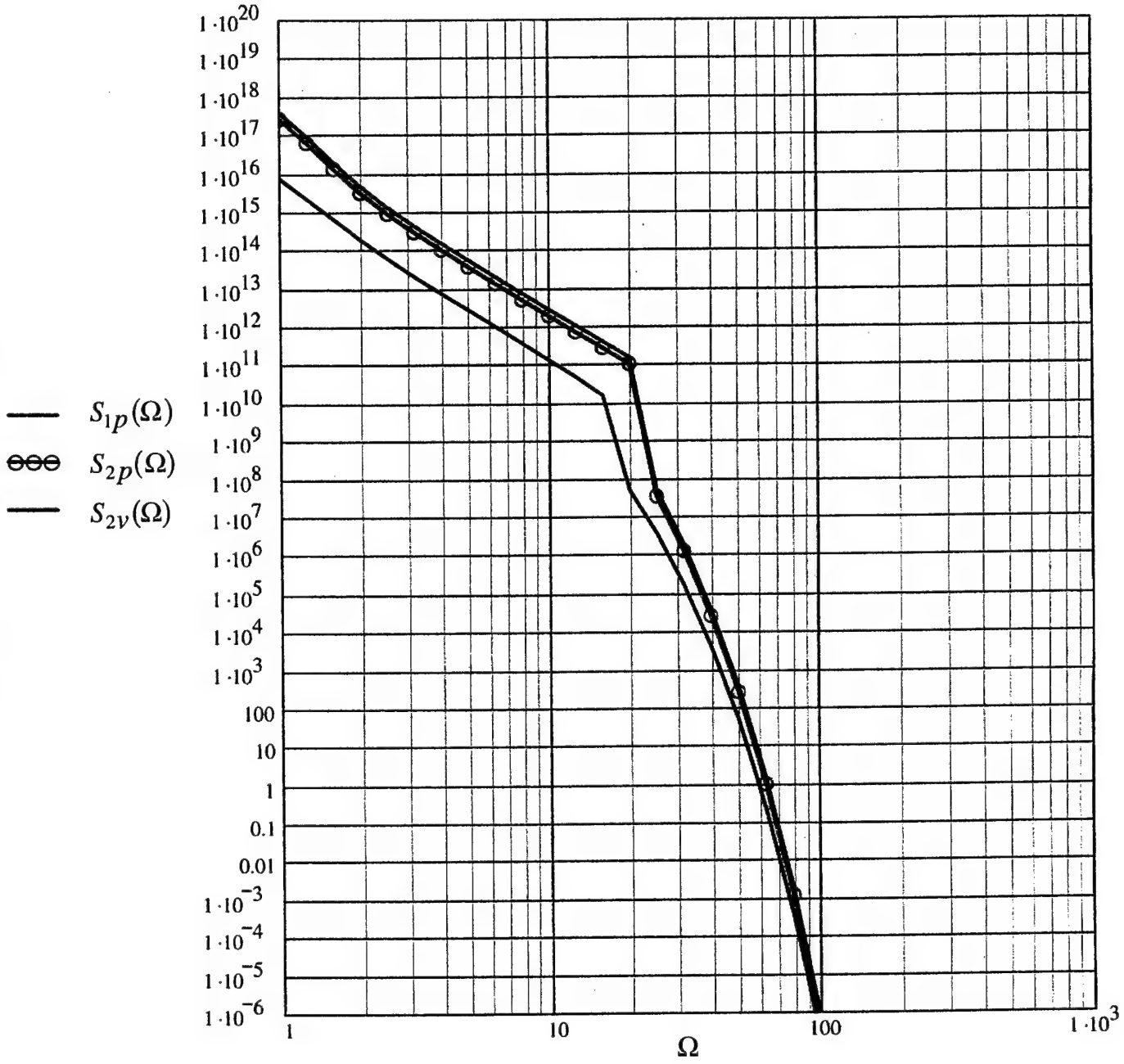

Fig. A7. Repeats Fig. A5, except that $\Omega_o^o(\Omega) = (2/5)\Omega$.

THIS PAGE INTENTIONALLY LEFT BLANK

REFERENCES

1. G. Maidanik and K.J. Becker, "Primitive Comparison of the Signal-to-Noise Ratios of Pressure and Velocity Planar Arrays," NSWCCD-SIG-97/256-7030 (1997).
2. G. Maidanik and K.J. Becker "Cursory and Primitive Comparison of the Signal-to-Noise Ratios of Pressure and Velocity Planar Arrays," NSWCCD-70--TR-1999/163 (June 1999).
3. M. Strasberg, "Flow Noise in Acoustic Particle-Velocity Sensors," Memorandum (29 April 1997).
4. G. Maidanik and J. Dickey, "Designing a negligible specular reflection coefficient for a panel with a compliant layer," Journal Acoustical Society of America **90**, 2139-2145 (1991).
5. G. Maidanik and J. Dickey, "A Boundary that Sustains a Negligible Specular Reflection Coefficient Over a Wide Frequency Band." Accepted for Publication in JASA.
6. M. Kim, "Caves, Prediction of Flow-Induced Noise in a Multiple-Layer System," Presentation (28 June 1999).
7. N.C. Martin, R. Barile and R.N. Brown, "Relative Flow Noise Performance of Pressure and Motion Sensing Arrays," Memorandum (12 June 1997).
8. G. Maidanik and K.J. Becker, "The Normalized Outputs to (TBL) of Pressure and Velocity Transducers and Their Sensitivities: Can the Conditioning Plate be Dispensed? Memorandum (3 Feb 2000).

THIS PAGE INTENTIONALLY LEFT BLANK

INITIAL DISTRIBUTION

Copies

2 NAVSEA 05T2
- 1 Taddeo
- 1 Biancardi

5 ONR/ONT
- 1 334 Tucker
- 1 334 Radlinski
- 1 334 Vogelsong
- 1 334 Main
- 1 Library

4 NRL
- 1 5130 Bucaro
- 1 5130 Williams
- 1 5130 Photiadis
- 1 Library

4 NUWC/NPT
- 1 Sandman
- 1 Harari
- 1 3332 Lee
- 1 Library

2 DTIC

2 Johns Hopkins University
- 1 Green
- 1 Dickey

2 ARL/Penn State University
- 1 Burroughs
- 1 Hwang

1 R.H. Lyons
- 1 Lyons

1 Cambridge Collaborative
- 1 Manning

1 Cambridge Acoustical Associates
- 1 Garrelick

1 J.G. Engineering Research
- 1 Greenspan

1 MIT
- 1 Dyer

Copies

1 Catholic Univ. of Am. Eng. Dept.
- 1 McCoy

2 Boston University
- 1 Pierce
- 1 Barbone

1 Penn State University
- 1 Koopman

2 Virginia Tech
- 1 Knight
- 1 Fuller

CENTER DISTRIBUTION

Copies	Code	Name
1	011	Corrado
2	0112	Douglas Halsall
1	20	
1	2040	Everstine
1	70	Covich
1	701	Sevik
3	7015	Fisher Hamly Vendittis
1	7020	Strasberg
1	7030	Maidanik
1	7203	Dlubac
7	7250	Shang Becker Bowers Carroll Maga Niemiec Vasudevan
1	842	Graesser
2	3421	(TIC-Carderock)